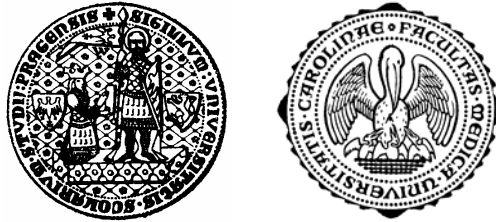


Charles University in Prague
First Faculty of Medicine

Academic program: biochemistry and pathobiochemistry



Mgr. Daniela Fornůsková

Studium poruch cytochrom c oxidasy a ATP synthasy na biochemické
a molekulární úrovni

Biochemical and molecular studies of cytochrome c oxidase
and ATP synthase deficiencies

PhD Thesis

Supervisor: Prof. MUDr. Jiří Zeman, DrSc.

Prague, 2010

Prohlášení:

Prohlašuji, že jsem závěrečnou práci zpracovala samostatně a že jsem řádně uvedla a citovala všechny použité prameny a literaturu. Současně prohlašuji, že práce nebyla využita k získání jiného nebo stejného titulu.

Souhlasím s trvalým uložením elektronické verze mé práce v databázi systému meziuniverzitního projektu Theses.cz za účelem soustavné kontroly podobnosti kvalifikačních prací.

V Praze, 2010

Mgr. Daniela FORNŮSKOVÁ

Podpis

Identifikační záznam

FORNŮSKOVÁ Daniela. *Studium poruch cytochrom c oxidasy a ATP synthasy na biochemické a molekulární úrovni. [Biochemical and molecular studies of cytochrome c oxidase and ATP synthase deficiencies]*. Praha, 2010. 93 stran. Disertační práce. Univerzita Karlova v Praze, 1. lékařská fakulta, Klinika dětského a dorostového lékařství. Vedoucí práce Prof. MUDr. Jiří Zeman, DrSc.

Identification record

FORNŮSKOVÁ Daniela. *Biochemical and molecular studies of cytochrome c oxidase and ATP synthase deficiencies. [Studium poruch cytochrom c oxidasy a ATP synthasy na biochemické a molekulární úrovni]*. Prague, 2010. 93 pages. PhD thesis. Charles University in Prague, First Faculty of Medicine, Department of Pediatrics and Adolescent Medicine. Supervisor Prof. Jiří Zeman, MD, PhD.

ABSTRAKT

Savčí organismus je plně závislý na systému oxidativní fosforylace (OXPHOS) jako hlavním zdroji produkce energie (ATP) v buňce. Poruchy OXPHOS mohou být způsobeny mutacemi v genech kódovaných mitochondriální DNA nebo jadernou DNA.

Část výzkumné práce je zaměřena na roli raně a pozdně se asemblujících, jaderně kódovaných, strukturních podjednotek cytochrom c oxidasy (CcO) a Oxa1l, lidského homologu kvasinkové mitochondriální Oxa1 translokasy, v biogenezi cytochrom c oxidasy a její funkci s využitím stabilní RNA interference COX4, COX5A, COX6A1 a OXA1L a ektopické exprese epitopově značených podjednotek Cox6a, Cox7a a Cox7b v buněčné linii HEK (lidské embryonální ledviny)-293. Naše výsledky ukazují, že zatímco podjednotky Cox4 a Cox5a jsou nezbytné pro asemblaci funkčního komplexu CcO, Cox6a podjednotka je důležitá pro její stabilitu. V buňkách se sníženou expresí OXA1L byla překvapivě zjištěna normální aktivita i hladina holoenzymu CcO, přestože inaktivace OXA1 u kvasinek vyvolá kompletní ztrátu aktivity CcO.

Při studiu poruch OXPHOS v izolovaných mitochondriích kosterního svalu, srdce, jater a frontálního kortexu získaných od pacientů s Leigh syndromem (mtDNA mutace 8363G>A), MERRF syndromem (mtDNA mutace 8344A>G) a MELAS syndromem (mtDNA mutace 3243A>G) jsme našli tkáňově specifické rozdíly v dopadu mt-tRNA mutací na OXPHOS mozku, které se významně lišily od dopadu těchto mutací v ostatních tkáních. Navíc jsme ukázali, že v případě mtDNA mikrolece 9205 Δ TA v ATP6 genu je výrazně omezena syntéza podjednotky a komplexu ATPasy a postižena biogeneze CcO.

Klíčová slova: mitochondrie, cytochrome c oxidasa, ATP syntasa (ATPasa), tkáňová specifita, asemblace proteinů, biogeneze, RNA interference (RNAi)

ABSTRACT

The mammalian organism fully depends on the oxidative phosphorylation system (OXPHOS) as the major energy (ATP) producer of the cell. Disturbances of OXPHOS may be caused by mutations in either mitochondrial DNA (mtDNA) or nuclear DNA.

One part of the thesis is focused on the role of early and late assembled nuclear-encoded structural subunits of cytochrome c oxidase (CcO) as well as Oxa1l, the human homologue of the yeast mitochondrial Oxa1 translocase, in the biogenesis and function of the human CcO complex using stable RNA interference of COX4, COX5A, COX6A1 and OXA1L, as well as expression of epitope-tagged Cox6a, Cox7a and Cox7b, in HEK (human embryonic kidney)-293 cells. Our results indicate that, whereas nuclear- encoded CcO subunits Cox4 and Cox5a are required for the assembly of the functional CcO complex, the Cox6a subunit is required for the overall stability of the holoenzyme. In OXA1L knockdown HEK-293 cells, intriguingly, CcO activity and holoenzyme content were unaffected, although the inactivation of OXA1 in yeast was shown to cause complete absence of CcO activity.

In addition, we compared OXPHOS protein deficiency patterns in mitochondria from skeletal muscle, heart, liver and frontal cortex of patients with Leigh (mtDNA mutation 8363G>A), MERRF (mtDNA mutation 8344A>G), and MELAS (mtDNA mutation 3243A>G) syndromes. Our data show new effects of mt-tRNA mutations on the brain which differ substantially from those described for other tissues. Furthermore, we found that mtDNA 9205 Δ TA microdeletion in the ATP6 gene prevents the synthesis of ATPase subunit a and also affects the biogenesis of CcO.

Key words: mitochondria, cytochrome c oxidase, ATP synthase (ATPase), tissue specificity, protein assembly, biogenesis, RNA interference (RNAi)

ACKNOWLEDGEMENTS

I would like to thank to my supervisor Prof. MUDr. Jiří Zeman, DrSc. for the opportunity to participate in the mitochondrial research, for the encouragement during the progress of this work whenever I needed and for much invaluable advice. This thesis would not have been possible without friendly atmosphere in our lab. Therefore I thank to all my colleagues from Laboratory for Study of Mitochondrial Disorders, especially to RNDr. Hana Hansíková, CSc. and RNDr. Jana Sládková, CSc. for their willing and helpful approach. Likewise, my special thanks belong to my colleague Mgr. Lukáš Stibůrek, PhD. for intense, often critical but inestimable and inspiring debates on various scientific subjects. Last but not least, I am grateful for patience and gracious support of my family and of my friend Ondřej.

Financially, the projects of this thesis were supported by grants from the Grant Agency of Charles University [grant number GAUK 153/2004/C] and [grant number GAUK 1/2006/R], the Grant Agency of Czech Republic [grant number GACR 303/03/H065], the Internal Grant Agency of the Ministry of Health of the Czech Republic [grant number IGA MZ NS 10581/3] and by institutional project [grant number MSM 0021620806].

LIST OF CONTENTS

ABBREVIATIONS	9
1 INTRODUCTION	11
2 AIMS OF THE STUDY	13
3 REVIEW OF THE LITERATURE	15
3.1. <i>Evolutionary trends in mitochondria</i>	15
3.2. <i>The main characteristic features of mitochondria</i>	18
3.3. <i>System of oxidative phosphorylation</i>	19
3.3.1. <i>Electron-transport chain</i>	19
3.3.1.1. <i>Complex I</i>	20
3.3.1.2. <i>Complex II</i>	22
3.3.1.3. <i>Complex III</i>	23
3.3.1.4. <i>Complex IV</i>	25
3.3.2. <i>Complex V</i>	29
3.3.3. <i>Transporters of ATP synthase substrates</i>	32
3.3.3.1. <i>Transport of ADP</i>	33
3.3.3.2. <i>Transport of Pi</i>	36
3.4. <i>Organization of OXPHOS, functional and structural relevance</i>	38
3.4.1. <i>Random diffusion vs. solid-state assembly of electron transfer enzymes</i>	38
3.4.2. <i>Supramolecular organization of ATP synthase and pleiotropic effects of its dysfunction</i>	42
3.4.3. <i>Tissue-specific physiological diversity of OXPHOS</i>	46
4 MATERIAL AND METHODS	48
4.1. <i>Tissues and cell lines</i>	48
4.2. <i>Ethics</i>	48
4.3. <i>Plasmid construction</i>	48
4.4. <i>Cell culture, transfections and flow cytometry</i>	49
4.5. <i>Isolation of mitochondria</i>	50
4.6. <i>Immunofluorescence</i>	50
4.7. <i>Laser scanning confocal microscopy</i>	51
4.8. <i>Sub-cellular and submitochondrial fractionation</i>	51
4.9. <i>Preparation of a polyclonal antibody to human Oxa11</i>	51
4.10. <i>Electrophoresis and Western blot analysis</i>	51
4.11. <i>Immunoprecipitation of Oxa11-FLAG protein</i>	53
4.12. <i>Spectrophotometric assays</i>	54
4.13. <i>High-resolution oxygraphy</i>	54
4.14. <i>Cytofluorimetric analysis of mitochondrial membrane potential</i>	55
4.15. <i>ATP synthesis</i>	55
4.16. <i>Biosynthesis of mitochondrial proteins</i>	56
4.17. <i>Protein determination</i>	56
4.18. <i>DNA analysis and sequencing</i>	56
4.19. <i>Restriction analysis</i>	56

4.20. Northern blot analysis	57
4.21. Quantitative RT-PCR (reverse transcription-PCR) analysis	57
4.22. Statistical analysis	58
5 RESULTS AND DISCUSSION	59
5.1. Characterization of the assembly and function of human nDNA-encoded CcO subunits 4, 5a, 6a, 7a and 7b (specific aim 1a)	59
5.2. Characterization of the biochemical properties of OXA1L, the human homologue of the yeast mitochondrial Oxa1 translocase, and study of its role for CcO biogenesis (specific aim 1b).....	61
5.3. Analysis of the tissue-specific effects of mt-tRNA point mutations in patients affected by Leigh syndrome (8363G>A), MERRF syndrome (8344A>G), and MELAS syndrome (3243A>G) on the steady-state levels and activity of OXPHOS complexes (specific aim 2a).....	63
5.4. Study of molecular and biochemical impact of mtDNA mutation in the ATP6 gene (9205ΔTA) on the biosynthesis of ATPase subunit a and its structural and functional consequences (specific aim 2b).....	65
6 CONCLUSIONS	68
7 SUMMARY	70
8 REFERENCES	71
9 LIST OF ORIGINAL ARTICLES.....	91
9.1. Journal articles.....	91
9.2. Abstracts in journals.....	91

ABBREVIATIONS

2D	two-dimensional
Δ	deletion
$\Delta\Psi$	potential difference
$\Delta\Psi_m$	mitochondrial membrane potential
ΔpH	proton gradient
AAC	ADP/ATP carrier
ADP	adenosine diphosphate
AMP	adenosine monophosphate
ATP	adenosine triphosphate
ATPase	adenosine triphosphatase
BN	blue native
bp	base pair
BSA	bovine serum albumin
CcO	cytochrome c oxidase, complex IV
CI	complex I
CII	complex II
CIII	complex III
CIV	complex IV
CMV	cytomegalovirus (RNA polymerase II) promoter
CN	colorless native
CNS	central nervous system
CoQ	coenzyme Q
COX	cytochrome c oxidase, complex IV
Cox#	cytochrome c oxidase structural subunit number #
CS	citrate synthase
CV	complex V
CytC	cytochrome c
dADP	deoxy-adenosine diphosphate
dATP	deoxy- adenosine triphosphate
dCTP	deoxy-cytosine triphosphate
DDM	n-dodecyl- β -D-maltoside
DMSO	dimethyl sulfoxide
DNA	deoxyribonucleic acid
EDTA	ethylenediaminetetraacetic acid
EGTA	ethylene glycol tetraacetic acid
FACS	fluorescent-activated cell sorting
FAD	flavin adenine dinucleotide
FADH ₂	flavin adenine dinucleotide reduced
FCCP	carbonyl cyanide <i>p</i> -trifluoromethoxyphenylhydrazone
FLAG	octapeptide tag sequence (N-DYKDDDDK-C, 1012 Da)
GFP	green fluorescent protein
HEK-293	human embryonic kidney - 293
IMAGE	integrated molecular analysis of genomes and their expression
IMM	inner mitochondrial membrane
IMS	intermembrane space
IRES-Neo	internal ribosome entry site - neomycin phosphotransferase
ISP	iron-sulfur protein
KD	knockdown
kDa	kilodalton

KO	knockout
MCA	metabolic flux control analysis
MDa	megadalton
MELAS	mitochondrial encephalopathy, lactic acidosis, and stroke like episodes
MERRF	myoclonic epilepsy and ragged-red fibers
mRNA	messenger ribonucleic acid
mt	mitochondrial
mt-tRNA	mitochondrial transfer ribonucleic acid
MW	molecular weight
n	nuclear
N side	negatively charged side
NAD ⁺	nicotinamide adenine dinucleotide
NADH	nicotinamide adenine dinucleotide reduced
NARP	neurogenic muscle weakness, ataxia, and retinitis pigmentosa
NS	non-silencing
nt	nucleotide(s)
OMM	outer mitochondrial membrane
ORF	open reading frame
OXA1	oxidase assembly 1
OXA1L	oxidase assembly 1-like
OXPHOS	oxidative phosphorylation system
P side	positively charged side
P ₅₀	partial pressure of oxygen at half-maximal respiration rate
PAGE	polyacrylamide gel electrophoresis
PBS	phosphate-buffered saline
PCR	polymerase chain reaction
PEO	progressive external ophthalmoplegia
Pi	inorganic phosphate
PIC	mitochondrial phosphate carrier
PMF	proton motive force
PVDF	polyvinylidene difluoride
QCR	ubiquinol:cytochrome c oxidoreductase, complex III
qRT-PCR	quantitative real-time PCR
RFLP	restriction fragment length polymorphism
RNA	ribonucleic acid
RNAi	RNA interference
ROS	reactive oxygen species
rRNA	ribosomal ribonucleic acid
SDH	succinate dehydrogenase
SDS	sodium dodecyl sulfate
shRNA	short hairpin RNA
shRNAmir	microRNA-adapted shRNA
STE	sucrose-Tris-EDTA medium
TBS	Tris-buffered saline
TMPD	<i>N,N,N',N'</i> -tetramethyl- <i>p</i> -phenylenediamine
TMRM	tetramethylrhodamine methyl ester
tRNA	transfer ribonucleic acid
UTR	untranslated region

1 INTRODUCTION

Mitochondria hold a central position in cellular bioenergetics. The most important mitochondrial energy-yielding reaction is performed by the oxidative phosphorylation system (OXPHOS) which is mainly composed of five large multi-subunit complexes (CI-CV) embedded in the inner mitochondrial membrane. The importance of mitochondria for cell viability is most dramatically apparent from diseases resulting from its malfunction. OXPHOS disorders, first recognized 50 years ago (Luft *et al.* 1962), have been found to be the most frequent cause of metabolic abnormality in pediatric neurology (DiMauro and Schon 2008; Zeviani *et al.* 1996) but often present with nonneurological symptoms (e. g. hepatic, cardiac, renal, gastrointestinal, endocrine, hematological symptoms, failure to thrive) (Di Donato 2009; Munnich *et al.* 1996) or can contribute to severe diseases of adulthood (e. g. Parkinson's disease, Alzheimer's disease, Type 2 diabetes mellitus) (Civitarese and Ravussin 2008; Lin and Beal 2006; Zeviani and Carelli 2007). The clinical and genetic variability of OXPHOS disorders makes it extremely difficult to estimate prevalence accurately; however, the general incidence of mitochondrial disease is approximately 1:5000 (Schaefer *et al.* 2004; Thorburn 2004). Since the OXPHOS is composed of 13 structural subunits encoded by mitochondrial DNA (mtDNA) and more than 70 structural polypeptides encoded by nuclear DNA (nDNA), primary OXPHOS disorders can be classified genetically according to whether the primary defect is in the nuclear or mitochondrial genome. Furthermore, 24 additional mtDNA-encoded genes are involved in mitochondrial translational apparatus and numerous nDNA-encoded genes are necessary for synthesis of prosthetic groups and assembly of OXPHOS complexes, stability of mtDNA and mitochondrial biogenesis (Fig. 1). Therefore, inheritance of these mutations may be autosomal recessive or dominant, X-linked or maternal (Smeitink *et al.* 2001b). MtDNA mutations, as it currently is believed, account for mitochondrial encephalopathy in 20% to 30% of pediatric patients and a higher proportion of adult patients with mitochondrial disorders (Lebon *et al.* 2003; Thorburn 2004).

At the metabolic level, the impact of OXPHOS disease can be classified as systemic consequences (e. g. pathological increase in concentration of the lactic acid, alanin or higher ketone body ratio) or consequences at the tissue and cellular level (bio-energy deficiency, redox or metabolite imbalance or elevated or disturbed production of reactive oxygen species (ROS)) (Smeitink *et al.* 2006). Although often assumed to be the primary effect of mitochondrial disease, sufficient supply of ATP to meet cellular needs is not necessarily the only factor or in some cases even the main factor in OXPHOS disease (Smeitink *et al.* 2006).

Biochemically, OXPHOS defects are classified based on the affected enzyme as isolated (only one OXPHOS enzyme is deficient) or combined (more than one complex deficiency is observed). Due to high complexity of genes which are involved in optional functioning of OXPHOS, some of which very likely remain to be identified, most patients are still classified clinically or biochemically, simply because the genetic defect has not yet been established. Moreover, very common and severe pathogenic manifestation of OXPHOS dysfunction - Leigh syndrome (see Chapter 3.3.1.1 for clinical details), for example, may be caused by mutations in more than 25 different genes (Kirby and Thorburn 2008), thus in many cases there is no clear candidate gene to investigate and many potential candidates may need to be analyzed (Tucker *et al.* 2010). Therefore, there is a great need to better understand the genetics of mitochondrial disease as well as biogenesis of OXPHOS, which will enable prenatal diagnoses and will deliver deeper understanding of mitochondrial function necessary for development of effective therapies (Koene and Smeitink 2009).

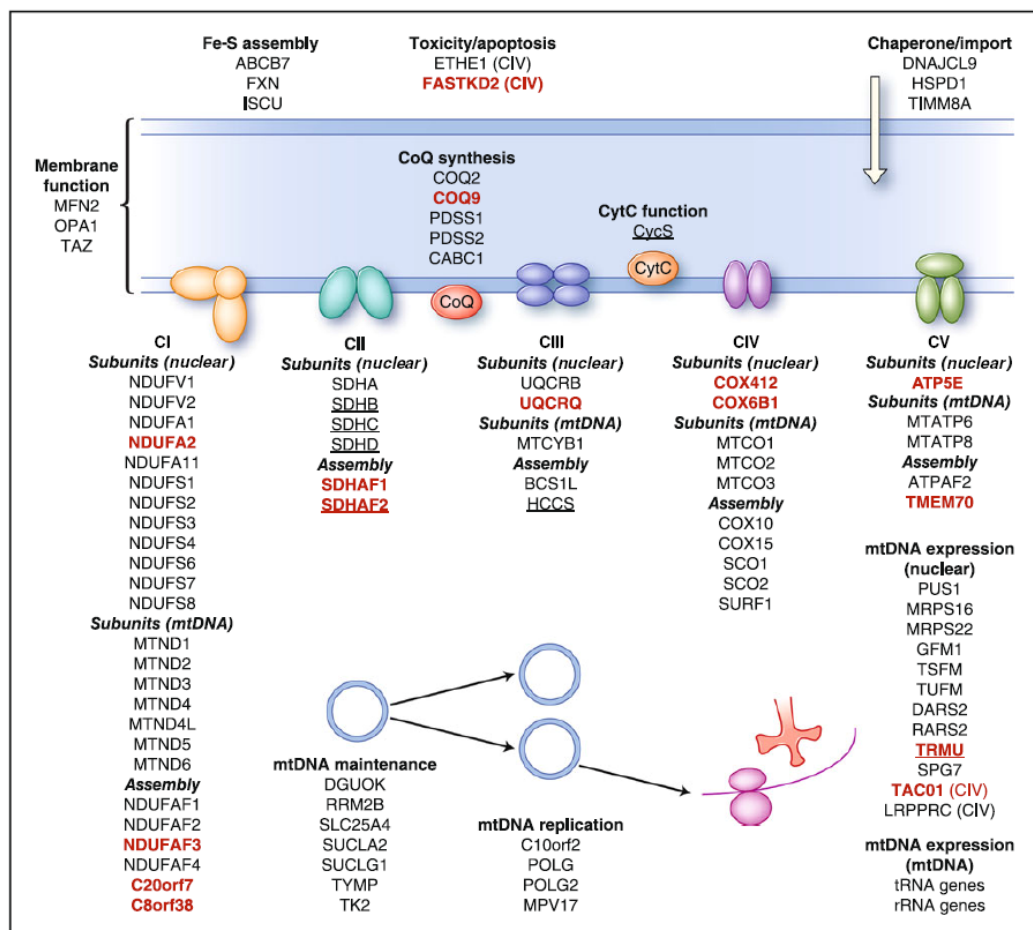


Figure 1 Genes associated with mitochondrial disease (Tucker *et al.* 2010). Mutations have been identified in genes encoding CI, CII, CIII, CIV, and CV subunits and assembly factors; genes involved in mitochondrial DNA (mtDNA) maintenance (via nucleotide metabolism), mtDNA replication, and mtDNA expression; genes affecting the electron carriers coenzyme Q (CoQ) and cytochrome *c* (CytC); genes affecting Fe-S assembly; and genes involved in protein import, toxicity/apoptosis, and membrane function. Recently identified genes are highlighted in red. Genes affecting oxidative phosphorylation for which mutations are not reported to cause neuropathology are underlined.

2 AIMS OF THE STUDY

Our laboratory for study of mitochondrial disorders specializes in biochemical and molecular diagnostics of OXPHOS deficiencies in the patients predominantly coming from Czech and Slovak Republics. One part of this thesis is based on the study of selected deleterious mutations of mtDNA in terms of their impact on OXPHOS steady-state levels and functioning in various patients' tissues. All analyzed mutations, especially those in genes coding for mt-tRNAs, usually affects more than one OXPHOS complex, thus they manifest as combined OXPHOS defects. We were interested in differences in OXPHOS deficiency patterns among various tissues.

Second part of this thesis is aimed at biogenesis of cytochrome c oxidase (CcO), the complex IV of OXPHOS, which plays central role in oxidative metabolism. Defective CcO functionality results in heterogeneous group of diseases predominantly affecting tissues with high-energy demands. For its medical relevance, CcO biogenesis has received significant attention and has been intensively studied by biochemical, genetic, spectroscopic and crystallographic means. Data from medical records of 180 CcO-deficient children identified in Poland, Czech and Slovak Republics, that means from area accounting for more than 50 million inhabitants, revealed fairly high mortality of CcO deficiency, relatively early onset of the diseases resulting from CcO deficiency and pretty severe clinical symptoms, encephalopathy to be the most common (Bohm *et al.* 2006). In this group, molecular basis of CcO deficiency, which is fundamental e. g. for prenatal diagnostics in affected families, still remains to be elucidated approximately in the half of cases. Therefore, the study of CcO assembly also became an important interest in our laboratory and of my thesis.

The specific aims of this thesis have been:

1) to study new aspects of the CcO assembly pathway

- a) Characterization of the assembly and function of human nuclear-encoded CcO subunits 4, 5a, 6a, 7a and 7b.
- b) Characterization of the biochemical properties of OXA1L, the human homologue of the yeast mitochondrial Oxal translocase, and study of its role for CcO biogenesis.

2) to study the molecular basis of selected mtDNA-encoded mutations and their impact on OXPHOS function

- a) Analysis of the tissue-specific effects of mt-tRNA point mutations in patients affected by Leigh syndrome (8363G>A), MERRF syndrome (8344A>G), and MELAS syndrome (3243A>G) on the steady-state levels and activity of OXPHOS complexes.

- b) Study of molecular and biochemical impact of mtDNA mutation in the ATP6 gene (9205 Δ TA) on the biosynthesis of ATPase subunit a and its structural and functional consequences.

3 REVIEW OF THE LITERATURE

3.1. Evolutionary trends in mitochondria

Mitochondria are the endosymbiotic semiautonomous ATP-generating organelles of eukaryotes. The divergence of mitochondria from bacteria and aerobic respiration in eukaryotes are conventionally associated with a global disaster about 2.0 billion years ago (Sicheritz-Ponten *et al.* 1998), when atmospheric oxygen levels increased rapidly, presumably from the accumulated activity of oceanic photosynthetic cyanobacteria (Andersson *et al.* 2003). A continuous presence of oxygen during the entire history of the biosphere, albeit primary at very low levels (Holland 1990), matches the ancient origins of the terminal oxidases characteristic of mitochondria as well as represented in the archaea and bacteria. Thus, the oxidative respiratory system was at the time of mitochondrial origin an ancient enzymatic system (Kurland and Andersson 2000). Phylogenetic reconstructions have by now provided convincing evidence that the various mitochondrial genomes have a single monophyletic origin in α -proteobacterial subdivision (Gray *et al.* 1999). A studying of mitochondrially encoded, chaperone and ribosomal proteins points specifically towards the Rickettsiaceae family (Andersson *et al.* 2003; Andersson *et al.* 1998; Viale and Arakaki 1994). A weakness of all current theories of mitochondrial origins is the uncertain identity of the host of the ancestral endosymbiont (Andersson *et al.* 2003; Lang *et al.* 1999). Phylogenomic reconstructions show that the characteristic eukaryotic complexity arose without any intermediate grades seen between the prokaryotic and eukaryotic levels of organization (Koonin 2010).

ATP production in eukaryotes from glucose and oxygen normally consists of two catabolic processes (Voet *et al.* 2006). First, the glycolytic system of the eukaryotes, which seems not to trace its origin back to the α -proteobacteria (Andersson *et al.* 2003), supply mitochondria (as well as the obligate parasites of the genus *Rickettsia*) with pyruvate. Second, pyruvate dehydrogenase complex and Krebs cycle catalyze oxidative conversion of pyruvate to H₂O and CO₂. Substrates of Krebs cycle do not come only from glycolysis, but also from beta-oxidation of fatty acids and proteolysis. Concomitantly to these catabolic processes, electrons are transferred via coenzymes NAD⁺ and FAD to pass into the mitochondrial electron-transport chain which produces a proton gradient across the mitochondrial membrane. The free energy stored in this electrochemical gradient drives the synthesis of ATP from ADP and phosphate through oxidative phosphorylation (Voet *et al.* 2006). The mechanistic principle of oxidative phosphorylation was first proposed by Peter Mitchell (Mitchell 1961) who received for chemiosmotic hypothesis Nobel prize in 1978.

The processes transforming the ancestral α -proteobacterium into the modern mitochondrion were obviously incremental and presumably spread over millions of years. Many ancestral mitochondrial genes have been lost, a smaller number of mitochondrial proteins have been transferred from the mitochondrial to the nuclear genome and the minimum of mitochondrial genes remained to be encoded by mitochondrial DNA (mtDNA). The tendency to transfer the vast majority of residual ancestral mitochondrial genes to the nuclear genome might have been favored for its well-developed sexual mechanisms compared to the asexual character of mitochondrial lineages which suggests that they might be particularly vulnerable to Muller's ratchet¹ (Kurland and Andersson 2000). Like a typical bacterial genome, many mtDNAs map as circular molecules, although linear mtDNA exist as well (Nosek *et al.* 1998). Although the genetic role of mtDNA appears to be universally conserved, this genome exhibits remarkable variation in conformation and size, which ranges from <6kbp in *Plasmodium falciparum* (the human malaria parasite) to >200kbp in land plants, as well as in actual gene content, arrangement and expression. The contrast between the expansive plant and condensed animal mitochondrial genomes in virtually every parameter (e. g. proportion of coding to noncoding sequence, rate of primary sequence divergence, conservation of gene order) suggests that these mtDNAs exhibit entirely opposite evolutionary trends (Gray *et al.* 1999).

The largest number of mitochondrial proteins, which have no bacterial or archaeal orthologues, constituted a novel "eukaryotic" group of mitochondrial proteins, which evidently evolved from the nuclear genome by duplication and functional divergence of sequences that predate the arrival of the endosymbiont ancestor of mitochondria (Karlberg *et al.* 2000). The phylogenetic clustering of the mitochondrial proteins into α -proteobacterial and eukaryotic homologues goes hand in hand with the functional profiles of the clusters (Kurland and Andersson 2000). Thus, the bacterial homologues seem to be mainly involved in translation and energy metabolism. In contrast, the eukaryotic proteins are typically associated with transport and regulatory functions. An important group of eukaryotic proteins, which originated subsequent to the integration of the endosymbiont into the eukaryotic cell, involves protein and ATP transport machinery (Andersson *et al.* 2003). Transport of mitochondrial precursor proteins to mitochondria is posttranslational process subsequent to their synthesis by cytosolic ribosomes. A recognition, import and sorting of mitochondrial precursor proteins based on their targeting sequence signals is mediated by translocases in the outer and inner membrane of mitochondria (Neupert and Herrmann 2007). The evolution of mitochondrial targeting system gave a possibility to the host cell to decorate the

¹ **Muller's ratchet** is the process by which the genomes of an asexual population accumulate deleterious mutations in an irreversible manner.

mitochondrial core complexes with a variety of new proteins, e. g. participating in the assembly of complexes or functioning in regulation. It is assumed, that the coevolution of the core α -proteobacterial components and the complementary eukaryotic nuclear components transformed the endosymbiont into an organelle (Kurland and Andersson 2000). The presence of ATP/ADP transporter systems made it possible for the mitochondriate cell to fully exploit the benefits of the high ATP yields obtained by aerobic respiration and may even have been critical for the transition from single cells to early, undifferentiated forms of multicellular eukaryotes (Pfeiffer *et al.* 2001).

3.2. The main characteristic features of mitochondria

Mitochondria display striking interspecies and inter-tissue variations in shape, connectivity, and inner membrane morphology (Mannella 2008). The general structure of mitochondrion is defined by its two membranes (Frey and Mannella 2000; Logan 2006). A topologically simple and limiting outer membrane enwraps the energy-transducing inner membrane whose surface area is considerably larger and which in turn encloses a protein-rich matrix. To accommodate the volume constraint imposed by the outer membrane, the inner membrane has numerous invaginations, the cristae, each of which can have one or more tubular connections to the membrane periphery (Mannella 2006b). In addition to the scaffold function of the inner membrane for the assembly and operation of the respiratory chain complexes, this highly pleomorphic structure provides the permeability barrier across which the respiratory machinery generates its chemiosmotic gradient. Electron tomographic analyses of various mitochondria provided overwhelming evidence that cristae are not simply random folds in the inner membrane but rather internal compartments formed by invaginations of the membrane, which originates at narrow neck-like segments referred as crista junctions. In other words, crista junctions delimit an intercrystal space, thereby presumably functionally restricting diffusion between intercrystal compartments and the peripheral intermembrane space (Mannella 2006a; Mannella 2006b; Mannella *et al.* 1997). The number of crista junctions and the morphology of the intercrystal space have been shown to change with the metabolic state of the mitochondria (Hackenbrock 1968; Mannella *et al.* 1997; Mannella *et al.* 1994) and can only be achieved by the inner membrane undergoing fusion and fission (Mannella *et al.* 2001). The relative activities of proteins involved in mitochondrial fusion and fission determine an overall morphology, integrity and turnover of the mitochondrial population as well as segregation and protection of mitochondrial DNA (Berman *et al.* 2008; Cerveny *et al.* 2007; Chen and Chan 2005; Scott *et al.* 2003). In many cases, mitochondria form a complex reticulum that interacts with other cellular components, in particular the cytoskeleton and endoplasmic reticulum (Mannella 2000; Rutter and Rizzuto 2000). Interaction of mitochondrial and endoplasmic reticulum networks and the connectivity state of mitochondria controls metabolic flow, production of ROS, protein transport, intracellular Ca^{2+} signaling and cell death (Csordas *et al.* 2006; de Brito and Scorrano 2008; Giorgi *et al.* 2009; Kakkar and Singh 2007; Szabadkai and Rizzuto 2007).

3.3. System of oxidative phosphorylation

Mitochondria comprise the site of most ATP production in eukaryotic cells by a process known as oxidative phosphorylation (Saraste 1999). This remarkably complex process, which is performed by system of oxidative phosphorylation (OXPHOS) (Fig. 2), requires four major events, electron transport (CI-CIV) and generation of a proton gradient (CI, CIII and CIV), transport of P_i and ADP and finally coupling the proton gradient to ATP synthesis (CV).

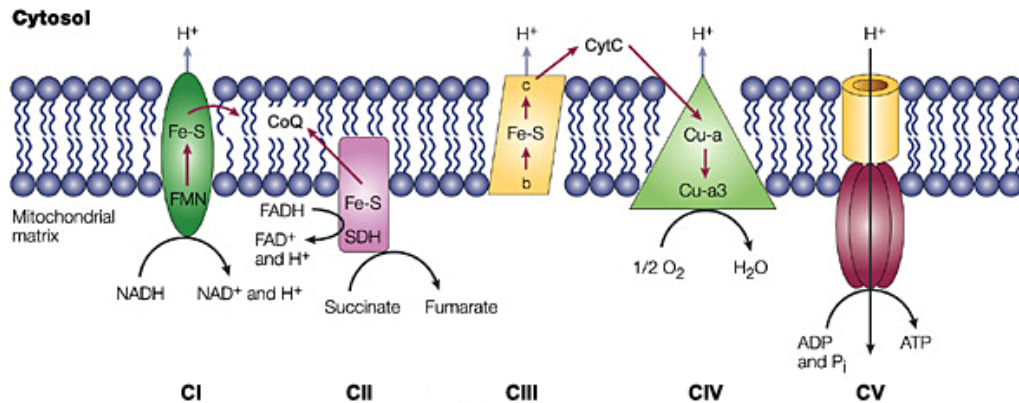


Figure 2 The complexes of OXPHOS (Eng *et al.* 2003). The diagram shows the five complexes of OXPHOS (CI – CV). Complexes I–IV are the electron-transport complexes, whereas complex V synthesizes ATP. Electrons are passed down the four complexes (black and red arrows) to molecular oxygen and then complex V generates ATP from ADP and P_i . The blue arrows show where the protons are pumped to the cytosolic side of the inter-membrane to generate an electrochemical gradient, and where proton movement back across complex V (the ATP synthase) is used to drive ATP synthesis.

3.3.1. Electron-transport chain

Oxidation of NADH and $FADH_2$ and transfer of electrons to O_2 is carried out by the electron transport chain also known as respiratory chain. Electrons travel through this chain from lower to higher standard reduction potentials through series of redox centers, so that the overall process is exergonic. Some of these redox centers are mobile, and others are components of integral membrane protein complexes (Fig. 2). The released energy is used at three locations within the chain (CI, CIII and CIV) to expel protons from the matrix into the IMS, resulting in a potential difference ($\Delta\Psi$) and proton gradient (ΔpH) across the IMM (Voet *et al.* 2006). The energy stored in this electrochemical proton gradient, generally referred to as proton motive force (PMF) can be used for chemical, osmotic and mechanical work. The PMF is dominated by $\Delta\Psi$, with ΔpH contributing ~15% to its total magnitude (Koopman *et al.* 2008; Nicholls and Ferguson 2002). In addition to crucial role of PMF in ATP synthesis, it is also used for a variety of other energy-dependent processes, which are (indirectly) driven by either $\Delta\Psi$ or ΔpH (Fig. 3).

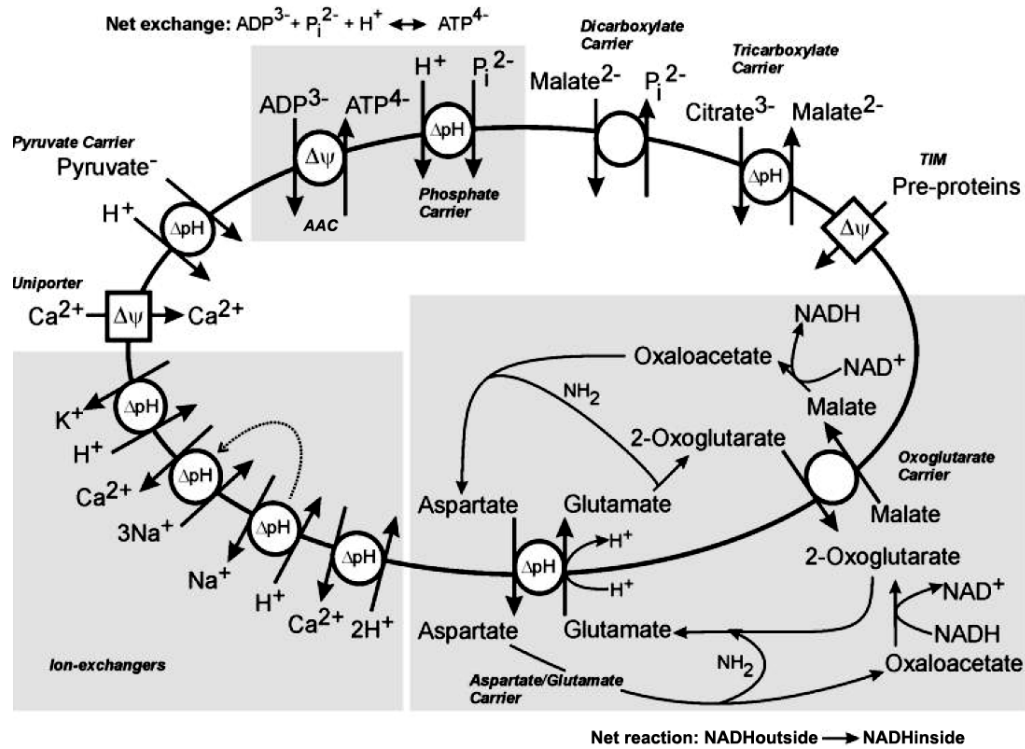


Figure 3 Processes driven by proton motive force (PMF) (Koopman *et al.* 2010). In addition to CV-mediated ATP generation, the PMF also is required for transport processes across the IMM. These processes are (indirectly) driven by either $\Delta\Psi$ or ΔpH . For instance, mitochondrial Ca^{2+} uptake, ATP/ADP exchange by the adenine-nucleotide translocator (AAC), trans-IMM Na^+ and K^+ fluxes (important in mitochondria volume regulation), and import of nDNA-encoded preproteins are $\Delta\Psi$ dependent, whereas several mitochondrial antiporters (aspartate/glutamate, H^+/K^+ , H^+/Na^+ , $2\text{H}^+/\text{Ca}^{2+}$) and symporters ($\text{H}^+/\text{pyruvate}$ and P_i/ADP) are ΔpH dependent. In this panel, indirect dependencies on ΔpH are marked by dotted lines.

3.3.1.1. Complex I

Complex I, NADH:ubiquinone oxidoreductase, is a very large integral membrane protein complex which oxidizes NADH, produced predominantly by the tricarboxylic acid cycle (Krebs cycle) and the β -oxidation of fatty acids, to regenerate the NAD^+ pool in the mitochondrial matrix. The transfer of two electrons from NADH which reduce ubiquinone (oxidized CoQ) to ubiquinol (reduced CoQ) in the membrane is coupled to the vectorial translocation of four protons across both the inner mitochondrial membrane and the plasma membrane of many bacteria thus contributing to generation of the proton motive force across the membrane. The ubiquinol is subsequently reoxidized by complex III (Hirst 2010).

Complex I has an unusual L-shaped structure, with one arm in the plane of the mitochondrial inner membrane, and one arm protruding into the matrix, both arms being of approximately equal length (Zickermann *et al.* 2009). The L-shaped structure of complex I, observed by electron microscopy, is conserved among species (Guenebaut *et al.* 1998; Radermacher *et al.* 2006), although the protein composition of the eukaryotic

and prokaryotic enzymes varies significantly. The 14 central subunits are conserved in prokaryotes and eukaryotes and harbor all bioenergetic core functions sufficient for energy transduction (Weidner *et al.* 1993). These core subunits consist of seven highly hydrophobic (in eukaryotes mtDNA-encoded) subunits (ND1, ND2, ND3, ND4, ND4L, ND5 and ND6; human nomenclature) and seven hydrophilic (in eukaryotes nDNA-encoded) subunits (NDUFV1, NDUFV2, NDUFS1, NDUFS2, NDUFS3, NDUFS7 and NDUFS8; human nomenclature). The eukaryotic enzyme, which accounts for a total mass in the range of 1MDa, contains numerous accessory subunits which vary between species and augment both enzyme domains. The function of these subunits is largely unknown, but they are very unlikely to participate directly in energy transduction (Koopman *et al.* 2010). In man and cow, there is 31 accessory subunits (Carroll *et al.* 2006). The conserved cofactors of complex I are a non-covalently bound FMN (flavin mononucleotide) and eight iron-sulfur clusters (Fe-S) with the iron coordinated with two to four cysteine side chains from the polypeptide. FMN accepts electrons from NADH (Gostimskaya *et al.* 2007; Grivennikova and Vinogradov 2006), Fe-S clusters transport electrons through the enzyme to ubiquinone. All Fe-S clusters are bound by the hydrophilic domain. Evidence was provided that mitochondrial complex I can undergo a so called active/deactive transition (Vinogradov 1998). To facilitate the proper buildup and stability of complex I protein, several assembly chaperones are required (Vogel *et al.* 2007).

The prokaryotic minimal form of complex I has been characterized e. g. from *Escherichia coli* (Weidner *et al.* 1993) or *Paracoccus denitrificans* (Usui *et al.* 1990). To establish a yeast genetic approach to complex I, obligate aerobic yeast *Yarrowia lipolytica* has been extensively used (Kerscher *et al.* 2002), since this enzyme is absent in fermentative yeasts like *Saccharomyces cerevisiae* (Buschges *et al.* 1994). Further eukaryotic model organisms are e. g. *Bos taurus* (Carroll *et al.* 2003), fungi *Neurospora crassa* (Marques *et al.* 2005) or plant *Arabidopsis thaliana* (Perales *et al.* 2005). Nevertheless, no high resolution structure of the whole complex I holoenzyme is available to date.

Isolated complex I deficiency is the most common cause of OXPHOS dysfunction (Smeitink *et al.* 2001a; Smeitink *et al.* 2001b). Clinical phenotypes of complex I deficiency can result from mutations in nuclear-encoded subunits, generally presenting in infancy and early childhood. Mutations in mtDNA-encoded subunits are more common in the late childhood or adolescence. Disease causing mutations have been described in all seven mtDNA-encoded structural subunits, twelve of the nDNA-encoded structural subunits and nDNA-encoded assembly factors NDUFAF2, NDUFAF1, C6orf66, C8orf38 and C20orf7 (Distelmaier *et al.* 2009; Janssen *et al.* 2006). MtDNA mutation-based diseases are inherited maternally, while nDNA

mutation-based diseases are mostly inherited in an autosomal recessive manner, although also X-linked inheritance has been described (Fernandez-Moreira *et al.* 2007). The most common and devastating clinical phenotype associated with early-onset complex I deficiency is Leigh syndrome, first described as subacute necrotizing encephalomyelopathy (Leigh 1951). Leigh syndrome is an early-onset, progressive neurological disorder characterized by motor and intellectual developmental delay, signs of brainstem and basal ganglia involvement, and increased lactate levels in blood and/or cerebrospinal fluid (Rahman *et al.* 1996).

3.3.1.2. Complex II

Complex II, succinate dehydrogenase (SDH) or succinate:ubiquinone oxidoreductase is a functional member of both the Krebs cycle (tricarboxylic acid cycle) and respiratory electron transfer chain. Within the Krebs cycle, SDH oxidizes succinate to fumarate in the mitochondrial matrix (or cytoplasm in bacteria) which is coupled to the reduction of ubiquinone in the membrane. SDH is the only OXPHOS complex to lack subunits encoded by the mitochondrial genome and the only respiratory complex not to pump protons across the membrane during its catalytic cycle. The physiological form of the mitochondrial SDH is most likely to be a monomer (Sun *et al.* 2005), unlike that for *Escherichia coli*, which is believed to be a trimer (Yankovskaya *et al.* 2003). Eukaryotic holoenzyme of SDH consists of equimolar amounts of four subunits, two of which, subunit A with a covalently bound FAD cofactor and subunit B containing three iron-sulfur clusters, form a hydrophilic catalytic head. This heterodimer is anchored in the inner membrane by hydrophobic tail composed of subunits C and D, which contain one heme b at the subunit interface each providing one of the two axial His ligands. The heme moiety is present in mammalian, yeast and *Escherichia coli* SDHs, but diverse SDH species vary in the number of heme groups as well as in the number of their hydrophobic subunits (Lemos *et al.* 2002; Sun *et al.* 2005). The electron transfer pathway in the oxidation of succinate by SDH involves initial reduction of a FAD cofactor followed by electron transfer through three Fe-S centers to ubiquinone (Hagerhall 1997). Two ubiquinone binding sites have been identified in SDH complexes in mammals and *Escherichia coli* (Sun *et al.* 2005; Yankovskaya *et al.* 2003). The high affinity ubiquinone site lies on the matrix side of the inner membrane and is formed by residues in subunits B, C and D. The second, low affinity ubiquinone site resides in the membrane closer to the intermembrane space. SDH is closely related to fumarate reductase (menaquinol:fumarate oxidoreductase), which catalyzes the opposite reaction to that of SDH during anaerobic respiration in bacteria (Kroger *et al.* 1992). Both enzymes are suggested to have evolved from a common ancestor.

Mutations of SDH genes can manifest themselves with a wide variety of clinical phenotypes in humans (Rustin and Rotig 2002). A mutation in SDHA gene for subunit A was described, first by Bourgeron *et al.* (1995), to contribute to complex II deficiency and Leigh syndrome (Bourgeron *et al.* 1995; Parfait *et al.* 2000) or late-onset optic atrophy, ataxia and myopathy (Birch-Machin *et al.* 2000). Mutations in genes coding for subunits B, C and D (SDHB, SDHC and SDHD respectively) have never been described in any of these progressive neurodegenerative syndromes related to mitochondrial complex II deficiencies, however, they cause the tumors observed in hereditary paraganglioma and/or pheochromocytoma (Baysal *et al.* 2000; Niemann and Muller 2000; Pasini and Stratakis 2009). Very recently, mutations in SDHAF1, encoding a new LYR-motif protein, were described to manifest as defective SDH and infantile leukoencephalopathy in patients (Ghezzi *et al.* 2009). Being a soluble protein, the authors concluded that SDHAF1 is not a stable component of the SDH complex and, therefore, must be an assembly factor.

3.3.1.3. Complex III

Complex III, ubiquinol:cytochrome c oxidoreductase (QCR) or bc_1 complex, is a component of the eukaryotic or bacterial respiratory chain and of the photosynthetic apparatus in purple bacteria. Every bc_1 complex (bacterial as well as mitochondrial) contains three common subunits with active redox centers. These catalytic core components are cytochrome b with two noncovalently attached b-type hemes b_L (also called b_{565}) and b_H (b_{562}), cytochrome c_1 with covalently attached heme c group and the “Rieske” iron-sulfur protein (ISP) with an [2Fe-2S] iron-sulfur cluster. The mitochondrial system contains additional nonredox subunits absent in the bacterial complexes (Hunte *et al.* 2000; Iwata *et al.* 1998; Schagger *et al.* 1986; Zhang *et al.* 1998), seven in yeast and eight in mammalian enzymes (Zara *et al.* 2009). The redox subunit b is encoded by mtDNA in these systems. In mitochondria, more than half of the total molecular mass of this structurally dimeric transmembrane protein complex protrudes into the matrix region, including two core proteins (Leonard *et al.* 1981; Xia *et al.* 1997). Both these subunits, Core1 and Core2, have been shown to be members of the mitochondrial processing peptidase family of proteins, suggesting that the QCR may be a bifunctional protein also involved in mitochondrial import protein processing (Braun *et al.* 1992; Braun and Schmitz 1995).

In respiratory chain, QCR functions to enable one molecule of ubiquinol, a two-electron carrier, to reduce two molecules of cytochrome c, a one-electron carrier (Voet *et al.* 2006). This occurs by a modified version of the “proton-motive Q cycle” of Mitchell (Mitchell 1976), that permits QCR to pump protons from the matrix to the intermembrane space and explains the main features of the enzyme activity (Brandt and

Trumpower 1994; Crofts *et al.* 1999a; Crofts *et al.* 1999b). The key trait of the model is that there are two separate binding sites for ubiquinone and ubiquinol. Ubiquinol is oxidized at the Q_o site of the complex in a bifurcated reaction, in which one electron is transferred to a high-potential chain and the other to a low-potential chain. The high-potential chain, consisting of the ISP, cytochrome c₁ and CytC, transfers one electron from ubiquinol to an acceptor (cytochrome c oxidase, Complex IV), what leaves a ubisemiquinone at the Q_o site. The low potential chain consists of two cytochrome b hemes (b_L and b_H, for low- and high-potential hemes), which serve as a pathway through which electrons are transferred across the coupling membrane from ubisemiquinone at the Q_o site to the Q_i site, at which ubiquinone binds and is reduced to ubiquinol. The two electrons at the Q_i site required for reduction of ubiquinone are provided in successive turnovers. The first electron at the Q_i site generates a relatively stable ubisemiquinone that is reduced to ubiquinol by the second electron. Thus, for every two ubiquinols that enter the Q cycle, one ubiquinol is regenerated. Proton translocation is the result of deprotonation of ubiquinol at the Q_o site (near the P side of the IMM) and protonation of the reduced ubiquinone at the Q_i site (near the N side of the IMM). The circuitous route of electron transfer in complex III is tied to the ability of CoQ to diffuse within the hydrophobic core of the membrane in order to bind to both the Q_o and Q_i sites. Binding of mobile CytC to subunit cytochrome c₁ of the enzyme is mainly mediated by nonpolar interactions (Lange and Hunte 2002). The exclusive reduction of heme b_L from Q_o-bound ubisemiquinone rather than the Rieske Fe-S cluster of the ISP protein, despite the greater reduction potential difference favoring the latter reaction, is secured by mechanic movement of the extrinsic domain of the Fe-S component after its reduction by ubiquinol from Q_o site to the proximity of heme c₁ group. Merely after oxidation of the Fe-S protein by the cytochrome, the subunit can move back to the docking interface on cytochrome b, close to the Q_o site to undergo further reduction by the ubiquinol (Zhang *et al.* 1998).

Complex III deficiency was first described by Spiro *et al.* (1970) in a 46-year-old man and his 16-year-old son with progressive ataxia, predominantly proximal muscle weakness, areflexia, extensor plantar responses and dementia. Studies of muscle mitochondria showed very loose coupling of oxidative phosphorylation and marked reduction in cytochrome b content, representing a defect in complex III (Spiro *et al.* 1970). Disorders related to complex III deficiency are clinically heterogeneous and relatively rare. Interestingly, absence of complex III was described to be associated with combined I-III deficiency, possibly due to structural importance of complex III for stability of complex I in the form of supercomplexes (see Chapter 3.4.1). Most of the cases of complex III deficiency are caused by mutations in the mtDNA-encoded cytochrome b subunit. Patients with these mutations usually present with an isolated

myopathy with ragged red fibers, characterized by exercise intolerance, weakness and myoglobinuria (Fernandez-Vizarra *et al.* 2009). Only one mutation in nDNA-encoded structural subunit has been described so far (Haut *et al.* 2003), a homozygous 4-bp deletion in the UQCRB gene, encoding the ubiquinone-binding protein presented with hypoglycemia and liver dysfunction. More than 20 pathogenic mutations have been reported in the complex III assembly factor BCS1L, dysfunction of which is associated with a wide variety of phenotypic manifestations, e. g. GRACILE syndrome (growth retardation, aminoaciduria, cholestasis, iron overload, lactic acidosis and early death), encephalopathy or Björnstad syndrome (sensorineural hearing loss and pili torti) (Fernandez-Vizarra *et al.* 2009).

3.3.1.4. Complex IV

Complex IV, cytochrome c oxidase (CcO), is the terminal enzyme complex of the mitochondrial electron-transport chain, which couples the electron transfer from reduced cytochrome c to molecular oxygen with vectorial proton translocation across the inner membrane. The mammalian CcO complex is composed of 13 different polypeptide subunits, encoded by both the nuclear and mitochondrial genomes. Mitochondrially encoded Cox1 and Cox2 form the redox site involved in electron transfer. Electrons enter the CcO complex at the binuclear copper site (Cu_A) in the Cox2 subunit, which also mediates electrostatic binding of cytochrome c (Zhen *et al.* 1999). From Cu_A , electrons pass to other metal centers in the Cox1 subunit, first to heme a and then to a heterobimetallic heme a_3/Cu_B center (Stiburek *et al.* 2006). Together with Cox3, mitochondrially encoded subunits constitute the evolutionarily conserved structural core of the enzyme. The remaining ten subunits (Cox4, Cox5a, Cox5b, Cox6a, Cox6b, Cox6c, Cox7a, Cox7b, Cox7c and Cox8), which are encoded by nuclear DNA, are associated with the surface of the complex core. These small polypeptides are required for the assembly and stability of the holoenzyme and are thought to function in the regulation of its activity (Fontanesi *et al.* 2008; Helling *et al.* 2008; Huttemann *et al.* 2008). Tissue-specific isoforms of subunits Cox4, Cox6a, Cox6b, Cox7a and Cox8 have been identified in mammals (Huttemann *et al.* 2001; Kadenbach *et al.* 2000). Most CcO subunits have one or more transmembrane domains, with the exception of Cox5a and Cox5b, which are located at the matrix side, and Cox6b, which is associated with the surface of the complex in the intermembrane space (Tsukihara *et al.* 1996).

Subunit Cox4 is the largest nuclear-encoded subunit of the complex. It was shown to be involved in the allosteric inhibition of CcO activity by ATP, which binds to the matrix portion of the subunit (Arnold and Kadenbach 1997). Isoforms 1 and 2 of Cox4 are encoded by two separate genes and are likely to differ with respect to ATP-induced inhibition of CcO activity (Horvat *et al.* 2006). In mammalian cells, the first step of

CcO assembly is the membrane integration of Cox1, followed by the association of the Cox4–Cox5a heterodimer (Stiburek *et al.* 2005) (Fig. 4B, C). Subunit Cox5a binds indirectly to subunit Cox1 via the matrix domain of subunit Cox4 and the extramembrane segment of Cox6c. Knockdown (KD) of both early-assembled subunits Cox4 and Cox5a, which we performed, resulted in accumulation of four subcomplexes consisting merely of subunit Cox1. The absence of Cox1–Cox4/Cox5a heterodimers confirmed further the interdependence of the assembly of Cox4 and Cox5a (Barrientos *et al.* 2009; Stiburek *et al.* 2005). Together with the lack of accumulation of higher-molecular-mass intermediates, our findings suggest that the assembly of the Cox4–Cox5a heterodimer with Cox1 is necessary for the subsequent association of Cox2, and thus for the rest of the assembly to proceed (Fornuskova *et al.* 2010).

Either under mild detergent conditions or when crystallized or reconstituted in phospholipids vesicles, the majority of mammalian CcO exists as a homodimer. Subunits involved in the stabilization of the dimeric state of CcO are Cox6a and Cox6b. Subunit Cox6a may also contribute to the formation of an interaction site for cytochrome c (Tsukihara *et al.* 1996). Subunit Cox6a (Nijtmans *et al.* 1998) and very likely also subunit Cox6b (Massa *et al.* 2008) were shown to associate with the complex, together with subunits Cox7a or Cox7b, at a very late stage of CcO assembly (Nijtmans *et al.* 1998) (Fig. 4A). The expression of FLAG-tagged versions of Cox7a2, Cox7b and Cox6a2 in both wild-type and Cox6a1-deficient backgrounds allowed us to elucidate for the first time the very late events in human CcO assembly (Fornuskova *et al.* 2010). We identified the particular entry points of these three subunits and demonstrated the significance of the CcO holoenzyme bands a₁ and a₂; detected e. g. by (Massa *et al.* 2008). According to our results, band a₁ probably represents the 13-subunit CcO holoenzyme (S4). In contrast, band a₂ lacks subunit Cox6a, which appears to be added as the last assembled structural subunit. Band a₂ (S4*) is formed by the addition of Cox7a2 and probably Cox6b1 (Massa *et al.* 2008) to the assembly intermediate S3. Finally, subunit Cox7b was found to join the assembling complex during or at the end of the formation of the assembly intermediate S3 (Fig. 4C). Furthermore, unlike COX4- and COX5A-KD mitochondria, in which the reduction in the holoenzyme band a₁ was accompanied by a more pronounced decrease in band a₂, Cox6a-deficient mitochondria retained significantly higher levels of the latter species. These results indicate that band a₂ represents another rate limiting step in human CcO assembly (Fornuskova *et al.* 2010).

The biogenesis of CcO is a complicated, sequential process that necessitates sophisticated coordination. Studies in yeast revealed that the CcO assembly requires more than 30 auxiliary proteins, encoded in the nuclear genome, that are essential for proper biogenesis of the CcO complex but are not part of the mature enzyme

(Barrientos *et al.* 2002; Winge and Tzagoloff 2009). These nonstructural factors (assembly factors), accomplish diverse functions at all the levels of the assembly process which include transcription and mRNA maturation, translation of CcO mitochondrial genes, as well as import into mitochondria of nuclear nDNA-encoded subunits and insertion of transmembrane subunits into the inner mitochondrial membrane. Essential additional roles involve heme a biosynthesis, copper homeostasis and insertion into the apoenzyme and formation of assembly intermediates (Fontanesi *et al.* 2008). A number of these factors were shown to have human homologues some of which were studied at the protein level (Stiburek *et al.* 2006). These include copper metallochaperones Sco1, Sco2, Cox11 and Cox17, which are involved in trafficking/insertion of copper ions into Cu_A and Cu_B centers in Cox2 and Cox1 subunits, respectively; inner membrane proteins Cox10, Cox15 and Surf1, which are required for synthesis and incorporation of heme a moieties into Cox1; and Oxa1 and Cox18 translocases, which are involved in the export/translocation of transmembrane segments of integral inner membrane proteins, including CcO subunits (Stiburek and Zeman 2010). In our laboratory, we addressed the role of human Oxa11, the human orthologue of the yeast Oxa1, in the biogenesis of OXPHOS. Oxa1 protein is a member of the evolutionarily conserved Oxa1/Alb3/YidC protein family, which is involved in the biogenesis of membrane proteins in mitochondria, chloroplasts and bacteria (Herrmann and Neupert 2003; Yi and Dalbey 2005). The predicted human Oxa11 shares 33% sequence identity with the corresponding yeast polypeptide. The inactivation of OXA1 in yeast was shown to cause pleiotropic OXPHOS defects, characterized mainly by the complete absence of CcO activity (Altamura *et al.* 1996), pointing to Oxa1 as essential factor for CcO biogenesis. Oxa11-depleted cells showed markedly decreased protein levels and ATP hydrolytic activity of the complex V and moderately reduced levels and activity of complex I. Intriguingly, the cytochrome oxidase activity and content of CcO, as well as the ascorbate/TMPD fuelled, sodium azide-sensitive oxygen uptake, were either unaffected or even increased when compared to negative controls (Stiburek *et al.* 2007). Since the yeast Oxa1 is strictly required for the N-terminal export of Cox2 precursor, it is possible that the complete absence of the N-terminal leader peptide in nascent human Cox2 might be responsible for the observed Oxa1-independent assembly of human CcO. The fact that human Oxa11 is able to partially restore the respiratory growth of yeast *oxa1* cells suggests that both proteins share at least basic functional features.

CcO deficiency, in addition to complex I deficiency, is frequent cause of mitochondrial encephalomyopathies. Although several pathogenic mutations in each of the three mitochondrially encoded CcO subunits (Shoubridge 2001) and two mutations in nDNA-encoded genes for structural subunits Cox4i2 (Shteyer *et al.* 2009) and Cox6b

(Massa *et al.* 2008) have been reported, the majority of fatal infantile CcO deficiencies identified so far result from autosomal recessive mutations in genes encoding CcO assembly factors (e. g. (Barrientos *et al.* 2009; Diaz 2010)). Indeed, two of the human CcO assembly factors, LRPPRC (leucine-rich pentatricopeptide repeat cassette) and TACO1 (translational activator of Cox1), both of which are involved in mitochondrial CcO mRNA translation, were identified primarily on the basis of their mutant phenotypes in human patients (Mootha *et al.* 2003; Weraarpachai *et al.* 2009).

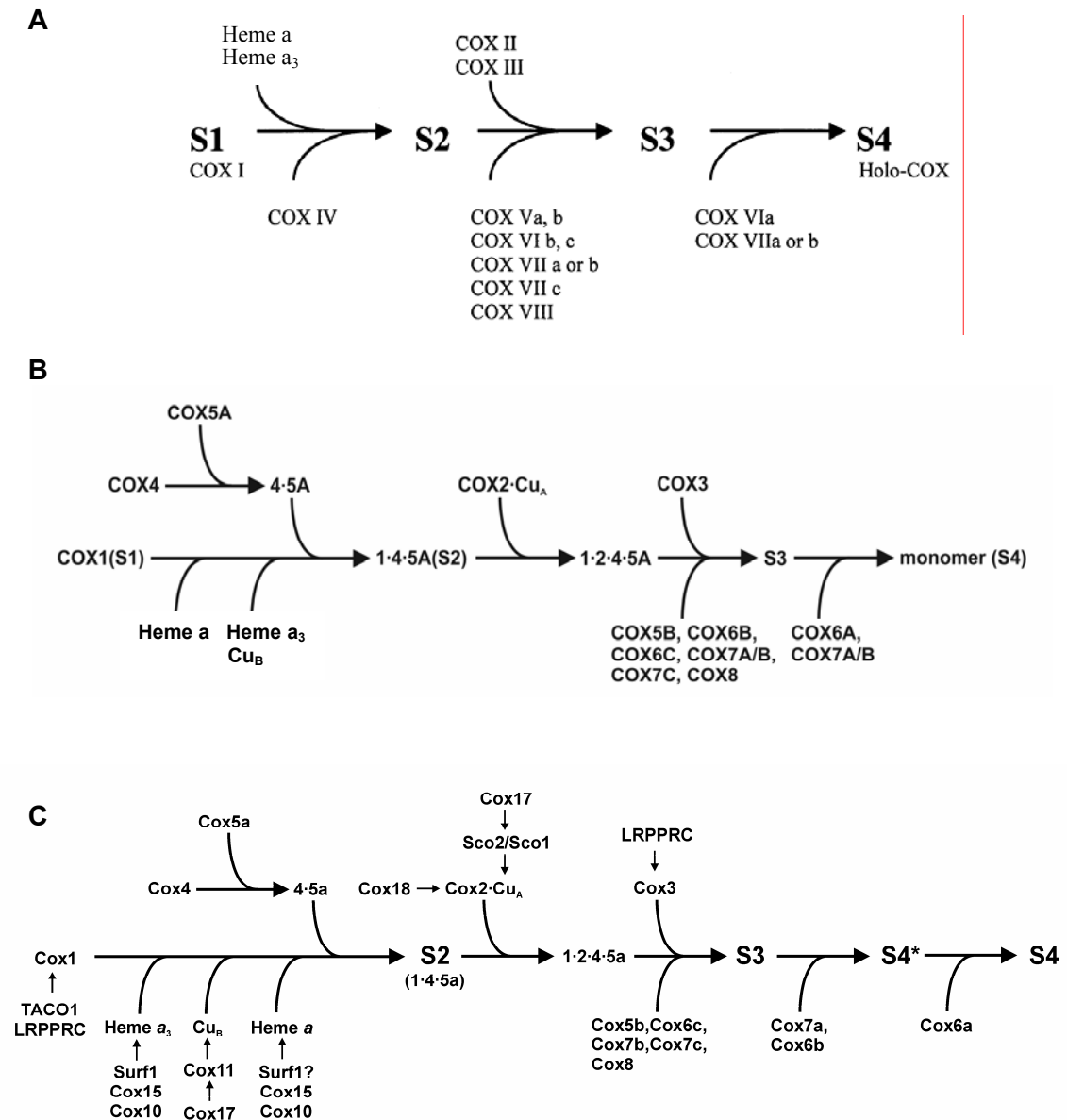


Figure 4 Models of the mammalian CcO assembly pathway according to Nijtmans *et al.* (1998) (A), Stiburek *et al.* (2005) (B) and Fornuskova *et al.* (2010) (C). Prosthetic groups and assembly factors are indicated. Roman (A) or Arabic (B, C) numerals denote CcO subunits within subcomplexes. S2 and S3 indicate assembly intermediates. S4 represents the 13-subunit CcO holoenzyme, and S4* indicates the late assembly intermediate that immediately precedes the formation of the holoenzyme.

3.3.2. Complex V

Complex V, F_1F_0 -ATP synthase or F-type ATPase is multisubunit enzyme nearly ubiquitous in the cell membranes of eubacteria, inner membranes of mitochondria and tylakoid membranes of chloroplasts (Boyer 1998). Under oxidative conditions, ATP synthase is a critically important for synthesis of ATP from ADP and P_i driven by a proton or sodium motive force (Meier *et al.* 2009; Meier *et al.* 2005; Pogoryelov *et al.* 2009; Preiss *et al.* 2010), thereby providing the vast majority of ATP in the cell. Under anaerobic conditions, eubacterial enzymes catalyze the reverse reaction and generate the proton motive force using energy liberated by hydrolysis of ATP produced by fermentation, whereas specific inhibitory mechanisms prevent the chloroplast and mitochondrial enzymes from carrying out the reverse reaction. Inhibition of the ATP hydrolysis activity of F_1 under certain conditions was shown in context of IF1 regulatory polypeptide (ATPase inhibitory factor 1) in mammals and Inh1p, Stf1p and Stf2p in yeast (Hong and Pedersen 2002; Walker 1994).

F_1F_0 -ATP synthase contains an extramembranous cytoplasmic F_1 part ($\alpha_3\beta_3\gamma\delta\epsilon$ in bacteria) and a membrane-embedded F_0 part (ab_2c_{10-12} in bacterial F_1F_0) (Fig. 5A). Both parts are linked by a peripheral and a central stalk. Overall, this large complex has eight different subunits in prokaryotes and 16-18 in mammals (Meyer *et al.* 2007), where the additional subunits are mostly in the stalk region. The central stalk, containing F_1 -subunits γ and ϵ , is associated with a ring of F_0 -subunits c . This central stalk/subunit c assembly constitutes the rotor in the fully assembled ATP synthase. In mitochondria (Fig. 5B), there is an additional subunit in the rotor, which is inconveniently called „ ϵ “ and has no equivalent in bacteria or chloroplasts. The mitochondrial „ δ “ subunit is the equivalent of the bacterial „ ϵ “ (Nakamoto *et al.* 2008). Peripheral stalk extends from the top (membrane distal) region of F_1 , along the external surface of the $\alpha_3\beta_3$ domain, and then reaches down into and across the membrane, where it is associated with subunit a (Walker and Dickson 2006). Its role is to act as stator which connects catalytic $\alpha_3\beta_3$ complex to the transport mediating subunit a . In most bacteria is made up of two copies of the helical b subunits (b_2) and the single δ subunit (the homologue of the bovine OSCP subunit). In some photosynthetic bacteria and chloroplasts, the two b subunits are similar but are the products of two genes (bb') (Nakamoto *et al.* 2008). In the mitochondrial complex, there is only one subunit b with two additional subunits in the peripheral stalk, d and F_6 (known as subunit h in *Saccharomyces cerevisiae* (Rubinstein *et al.* 2005)) and four additional membranous subunits e , f , g and A_6L are associated with subunit a (Dickson *et al.* 2006). Unlike the situation in bovine heart where are subunits e and g tightly bound as the part of monomeric ATP synthase, yeast subunits e and g as well as k were proposed to be a dimer-specific (Arnold *et al.* 1998). Subunit a

(ATP6 gene) and A6L (ATP8) are encoded by mammalian mtDNA, whereas yeast mitochondrial genome codes also for the ATP synthase subunit c, (ATP9).

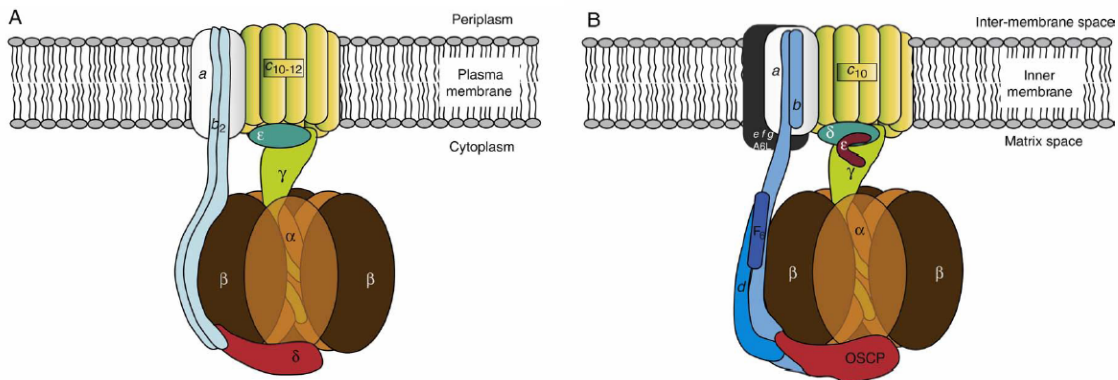


Figure 5 Schematic representation of the bacterial and mitochondrial F_1F_0 -ATP synthases (Kucharczyk *et al.* 2009). The enzyme of *Escherichia coli* (A), with a subunit stoichiometry of $\alpha_3\beta_3\gamma\delta\epsilon ab_2c_{10-12}$, is organized in four subdomains, i.e. the catalytic headpiece ($\alpha_3\beta_3$), the central rotor stalk ($\gamma\epsilon$), the stator stalk ($b_2\delta$), and the proton channel (ac_{10-12}). The human mitochondrial enzyme (B) contains the additional subunit ϵ in the central stalk ($\gamma\delta\epsilon$); the stator stalk is composed of one subunit b, subunits d, F6, f and OSCP; subunit c is present in 10 copies and subunits e and g mediate enzyme dimerization.

The F_1 part contains three catalytic sites, which lie mainly in β -subunits at interfaces with α -subunits. The study of these catalytic sites (Weber and Senior 2000) indicated that F_1 part is effectively a trimeric complex of three α and three β subunits that displays strong negative cooperativity of substrate binding and, at the same time, strong positive cooperativity of enzymatic activity. To explain these unusual properties, Paul Boyer proposed mechanism named as binding change hypothesis (or also alternating site hypothesis) (Boyer 1993). The key feature of this hypothesis is that three interacting catalytic $\alpha\beta$ -protomers are each in a different conformational state at any one time. One binds substrates and products loosely, one binds them tightly and one does not bind them at all. The cyclic nature of the binding change mechanism led Boyer to propose that the binding changes are driven by the rotation of the catalytic assembly ($\alpha_3\beta_3$) with respect to other portions of the F_1F_0 ATPase (Boyer 1993; Boyer 2000). We know now that C-terminal region of the γ -subunit penetrates $\alpha_3\beta_3$ domain in asymmetric manner and as it rotates, it brings about a series of conformational changes given by this asymmetry of the central stalk (Walker and Dickson 2006). Each 360° rotation of the central stalk in a clockwise manner (as viewed from the membrane) inside the F_1 domain generates three ATP molecules, and the rotation of the central stalk proceeds, to a first approximation, in 120° steps. If each c subunit translocates one proton, and if it takes the energy for translocation of three or four protons to synthesize one ATP molecule, then three or four small rotations (each through an angle that depends on the number of c subunits in the ring) are required to drive a 120° rotation of $\gamma\epsilon$ relative to the $\alpha_3\beta_3$ domain. During the rotation of the central stalk, energy is stored transiently,

presumably in an elastic element, and then released in a quantum to drive each 120° step (Beke-Somfai *et al.* 2010; Capaldi and Aggeler 2002; Nakamoto *et al.* 2008; Tsunoda *et al.* 2001). The two most obvious candidates for such elastic element are the α -helical region of the γ -subunit in the central stalk and the peripheral stalk (Walker and Dickson 2006).

In humans, the most common cause of ATPase defects are missense heteroplasmic mtDNA mutations in the ATP6 gene for subunit a, which affect the protonophoric function of ATPase (Hutcheon *et al.* 2001; Stock *et al.* 1999). Higher prevalence show 8993T>G(C) mutations (Ciafaloni *et al.* 1993; Holt *et al.* 1990; Puddu *et al.* 1993; Shoffner *et al.* 1992; Tatuch *et al.* 1994) which change Leu¹⁵⁶ to Arg or Pro. At a lower mutation load, they manifest as neurogenic muscle weakness, ataxia, and retinitis pigmentosa (NARP syndrome); at heteroplasmy exceeding 90% they present as maternally inherited Leigh syndrome (severe and fatal encephalopathy). Less common are 9176T>G(C) mutations, which change Leu²¹⁷ (Carrozzo *et al.* 2001; Dionisi-Vici *et al.* 1998; Thyagarajan *et al.* 1995), or a 8851T>G mutation (De Meirleir *et al.* 1995) that changes Trp¹⁰⁹, all manifesting also as striatal necrosis syndromes (Schon *et al.* 2001). Impairment of the ATPase H⁺ channel results often, but not always, in decreased ATP production, whereas the ATPase hydrolytic activity remains largely unchanged (Houstek *et al.* 1995b; Tatuch and Robinson 1993). Otherwise, a mutation in which A8527G changes the ATPase 6 initiation codon AUG into GUG (Met > Val), has been found in an adult patient with neuropathy, mental retardation, myopathy and retinopathy (Dubot *et al.* 2004). More rarely, ATP synthase dysfunction can be caused by a mutation in the ATP8 gene (Jonckheere *et al.* 2008). A homoplasmic nonsense mutation in overlapping region of ATP6 and ATP8 gene, which results in truncated A6L protein without the last 14 amino acids, has been detected in a 16-year-old patient with hypertrophic cardiomyopathy and neuropathy. A different type of pathogenic mechanism represents mtDNA 2bp microdeletion 9205delTA, which was found in a newborn with transient lactic acidosis (Seneca *et al.* 1996) and also in our patient, a child with encephalopathy and severe psychomotor retardation (Jesina *et al.* 2004). A 9205delTA mutation removes the stop codon of the ATP6 gene and affects the cleavage site between the ATP6 and COX3 transcripts.

Our study on fibroblasts with primary defects in mitochondrial ATP synthase due to heteroplasmic mtDNA mutations in the ATP6 gene, affecting protonophoric function or synthesis of subunit a, show that at high mutation loads, mitochondrial membrane potential $\Delta\Psi_m$ at state 4 is normal, but ADP-induced discharge of $\Delta\Psi_m$ is impaired and ATP synthesis at state 3-ADP is decreased. Increased $\Delta\Psi_m$ and low ATP synthesis is also found when the ATPase content is diminished by altered biogenesis of the enzyme complex. Irrespective of the different pathogenic mechanisms, elevated $\Delta\Psi_m$ in primary

ATPase disorders could increase mitochondrial production of ROS and decrease an energy provision (Vojtiskova *et al.* 2004).

A distinct group of inborn defects of ATP synthase is represented by the enzyme deficiency due to nuclear genome mutations which are very rare and characterized by a selective inhibition of ATP synthase biogenesis. ATPase deficiency of possible nonmitochondrial origin was first described in a child with 3-methylglutaconic aciduria and severe lactic acidosis (Holme *et al.* 1992). Extremely low ATPase activity and low, tightly coupled respiration rates were observed in muscle mitochondria, but no mutation was found in mtDNA genes encoding ATPase subunits. A nuclear origin of ATP synthase deficiency was demonstrated for the first time in 1999 (Houstek *et al.* 1999) in a new type of fatal mitochondrial disorder: a child with severe lactic acidosis, cardiomegaly, and hepatomegaly died 2 days after birth. 70 to 80% decrease in ATPase activity and ATP production was associated with a corresponding selective decrease in the ATPase complex, which had normal size and subunit composition. Increased biosynthesis of the β subunit with a very short half-life contrasted with decreased biosynthesis of the assembled ATPase and indicated assembly defect at the level of F₁-ATPase. Cybrid cells made of patient fibroblasts fully complemented the ATPase defect and confirmed the nuclear origin of impaired biogenesis of the enzyme complex (Houstek *et al.* 1999). In 2004, the search for the disease-causing gene resulted in the identification of a homozygous missense mutation in the third exon of the ATP12 (ATPAF2) gene which replaced tryptophan 94 with arginine. The mutation was found in a patient with severe encephalopathy and it was confirmed that the primary defect was in the assembly of the F₁ catalytic part of ATP synthase (De Meirleir *et al.* 2004). In 2008, the expression profiling and homozygosity mapping identified a mutation in the second intron of TMEM70 encoding a 30kDa mitochondrial protein of unknown function. The mutation leading to aberrant splicing and loss of *TMEM70* transcript was found in 24 patients (Cizkova *et al.* 2008). This protein turned out to be a novel ancillary factor of ATP synthase biogenesis, interestingly, the first one specific for higher eukaryotes. The first case of a mitochondrial disease due to a mutation in a nuclear encoded structural subunit of ATP synthase was described most recently. Missense mutation in ATP5E gene coding for ϵ subunit replaced tyrosine 12 with cysteine in patient with neonatal onset, lactic acidosis, 3-methylglutaconic aciduria, mild mental retardation and developed peripheral neuropathy (Mayr *et al.* 2010).

3.3.3. Transporters of ATP synthase substrates

The net efflux of phosphate across the inner mitochondrial membrane occurs to a great extent as γ -phosphate of ATP via the adenine nucleotide carrier, which catalyses efflux of ATP in exchange for ADP. Moreover, ADP as well as inorganic phosphate

(Pi) must be transported into the mitochondrial matrix to be utilized for oxidative phosphorylation.

3.3.3.1. Transport of ADP

The protein, which mediates link between the mitochondrial and cytosolic compartments of all aerobic eukaryotic cells by catalysis of the transmembrane exchange between ATP from oxidative phosphorylation generated inside mitochondria and cytosolic ADP, is ADP/ATP carrier (AAC) or translocase. The popular term adenine nucleotide transporter (ANT) is misleading since this term also implies transport of AMP which is explicitly excluded by the AAC (Klingenberg 2008). The transported substrates are large, hydrophilic, highly charged molecules, averse to low dielectric membrane environment, thus their transport through biomembranes requires a carrier with highly efficient catalytic qualities. Paradoxically to this point, transport by AAC requires adenine nucleotides with their full charge as ATP^{4-} and ADP^{3-} and the less charged AMP is excluded from both uptake and efflux. dADP and dATP are transported at 10-15% the rates of their ribose homologues. Concerning the base moiety, a stringent specificity for adenine is maintained, excluding most other bases (Duce and Vignais 1969; Pfaff and Klingenberg 1968). With AAC reconstituted vesicles, also a 1:1 exchange of pyrophosphate (PPi) against ADP was characterized (Kramer and Klingenberg 1985). Although a fractional charge, corresponding to a partial ADP^{3-} - ATP^{3-} transport cannot be ruled out and may serve to adjust the energy share used in the exchange in dependence on $\Delta\psi$ and ΔpH , various studies substantiate a fully electric ATP^{4-} - ADP^{3-} exchange (LaNoue *et al.* 1978; Villiers *et al.* 1979; Wulf *et al.* 1978). Under *in vivo* conditions, ADP and ATP are offered simultaneously at varying proportions. In the energized state, ATP is released preferably to ADP but in the uncoupled state ADP leaves the mitochondria more rapidly than ATP (Klingenberg 1980), although equal rates should be expected, just as observed for uptake (Klingenberg 2008). This can be explained by considering that in the mitochondria the nucleotides are present mostly as the Mg^{2+} complexes which are not transported and thus the concentration of free ATP which binds Mg^{2+} about 5-times tighter than ADP (Heldt *et al.* 1972) is decreased more than of ADP (Klingenberg 2008). Without membrane potential the AAC can catalyze the four exchange combinations of ADP and ATP, two homoexchange modes (ATP-ATP, ADP-ADP) and two heteroexchange modes (ATP-ADP, ADP-ATP) at nearly equal rates. Only the ADP-ATP mode (ADP uptake, ATP release) is productive for the ATP delivery whereas the ATP-ADP mode is counter-productive. The homo-modes are diverting exchange capacity. The membrane potential skews this distribution in favor of the ADP-ATP mode and suppresses the ATP-ADP mode (Klingenberg 2008). The central role of the AAC in oxidative

metabolism requires high expression levels in most eukaryotic cells exceeding other transporters.

The amino acid sequence of the AAC was first established in the bovine heart (Aquila *et al.* 1982). The sequence comprising 297 amino acids is likely to be segmented into three similar domains, each featuring two helices with a total of six transmembrane helices (Saraste and Walker 1982). It closely resembles the typical structure of members of the mitochondrial carrier protein family. The striking sequence RRRMMM regarded as an AAC signature was present in all forthcoming AAC sequences, such as of *Neurospora crassa* (Arends and Sebald 1984) and *Saccharomyces cerevisiae* (Adrian *et al.* 1986). By using cross-linking and analytical ultracentrifuge techniques it was shown that the AAC as well as the mitochondrial uncoupling protein, at least in the solubilized state, forms a homodimer (Hackenberg and Klingenberg 1980; Lin *et al.* 1980). A dimer state of yeast yAAC2 was demonstrated using native gel electrophoresis of mitochondria (Ryan *et al.* 1999).

First in yeast and then in other organisms, particularly in mammals, genes of AAC isoform were identified. *Saccharomyces cerevisiae* contains three genes (AAC1, AAC2 also known as PET9, AAC3) for AAC isoforms. yAAC2 is the principal AAC in aerobic yeast. The study of involved promoters and transcription factors showed the N-terminal extension of yAAC2 which is instrumental for the high expression level (Betina *et al.* 1995). yAAC1 is barely expressed (Lawson *et al.* 1990). yAAC3 is obligatory for anaerobic growth (Drgon *et al.* 1991; Kolarov *et al.* 1990) and is suggested to act in reversed order, supplying ATP from glycolysis to the mitochondria. Notably, in the obligate aerob *Neurospora crassa* only one ncAAC gene has been found (Arends and Sebald 1984). In man as well as in cow, four tissue-specific isoforms were described. h- and bAAC1 is predominantly expressed in skeletal and cardiac muscles (Stepien *et al.* 1992). hAAC2 expression is strongly stimulated by growth factor in fibroblasts (Ku *et al.* 1990) and also increased in neoplastic cells (Torrioni *et al.* 1990) as well in early myoblasts (Stepien *et al.* 1992) indicating that this isoform is related to enhanced glycolysis in the proliferating cells and has the role of supplying glycolytic ATP into the mitochondria, similarly as suggested for yAAC3 in yeast. At very low level, hAAC3 is expressed in brain, liver, kidney, heart and skeletal muscle (Stepien *et al.* 1992) and hAAC4 in liver and testis, marginally in brain (Dolce *et al.* 2005). Overall, the sequence differences in AAC isoforms are small, as compared to those in the yeast, retaining about 85% identity, with the exception of h- and bAAC4 with only 66-68% identity to the other isoforms (Dolce *et al.* 2005).

Mutations in hAAC1 gene (SLC25A4) have been shown predominantly to result in autosomal dominant progressive external ophthalmoplegia and familial hypertrophic cardiomyopathy. Kaukonen *et al.* (2000) identified a missense mutation in the AAC1

gene (A114P) in 5 families with autosomal dominant progressive external ophthalmoplegia (PEOA2). The analogous mutation in yeast caused a respiratory defect. The authors also identified mutations in the AAC1 gene (V289M) in a sporadic case of PEO (Kaukonen *et al.* 2000). Chen (2002) determined that the A128P mutation of the *Saccharomyces cerevisiae* yAAC2 protein, equivalent to A114P in human AAC1, does not always affect respiratory growth. Rather, expression of A128P resulted in depolarization, structural swelling, disintegration of mitochondria and ultimately an arrest of cell growth in a dominant-negative manner. The author proposed that the A128P mutation may induce an unregulated channel, allowing free passage of solutes across the inner membrane, rather than interfere specifically with ATP/ADP exchange (Chen 2002). Fontanesi *et al.* (2004) introduced dominant-acting missense mutations associated with PEO into yAAC2, the yeast ortholog of human AAC1. Expression of the equivalent mutations in aac2-defective haploid strains of *Saccharomyces cerevisiae* resulted in a marked growth defect on nonfermentable carbon sources and a concurrent reduction of the amount of mitochondrial cytochromes, cytochrome c oxidase activity and cellular respiration. The AAC2 pathogenic mutants showed a significant defect in ADP versus ATP transport compared with wildtype AAC2. The aac2 mutant alleles were also inserted in combination with the endogenous wildtype AAC2 gene. The heteroallelic strains behaved as recessive for oxidative growth and petite-negative phenotype. In contrast, reduction in cytochrome content and increased mtDNA instability appeared to behave as dominant traits in heteroallelic strains (Fontanesi *et al.* 2004). Palmieri *et al.* (2005) first reported a recessive mutation in the AAC1 gene in a sporadic patient who presented with hypertrophic cardiomyopathy, exercise intolerance and lactic acidosis but without ophthalmoplegia. A muscle biopsy showed numerous ragged-red fibers and Southern blot analysis disclosed multiple mtDNA deletions. Homozygous mutation 368C>A in AAC1 gene converting a highly conserved alanine into an aspartic acid at codon 123 was found. The equivalent mutation in AAC2, the yeast ortholog of human AAC1, resulted in a complete loss of transport activity and in the inability to rescue the severe OXPHOS phenotype displayed by WB-12, an AAC1/AAC2 defective strain. Interestingly, exposure to ROS scavengers dramatically increased the viability of the WB-12 transformant, suggesting that increased redox stress is involved in the pathogenesis of the disease (Palmieri *et al.* 2005).

In mouse, two AAC isoforms, mAAC1 and mAAC2, were described (Levy *et al.* 2000). A knockout of heart/muscle specific isoform (mAAC1) (Graham *et al.* 1997) revealed ragged-red fibers in skeletal muscle and cardiac hypertrophy accompanied by dramatic proliferation of mitochondria. In mutant adults, a lactic acidosis and severe exercise intolerance were observed. Muscle specific AAC1 isoform with low expression in myoblasts, is settled to be predominantly expressed by muscle development (Stepien

et al. 1992). Surprisingly, the absence of mAAC1 in knockout mouse was not compensated by an increase in the other AAC isoform. Interestingly, comparable observations were characterized in context of cytochrome c oxidase isoforms of structural subunit Cox6a. Liver-type subunit Cox6a (Cox6a1/Cox6aL) is found in all non-muscle tissues, whereas heart/muscle-type subunit Cox6a (Cox6a2/Cox6aH), encoded by a different gene, is expressed only in striated muscles (Schlerf *et al.* 1988). Mature Cox6a1 and Cox6a2 subunits share lower intra-species (approx. 60%) than inter-species (80–88%) amino acid sequence identity in humans, rats and cows (Fabrizi *et al.* 1992). The tissue-specific pattern of these isoforms is also (similarly to AAC isoforms) established during tissue differentiation (Bonne *et al.* 1993; Kim *et al.* 1995; Taanman *et al.* 1992). A switch from COX6A1 to COX6A2 isoforms was described to occur during mammalian postnatal development in skeletal muscle and heart as well as during differentiation of myogenic cells *in vitro*, and is assumed to be essential for normal function of tissues with high aerobic metabolic demands (Kim *et al.* 1995; Taanman *et al.* 1992). In the heart of mice lacking the COX6A2 gene, the content of CcO comprising Cox6a1 appeared to be unchanged; in other words, without apparent compensation by induction of the expression of subunit Cox6a1 in the knockout heart (Radford *et al.* 2002). In our study (Fornuskova *et al.* 2010), used HEK-293 cells are derived from embryonic kidney tissue, which is specific by almost exclusive (both prenatal and postnatal) expression of the COX6A1 isoform (Bonne *et al.* 1993; Kim *et al.* 1995; Taanman *et al.* 1992). Indeed, the vast majority of the *COX6A* transcripts in HEK-293 cells is represented by the *COX6A1* isoform. Similar to the results from mCOX6A2-KO and mAAC1-KO, the decrease in the major isoform in our COX6A1-KD cells was not accompanied by up-regulation of the minor isoform (COX6A2). However, ectopic expression of Cox6a2 in COX6A1-KD cells tends to complement the CcO defect (Fornuskova *et al.* 2010). It appears that the mechanisms responsible for maintenance of tissue-specific patterns of COX6A as well as AAC isoforms cannot react in response to actual cellular state. In contrast, it is also possible that the pronounced biochemical defect still did not provoke sufficient physiological impairment, which would otherwise trigger the expression of the minor subunit.

3.3.3.2. Transport of Pi

A smaller fraction of phosphate may be transported by the dicarboxylate carrier, which catalyzes a Pi/dicarboxylate or Pi/Pi exchange (Wohlrab 1986). Furthermore, the protein, which is mainly responsible for phosphate transport, is the mitochondrial phosphate carrier (PIC) also named as phosphate transport protein (PTP) (Fig. 3). Three different modes of PIC action were elucidated. Homologous phosphate/phosphate (Pi^-/Pi^-) antiport, heterologous phosphate/hydroxyl (Pi^-/OH^-) antiport or phosphate/proton

(Pi^-/H^+) symport represents the physiological transport mode of unidirectional phosphate uptake. In the functionally active catalytic complex, two binding sites have to be simultaneously occupied in the transport cycle thus forming a ternary complex. The lack of any dependence on the electrical potential confirmed the electroneutrality of the transport reaction (Wohlrab 1986), which is, however, dependent on the membrane pH gradient as driving force of the mitochondrial phosphate carrier (Wohlrab and Flowers 1982). Kinetic modeling of the pH dependence of the unidirectional phosphate transport reaction favors the Pi^-/OH^- antiport rather than Pi^-/H^+ symport (Stappen and Kramer 1994). In addition to the physiological transport mode, PIC can undergo a functional shift from coupled antiport to uncoupled uniport after modification of cysteine residues by mercurial reagents (Stappen and Kramer 1993). A similar shift has been observed for the ATP/ADP and the carnitine carrier from mitochondria (Kramer 1998).

The amino acid sequence of the phosphate carrier from several species including bovine (Runswick *et al.* 1987) or human (Dolce *et al.* 1991) heart and yeast (Phelps *et al.* 1991) has been determined. It closely resembles the typical structure of members of the mitochondrial carrier protein family with subunits of six transmembrane segments and a molecular mass of ~32 kDa (Aquila *et al.* 1985; Kuan *et al.* 1995). Similarly to many mitochondrial transport proteins (Wohlrab 2009; Wohlrab 2010), PIC appears to function as homodimer (Phelps and Wohlrab 2004; Schroers *et al.* 1998; Wohlrab 2004). Among the family members, the mammalian, but not the yeast, PIC is exceptional in having a processed N-terminal sequence that helps to target the protein into mitochondria (Zara *et al.* 1992). Only one gene for the PIC has been detected in human (SLC25A3) and cow (Dolce *et al.* 1994), in both, with two closely related exons named 3A and 3B which appear to be alternatively spliced (Dolce *et al.* 1994). At transcript and protein levels, two PIC isoforms (A and B) has been demonstrated. PIC-A is present only in heart and skeletal muscles, whereas PIC-B is ubiquitous (Fiermonte *et al.* 1998). The recombinant, reconstituted isoforms exhibit similar substrate specificity and inhibitor sensitivity, but they differ in kinetic parameters.

Mayr *et al.* (2007) described the first patients with mitochondrial phosphate carrier deficiency caused by a homozygous mutation in the SLC25A3 gene, i. e. 215G>A transition in alternatively spliced exon 3A, resulting in an amino acid substitution of Gly⁷² to Glu. Two siblings showed lactic acidosis, hypertrophic cardiomyopathy, and muscular hypotonia and died within the first year of life. Functional investigation of intact mitochondria showed a deficiency of ATP syntase in muscle but not in fibroblasts, which correlated with the tissue-specific expression of exon 3A in muscle versus exon 3B in fibroblasts (Mayr *et al.* 2007).

3.4. Organization of OXPHOS, functional and structural relevance

The molar ratios of the respiratory components of mitochondria from different species as well as from different organs of the same species vary significantly (Lenaz and Genova 2007). These different stoichiometries could reflect the adaptability of the tissues to a variable energy demand. In bovine heart, the main components of OXPHOS best fit unit stoichiometry of 1 complex I : 1.3 complex II : 3 complex III : 6.7 complex IV (Schagger and Pfeiffer 2001). For each complex IV are 0.5 unit of ATP synthase and 3-5 units of the ADP/ATP translocase (Capaldi 1982). The amount of CoQ is in considerable molar excess to complex III and CytC is usually in slight molar excess to complex IV (Lenaz and Genova 2009).

3.4.1. Random diffusion vs. solid-state assembly of electron transfer enzymes

In the prevalent view, the large enzymatic complexes are randomly distributed in the lipid bilayer of the inner membrane and functionally connected by lateral diffusion of small redox molecules, i. e., coenzyme Q and cytochrome c. All these components undergo independent lateral diffusion in the plane of the membrane, however, diffusion rates of mobile electron carriers are faster than those of the bulkier macromolecular complexes. The diffusion-coupled collision frequencies may be either higher or lower than any given reaction step within the complexes, and consequently electron transfer would be either reaction limited or diffusion limited. Such a random liquid-state organization is usually referred as fluid mosaic model, random diffusion model or random collision model of electron transfer (Lenaz and Genova 2007; Lenaz and Genova 2009) and was essentially based on the isolation of functional individual complexes (Hatefi 1985), on the failure of electron microscopic and liposomal fusion studies to identify associations of complexes (Capaldi 1982), and on the pool behavior of CoQ and CytC in bovine mitochondria (Gupte and Hackenbrock 1988; Kroger and Klingenberg 1973).

Alternatively, the components of the chain form aggregates ranging from small clusters of few complexes to the extreme of a solid-state assembly. The aggregates may be either permanent or transient, but their duration in time must be larger than any electron transfer turnover to show kinetic differences from the previous model (Lenaz and Genova 2007; Lenaz and Genova 2009). The evidence that the respiratory chain complexes are associated to form specific stoichiometric supramolecular units with well defined structure provided the electrophoretic analyses by both BN-PAGE and colorless native PAGE (CN-PAGE) supporting the idea of highly ordered associations of the respiratory supercomplexes and discarding most doubts on artificial interactions. The interactions may be species- or kingdom- specific (Schagger and Pfeiffer 2000; Vonck

and Schafer 2009) presumably within the plane of the membrane, whereas the matrix-exposed protein domains are in close vicinity but probably do not substantially interact (Dudkina *et al.* 2005).

In bovine heart mitochondria, complexes I-III interactions were apparent from the presence of about 17% of total complex I in the form of I₁III₂ supercomplex that was found further assembled into two major supercomplexes (respirasomes) comprising different copy numbers of complex IV (I₁III₂IV₁ and I₁III₂IV₂ contain 54% and 9% of total complex I, respectively). Only 14-16% of total complex I, 40-42% of complex III and majority of complex IV (>85%) was found in free form in the presence of digitonin (Schagger and Pfeiffer 2001). Associations of complex II with other complexes of the OXPHOS system could not be identified under the conditions of BN-PAGE (Lenaz and Genova 2009). However, Acin-Perez and colleagues demonstrated recently that some of the previously identified mammalian supercomplexes contain also complex II, and complex V, as well as electron carriers CoQ and CytC (Acin-Perez *et al.* 2008).

In *Saccharomyces cerevisiae*, complex I is absent and replaced by three NADH dehydrogenases. Compared to bovine heart mitochondria, yeast complex IV does not occur significantly in free form. It is quantitatively associated with complex III, and the amount of the supercomplexes formed depends on the amount of complex IV available at different growth conditions. The amount of supercomplexes seems to reflect the demand of the cell for energy supply via the OXPHOS system (Schagger and Pfeiffer 2000). Stable supercomplexes of complexes III and IV were isolated also from several bacteria, e. g. from *Paracoccus denitrificans* (Berry and Trumpower 1985), the thermophilic *Bacillus* PS3 (Sone *et al.* 1987), the thermoacidophilic archaeon *Sulfolobus* sp. strain 7 (Iwasaki *et al.* 1995a; Iwasaki *et al.* 1995b) and *Corynebacterium glutamicum* (Niebisch and Bott 2003).

Supercomplexes are stabilized by cardiolipin (Claypool *et al.* 2008; McKenzie *et al.* 2006; Pfeiffer *et al.* 2003), an anionic phospholipid consisting of two phosphatidyl residues that are linked by a glycerol moiety (Lecocq and Ballou 1964; Macfarlane 1964). Cardiolipin is exclusively found in bacterial and mitochondrial membranes, which are designed to generate an electrochemical potential for substrate transport and ATP synthesis (Schlame *et al.* 2000). It is buried within the protein complexes having important structural and catalytic role (Lange *et al.* 2001; Sedlak and Robinson 1999).

Although, from a structural point of view, little doubt exists that respiratory chain complexes are organized, at least in part, as supramolecular aggregates, characterization of the supercomplexes by biochemical functional analysis is still poor. The close proximity of the enzymes catalyzing consecutive reactions enables increased metabolic flow in the pathway by ensuring the substrate channeling of quinones and/or CytC and sequestration of reactive intermediates like ubisemiquinone, which can react with

oxygen to generate superoxide anion radical (Grivennikova and Vinogradov 2006; Schagger and Pfeiffer 2000). Kinetic testing using metabolic flux control analysis (see Chapter 3.4.3) can discriminate whether the enzyme complexes are independently embedded in the lipid bilayer of the inner membrane and connected by randomly diffusing mobile electron carriers or functions as the part of multicomplex units with direct electron channeling between complexes. The former model implies that each enzyme may be rate-controlling to a different extent, whereas in the latter, the whole metabolic pathway would behave as a single supercomplex and inhibition of any one of its components would elicit the same flux control. In bovine heart mitochondria particles and submitochondrial particles, both complexes I and III were found to be highly rate-controlling over NADH oxidation, a strong kinetic evidence suggesting the existence of functionally relevant association between the two complexes, whereas complex IV appears randomly distributed, indicating that electron transfer occurs via a random pool of CytC molecules. Moreover, complex II is fully rate-limiting for succinate oxidation, clearly indicating the absence of substrate channeling toward complexes III and IV (Bianchi *et al.* 2004). The presence of a large excess of free complex IV (Schagger and Pfeiffer 2001) is in line with this conclusion, however, this fact also prevents, using this approach, to exclude substrate channeling within those complex IV units that are bound in a respirasome. Interestingly, in yeast, where the majority of complexes III and IV is associated in form of III-IV supercomplex, overall quinol oxidase rate (rate of complexes III-IV) was significantly decreased after DDM treatment of digitonin-solubilized yeast mitochondria. Indeed, the decrease in quinol oxidase activity was observed in the same range of DDM as dissociation of supercomplexes III-IV was detected by BN-PAGE (Schagger and Pfeiffer 2000). Taken together, substrate channeling of electrons in bovine heart mitochondria, which was confirmed between complexes I and III, may occur also between complexes III and IV but is not required for electron transfer (Genova *et al.* 2008).

In addition, the supercomplex assembly appears to play role in structural stabilization of individual complexes. Analysis of the structural integrity of human respirasomes in patients with defined defects of individual respiratory chain complexes (Schagger *et al.* 2004) provided evidence that a loss of complex III prevented respirasome formation and led to secondary loss of complex I, therefore primary complex III assembly deficiencies presented as combined complex III/I defects. Conversely, absence of complex I did not influence stability of complex III. Also several other studies in mutants and patients suggested that complex III is involved in the assembly and stabilization of complex I (Acin-Perez *et al.* 2004; Blakely *et al.* 2005; Stroh *et al.* 2004). Moreover, Marques *et al.* (2007) studied biogenesis of complex I in *Neurospora crassa* using a collection of deletion mutants that can survive for the

presence of alternative NADH dehydrogenases. They found that the biogenesis of complex I is obligatorily linked with its assembly in supercomplexes. Furthermore, complex I of *nuo51* mutant, that lacks the NADH-binding 51kDa subunit and is enzymatically inactive, is assembled into supercomplexes like those found in wild-type mitochondria, showing that a major function of supercomplex organization might be non-catalytic, but rather to direct assembly of the respiratory complexes (Marques *et al.* 2007).

Regarding structural relevance of complex IV for stability of complex I, the recent evidence is not so straightforward. In the study of Schagger *et al.* (2004), complex IV deficiency led to normal steady-state levels of complexes I and III (Schagger *et al.* 2004). However, similar authors observed reduced stability of complex I under the conditions of BN-PAGE and substantial decrease in NADH-ubiquinone oxidoreductase activity in the mutant strain of *Paracoccus denitrificans* lacking complex IV (Stroh *et al.* 2004). Similarly, the total loss of CcO in a mouse COX10-knockout model (Diaz *et al.* 2006) as well as substantial decrease of CcO due to RNAi KD of Cox4 in murine cultured cells (Li *et al.* 2007) resulted in decreased stability and activity of complex I. Nevertheless, the knockdown of Cox4 and Cox5a in *Caenorhabditis elegans* led to enzymatic defect of complex I with otherwise normal amount of the assembled complex (Suthammarak *et al.* 2009). In contrast, the CcO deficiency in our COX4-, COX5A- and COX6A-KD cells did not lead to any significant changes in the amount and/or activity of other OXPHOS complexes, including complex I (Fornuskova *et al.* 2010). Similarly, normal levels and activity of complex I were also found in murine COX5BKD cells with severe CcO deficiency (Galati *et al.* 2009).

Another aspect of supercomplex assembly concerns at what stage of biogenesis of respiratory complexes are the supercomplexes organized. In four *Neurospora crassa* deletion mutants of complex I membrane arm subunits *nuo9.8*, *nuo11.5* and *nuo20.8*, 2D BN-SDS immunoblots of digitonin-solubilized mitochondria detected that subcomplexes of peripheral arm containing at least the 30.4kDa subunit and accumulating in these samples comigrate with III/IV supercomplexes and/or the prohibitin complex, thus pointing to them as putative candidates for interaction partners (Marques *et al.* 2007). In another study, Mick *et al.* (2007) investigated the role of Shy1, the yeast homolog of human Surf1, in the assembly of complex IV from *Saccharomyces cerevisiae* by analyzing the nature of intermediate subcomplexes by gel electrophoresis. They found that complex IV associates with complex III already in the form of incomplete subcomplexes, and that some of the late assembled subunits are probably added directly to the III/IV supercomplex (Mick *et al.* 2007). An example of such a subunit is Cox13, the yeast homologue of human Cox6a (Brandner *et al.* 2005). We performed BN/PAGE immunoblots in our CcO deficient samples with

knockdown of selected structural CcO subunits, including subunit Cox6a. In all samples, including controls, additional spots that migrated at the level of supercomplexes in the first dimension, but with apparent molecular masses lower than that of the CcO holoenzyme were detected. These spots were most apparent in COX5A-KD mitochondria, which exhibited the most severe CcO holoenzyme defect and the highest accumulation of incomplete CcO assemblies (Fornuskova *et al.* 2010). Although we cannot exclude the removal of some of the peripheral subunits because of detergent treatment, these spots might represent incomplete CcO assemblies that are already present in supercomplexes. Collectively, subcomplexes resulting from pathological conditions as well as those accumulating in the mitochondria under physiological conditions seem to be capable, at least to some extent, to assemble into supercomplexes.

3.4.2. Supramolecular organization of ATP synthase and pleiotropic effects of its dysfunction

While prokaryotic ATP synthase is thought to occur exclusively as a monomer, mitochondrial ATP synthase adopts supramolecular structures that have been found in a large range of organisms. Originally, ATP synthases arrangements were observed by electron microscopy of deep-etched *Paramecium* mitochondria as a double row of particles, which form a zipper-like array along the outer curved margin of the helically shaped tubular cristae (Allen *et al.* 1989), however, the same approach failed to reveal a similar arrangement in mammalian specimens (Allen *et al.* 1989). Therefore, it was unclear whether or not the dimer ribbons were a special feature of ciliate mitochondria. Ten years later, rows of F₁ parts were also seen by cryo-electron tomography of *Neurospora crassa* mitochondria (Nicastro *et al.* 2000) and then by atomic force microscopy in yeast (Buzhynskyy *et al.* 2007) and by cryo-tomography in rat and bovine mitochondria (Strauss *et al.* 2008) indicating that the ribbons of ATP synthase dimers are rather common to all eukaryotes. Furthermore, dimeric and occasionally higher oligomeric forms of ATP synthase were isolated with high yield by native gel electrophoresis after mild detergent treatment of mitochondrial membranes, first in yeast (Arnold *et al.* 1998) and later in mammalian (Schagger and Pfeiffer 2000) and plant (Eubel *et al.* 2003) mitochondria. A gentle separation by CN-PAGE, without the use of Coomassie stain, promotes the retention of even-numbered oligomers like tetramers, hexamers and octamers suggesting that oligomeric ATP synthase is formed from dimeric building blocks (Wittig and Schagger 2005). A higher digitonin/protein ratio, used for membrane solubilization, induces breakdown of the oligomers into dimers and monomers.

Association between the two ATP synthases in a dimer occurs via the F_o parts which are linked together so that the dimer adopts a V-like structure. The dimer ribbons

seem to assemble from two dimer types assigned as “true dimer” and “pseudo dimer” (Dudkina *et al.* 2006). The former appears to be characterized by large angle (70-90°) between the ATP synthase monomers across both rows and the latter is characteristic by rather small angle (20-35°) made up of neighbors within a row (Vonck and Schafer 2009; Wittig and Schagger 2009). In *Saccharomyces cerevisiae*, it has been shown that subunits e and g that are not involved in the ATPase or ATP synthase activity are essential actors for dimerization (Arnold *et al.* 1998) and oligomerization (Fronzes *et al.* 2006). Both subunits are F_o components with a single transmembrane span (Belogrudov *et al.* 1996). Other components such as subunit 4, the homologous subunit to the b-subunit of beef ATP synthase, and other proteins of the peripheral stalk are involved *in vivo* in the interactions between monomers (Fronzes *et al.* 2006; Gavin *et al.* 2005; Wittig and Schagger 2008).

Deletion mutants of e and g not only lacked ATP synthase dimers but also had altered inner membrane morphology with the inner membranes forming onion-like structures. Thus, the association of ATP synthase dimers was strongly suggested to be involved in the control of the biogenesis of the inner mitochondrial membrane (Giraud *et al.* 2002; Paumard *et al.* 2002). Strauss *et al.* (2008) further characterized in bovine and rat mitochondria, that the dimer ribbons are associated with a sharp bend (~ 60°) in the lipid bilayer implying that the ATP synthase arrays are a key factor in shaping cristae morphology (Strauss *et al.* 2008). Cristae are perhaps the most notable ultrastructural feature of active mitochondria. Numerical simulation indicates that, although the electrochemical potential must be the same along the entire inner membrane surface under equilibrium conditions, the local pH gradient, and hence the ΔpH contribution to the proton motive force is significantly higher in regions of high membrane curvature (Strauss *et al.* 2008). As the ΔpH contribution seems to be more effective than $\Delta\Psi$ in driving ATP synthesis (Kaim and Dimroth 1999), this would suggest that a position of the ATP synthase at the apex of mitochondrial cristae is optimal for ATP production.

ATP synthase is fundamentally dependent on the phosphate (PIC) and adenine nucleotide (AAC) carriers (Kaplan 2001), which are responsible for transport of Pi and ADP, the substrates for ATP synthesis, to the mitochondrial matrix (see Chapter 3.3.3). Each carrier consists of a single polypeptide chain in dimeric form and both were found to sub-fractionate under the mild conditions in complex with ATP synthase as ATP synthase/PIC/AAC supercomplex of 1:1:1 stoichiometry named also as “ATP synthasome” (Ko *et al.* 2003). A likely location of PIC and AAC is adjacent to one another and although they are near the more centrally located subunit c ring of ATP synthase F_o part, do not overlap with it (Chen *et al.* 2004).

In some yeast mutants of complex V subunits, combined deficiencies in complexes IV and V were found. The complex IV was affected more than the other respiratory enzymes in strains with mutation in ATP4 (Paul *et al.* 1989), ATP6 (Choo *et al.* 1985), ATP8 (Marzuki *et al.* 1989), ATP9 (Hadikusumo *et al.* 1988) or ATP17 (Spannagel *et al.* 1997), however, high level of petite production, i. e. cells bearing large deletions in the mtDNA or totally lacking mtDNA, rendered the interpretation difficult. More recently, Δ atp6 (Rak *et al.* 2007), Δ atp1 and Δ atp2 (Marsy *et al.* 2008) mutant strains with minimal petite production also showed substantial decrease in the accumulation of complex IV. Interestingly, no decrease in complex IV levels was observed in uncoupled complex V mutants of ATP3, ATP16 or ATP15 genes (coding for subunits γ , δ and ϵ , respectively) where maintenance of a mitochondrial potential was found to be severely compromised by massive proton leaks through the F_0 (Duvezin-Caubet *et al.* 2003; Guelin *et al.* 1993; Xiao *et al.* 2000). Therefore, it was hypothesized that reduction of the amount of complex IV would be observed only in complex V mutants unable to dissipate the proton gradient. Indeed, blocking proton translocation in wild-type yeast cells with use of oligomycin also induced a strong quantitative deficit in complex IV, which was reversible when the cells were returned to an oligomycin-free medium (Marsy *et al.* 2008).

In tightly coupled mitochondria, the oxygen consumption rate and ATP synthesis activity depend on each other (Kadenbach 2003). The first mechanism of respiratory control suggest that an uptake of ADP into mitochondria stimulates the ATP synthase, thereby decreasing proton motive force, which in consequence stimulates the activity of the three proton pumps and thus mitochondrial respiration (Nicholls and Ferguson 2002); the proton pumps are inhibited at high membrane potential (150-200 mV). The second mechanism of respiratory control, however, involves allosteric inhibition of cytochrome c oxidase by ATP at high intramitochondrial ATP/ADP ratios (Arnold and Kadenbach 1997; Kadenbach and Arnold 1999) which is suggested to keep *in vivo* the mitochondrial membrane potential at low values (Lee *et al.* 2001), close to optimal values for the synthesis of ATP by the ATP synthase (100-140mV) (Kaim and Dimroth 1999). Thus in the system with minimal or no activity of ATP synthase, low energy provision (low ATP) can presumably stimulate cytochrome c oxidase activity, which in turn increases membrane potential without its dissipation by ATP synthase. At high mitochondrial membrane potentials (>140 mV), an exponential increase of mitochondrial ROS production occurs (Korshunov *et al.* 1997; Liu 1999), which could be prevented by an uncoupler treatment (Houstek *et al.* 2004). High membrane potential across the inner membrane would also hamper import of glycolytic ATP into mitochondria unable to perform oxidative phosphorylation (Brustovetsky *et al.* 1996), since this is an electrogenic reaction exchanging four against three negative charges by

reversal of the ADP/ATP translocase (see Chapter 3.3.3.1). Defective OXPHOS presumably tends to lower the respiratory chain in attempt to prevent either a too high membrane potential or the accumulation of reduced intermediary components of the respiratory chain. In accordance with the second mechanism of respiratory control, the pleiotropic effects of severe complex V deficiency are mainly striking for complex IV.

In human skin fibroblasts from Leigh patients with ATP synthase deficiency due to mtDNA 8993T>C heteroplasmic mutation (>95%) in ATP6 gene, the pleiotropic effects similar to those observed in yeast mutants with ATP synthase deficiency (Rak *et al.* 2007) were absent (Marsy *et al.* 2008). In our study, we investigated impact of mitochondrial tRNA mutations on the amount and stability of OXPHOS in various tissues including skeletal muscle, heart, frontal cortex and liver (Fornuskova *et al.* 2008). In skeletal muscle and heart, the patterns of OXPHOS deficiencies were typical for mutations affecting mt-tRNA^{Leu(UUR)} and mt-tRNA^{Lys} with respect to abundance of respective codons in mitochondrially-translated subunits of OXPHOS, i. e. isolated defect of complex I in the patient with a mutation in mt-tRNA^{Leu(UUR)} and combined severe deficiency of complexes I and IV in patients with mutations in mt-tRNA^{Lys} (complex V was also significantly decreased, albeit less than complexes I and IV). Accordingly, immunoblotting of BN/SDS/PAGE in skeletal muscle of patient with dysfunctional mt-tRNA^{Lys} detected the level of free S1 subcomplex (related to free mtDNA-encoded subunit Cox1 of complex IV with most abundant AAR codons specific for Lys) to be below the detection limit of the method what very likely reflected the limiting character of this subunit in the holoenzyme assembly and clearly demonstrated aberrant CcO assembly due to dysfunction of mt-tRNA^{Lys}. However, in frontal cortex mitochondria of both types (with affected mt-tRNA^{Leu(UUR)} as well as mt-tRNA^{Lys}), the patterns of OXPHOS deficiencies differed substantially from those observed in other tissues, what was particularly striking for ATP synthase. Surprisingly, in the frontal cortex of the patient with mutation in mt-tRNA^{Leu(UUR)}, whose ATP synthase level was below the detection limit, the assembly of complex IV appeared to be hindered by some factor other than the availability of mtDNA-encoded subunits, based on the massive accumulation of all three mitochondrially encoded subunits, either free or partially assembled. Although the Cox1 subunit was shown to be a key regulatory target for CcO reduction in yeast cells (Rak *et al.* 2007), hindered CcO assembly in frontal cortex of our patient (Fornuskova *et al.* 2008) employing other mechanism might be comparable to pleiotropic (presumably protective) effects of very severe ATP synthase deficiencies observed in yeast mutants (Marsy *et al.* 2008; Rak *et al.* 2007).

3.4.3. Tissue-specific physiological diversity of OXPHOS

Mitochondria of various tissues exhibit large diversity in mitochondrial shape and organization with an important variability of organellar section profile, intracellular localization and heterogeneity (Benard *et al.* 2006). Accordingly, the different tissues present with large differences in the composition of the OXPHOS machinery and the organization of mitochondria, which could reflect their variable physiological activity. The tissue specific nature of mitochondria was proposed to contribute to the observed tissue variation in the control of oxidative phosphorylation, which was studied by metabolic flux control analysis (MCA). MCA is usually performed by titrating the whole respiratory chain activity (global flux) and its single steps with inhibitors of the individual complexes thus quantitatively expressing the effect of a perturbation of a step on a flux. It allows determination of control coefficients or threshold curves. The control coefficients are calculated from the measured per cent changes in the enzyme activities upon the addition of a small concentration of specific inhibitors (Groen *et al.* 1982; Rossignol *et al.* 2000). In the case of the threshold curves, each point represents the respiratory rate inhibition percentage as a function of inhibition percentage of the isolated step activity for the same inhibitor concentration. The threshold curves exhibit two types according to their profile (Mazat *et al.* 2000). Type I threshold curves present a large plateau phase followed by a steep breakage allowing a precise determination of the threshold value, whereas in type II, a plateau is no longer apparent and the threshold value is hardly defined. Threshold curve profiles can be explained by an excess of enzyme activity that accounts for the plateau phase of type I threshold curves. Conversely, in the case of no excess of enzyme activity, the isolated step inhibition will have a direct effect on the flux (type II profile), so the threshold curve will no longer have a plateau phase. Type I threshold curves for complexes I and III and type II threshold curves for oxidative phosphorylation network (ATP synthase, AAC, PIC) were observed in mitochondria originated from various rat tissues (muscle, heart, brain, liver and kidney). Complex IV presented the two profiles according to the tissue with a type I in the liver, the brain and the kidney and a type II in the muscle and the heart (Rossignol *et al.* 1999). The authors proposed two tissue groups, each characterized by similar threshold values (determined from threshold curves). The first group included the muscle and the heart and the second group encompassed the kidney and the brain. The liver could be associated to either one or the other of these two groups according to the complex considered. Based on the control coefficient distribution, two slightly different tissue groups were obtained by the same authors (Rossignol *et al.* 2000). The muscle and the heart on the one hand, controlled essentially at the level of the respiratory chain and the liver, the kidney and the brain on the other hand, controlled mainly at the phosphorylation level by ATP synthase and the phosphate carrier. Indeed,

when we studied tissue-specific impact of mt-tRNA mutations with comparable tissue heteroplasmy on OXPHOS deficiency patterns using Western immunoblotting, the observed steady-state levels of OXPHOS complexes suggested that the brain ATP synthase is most sensitive to disturbances of the mitochondrial translational system, however, in the skeletal muscle and the heart, steady-state levels of respiratory chain complexes I (and IV) were most severely affected. In skeletal muscle and heart, the preferential deficiency of complex I and also IV is in line with the particular abundance and distribution of codons for affected mt-tRNAs in mitochondrially-translated subunits of these complexes (Fornuskova *et al.* 2008).

Finally, when the tissue diversity of OXPHOS was considered also based on mitochondrial morphology, overall mitochondrial content, relative and absolute content of respiratory chain complexes II, III and IV, their kinetics and stoichiometry with respective substrate as well as global functioning of the respiratory chain, three groups of tissues were obtained. The first group, skeletal muscle and heart, presented with the highest OXPHOS capacity and a low resistance against the occurrence of respiratory chain perturbation. The second group, liver and kidney, was characterized by a lower OXPHOS capacity and a lower sensitivity to OXPHOS defects. The third group, which contained solely the brain, was between the first and the second group regarding the OXPHOS capacity and flux response (Benard *et al.* 2006).

Taken together, oxidative phosphorylation capacity is highly variable and diverse in tissues. It appears to be determined by different combinations of the mitochondrial content, the amount of respiratory chain complexes and their intrinsic activity. Tissue specificity of these parameters can partly explain the tissue specificity of mitochondrial deficiencies.

4 MATERIAL AND METHODS

4.1. Tissues and cell lines

Human samples for analyses were obtained from patients with mtDNA microdeletion 9205 Δ TA, from three patients harboring two mutations in mt-tRNA^{Lys} (8363G>A and 8344A>G) or one mutation in mt-tRNA^{Leu(UUR)} (3243A>G), as well as from age-related controls. Open muscle biopsies from the tibialis anterior muscle were frozen at -80°C. Post-mortem tissue specimens obtained at autopsy of patients with mtDNA mutations 8363G>A and 3243A>G, and controls were frozen less than 2 h after death. The studies were performed in available stored material from the muscle (tibialis anterior), heart, liver, and brain (frontal cortex). Fibroblast cultures were established from skin biopsies. HEK-293 cells (CRL-1573) were obtained from A.T.C.C. (Manassas VA, U.S.A.).

4.2. Ethics

All studies were carried out in accordance with the Declaration of Helsinki of the World Medical Association and were approved by the Committees of Medical Ethics at all collaborating institutions. Informed consent was obtained from investigated individuals or their parents.

4.3. Plasmid construction

The nucleotide sequences of 33 different candidate miR-30-based shRNAs [shRNAmirs (microRNA-adapted shRNAs)] targeted to COX4I1, COX5A and COX6A1 mRNAs were designed with shRNA Retriever (<http://katahdin.cshl.org/siRNA/RNAi.cgi?type=shRNA>). The nucleotide sequences of eight different shRNAmirs targeted to the coding sequence of human OXA1L were downloaded from the publicly accessible RNAi Codex database (Olson *et al.* 2006). The corresponding 97-mer oligonucleotides were synthesized (Invitrogen) and used as template sequences for PCR amplification to produce clonable double-stranded products. The corresponding XhoI/EcoRI restriction fragments were inserted downstream of the CMV-GFP-IRESNeo expression cassette of the lentiviral pCMV-GIN-Zeo vector (Open Biosystems). The negative control (non-silencing) shRNAmir pCMV-GIN-Zeo derivative was obtained from Open Biosystems. The coding sequences of COX7A2 (IMAGE ID: 40002220) and COX7B (IMAGE ID: 3861730) were amplified from the respective full-length cDNA clones (ImaGenes), fused to the C-terminal FLAG epitope and cloned (EcoRI/NotI) into the modified pmaxFP-Red-N plasmid (Amaya). The full length human OXA1L coding sequence (IMAGE ID: 40017377) was amplified and inserted into the C-FLAG fusion mammalian expression vector pCMV-Tag4a (Stratagene). The fidelity of all constructs was confirmed by automated DNA

sequencing. Plasmids pReceiver-M02 (EXC0224) and pReceiver-M13 (EX-C0224) (GeneCopoeia) were used to express Cox6a2 and Cox6a2-FLAG respectively.

4.4. Cell culture, transfections and flow cytometry

Fibroblast cultures were grown in Dulbecco's modified Eagle's medium supplemented with 10% (v/v) fetal calf serum (Sigma) at 37°C in 5% CO₂. Cells were grown to ~90% confluence and harvested using 0.05% (w/v) trypsin and 0.02% (w/v) EDTA. Detached cells were diluted with an ice-cold culture medium, sedimented by centrifugation and washed twice in PBS (Sigma).

HEK-293 cells were grown at 37°C in a 5% (v/v) CO₂ atmosphere in high-glucose Dulbecco's modified Eagle's medium (PAA) supplemented with 10% (v/v) fetal bovine serum Gold (PAA). Cell lines stably expressing shRNAmir were prepared using the Nucleofector™ device (Amaxa) and the HEK-293 cell-specific transfection kit. At 48 h after the transfection the cells were split into culture medium containing 720 µg/ml of G418 sulfate (Clontech) and antibiotic-resistant colonies were selected over a period of three weeks. The cells were further maintained in the presence of 720 µg/ml G418.

The GFP fluorescence of stable G418-resistant HEK-293 cells was measured with a FACSCalibur flow cytometer and analyzed using the Cell Quest 3.3 application (Becton Dickinson).

The transient expression of Oxa11 or selected CcO subunits in HEK-293 cells was accomplished using the Lipofectamine 2000 reagent (Invitrogen) or the Express-In Transfection Reagent (Open Biosystems). To obtain optimal accumulation of the CcO subunit polypeptides, the cells were transfected twice consecutively, leading to transgene expression for a total of 4 days.

To assess the efficiency of the shRNAmir constructs interfering with *OXA1* transcripts, HEK-293 cells were co-transfected using a Nucleofector™ device with either one of the eight OXA1L-targeted shRNA constructs or the negative control (non-silencing) shRNA construct and with the OXA1L-FLAG expression construct. At 48 h after the transfection, the cells were lysed and the expression level of the Oxa11-FLAG fusion protein was examined by immunoblot analysis. The three OXA1L-targeted constructs that contained shRNA 1 (mp_id 433861, 5'-CAAGTTAGCAGGAGACCAT-3'), shRNA 2 (mp_id 19616, 5'-CCTACAACCTGGAAAGGAT-3') and shRNA 3 (mp_id 19615, 5'-GAGACCATATTGAGTATTA-3') (RNAi Codex) showed the highest potential to interfere with the expression of Oxa11-FLAG protein in the transient assay. For the generation of stable transfectants, HEK-293 cells (10⁶) were transfected using a Nucleofector™ device with the three functionally validated OXA1L-targeted shRNA constructs, the negative control (non-silencing) shRNA construct and with the empty vector.

4.5. Isolation of mitochondria

Mitochondria were isolated from fibroblasts by a hypo-osmotic shock method (Bentlage *et al.* 1996). The freshly harvested cells were disrupted in 10 mM Tris buffer (pH 7.4) and quickly homogenized in a Teflon/glass homogenizer at 4°C. Sucrose was added to a final concentration of 0.25 M immediately after homogenization. The nuclei were removed by centrifugation for 10 min at 4°C and 600 g and the mitochondrial fraction was isolated from the postnuclear supernatant by centrifugation for 10 min at 4°C and 10 000 g. The mitochondrial pellet was washed and finally resuspended in 0.25 M sucrose, 2 mM EGTA, 40 mM KCl and 20 mM Tris, pH 7.4, and stored at -70°C. Mitoplasts were prepared from fibroblasts as described previously (Klement *et al.* 1995). In brief, trypsinized cells suspended in isotonic STE medium [0.25 M sucrose, 10 mM Tris, pH 7.4, 1 mM EDTA, 1% (w/v) Protease inhibitor cocktail (Sigma)] were treated with digitonin (0.4 mg/mg of protein; Fluka) on ice for 15 min. The suspension was diluted 10-fold with STE and centrifuged for 10 min at 4°C and 12 000 g. The pellet was washed by centrifugation and resuspended in STE to a final concentration of 1–2 mg of protein/ml. Based on immunodetection and enzyme activity measurements, >95% of the mitochondrial inner membrane proteins were recovered in this fraction.

To isolate mitochondria from HEK-293 cells, collected and thawed cells were resuspended in STE buffer, homogenized in a glass/glass homogenizer at 4°C. Unbroken cells and nuclei were removed by centrifugation for 15 min at 4°C and 600 g and the mitochondrial fraction was isolated from the postnuclear supernatant by centrifugation for 25 min at 4°C and 10 000 g. The mitochondrial pellet was washed, resuspended in STE buffer (2.5 volume of the mitochondrial pellet) and stored at -80°C.

Muscle mitochondria were isolated according to (Schagger and von Jagow 1991), but without use of protease. Tissue samples were homogenized at 4°C in a KCl medium (100 mM KCl, 50 mM Tris, 2 mM EDTA, 10 mg/ml aprotinin, pH 7.5). The homogenate was centrifuged for 10 min at 4°C and 600 g, the supernatant was filtered through a 100 µm nylon screen, and mitochondria were sedimented by centrifugation for 10 min at 4°C and 10 000 g. The mitochondrial pellet was washed by centrifugation and resuspended to a final protein concentration of 20-25 mg/ml.

4.6. Immunofluorescence

HEK-293 cells (1.5×10^5) grown on 70 mm² glass chamber slides (BD Falcon) were transfected with an OXA1L-FLAG expression construct using the Lipofectamine 2000 reagent. At 24 h after the transfection, the cells were incubated with 200 nM MitoTracker Red CMX Ros (Molecular Probes) for 15 min, and then fixed and permeabilized with PBS, 4% (v/v) paraformaldehyde and 0.1% (v/v) Triton X-100 solutions, respectively. Subsequently, the cells were incubated in PBS containing

10% (w/v) BSA for 1 h at 37°C to block non-specific binding. Immunocytochemical detection was then performed with a monoclonal M2 anti-FLAG antibody (1:1000) and with an anti-mouse IgG₁ Alexa Fluor® 488 antibody (1:500).

4.7. Laser scanning confocal microscopy

xyz images sampled according to the Nyquist criterion were acquired using a Nikon Eclipse TE2000 microscope equipped with a *C1si* confocal scanning head and an Apo TIRF 60× (N.A. 1.49) objective. The 488 nm and 543 nm laser lines and appropriate 515±15 and 590±15 nm band pass filter sets were used for excitation and fluorescence detection, respectively. Individual channel images were acquired separately. Images were restored using the measured point spread function (PSF) and the classic maximum likelihood deconvolution algorithm in Huygens Professional Software (SVI).

4.8. Sub-cellular and submitochondrial fractionation

The postnuclear supernatant from 10⁷ HEK-293 cells (see Chapter 4.5) was centrifuged at 10 000 g for 25 min to pellet the mitochondria. The resulting supernatant corresponding to the cytoplasmic fraction was collected, and the mitochondrial pellet was washed once with STE buffer. For sonical disruption, isolated mitochondria were adjusted to a protein concentration of 2.5 mg/ml, sonicated and centrifuged at 100 000 g for 30 min. Alkaline sodium carbonate extraction of mitochondrial membranes was performed essentially as described (Fujiki *et al.* 1982).

4.9. Preparation of a polyclonal antibody to human Oxa11

An Oxa11-specific antibody was prepared by Open Biosystems. An Oxa11-specific antiserum was generated by immunizing chicken with a synthetic peptide (KLH-coupled) corresponding to the C-terminal part of human Oxa11 (CKPKSKYPWHDT). The polyclonal antibody to human Oxa11 was affinity-purified from the total IgY with the respective peptide-packed column. The specificity of the produced antibody was tested by immunodetection of the Oxa11-FLAG fusion protein.

4.10. Electrophoresis and Western blot analysis

In cultured skin fibroblasts, BN-PAGE (Schagger and von Jagow 1991) was used for the separation of native mitochondrial OXPHOS complexes on 6–15% (w/v) polyacrylamide gradient minigels (Mini Protean system; Bio-Rad) as described previously (Klement *et al.* 1995). Mitoplasts were pelleted by centrifugation for 10 min at 4°C and 10 000 g, and solubilized using 1 g of DDM/g of protein for 20 min on ice in a buffer containing 1.75 M aminocaproic acid, 2 mM EDTA and 75 mM Bis-Tris (pH 7.0). Samples were centrifuged for 20 min at 20 000 g and Serva Blue G dye was added

to collected supernatants at a concentration of 0.1 g/g of detergent. Electrophoresis was performed at 50 V for 30 min and then at 90 V. SDS/PAGE (Schagger and von Jagow 1987) was performed on 10% (w/v) polyacrylamide slab minigels, and analysis of [³⁵S] methionine-labelled proteins was performed on a 16 cm long 15-20% (w/v) gradient polyacrylamide slab gels (Protean system; Bio-Rad). The samples were boiled for 3 min in sample lysis buffer [2% (v/v) mercaptoethanol, 4% (w/v) SDS, 10 mM Tris/HCl, 10% (v/v) glycerol]. For 2D analysis, strips of the first-dimension BN-PAGE gel were incubated for 1 h in 1% (w/v) SDS and 1% (v/v) mercaptoethanol and then subjected to SDS/PAGE (10% polyacrylamide) for separation in the second dimension (Schagger and von Jagow 1987). Gels were blotted onto Hybond C-extra nitrocellulose membranes (Amersham) by semi-dry electrotransfer for 1 h at 0.8 mA/cm² and the membrane was blocked in PBS containing 0.2% (v/v) Tween 20. The membranes were used whole or were cut according to molecular mass markers into portions containing individual OXPHOS complexes or their subunits. Membranes were incubated for 3 h with primary antibodies diluted in PBS containing 2% (w/v) BSA. Previously characterized polyclonal antibodies were used at the indicated titres: those against the F₀c subunit of ATPase (1:900) (Houstek *et al.* 1995a) and those against the F₀a (ATP6) subunit of ATPase (1:500) (Dubot *et al.* 2004). In addition, we used monoclonal antibodies against complex IV subunits Cox1 (1:330), Cox4 (1:670) and Cox6c (1:200), complex I subunit NADH39 (1:250) and the 70 kDa flavoprotein subunit of SDH (SDHA) (1:2000), all obtained from Molecular Probes, as well as subunit F₁-α of ATPase (1:200 000 (Moradi-Ameli and Godinot 1983). Incubation with peroxidase-labelled secondary antibodies in PBS with 2% (w/v) BSA was performed for 1 h using either goat anti-mouse IgG (1:1000; Sigma A8924) or goat anti-rabbit IgG (1:1000; Sigma F0382). The chemiluminescence reaction with an ECL® kit (Amersham) was detected on an LAS 1000 instrument (Fuji) and the signal was quantified using Aida 2.11 Image Analyzer software.

In bioptic or autoptic tissues, proteins were electroblotted from the gels onto Immobilon™-P PVDF membranes (Millipore) using semi-dry transfer for 60-90 min at a constant current of 0.6-0.8 mA/cm². Membranes were air-dried overnight, rinsed twice with 100% (v/v) methanol, and blocked in TBS and 10% (w/v) non-fat dried milk for 1-2 h. Primary detection of BN/PAGE-blot was performed with mouse monoclonal antibodies raised against the complex I subunit NDUFA9 (2 µg/ml), ATP synthase subunit F₁-α (2-3 µg/ml), complex III subunit Core2 (0.5 µg/ml), complex IV subunit Cox2 (0.5–1 µg/ml), and complex II subunit 70 kDa protein (1 µg/ml) (Mitosciences), at indicated dilutions. Primary detection of two-dimensional BN/SDS/PAGE-blot for the CcO assembly was performed as described previously (Stiburek *et al.* 2005). Blots were incubated with primary antibodies in TBS, 0.3% (v/v) Tween 20 and 2% non-fat

dried milk for 2 h. Secondary detection was carried out with a goat anti-mouse IgG-horseradish peroxidase conjugate (1:1000–1:4000; Sigma A8924) in TBS, 0.1% Tween 20 and 2% non-fat dried milk, for 1 h. The immunoblots were developed with SuperSignal West Femto Maximum Sensitivity Substrate (Pierce). Signal acquisition was performed using either a VersaDoc 4000 imaging system (Bio-Rad Laboratories) or Kodak BioMax Light films (Eastman Kodak Co.). Digital images were analyzed using the Quantity One application (Bio-Rad Laboratories). All blotting experiments were repeated with independently isolated mitochondrial samples. Duplicate experiments yielded consistent results.

In HEK-293 cells, protein sample preparations, electrophoresis, immunoblot analysis and signal acquisition for SDS, BN (blue native) and BN/SDS/PAGE immunoblot analysis were performed essentially as described above for bioptic and autoptic tissues. Monoclonal antibodies against the mitochondrial outer membrane protein porin, CcO subunits Cox1, Cox2, Cox4, Cox5a, Cox6a1 and Cox6c, the 70 kDa flavoprotein subunit of SDH (SDHA), complex III subunit Core2, complex I subunits NDUFA9 and NDUFB6, complex V subunits F₁- α , F₁- β , subunit d and OSCP, and pyruvate dehydrogenase (PDH) subunit E2 were obtained from Mitosciences. The mouse monoclonal antibody to mtHSP70 was from Alexis Biochemicals. Polyclonal antibodies to α -tubulin and eIF2 α were from Cell Signaling Technology, and the monoclonal anti-FLAG antibody was from Sigma. For analysis of respiratory supercomplexes by BN/SDS/PAGE and BN/BN/PAGE, isolated mitochondria were extracted using digitonin (detergent/protein ratio of 6). Primary detection of BN/SDS/PAGE and BN/BN/PAGE immunoblots was performed with mouse monoclonal antibodies (Mitosciences) raised against the complex I subunit NDUFB6, complex III subunit Core1 and complex IV subunit Cox1. The first dimension gel strips for BN/BN/PAGE immunodetection were soaked in cathode buffer containing 0.1% DDM for 15 min and then in cathode buffer containing 0.02% DDM for another 15 min. The second dimension of BN-PAGE separation was performed in the presence of 0.02% DDM as described in (Wittig *et al.* 2006).

4.11. Immunoprecipitation of Oxa11–FLAG protein

HEK-293 cells ($\sim 10^6$) were transiently (48 h) transfected with the Oxa11–FLAG expression construct, lysed with a buffer containing 1% Triton X-100, 150 mM NaCl, 1 mM EDTA and 50 mM Tris/HCl (pH 7.4), and the lysate was incubated for 6 h at 4°C with previously washed 50 μ l of an ANTI-FLAG® M2 affinity agarose resin (flagipt-1; Sigma). Subsequently, the resin was washed five times with a buffer containing 150 mM NaCl, 50 mM Tris/HCl (pH 7.4), and the bound protein was eluted by competition with 3 \times FLAG peptide. Finally, the eluted immunoprecipitate was combined with SDS sample buffer and resolved using SDS/PAGE.

4.12. Spectrophotometric assays

The activities of respiratory chain complexes were measured spectrophotometrically with a UV-2401PC instrument (Shimadzu). The activities of the mitochondrial enzymes NADH:coenzyme Q₁₀ reductase (NQR, complex I), succinate:coenzyme Q₁₀ reductase (SQR, complex II), succinate:cytochrome c reductase (SCCR, complex II+III), NADH:cytochrome c reductase (NCCR, complex I+III), coenzyme Q₁₀:cytochrome c reductase (QCCR, complex III), and cytochrome c oxidase (COX, CcO, complex IV) were measured spectrophotometrically by standard methods at 37°C in muscle homogenate and isolated muscle mitochondria (Fischer *et al.* 1986; Makinen and Lee 1968) or in cultured fibroblasts (Chowdhury *et al.* 2000). In HEK-293 cells, rotenone-sensitive complex I activity (NADH:ubiquinone oxidoreductase) was measured by incubating 45 µg of mitochondrial protein in 1 ml of assay medium (50 mM Tris/HCl, pH 8.1, 2.5 mg/ml BSA, 50 µM decylubiquinone, 0.3 mM KCN and 0.1 mM NADH without or with 3 µM rotenone). The decrease in absorbance at 340 nm due to the NADH oxidation was followed. Complex II activity (succinate:2,6-dichloroindophenol oxidoreductase) was measured by incubating 20 µg of mitochondrial extract in 1 ml of assay medium (10 mM potassium phosphate, pH 7.8, 2 mM EDTA, 1 mg/ml BSA, 0.3 mM KCN, 10 mM succinate, 3 µM rotenone, 0.2 mM ATP, 80 µM 2,6-dichloroindophenol, 1 µM antimycin and 50 µM decylubiquinone). The decrease in absorbance at 600 nm due to the reduction of 2,6-dichloroindophenol was monitored. CcO activity was measured by incubating 15–18 µg of mitochondrial protein in 1 ml of assay medium (40 mM potassium phosphate, pH 7.0, 1 mg/ml BSA, 25 µM reduced cytochrome c and 2.5 mM DDM) and the oxidation of cytochrome c (II) at 550 nm was monitored. All assays were performed at 37°C. The total protein was determined using the method of Lowry (Lowry *et al.* 1951).

Aurovertin-sensitive ATP hydrolytic activity was measured in a ATP-regenerating system as described in (Baracca *et al.* 1989). Mitochondria (8-22 µg of protein/ml) were incubated in a medium containing 40 mM Tris (pH 7.4), 5 mM MgCl₂, 10 mM KCl, 2 mM phosphoenolpyruvate, 0.2 mM NADH, 1 µg/ml rotenone, 0.1% (w/v) BSA, 5 units of pyruvate kinase and 5 units of lactate dehydrogenase for 2 min. The reaction was started by the addition of 1 mM ATP and the rate of NADH oxidation, equimolar to ATP hydrolysis, was monitored as the decrease in absorbance at 340 nm. Sensitivity to aurovertin was determined by parallel measurements in the presence of 2 µM inhibitor.

4.13. High-resolution oxygraphy

Oxygen consumption in cultured fibroblasts was determined at 30°C as described in (Chowdhury *et al.* 2000; Pecina *et al.* 2003) using an Oxygraph-2k (Oroboros). Freshly harvested fibroblasts were suspended in a KCl medium (80 mM KCl, 10 mM Tris/HCl, 3 mM MgCl₂, 1 mM EDTA, 5 mM potassium phosphate, pH 7.4) and cells

were permeabilized by digitonin (0.1 mg of detergent/mg of protein). Respiratory substrates and inhibitors were used at the concentrations indicated. Oxygen consumption was expressed in pmol of oxygen/s per mg of protein. CcO activity was measured with 5 mM ascorbate and 1 mM TMPD, and was corrected for substrate autooxidation (determined as oxygen uptake insensitive to 0.33 mM KCN).

Muscle fibers were separated mechanically according to (Kunz *et al.* 1993), and oxygen consumption by saponin-skinned muscle fibers was determined using multiple substrate inhibitor titrations as described (Wenchich *et al.* 2003).

The oxygen consumption of digitonin-permeabilized HEK-293 cells was measured at 30°C using an OROBOROS Oxygraph (Anton Paar) in a medium containing 0.5 mM EGTA, 3 mM MgCl₂, 60 mM potassium lactobionate, 20 mM taurine, 10 mM KH₂PO₄, 110 mM sucrose, 1 g/l BSA, 20 mM Hepes (pH 7.1). The measurements were carried out in the presence of 30-75 µg/ml of digitonin, 2.5 µM antimycin A, 2 mM ascorbate, 500 µM TMPD and 0.5-1.5 µM FCCP. Respiration was inhibited by the addition of sodium azide to a final concentration of 10 mM. The P₅₀ (partial pressure of oxygen at the half-maximal respiration rate) value was measured in the presence of 0.5 µM FCCP and 10 mM succinate essentially as described in (Pecina *et al.* 2004). All measurements were performed independently three to six times for each cell line.

4.14. Cytofluorimetric analysis of mitochondrial membrane potential

Freshly harvested fibroblasts were resuspended in 80 mM KCl, 10 mM Tris/HCl (pH 7.4), 3 mM MgCl₂, 1 mM EDTA, 5 mM potassium phosphate and 10 mM succinate at a protein concentration of 1 mg/ml. Cells (~10⁴ per each measurement) were permeabilized by 0.1 mg digitonin per mg protein (Sigma) and stained with 20 nM TMRM (Molecular Probes) for 15 min at room temperature. ADP, inhibitors, or both were added at indicated concentrations 1 min before cytofluorometric measurements, which were performed as described elsewhere (Floryk and Houstek 1999) on a FACSort flow cytometer (Becton Dickinson) equipped with an argon laser, 488 nm. The TMRM signal was analyzed in the FL2 channel, equipped with a band pass filter 585±21 nm; the photomultiplier value of the detector was at 631 V in FL2. Data were acquired in log scale using CellQuest (Becton Dickinson) and analyzed with WinMDI 2.8 software (TSRI). Arithmetic mean values of the fluorescence signal in arbitrary units were determined for each sample for the purpose of subsequent graphic representation.

4.15. ATP synthesis

The rate of ATP synthesis was measured at 37°C in 150 mM KCl, 25 mM Tris/HCl, 10 mM potassium phosphate, 2 mM EDTA and 1% (w/v) BSA, pH 7.2, using 0.5 mM ADP and 10 mM succinate or 10 mM pyruvate + 10 mM malate (or

ketoglutarate + malate) as substrate, as described previously (Wanders *et al.* 1996). Protein concentration was 1 mg/ml. For permeabilization of fibroblasts and cybrids, 0.1 and 0.03 mg of digitonin/mg of protein, respectively, was used. The reaction was started by addition of the cells and performed for the indicated time intervals. Reaction mixture aliquots of 200 µl were added to 200 µl of DMSO, and ATP content was determined in DMSO-quenched samples by a luciferase assay according to (Ouhabi *et al.* 1998). ATP production was expressed in nmol of ATP/min per mg of protein.

4.16. Biosynthesis of mitochondrial proteins

Growth medium was removed from cultured fibroblasts, and the cells were rinsed with methionine-free medium without serum (Gibco medium 21013; 1 mM pyruvate, 2 mM glutamine and 30 mg/l cysteine) and incubated in the same medium containing 10% (v/v) dialysed fetal calf serum and 100 µg/ml emetine for 10 min. The cells were labelled for 3 h with 300 µCi/ml L-[³⁵S] methionine, as described in (Chomyn 1996). The products were separated by 15-20% (w/v) polyacrylamide gradient SDS-PAGE. A small aliquot of the samples prepared for electrophoresis was used to measure the total incorporation of radioactivity in the mitochondrial fraction as trichloroacetic acid-precipitable counts. The radioactivity of proteins was quantified in dried gels using a BAS-5000 system (Fuji). Labelled proteins were identified according to their molecular mass as reported previously in *ex vivo* translation assays (Chomyn 1996).

4.17. Protein determination

The protein content was measured by the Bradford or Micro BCA protein kit assays (Bio-Rad Laboratories), using BSA as a standard. Samples were sonicated for 20 s prior to protein determination.

4.18. DNA analysis and sequencing

Total genomic DNA from muscle and cultured fibroblasts was isolated by phenol extraction. The entire mtDNA was amplified in six overlapping fragments by PCR (7-3148, 2073-5719, 5645-8815, 8403-11 132, 11 005-14 684 and 13 863-136). Purified fragments were sequenced on the automatic sequencer ALF Express II (Amersham Biosciences) using cycle sequencing with 41 Cy5-labelled internal sequencing primers or on an AbiPrism 3100 Avant Genetic Analyzer (Applied Biosystems).

4.19. Restriction analysis

To determine the amount of mtDNA mutations, PCR/RFLP (restriction fragment length polymorphism) analysis method was performed. 9205delTA microdeletion was quantified according to (Chrzanowska-Lightowlers *et al.* 2004) using the mismatched (bold) primers 5'-CCT CTA CCT GCA CGA CAA **TGC** A-3' (forward) and 5'-CGT

TATGCATTGGAAGTGAAATCA C-3' (reverse), which introduce two novel NsiI restriction sites in the case of the wild-type mtDNA and one NsiI restriction site in the case of mutant mtDNA. PCR products were radioactively labelled with [α -³²P]dCTP in the final cycle of PCR and run on a non-denaturing 13% (w/v) polyacrylamide gel after complete digestion. To quantify 8363G>A mutation, PCR products (8279–8485) were radioactively labelled with [α -³²P]dCTP in the final cycle of PCR, and run on a non-denaturing 10% (w/v) polyacrylamide gel after complete digestion with TspRI (New England BioLabs). The mutation abolishes one of two TspRI restriction sites on the fragment. The levels of heteroplasmy of the prevalent 3243A>G and 8344A>G mutations were determined as described elsewhere (Brantova *et al.* 2006). The proportions of wild-type to mutant mtDNA were measured using PhosphorImager and ImageQuant software (Molecular Dynamics).

4.20. Northern blot analysis

Total RNA was isolated from cultured fibroblasts by phenol/guanidium thiocyanate/chloroform extraction (Sambrook and Russell 2001). ~20 μ g of total RNA per lane was separated through a 1.2% (w/v) agarose/formaldehyde gel and transferred to a Hybond-N nylon membrane (Amersham) in 20 \times SSC (1 \times SSC is 0.15 M NaCl/0.015 M sodium citrate). The membrane was prehybridized for 2 h at 45°C in 5 \times SSC, Denhardt's solution, 0.5% SDS and 100 μ g/ml sonicated herring sperm. The membranes were hybridized overnight at 45°C with [α -³²P]dCTP-labelled probes corresponding to regions of the genes ATP6 (8361–9060), COX3 (9269–9912), ND1 (3313–4252) and COX1 (6120–6960). The radioactivity was detected by PhosphorImager and ImageQuant software (Molecular Dynamics).

4.21. Quantitative RT-PCR (reverse transcription–PCR) analysis

Total RNA was isolated from cultured fibroblasts using RNA Blue reagent (Top-Bio, Prague, Czech Republic). Following DNase I treatment (Invitrogen), first-strand cDNA was synthesized from 1 μ g RNA aliquots with 200 units SuperScript II reverse transcriptase using either 200 ng of random hexamer primers or 500 ng of oligo(dT)_{12–18} (all Invitrogen) according to the manufacturer's instructions. Real-time quantitative RT-PCR was performed on a LightCycler instrument (Roche Diagnostics) using a QuantiTect SYBR Green PCR kit (Qiagen). PCR reactions were performed on cDNAs using primer pairs specific for the ATP6 gene transcript (forward, 5'-CCT TAT GAG CGG GCA CAG T-3'; reverse, 5'-CAG GGC TAT TGG AA-3'; nt 8846–8994), for the COX3 gene transcript (forward, 5'-GCC CTC TCA GCC CTC CTA ATG-3'; reverse, 5'-GTG GCC TTG GTA TGT GCT TTC TCG-3'; nt 9267–9416), for the ATP6–COX3 gene transcript (forward, 5'-AAT CCA AGC CTA CGT TTT CAC ACT-3'; reverse, 5'-TAG GCC GGA GGT CAT TAG G-3'; nt 9150–9299), for the

CYTB gene transcript (forward, 5'-GACCTCCCCACCCCATCCA-3'; reverse, 5'-AAA GGC GGT TGA GGC GTC TG-3'; nt 14 804– 14 935) and for the ND1 gene transcript (forward, 5'-CAA CCT CAA CCT AGG CCT CCT-3'; reverse, 5'-ACG GCT AGG CTA GAG GTG GC-3'; nt 3595–3644). The primer pair for ATP6–COX3 was designed to flank the splice site of the ATP6–COX3 transcript. Amplified regions of the ATP6 or COX3 transcript were present in both processed and unprocessed RNAs. All reactions were run at an annealing temperature of 60°C. The PCR mixture contained 5 µl of 2×SYBR Green PCR Master Mix, 2 µl of 100×diluted reverse transcription product and 200 nM of each primer in a total volume of 10 µl. All reactions were performed in triplicate. For each primer pair, non-template controls were included to check for the absence of contaminants and primer dimers that would interfere with quantification when SYBR Green is used. The external standard curve was generated in parallel for all reactions using serial dilutions of cDNA synthesized from control RNA. For each sample, the relative amounts of ATP6, COX3, CYTB, ND1 and unprocessed ATP6–COX3 transcripts were determined from the standard curves. Each sample was analyzed in two separate experiments.

Total RNA from HEK-293 cells was isolated using TriReagent solution (MRC). First-strand cDNA was synthesized from 4 µg of total RNA with the use of Superscript III reverse transcriptase (Invitrogen) and Oligo-dT primers (Promega). Pre-amplification and relative quantification was performed according to the manufacturer's instructions (Applied Biosystems). Ten pre-amplification cycles were run with 12.5 µl of cDNA and a 0.05×pooled mixture of eight TaqMan Gene Expression Assays [Hs00971639_m1, COX4I1; Hs00261747_m1, COX4I2; Hs01924685_g1, COX6A1; Hs00193226_g1, COX6A2; Hs00427620_m1, TBP (TATA-box-binding protein); Hs00173304_m1, PPARGC1A (peroxisome-proliferator-activated receptor γ co-activator 1 α); Hs00188166_m1, SDHA (succinate dehydrogenase complex subunit A; Hs01082775_m1, TFAM (transcription factor A, mitochondrial)]. Relative quantification was performed in duplicates twice on the 7300 Real-Time PCR System (Applied Biosystems). The transcript levels of all mRNAs were normalized to the level of TBP mRNA. Because the amplification efficiency of the reference and target genes was the same, the comparative $\Delta\Delta C^t$ method was used for relative quantification.

4.22. Statistical analysis

A Student's t test was performed using Microsoft Excel. Results are expressed as mean±S.D. A *P* value of less than 0.05 was considered as statistically significant, and asterisks are used to denote significance as follows: **P*<0.05; ** *P* <0.01; *** *P* <0.001.

5 RESULTS AND DISCUSSION

5.1. Characterization of the assembly and function of human nDNA-encoded CcO subunits 4, 5a, 6a, 7a and 7b (*specific aim 1a*)

Fornuskova D, Stiburek L, Wenchich L, Vinsova K, Hansikova H and Zeman J

Novel insights into the assembly and function of human nuclear-encoded cytochrome c oxidase subunits 4, 5a, 6a, 7a and 7b.

Biochem J 2010; 428: 363-374.

To study the role of nuclear-encoded cytochrome c oxidase (CcO) structural subunits Cox4, Cox5a and Cox6a as well as the sequence of late events in the CcO assembly pathway, we prepared stable HEK-293 knockdown lines using microRNA-adopted design evoking RNA interference of *COX4*, *COX5A* and *COX6A1*. Furthermore, we used ectopic expression of C-end epitope-tagged Cox6a, Cox7a and Cox7b in wild-type HEK-293 cells and *COX6A* knockdowns to elucidate entry points of these subunits into the CcO assembly pathway. To estimate functionality and integrity of OXPHOS in context of CcO deficiency, we employed quantitative real-time RT-PCR, isolation of crude mitochondrial fraction by cellular fractionation and differential centrifugation, spectrophotometric enzyme activity assays, high-resolution respirometry and blue-native (BN), denaturing (SDS) and two-dimensional (BN/SDS or BN/BN) PAGE with downstream immunoblot detections using monoclonal antibodies against various mitochondrial proteins.

Knockdown of Cox4, Cox5a and Cox6a resulted in reduced CcO activity, diminished affinity of the residual enzyme for oxygen, decreased CcO holoenzyme and CcO dimer levels, increased accumulation of CcO subcomplexes and gave rise to an altered pattern of respiratory supercomplexes. An analysis of the patterns of CcO subcomplexes found in both knockdown and overexpressing cells identified a novel CcO assembly intermediate, identified the entry points of three late-assembled subunits and demonstrated directly the essential character as well as the interdependence of the assembly of Cox4 and Cox5a. The ectopic expression of the heart/muscle-specific isoform of the Cox6 subunit (*COX6A2*) resulted in restoration of both CcO holoenzyme and activity in *COX6A1*-knockdown cells. This was in sharp contrast with the unaltered levels of *COX6A2* mRNA in these cells suggesting the existence of a fixed expression

programme. The normal amount and function of respiratory complex I in all of our CcO-deficient knockdown cell lines suggest that, unlike non-human CcO-deficient models, even relatively small amounts of CcO can maintain the normal biogenesis of respiratory complex I in cultured human cells.

I contributed fundamentally to this study by designing the research, cloning of pCMV-GIN-ZEO plasmid derivatives coding for candidate shRNAs to achieve the most efficient knockdown, maintaining the HEK-293 cell culture, carrying out expression cloning, preparation of knockdown cell lines and transiently transfected cellular materials, performing mitochondrial isolations and all Western blot analyses and by writing the paper.

Novel insights into the assembly and function of human nuclear-encoded cytochrome *c* oxidase subunits 4, 5a, 6a, 7a and 7b

Daniela FORNUSKOVA, Lukas STIBUREK, Laszlo WENCHICH, Kamila VINSOVA, Hana HANSIKOVA and Jiri ZEMAN¹

Department of Pediatrics, First Faculty of Medicine, Charles University in Prague, Ke Karlovu 2, Prague 2, 128 08, Czech Republic

Mammalian CcO (cytochrome *c* oxidase) is a hetero-oligomeric protein complex composed of 13 structural subunits encoded by both the mitochondrial and nuclear genomes. To study the role of nuclear-encoded CcO subunits in the assembly and function of the human complex, we used stable RNA interference of *COX4*, *COX5A* and *COX6A1*, as well as expression of epitope-tagged Cox6a, Cox7a and Cox7b, in HEK (human embryonic kidney)-293 cells. Knockdown of Cox4, Cox5a and Cox6a resulted in reduced CcO activity, diminished affinity of the residual enzyme for oxygen, decreased holoCcO and CcO dimer levels, increased accumulation of CcO subcomplexes and gave rise to an altered pattern of respiratory supercomplexes. An analysis of the patterns of CcO subcomplexes found in both knockdown and overexpressing cells identified a novel CcO assembly intermediate, identified the entry points of three

late-assembled subunits and demonstrated directly the essential character as well as the interdependence of the assembly of Cox4 and Cox5a. The ectopic expression of the heart/muscle-specific isoform of the Cox6 subunit (*COX6A2*) resulted in restoration of both CcO holoenzyme and activity in *COX6A1*-knockdown cells. This was in sharp contrast with the unaltered levels of *COX6A2* mRNA in these cells, suggesting the existence of a fixed expression programme. The normal amount and function of respiratory complex I in all of our CcO-deficient knockdown cell lines suggest that, unlike non-human CcO-deficient models, even relatively small amounts of CcO can maintain the normal biogenesis of this respiratory complex in cultured human cells.

Key words: cytochrome *c* oxidase, protein assembly, respiratory supercomplex, RNA interference (RNAi).

INTRODUCTION

Cytochrome *c* oxidase (CcO), the terminal enzyme complex of the mitochondrial electron-transport chain couples the electron transfer from reduced cytochrome *c* to molecular oxygen with vectorial proton translocation across the inner membrane. The mammalian CcO complex is composed of 13 different polypeptide subunits, which are encoded by both the nuclear and mitochondrial genomes. Mitochondrially encoded Cox1 and Cox2 form the redox site involved in electron transfer. Electrons enter the CcO complex at the binuclear copper site (Cu_A) in the Cox2 subunit, which also mediates electrostatic binding of cytochrome *c* [1]. From Cu_A, electrons pass to other metal centres in the Cox1 subunit, first to haem *a* and then to a heterobimetallic haem *a*₃/Cu_B centre [2]. Together with Cox3, mitochondrially encoded subunits constitute the evolutionarily conserved structural core of the enzyme. The remaining ten subunits, which are encoded by nuclear DNA, are associated with the surface of the complex core. These small polypeptides are required for the assembly and stability of the holoenzyme and are thought to function in the regulation of its activity [3–5]. Tissue-specific isoforms of subunits Cox4, Cox6a, Cox6b, Cox7a and Cox8 have been identified in mammals [6,7]. Most CcO subunits have one or more transmembrane domains, with the exception of Cox5a and Cox5b, which are located at the matrix side, and Cox6b, which is associated with the surface of the complex in the intermembrane space [8].

Subunit Cox4 is the largest nuclear-encoded subunit of the complex. It was shown to be involved in the allosteric inhibition

of CcO activity by ATP, which binds to the matrix portion of the subunit [9]. Isoforms 1 and 2 of Cox4 are encoded by two separate genes and are likely to differ with respect to ATP-induced inhibition of CcO activity [10]. In mammalian cells, the first step of CcO assembly is the membrane integration of Cox1, followed by the association of the Cox4–Cox5a heterodimer [11]. Subunit Cox5a binds indirectly to subunit Cox1 via the matrix domain of subunit Cox4 and the extramembrane segment of Cox6c. Subunit Cox6a is involved in the stabilization of the dimeric state of CcO and may contribute to the formation of an interaction site for cytochrome *c* [8]. Liver-type subunit Cox6a (Cox6a1/Cox6aL) is found in all non-muscle tissues, whereas heart/muscle-type subunit Cox6a (Cox6a2/Cox6aH), which is encoded by a different gene, is expressed only in striated muscles [12]. Subunit Cox6a was shown to associate with the complex, together with subunits Cox7a or Cox7b, at a very late stage of CcO assembly [13].

In the present study, we generated HEK (human embryonic kidney)-293 cell lines with stably [shRNA (short hairpin RNA)] down-regulated levels of CcO subunits Cox4, Cox5a and Cox6a. We analysed the steady-state levels of the CcO holoenzyme and the presence and composition of CcO subcomplexes. We have demonstrated directly that depletion of each of the selected subunits results in decreased levels of CcO with a parallel accumulation of CcO subcomplexes and unassembled subunits. These changes were accompanied by a reduction in the activity of CcO and a decreased affinity of CcO for oxygen. The subunit composition of CcO subcomplexes in Cox6a-depleted cells, along with analyses of the ectopic expression of subunits Cox7a2 and Cox7b in these cells, provided novel insights into the late stages

Abbreviations used: BN, blue native; CcO, cytochrome *c* oxidase; DDM, n-dodecyl- β -D-maltoside; FCCP, carbonyl cyanide *p*-trifluoromethoxyphenylhydrazone; HEK, human embryonic kidney; KD, knockdown; NDUFB6, NADH dehydrogenase (ubiquinone) 1 β subcomplex 6; *P*₅₀, partial pressure of oxygen at half-maximal respiration rate; qRT-PCR, quantitative real-time PCR; RNAi, RNA interference; SDHA, succinate dehydrogenase complex subunit A; shRNA, short hairpin RNA; shRNAmir, microRNA-adapted shRNA; SQR, succinate:coenzyme Q₁₀ reductase, complex II; TBP, TATA-box-binding protein; TMPD, *N,N,N',N'*-tetramethyl-*p*-phenylenediamine; UTR, untranslated region.

¹ To whom correspondence should be addressed (email jzem@lf1.cuni.cz).

of human CcO assembly. Moreover, CcO deficiency in *COX6A1*-KD (knockdown) cells was complemented by ectopic expression of the Cox6a2 isoform. We have demonstrated further that CcO deficiency in *COX5A*- and *COX6A*-KD cells affects the formation of respiratory supercomplexes containing the dimeric form of CcO.

EXPERIMENTAL

Plasmid construction

The nucleotide sequences of 33 different candidate miR-30-based shRNAs [shRNAmirs (microRNA-adapted shRNAs)] targeted to *COX4I1*, *COX5A* and *COX6A1* mRNAs were designed with shRNA Retriever (<http://katahdin.cshl.org/siRNA/RNAi.cgi?type=shRNA>), synthesized and cloned into the pCMV-GIN-ZEO plasmid (Open Biosystems) as described previously [14]. A pCMV-GIN-ZEO derivative that expresses negative control (non-silencing) shRNAmir was obtained from Open Biosystems. The coding sequences of *COX7A2* (GenBank® accession number BC100852; IMAGE ID: 40002220) and *COX7B* (GenBank® accession number BC018386; IMAGE ID: 3861730) were amplified from the respective full-length cDNA clones (ImaGenes), fused to the C-terminal FLAG epitope and cloned (EcoRI/NotI) into the modified pmaxFP-Red-N plasmid (Amaya). The fidelity of all constructs was confirmed by automated DNA sequencing. Plasmids pReceiver-M02 (EX-C0224) and pReceiver-M13 (EX-C0224) (GeneCopeia) were used to express Cox6a2 and Cox6a2-FLAG respectively.

Cell culture and transfection

HEK-293 cells (CRL-1573) were obtained from A.T.C.C. (Manassas, VA, U.S.A.) and grown at 37 °C in a 5% (v/v) CO₂ atmosphere in high-glucose Dulbecco's modified Eagle's medium (PAA) supplemented with 10% (v/v) fetal bovine serum Gold (PAA). Cell lines stably expressing shRNAmir were prepared using the Nucleofector™ device (Amaya) essentially as described previously [14]. The transient expression of selected CcO subunits in HEK-293 cells was accomplished using the Express-In Transfection Reagent (Open Biosystems).

Reverse transcription and qRT-PCR (quantitative real-time PCR)

Total RNA was isolated from HEK-293 cells using TriReagent solution (MRC). First-strand cDNA was synthesized from 4 µg of total RNA with the use of Superscript III reverse transcriptase (Invitrogen) and Oligo-dT primers (Promega). Pre-amplification and relative quantification was performed according to the manufacturer's instructions (Applied Biosystems). Ten pre-amplification cycles were run with 12.5 µl of cDNA and a 0.05× pooled mixture of eight TaqMan Gene Expression Assays [Hs00971639_m1, *COX4I1*; Hs00261747_m1, *COX4I2*; Hs01924685_g1, *COX6A1*; Hs00193226_g1, *COX6A2*; Hs00427620_m1, *TBP* (TATA-box-binding protein); Hs00173304_m1, *PPARGC1A* (peroxisome-proliferator-activated receptor γ co-activator 1 α); Hs00188166_m1, *SDHA* (succinate dehydrogenase complex subunit A; Hs01082775_m1, *TFAM* (transcription factor A, mitochondrial)]. Relative quantification was performed in duplicates twice on the 7300 Real-Time PCR System (Applied Biosystems). The transcript levels of all mRNAs were normalized to the level of *TBP* mRNA. Because the amplification efficiency of the reference and target genes was the same, the comparative $\Delta\Delta C^t$ method was used for relative quantification.

Immunoblot analysis

Protein sample preparation and signal acquisition for SDS, BN (blue native) and BN-SDS/PAGE immunoblot analysis were performed essentially as described in [11,14]. The immunoblots were developed with SuperSignal West Femto Maximum Sensitivity Substrate (Thermo Scientific). For analysis of respiratory supercomplexes by BN-SDS/PAGE and BN/BN-PAGE, isolated mitochondria were extracted using digitonin (detergent/protein ratio of 6). Primary detection of BN-SDS/PAGE and BN/BN-PAGE immunoblots was performed with mouse monoclonal antibodies (Mitosciences) raised against the complex I subunit NDUFB6 [NADH dehydrogenase (ubiquinone) 1 β subcomplex 6], complex III subunit Core1 and complex IV subunit Cox1. The first dimension gel strips for BN/BN-PAGE immunodetection were soaked in cathode buffer containing 0.1% DDM (n-dodecyl- β -D-maltoside) for 15 min and then in cathode buffer containing 0.02% DDM for another 15 min. The second dimension of BN-PAGE separation was performed in the presence of 0.02% DDM as described in [15].

Spectrophotometric assays

The activities of respiratory chain complexes were measured spectrophotometrically with a UV-2401PC instrument (Shimadzu). Rotenone-sensitive complex I activity (NADH:ubiquinone oxidoreductase) was measured by incubating 45 µg of mitochondrial protein in 1 ml of assay medium (50 mM Tris/HCl, pH 8.1, 2.5 mg/ml BSA, 50 µM decylubiquinone, 0.3 mM KCN and 0.1 mM NADH without or with 3 µM rotenone). The decrease in absorbance at 340 nm due to the NADH oxidation was followed. Complex II activity (succinate:2,6-dichloroindophenol oxidoreductase) was measured by incubating 20 µg of mitochondrial extract in 1 ml of assay medium (10 mM potassium phosphate, pH 7.8, 2 mM EDTA, 1 mg/ml BSA, 0.3 mM KCN, 10 mM succinate, 3 µM rotenone, 0.2 mM ATP, 80 µM 2,6-dichloroindophenol, 1 µM antimycin and 50 µM decylubiquinone). The decrease in absorbance at 600 nm due to the reduction of 2,6-dichloroindophenol was monitored. CcO activity was measured by incubating 15–18 µg of mitochondrial protein in 1 ml of assay medium (40 mM potassium phosphate, pH 7.0, 1 mg/ml BSA, 25 µM reduced cytochrome *c* and 2.5 mM DDM) and the oxidation of cytochrome *c* (II) at 550 nm was monitored. All assays were performed at 37 °C. The total protein was determined using the method of Lowry [16].

High-resolution respirometry and oxygen kinetics

Oxygen consumption measurements were performed as described previously [14], except that the cells were permeabilized with 50–75 µg/ml digitonin and 0.5 µM FCCP (carbonyl cyanide *p*-trifluoromethoxyphenylhydrazone) was used to uncouple and maximally stimulate respiration. The P_{50} (partial pressure of oxygen at the half-maximal respiration rate) value was measured in the presence of 0.5 µM FCCP and 10 mM succinate essentially as described in [17]. All measurements were performed independently three to six times for each cell line.

RESULTS

Cox4i1 and Cox6a1 isoforms account for the majority of Cox4 and Cox6a transcripts expressed in HEK-293 cells under normal conditions

Because two tissue-specific isoforms of subunits Cox4 and Cox6a were described in humans, we measured the levels of *COX4I1*,

COX4I2, *COX6A1* and *COX6A2* mRNAs in HEK-293 cells. To quantify both isoforms using qRT-PCR, pre-amplification of the cDNA was necessary. The transcript levels of all mRNAs were normalized to the level of *TBP* mRNA. The relative normalized level of *COX4I1* mRNA was found to be $\sim 2 \times 10^5$ times higher than *COX4I2*, whereas the relative normalized level of *COX6A1* mRNA was $\sim 5 \times 10^6$ times higher than that of *COX6A2* (Figure 1A). This finding suggests that the vast majority of Cox4 and Cox6a expressed and assembled within the CcO complex in HEK-293 cells are represented by Cox4i1 and Cox6a1 tissue isoforms.

Subunits Cox4, Cox5a and Cox6a are depleted in HEK-293 cells by the stable expression of shRNAmir

Owing to the considerably long half-life of the CcO complex [2] and the relatively large amount of material required for subsequent analyses, a stable vector-based RNAi (RNA interference) approach was utilized to down-regulate the expression of Cox4, Cox5a and Cox6a in HEK-293 cells. We designed and constructed 13, nine and 11 pCMV-GIN-ZEO derivatives encoding miR-30-based shRNAs (shRNAmirs) targeting human *COX4I1*, *COX5A* and *COX6A1* mRNAs respectively. These plasmids were used to generate stable KD in HEK-293 cells. Six out of the 33 produced cell lines, which were found to have substantially lower levels of the target proteins, were selected for further analyses (Figure 1B).

The residual levels of the target subunits in mitochondrial preparations were quantified using denaturing Western blots. Serial dilutions of protein isolated from the mitochondria of the control line expressing non-silencing shRNA were loaded on the same gels as the KD samples so that the steady-state levels of the respective polypeptides in KD cells could be assessed as a percentage of the control values (see Supplementary Figure S1 at <http://www.BiochemJ.org/bj/428/bj4280363add.htm>). The residual amount of the Cox4 polypeptide was found to be 45% in *COX4I1* (sh1) KD and 55% in *COX4I1* (sh14) KD mitochondria. In the *COX5A* (sh5) KD and *COX5A* (sh7) KD samples, the amount of Cox5a polypeptide was decreased to 35 and 20% respectively. The Cox6a1 polypeptide was decreased to 25 and 35% in *COX6A1* (sh11) KD and *COX6A1* (sh12) KD mitochondria respectively.

Relative normalized mRNA levels ($2^{-\Delta\Delta C_t} \times 100$) of the major *COX4I1* and minor *COX4I2* isoform were 33 and 24% in the *COX4I1* (sh1) KD sample, and 18 and 77% in the *COX4I1* (sh14) KD sample respectively. The relative normalized mRNA levels of the major *COX6A1* and minor *COX6A2* isoform accounted for 13 and 21% in the *COX6A1* (sh11) KD sample, and 12 and 105% in the *COX6A1* (sh12) KD sample respectively.

Steady-state levels of a subset of respiratory chain subunits as well as several other mitochondrial proteins are not affected in *COX4*-, *COX5A*- and *COX6A*-KD cells

The mitochondrial preparations used to quantify target subunits were utilized for SDS/PAGE immunodetection to determine the steady-state levels of selected CcO subunits, representative respiratory chain subunits and several other mitochondrial proteins (see Supplementary Figure S1).

Depletion of subunit Cox4 led to a reduction in the level of Cox5a to 45% in *COX4I1* (sh1) KD and 55% in *COX4I1* (sh14) KD samples compared with the control. The levels of Cox1 and Cox2 were both 80 and 90% of the control values in *COX4I1* (sh1) and (sh14) KD samples respectively. Depletion of subunit Cox5a resulted in a decrease in the levels of Cox4 and Cox2 to 35% in *COX5A* (sh5) KD and 20% in *COX5A* (sh7) KD, whereas the level of Cox1 remained unchanged. Down-regulation of subunit Cox6a

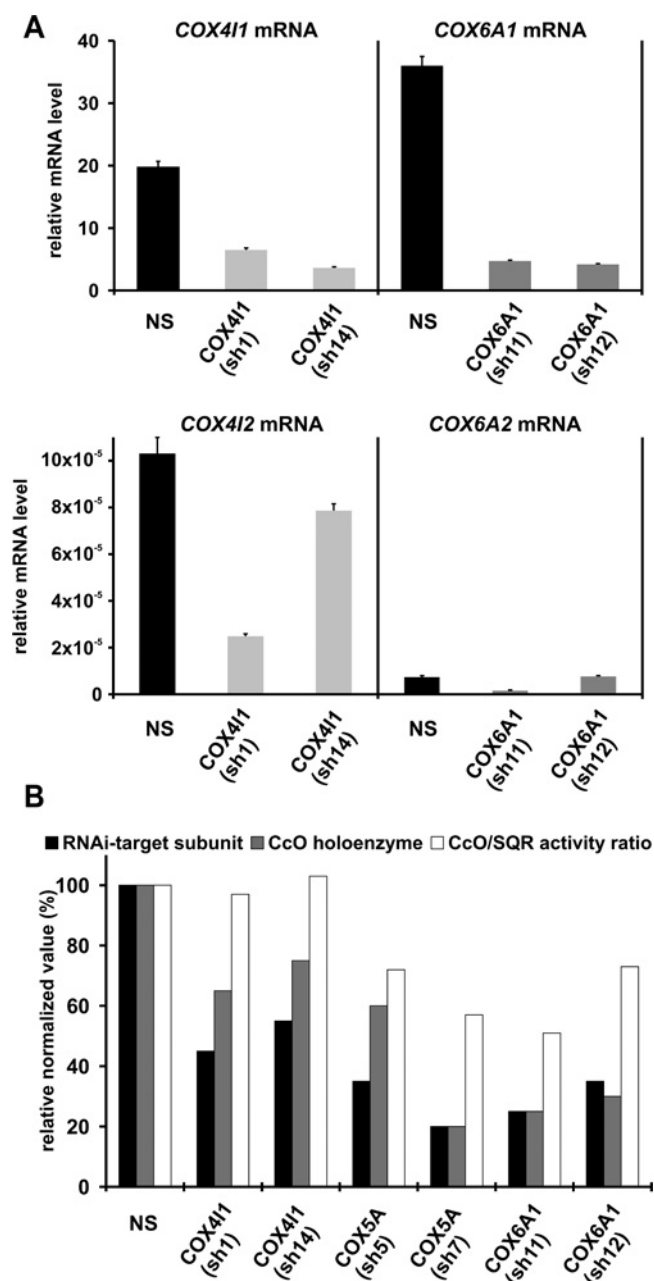


Figure 1 Levels of *COX4* and *COX6A* mRNAs and the effects of shRNA KD of *COX4I1*, *COX5A* and *COX6A1* in HEK-293 cells

(A) mRNA levels of *COX4* and *COX6A* isoforms in control and *COX4* and *COX6A1*-KD HEK-293 cells, normalized to the level of *TBP* mRNA ($2^{-\Delta\Delta C_t}$). (B) The relationship between the residual target subunit, content of CcO and its enzyme activity. The residual level of the target subunit was determined by SDS/PAGE of mitochondrial protein samples ($\sim 30 \mu\text{g}$) and Western blotting. The amount of CcO holoenzyme was determined by BN (5–15% acrylamide gradient)-PAGE of mitochondrial proteins ($\sim 20 \mu\text{g}$) solubilized using 1.1% DDM (4.8 DDM/protein) followed by Western blotting. Immunoreactive material was visualized by chemiluminescence. For the loading control, the amount of target subunit was normalized to that of subunit SDHA of complex II and to the outer membrane protein porin. The amount of CcO holoenzyme was normalized to that of complex II. The final values are expressed relatively to control (NS) sample, which was arbitrarily set at 100%. The CcO activity was determined by measuring the rate of cytochrome *c* oxidation (nmol/min per mg of mitochondrial protein) and normalized to the activity of complex II (SQR) (CcO/SQR ratio), which was determined by measuring the rate of 2,6-dichloroindophenol reduction (nmol/min per mg of mitochondrial protein). For comparison with the level of RNAi-target subunit and CcO content, the CcO/SQR ratio of the mean activity values was, in turn, expressed relative to the CcO/SQR ratio value obtained in the control (NS) sample, which was arbitrarily set at 100%. NS, mitochondria from HEK-293 cells expressing the non-silencing control shRNAmir.

caused a reduction in the levels of subunits Cox1, Cox2, Cox4 and Cox5a to 80 % of the control values. The steady-state levels of PDH-E2 (pyruvate dehydrogenase subunit E2), porin, cytochrome *c*, the 70-kDa flavoprotein subunit of SDHA, the ATP synthase subunit F_1 - β (ATPase F_1 - β), complex III core protein 2 and the complex I subunit NDUFA9 [NADH dehydrogenase (ubiquinone) 1 α subcomplex 9] were not changed compared with the control.

Depletion of subunits Cox4, Cox5a and Cox6a decreases the quantity of CcO holoenzyme and increases an accumulation of CcO subcomplexes

To study the impact of the depletion of subunits Cox4, Cox5a and Cox6a on CcO holoenzyme levels, we performed 5–15 % BN-PAGE Western blot analyses. The same mitochondrial fractions used for SDS/PAGE Western blots were solubilized in DDM and analysed along with serial dilutions of control samples (Figure 2A). The amount of CcO holoenzyme was diminished to 65 % of the control value in *COX4I1* (sh1) KD and to 75 % of the control value in *COX4I1* (sh14) KD samples. The *COX5A* (sh7) and (sh5) KD samples showed a decrease in the amount of the CcO holoenzyme to 20 and 60 % of the control values respectively. In *COX6A1* (sh11) KD and *COX6A1* (sh12) KD samples, CcO holoenzyme was reduced to 25 and 30 % of the control values respectively.

To investigate the assembly pattern of CcO, we performed BN-PAGE as well as two-dimensional BN-SDS/PAGE, in which we utilized 8–16 % polyacrylamide gradients followed by Western blot analysis of the selected subunits. The BN anti-Cox1 immunoblots revealed the presence of several distinct bands in KD mitochondria, which were denoted *a–e* (Figure 2B). The holoenzyme band *a* was, in fact, found to be composed of two bands (*a*₁ and *a*₂) [18]. *COX6A1*-KD mitochondria showed a reduction in the levels of both bands *a*₁ and *a*₂ to 20 % of the control values (Figures 2B and 2C). In contrast, the decrease in band *a*₁ in *COX4*- and *COX5A*-KD samples, which was comparable with that for *COX6A1*-KD mitochondria, was accompanied by a more profound reduction in the amount of band *a*₂ (Figures 2B and 2C). In addition to band *a*, anti-Cox1 immunoblotting detected three faster migrating bands (*b*, *x* and *c*) in all samples with approximate molecular masses of 180, 155 and 110 kDa respectively. Band *b*, which was barely discernible between control, *COX4*-KD and *COX5A*-KD mitochondria, was increased in *COX6A*-KD samples (Figure 2B). This band probably represents the previously identified assembly intermediate S3 (Figure 2D) [2]. Band *x*, which was almost undetectable in controls and slightly increased in *COX6A*-KD mitochondria, was markedly increased in the *COX5A* (sh7) KD sample. Despite its high apparent molecular mass, this band was detectable only with the anti-Cox1 antibody. Band *c*, which was detected in all samples, was increased in *COX4*- and *COX5A*-KD mitochondria. This band was detected with antibodies against Cox1, Cox4 and Cox5a in *COX6A1*-KD samples, but only with the anti-Cox1 antibody in *COX4*- and *COX5A*-KD samples (Figure 2D). Finally, bands *d* and *e*, with approximate molecular masses of 100 and 85 kDa respectively, were found only in *COX4*- and *COX5A*-KD samples. These bands were increased in the severely CcO-deficient *COX5A* (sh7) KD sample and were detected exclusively with the anti-Cox1 antibody.

Whereas CcO activity is significantly decreased, activities of respiratory chain complexes I, II and III are not affected in *COX5A*- and *COX6A1*-KD cells

To assess residual CcO activity in mitochondrial preparations, we determined CcO activity and normalized it to the activity of SQR (succinate:coenzyme Q₁₀ reductase, complex II) (Figure 1B).

The same mitochondrial preparations used in the electrophoretic analyses were utilized in these assays. The relative CcO/SQR ratio values obtained for mitochondria from the *COX4I1* (sh1) (97 %) and *COX4I1* (sh14) (103 %) KD cells were comparable with that obtained for control cells. In *COX5A* (sh5) KD and *COX5A* (sh7) KD mitochondria, the relative normalized CcO/SQR ratio accounted for 72 and 57 % of the control values respectively. The mitochondrial preparations from *COX6A1* (sh11) KD and *COX6A1* (sh12) KD cells revealed a decrease in the CcO/SQR ratio to 51 and 73 % of the control values respectively. The activities of the remaining respiratory chain complexes were found to be unchanged in all of the KD samples investigated (results not shown).

Isolated CcO deficiency due to *COX5A* and *COX6A1* KD affects the organization of respiratory supercomplexes in HEK-293 cells

To study the impact of *COX5A* and *COX6A1* KD on the composition of respiratory chain supercomplexes, mitochondrial fractions were solubilized with digitonin (digitonin/protein ratio of 6) and analysed by BN-SDS/PAGE and BN/BN-PAGE Western blotting. Both approaches showed that *COX5A* and *COX6A1* KD significantly decreased the levels of the dimeric form of the CcO holoenzyme (Figure 3). Furthermore, BN/BN-PAGE Western blots revealed markedly reduced levels of supercomplexes III₂IV₂ and I₁III₂IV₂, which apparently contained the dimeric form of the CcO holoenzyme (Figure 3B). In contrast, the amount of the major mammalian supercomplex I₁III₂IV₁ was normal or slightly increased (Figure 3B). The appearance of the faint spot corresponding to undissociated IV₂ below the spot corresponding to III₂ of the III–IV-containing supercomplex substantiates the presence of the III₂IV₂, rather than the III₂IV₁ supercomplex in the samples (Figure 3B, long exposure). The two spots migrating above complex I probably represent undissociated supercomplexes (e.g. I₁III₂IV₁ and I₁IV₁) [19].

In all samples, including the controls, BN/BN-PAGE immunoblots revealed additional spots that migrated at the level of supercomplexes in the first dimension, but had apparent molecular masses lower than that of the CcO holoenzyme (Figure 3B). These spots were most apparent in *COX5A*-KD mitochondria, which exhibited the most severe CcO holoenzyme defect and the highest accumulation of incomplete CcO assemblies (Figure 2B). Indeed, these spots might represent CcO assembly intermediates already in the form of respiratory supercomplexes.

Normal normoxic respiration is accompanied by increased P_{50} values in *COX5A*- and *COX6A1*-KD cells

To further characterize mitochondrial respiratory function in *COX5A* (sh7) KD and *COX6A1* (sh11) KD cells, we performed high-resolution respirometry using the Oroboros Oxygraph. The only difference observed in this assay was diminished oxygen consumption (~80 % of control) after the addition of ascorbate/TMPD (*N,N,N,N'*-tetramethyl-*p*-phenylenediamine) substrates in *COX5A* (sh7) KD cells (Figure 4A). Therefore we analysed the respiratory response of the cells to low oxygen. The digitonin-permeabilized cells were treated with FCCP to uncouple and maximally stimulate respiration (state 3u) and were then treated with succinate. The oxygen kinetics were quantified by determining the P_{50} . The average P_{50} value was 0.072 ± 0.02 (S.D.) kPa ($n = 6$) in control (non-silencing) cells, 0.163 ± 0.01 kPa ($n = 5$) in *COX5A* (sh7) KD cells and 0.105 ± 0.01 kPa ($n = 3$) in *COX6A1* (sh11) KD samples (Figure 4B). Thus the P_{50} value was elevated more than 2-fold in *COX5A* (sh7) KD and ~1.5-fold in *COX6A1* (sh11) KD cells.

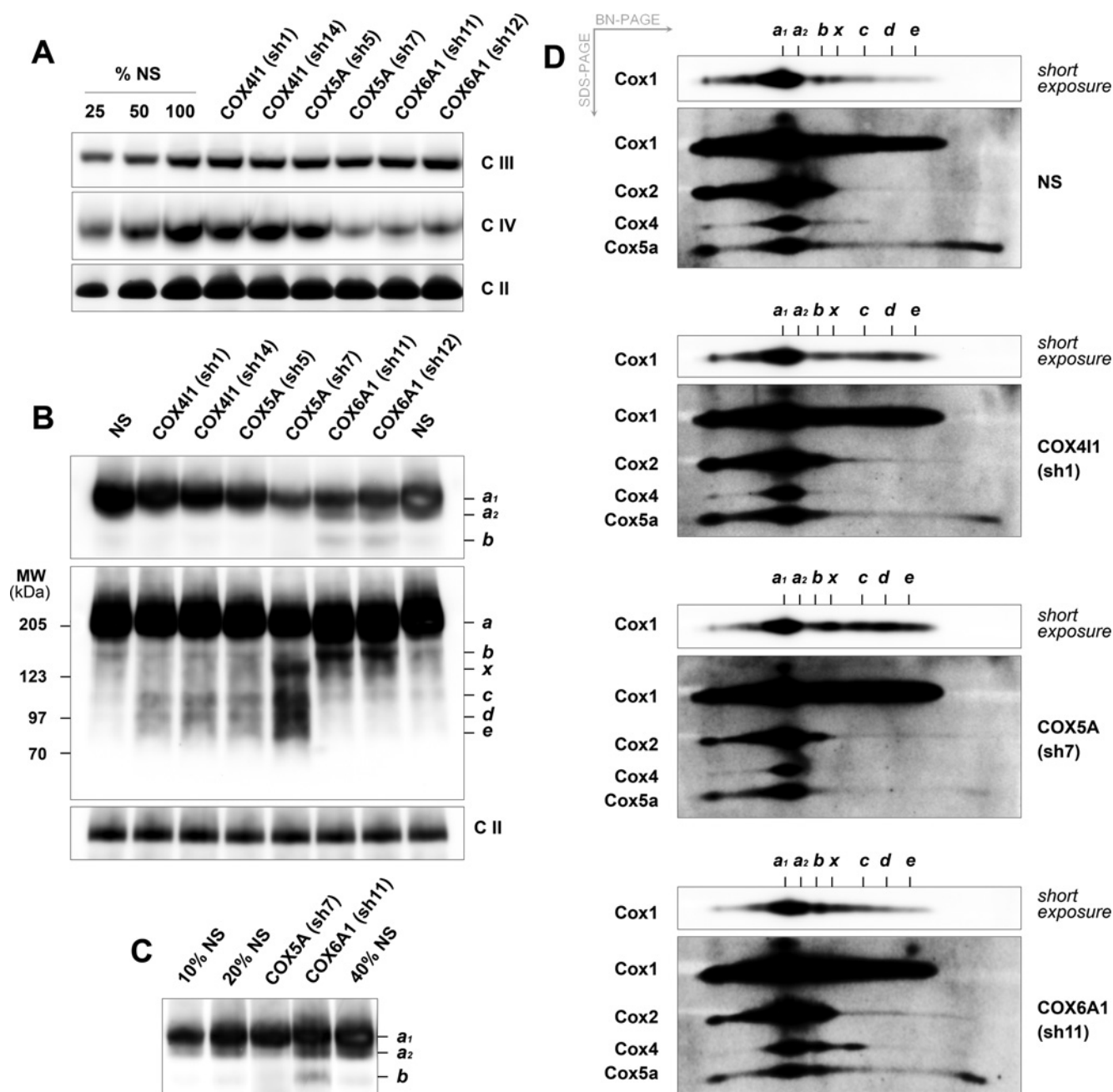


Figure 2 Levels of CcO holoenzyme and the assembly pattern of CcO in *COX4*-, *COX5A*- and *COX6A1*-KD mitochondria

(A) Equal amounts ($\sim 20 \mu\text{g}$) of mitochondrial protein prepared by solubilization using 1.1% DDM (4.8 DDM/protein) and serial dilutions of non-silencing control samples (NS) were resolved by BN (5–15% acrylamide gradient)-PAGE and subjected to Western blot analysis with an anti-Cox1 antibody. (B) Mitochondrial proteins ($\sim 25 \mu\text{g}$) prepared by solubilization using 1.1% DDM (4.8 DDM/protein) were resolved by BN (8–16% acrylamide gradient)-PAGE and subjected to Western blot analysis with an anti-Cox1 antibody. Both short (upper panel) and long (lower panel) exposures are shown. Equal loading was verified using antibodies against the complex II subunit SDHA and the complex III subunit Core 2 (A, B). (C) The same protein samples as in (B) were fractionated using BN (7–10% acrylamide gradient)-PAGE and subjected to Western blot analysis with an anti-Cox1 antibody. The amount of protein loaded per lane was normalized to the signal of the holoenzyme band a_1 . (D) The same protein samples as in (B) ($\sim 35 \mu\text{g}$) were resolved by two-dimensional BN (8–16 acrylamide gradient)-SDS (13% acrylamide) or 13% BN-SDS/PAGE and subjected to Western blot analysis with a cocktail of antibodies specific for subunits Cox1, Cox2, Cox4 and Cox5a. The migration direction of the first, native (BN-PAGE), and the second, denaturing (SDS/PAGE), dimension are marked with grey arrows. The positions of bands a – e and the molecular mass (MW) of complex II (123 kDa), the SDHA–SDHB (succinate dehydrogenase complex subunit B) subcomplex (97 kDa) and SDHA (70 kDa) are indicated. Both short and long Cox1-specific exposures are shown. Immunoreactive material was visualized by chemiluminescence (A–D).

Overexpression of the Cox6a2 isoform complements the quantitative CcO holoenzyme defect of *COX6A1*-KD cells

Despite the substantial decrease in CcO holoenzyme levels, the levels of heart/muscle-specific *COX6A2* mRNA remained low in Cox6a1-depleted CcO-deficient cells (Figure 1A). Therefore we

tested whether the Cox6a2 isoform can substitute for subunit Cox6a1 during CcO assembly in HEK-293 cells. To obtain optimal accumulation of the subunit polypeptide, the cells were transfected twice consecutively, leading to transgene expression for a total of 4 days. Both untagged and FLAG-tagged forms were used to transfect wild-type and *COX6A1*-KD cells. This analysis

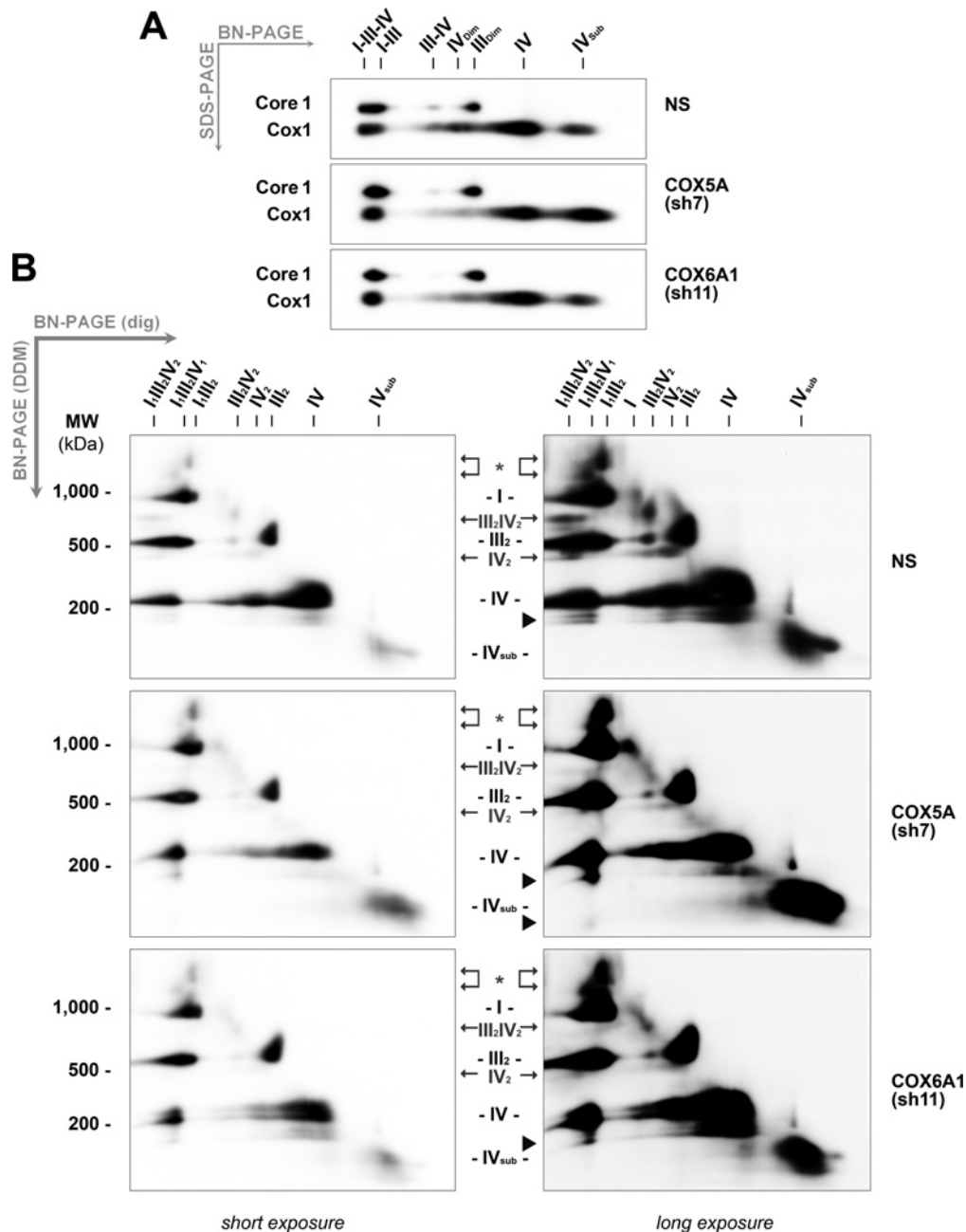


Figure 3 Supramolecular organization of CcO in *COX5A*- and *COX6A1*-KD cells

(A) Digitonin-solubilized (6 digitonin/protein) mitochondrial proteins were separated by two dimensional BN (5–12% acrylamide gradient)-SDS (10% acrylamide)/PAGE (~45 μ g) and subjected to Western blot analysis with antibodies specific for the complex III subunit Core 1 and the complex IV subunit Cox1. IV_{Dim} and III_{Dim} indicate complex IV and III homodimers respectively, and IV_{Sub} indicates CcO subcomplexes. NS, non-silencing control samples. The migration direction of the first, native (BN-PAGE), and the second, denaturing (SDS-PAGE), dimension are indicated with grey arrows. (B) The same protein preparations as in (A) (~45 μ g) were fractionated using two-dimensional BN (4–13% acrylamide gradient)/BN (4–15% acrylamide gradient)-PAGE and subjected to Western blot analysis with a cocktail of antibodies specific for the complex I subunit NDUFB6, the complex III subunit Core 1 and the complex IV subunit Cox1. The migration direction of the first (dig) and the second (DDM) dimension are indicated with grey arrows. Complexes from the first BN-PAGE that retained their masses after two-dimensional BN-PAGE are found on a diagonal. Supercomplexes that dissociated into individual complexes were detected below the diagonal. The small arrows indicate supramolecular assemblies of respiratory complexes that did not dissociate in the second dimension. Asterisks indicate undissociated supercomplexes of higher molecular masses than complex I. Arrowheads denote spots migrating in the first dimension at the level of supercomplexes, but with apparent molecular masses (MW) lower than that of the CcO holoenzyme. Immunoreactive material was visualized by chemiluminescence (A and B).

was simplified by the fact that both *COX6A1* shRNAmirs used to prepare the KD cells targeted the 3'-UTR (untranslated region) of *COX6A1* mRNA, which was not present in our Cox6a2 expression constructs.

The ectopic expression of the Cox6a2 isoform in *COX6A1* (sh11) KD cells led to the restoration of wild-type CcO

levels. The total pool of CcO in these cells consisted of the Cox6a2-containing enzyme as well as residual Cox6a1-containing molecules (~25%) (Figure 5B). Therefore both untagged (Figures 5A and 5B) and FLAG-tagged (Figures 5A and 5C) Cox6a2 polypeptides could substitute for the Cox6a1 isoform during CcO assembly in HEK-293 cells. From these experiments,

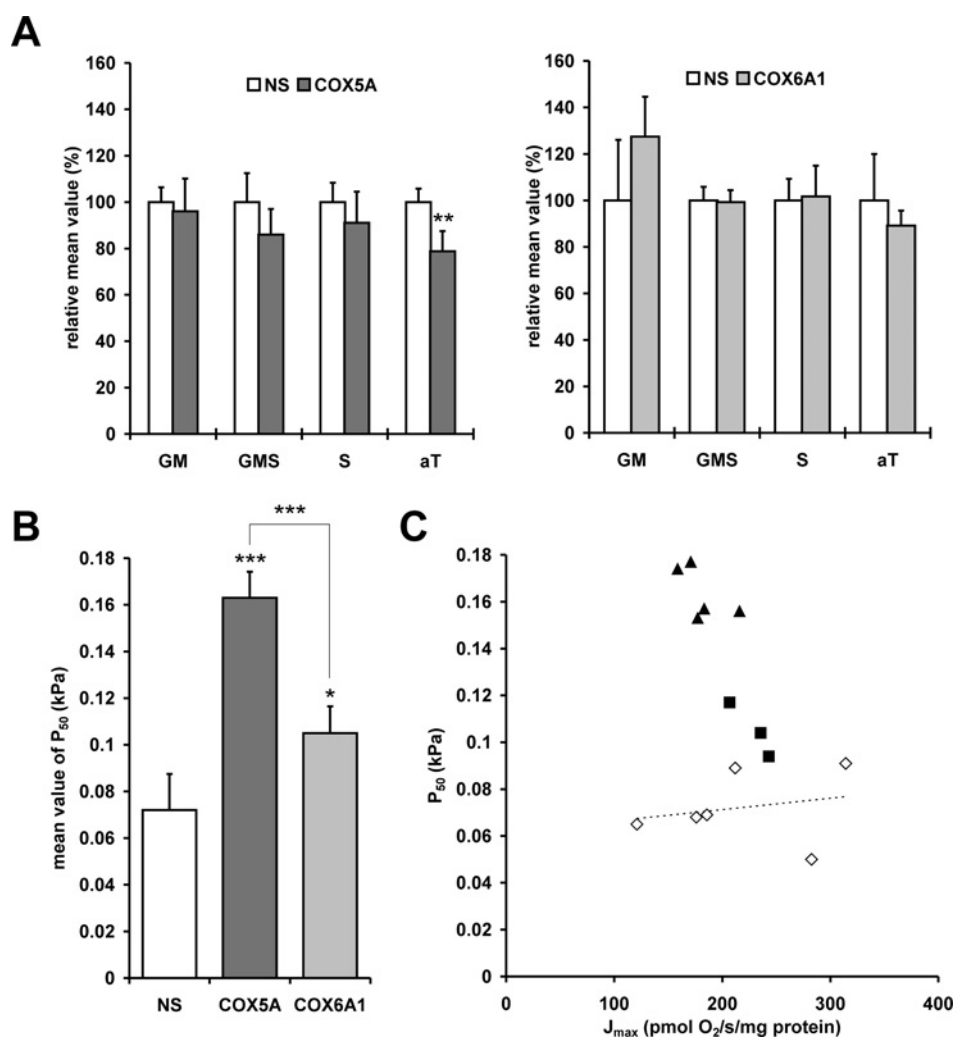


Figure 4 High-resolution respirometry in permeabilized (digitonin-treated) uncoupled (FCCP-treated) *COX5A*- and *COX6A1*-KD cells

(A) Respiration at environmental normoxic levels of oxygen. The mean rate of oxygen consumption (pmol of O_2 /s per mg of protein) in KD cells was expressed relative to the non-silencing control (NS) mean value, which was arbitrarily set at 100%. GM, relative respiration after addition of glutamate and malate (rotenone-sensitive); GMS, relative respiration after addition of glutamate, malate and succinate (antimycin A-sensitive); S, relative respiration after addition of succinate (antimycin A-sensitive); aT, relative respiration after addition of ascorbate and TMPD (sodium azide-sensitive). (B) Mean P_{50} values in cells supplied by succinate. Results in (A) and (B) are means \pm S.D. (C) The relationship of P_{50} and protein-specific oxygen flux. P_{50} values from individual measurements were plotted as a function of protein-specific oxygen flux (J_{max}). \diamond , Control sample (NS); \blacktriangle , *COX5A* (sh7) KD cells; \blacksquare , *COX6A1* (sh11) KD cells. * $P < 0.05$; ** $P < 0.01$; *** $P < 0.001$.

it was also apparent that ectopic expression of Cox6a2 in wild-type HEK-293 cells increased the amount of CcO holoenzyme (band a_1) as well as the level of band a_2 . In all transfected samples, including controls, an increase in the amount of the assembly intermediate S3 (band b) was observed, probably as a result of the transfection treatment (Figures 5A and 5B).

The consequences of increased CcO content after ectopic expression of the Cox6a2 isoform in *COX6A1*-KD cells were analysed by spectrophotometric measurement of CcO activity. CcO activity in Cox6a2-FLAG expressing cells, which was normalized to the activity of the control enzyme (SQR), did not change significantly compared with either untreated wild-type cells or wild-type cells transfected with the control vector (1.26–1.29). In *COX6A1*-KD cells, ectopic expression of the Cox6a2-FLAG isoform led to a ~ 1.5 -fold increase in CcO/SQR activity ratio compared with transfection with the control vector (CcO/SQR ratio was 0.75 and 0.49 respectively) (Figure 5D).

Subunit Cox7a2 enters the CcO assembly after Cox7b, but before Cox6a2

To elucidate the entry points of subunits Cox7a2 and Cox7b with respect to the formation of the assembly intermediate S3, which shows increased accumulation in *COX6A1*-KD cells, we transfected *COX6A1*-KD cells with expression constructs containing Cox7a2- and Cox7b-coding sequences fused to a C-terminal FLAG epitope. To obtain optimal accumulation of the subunit polypeptides, the cells were transfected twice consecutively, leading to transgene expression for a total of 4 days. Subsequently, isolated mitochondria were resolved by BN (7–10% acrylamide gradient)-PAGE and subjected to Western blot analysis using antibodies specific to Cox1 and the FLAG epitope. No changes in the amount of the CcO holoenzyme or S3 intermediate were observed in *COX6A1*-KD mitochondria upon expression of these polypeptides (Figure 5C).

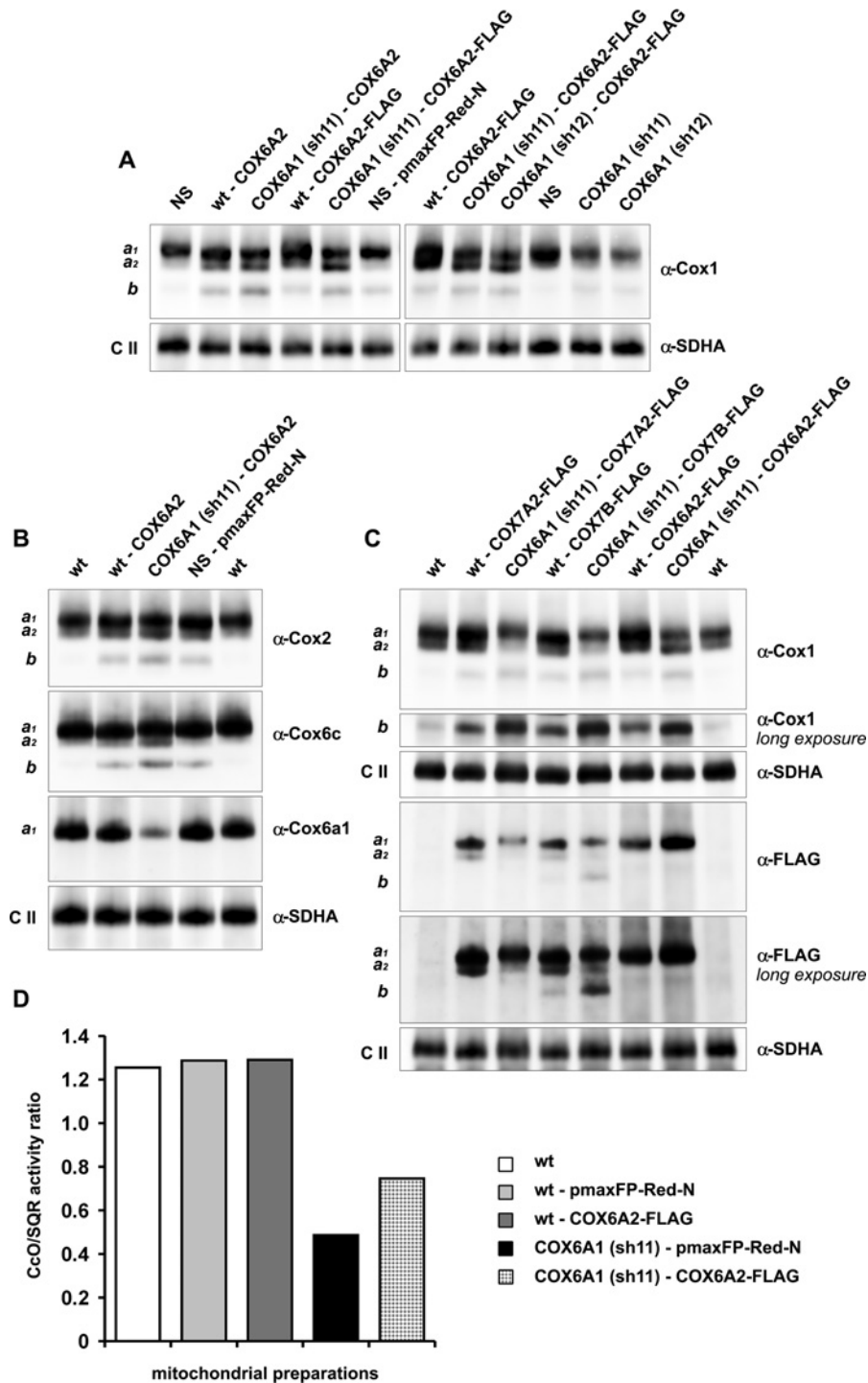


Figure 5 Expression of FLAG-tagged versions of Cox6a2, Cox7a2 and Cox7b in wild-type and *COX6A1*-KD HEK-293 cells

(**A** and **B**) Equal amounts (~ 20 – $50 \mu\text{g}$) of mitochondrial protein were solubilized using 1.1% DDM (4.8 DDM/protein) and resolved by BN (7–10% acrylamide gradient)-PAGE and subjected to Western blot analysis with antibodies specific to Cox1 (**A**), Cox2, Cox6c and Cox6a1 (**B**). (**C**) Equal amounts of mitochondrial protein solubilized using 1.1% DDM (4.8 DDM/protein) were resolved by BN (7–10% acrylamide gradient)-PAGE and subjected to Western blot analysis with antibodies specific to the Cox1 subunit ($\sim 20 \mu\text{g}$ of protein loaded per lane) and FLAG epitope ($\sim 60 \mu\text{g}$ of protein loaded per lane). Both short and long exposures are shown. (**A**–**C**) Equal loading was verified using an antibody against the complex II subunit SDHA. Positions of the various assembly forms of complex IV (*a* and *b*) and holoenzyme of complex II (**C II**) as well as specificity of the antibodies (in the right hand margin) are indicated. Immunoreactive material was visualized by chemiluminescence. (**D**) CcO activity was determined by measuring the rate of cytochrome *c* oxidation (nmol/min per mg of mitochondrial protein) and normalized to the activity of complex II (SQR) (CcO/SQR ratio), which was determined by measuring the rate of 2,6-dichloroindophenol reduction (nmol/min per mg of mitochondrial protein). NS, mitochondria from stable HEK-293 cells expressing the non-silencing control shRNAmir; wt, mitochondria from wild-type HEK-293 cells; wt - COX6A2, mitochondria from wild-type HEK-293 cells transiently transfected with a construct encoding the Cox6a2 subunit; wt - COX6A2-FLAG, mitochondria from wild-type HEK-293 cells transiently transfected with a construct encoding the FLAG epitope-tagged Cox6a2 subunit; wt - COX7A2-FLAG, mitochondria from wild-type HEK-293 cells transiently transfected with a construct encoding the FLAG epitope-tagged Cox7a2 subunit; wt - COX7B-FLAG, mitochondria from wild-type HEK-293 cells transiently transfected with a construct encoding the FLAG epitope-tagged Cox7b subunit; wt - pmaxFP-Red-N, mitochondria from wild-type cells transiently transfected with control plasmid pmaxFP-Red-N encoding a fluorescent marker; COX6A1

In contrast with the anti-Cox1 immunoblot, which detected the S3 intermediate in all of the analysed samples (Figure 5C, long exposure of band *b*), the FLAG-specific antibody cross-reacted with this assembly intermediate only in mitochondria from cells expressing Cox7b-FLAG. The fact that Cox1-specific, but not FLAG-specific, antibodies detected S3 in the samples expressing Cox7a2-FLAG indicated that, unlike Cox7b, Cox7a2 is incorporated after the formation of the assembly intermediate S3 (Figure 5C).

Mitochondrial preparations from cells transfected with the Cox6a2-FLAG construct were also analysed for the presence of expressed subunits in the late assembly forms of CcO. Despite the high cross-reactivity of both bands *a*₁ and *a*₂ with the anti-Cox1 antibody in these samples, the FLAG-specific antibody detected band *a*₂ only in Cox7a2-FLAG- and Cox7b-FLAG-expressing samples (Figure 5C). Furthermore, when endogenous Cox6a1 was probed, only *a*₁ was detected in samples, whereas both bands *a*₁ and *a*₂ were confirmed with antibodies specific to Cox1, Cox2 or Cox6c (Figures 5A and 5B). These results indicate that subunit Cox6a is incorporated after the formation of band *a*₂, probably as the last structural subunit incorporated into the human CcO complex.

DISCUSSION

CcO is a crucial cellular enzyme with a central role in oxidative metabolism [2,20]. The significant interest in the biogenesis of CcO stems from its clinical importance. Defective CcO biogenesis is frequently related to severe mitochondrial diseases that often involve tissues with a high energy demand [2,21,22].

It was demonstrated previously in various non-human eukaryotic models that KD of Cox4 or Cox5a affects CcO holoenzyme content [23–26]. Deficiency of subunit Cox6a was described to cause severe CcO deficiency in *Drosophila* [27] and mice [28]. However, the yeast Cox6a homologue is dispensable for assembly of the yeast CcO complex [29]. In the present study, we have demonstrated that the impact of stable down-regulation of Cox4i1, Cox5a and Cox6a1 in cultured human cells on the content of CcO corresponds to similar studies in higher eukaryotes. Furthermore, our results provide detailed KD-specific patterns of CcO assembly intermediates and indicate several novel aspects of the sequential incorporation of subunits during the assembly process, including identification of a novel assembly intermediate in human CcO assembly.

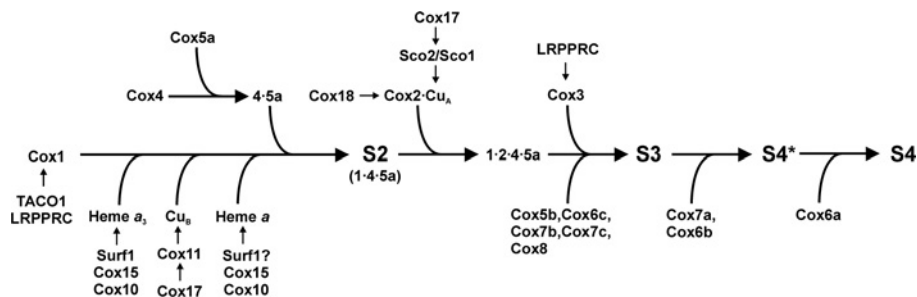
Overall, the accumulation of CcO subcomplexes seen in our KD cells reflected the proposed entry of individual subunits into the assembly. The effects of *COX6A* KD on CcO subcomplex pattern was manifested mainly by the marked increase in the assembly intermediate S3. Unlike *COX4*- and *COX5A*-KD mitochondria, in which the reduction in the holoenzyme band *a*₁ was accompanied by a more pronounced decrease in band *a*₂, *Cox6a*-deficient mitochondria retained significantly higher levels of the latter species. These results indicate that band *a*₂ represents another rate-limiting step in human CcO assembly. Both Cox6a and Cox6b subunits, which are thought to be responsible for dimerization

of CcO, are the first to dissociate from the bovine complex under various destabilizing conditions [30,31]. Thus it appears plausible that the elevated levels of the assembly intermediate S3 in *COX6A*-KD cells could stem from compromised binding of Cox6b, which might be contingent upon the concomitant assembly of Cox6a. KD of both early-assembled subunits Cox4 and Cox5a resulted in accumulation of four subcomplexes consisting merely of subunit Cox1. The absence of Cox1-Cox4/Cox5a heterodimers confirmed further the interdependence of the assembly of Cox4 and Cox5a [11,32]. Together with the lack of accumulation of higher-molecular-mass intermediates, our findings suggest that the assembly of the Cox4-Cox5a heterodimer with Cox1 is necessary for the subsequent association of Cox2, and thus for the rest of the assembly to proceed. The Cox1-containing subcomplex *x* of ~155 kDa, which apparently does not contain any of the CcO subunits that we tested, was found to be particularly increased in *COX5A*-KD mitochondria. The composition and migration of this subcomplex suggests that it might represent an off-path complex that is not relevant to the normal route of assembly. However, the other samples, including controls, contained small amounts of this subcomplex as well. A similar situation in terms of discrepancy between subunit composition and the apparent molecular mass was observed in the case of the 110 kDa subcomplex *c* from *COX4*- and *COX5A*-KD mitochondria. These results strongly suggest that individual CcO subunits as well as CcO subcomplexes associate during the assembly with several non-subunit proteins, as reported for yeast Cox1 [33]. The expression of FLAG-tagged versions of Cox7a2, Cox7b and Cox6a2 in both wild-type and Cox6a1-deficient backgrounds allowed us to elucidate for the first time the very late events in human CcO assembly. We identified the particular entry points of these three subunits and demonstrated the significance of the CcO holoenzyme bands *a*₁ and *a*₂. According to our results, band *a*₁ probably represents the 13-subunit CcO holoenzyme (S4). In contrast, band *a*₂ lacks subunit Cox6a, which appears to be added as the last assembled structural subunit. Band *a*₂ (S4*) is formed by the addition of Cox7a2 and probably Cox6b1 [18] to the assembly intermediate S3. Finally, subunit Cox7b was found to join the assembling complex during or at the end of the formation of the assembly intermediate S3 (Scheme 1).

The amount of CcO holoenzyme in *COX5A* (sh7) KD and both *COX6A1*-KD samples corresponded to the residual content of the targeted subunits. On the basis of our assertion that the Cox6a subunit completes the assembly of the CcO holoenzyme, the amount of fully assembled CcO seems to be strictly contingent upon the amount of the residual Cox6a. Furthermore, transient overexpression of subunit Cox6a in wild-type HEK-293 cells increased the content of CcO holoenzyme. Lower levels of S3 intermediate and a shift in the *a*₁/*a*₂ ratio towards *a*₁ in *COX5A* (sh7) KD samples suggest changes in the kinetics of CcO assembly in terms of the increased utilization of intermediates subsequent to the integration of Cox5a, thereby increasing the level of complete CcO complex to the level of Cox5a. A similar reduction in the levels of RNAi-target subunits in *COX5A* (sh5) KD and *COX6A1* (sh12) KD cells resulted in a milder reduction of

Figure 5 Continued

(sh11) - *COX6A2*, mitochondria from stable *COX6A1* (sh11) KD cells transiently transfected with a construct encoding the Cox6a2 subunit; *COX6A1* (sh11) or (sh12) - *COX6A2*-FLAG, mitochondria from stable *COX6A1* (sh11) or (sh12) KD cells transiently transfected with a construct encoding the FLAG epitope-tagged Cox6a2 subunit; *COX6A1* (sh11) - *COX7A2*-FLAG, mitochondria from stable *COX6A1* (sh11) KD cells transiently transfected with a construct encoding the FLAG epitope-tagged Cox7a2 subunit; *COX6A1* (sh11) - *COX7B*-FLAG, mitochondria from stable *COX6A1* (sh11) KD cells transiently transfected with a construct encoding the FLAG epitope-tagged Cox7b subunit; *COX6A1* (sh11) - pmaxFP-Red-N, mitochondria from stable *COX6A1* (sh11) KD cells transiently transfected with control plasmid pmaxFP-Red-N encoding a fluorescent marker; NS - pmaxFP-Red-N, mitochondria from NS cells transiently transfected with control plasmid pmaxFP-Red-N encoding a fluorescent marker.



Scheme 1 Proposed model of the mammalian CcO assembly pathway

Prosthetic groups and assembly factors are indicated. Arabic numerals denote CcO subunits within subcomplexes. S2 and S3 indicate previously identified assembly intermediates. S4 represents the 13-subunit CcO holoenzyme, and S4* indicates the late assembly intermediate that immediately precedes the formation of the holoenzyme (see the text for details).

CcO holoenzyme levels in Cox5a-deficient cells. This observation suggests the existence of different threshold values for the availability of various CcO subunits during enzyme assembly. The diminished content of CcO holoenzyme in our KD cells resulted in a milder reduction in specific CcO activity. Indeed, the relatively mild Cox4 reduction in *COX4I1*-KD cells resulted in virtually normal CcO activity. These observations are in line with the well-established high excess capacity of CcO [20,34].

Diaz et al. [35] demonstrated that the total loss of CcO leads to complex I deficiency in a mouse *COX10*-knockout model. Furthermore, RNAi KD of Cox4 in murine cultured cells resulted in decreased stability and activity of complex I [24]. A similar effect of *COX4*- and *COX5A*-KD on complex I was described in *Caenorhabditis elegans*, where the content of complex I was normal, but its enzymatic activity was reduced significantly [23]. In contrast, the CcO deficiency in our *COX4*-, *COX5A*- and *COX6A*-KD cells did not lead to any significant changes in the amount and/or activity of other complexes of oxidative phosphorylation system, including complex I. Similarly, normal levels and activity of complex I were also found in murine *COX5B*-KD cells with severe CcO deficiency [36]. Further work is needed to establish the potential role of fully assembled CcO in complex I biogenesis.

High-resolution respirometry in our CcO-deficient cellular model showed significantly increased P_{50} values. This may indicate either a change in mitochondrial capacity or decreased affinity for oxygen ($=1/P_{50}$) of the residual CcO [20]. The lack of a significant decrease in maximal (state 3u) normoxic respiration in our KD cells argues against the possibility that P_{50} is increased due to lower mitochondrial capacity. The second possibility, which involves a decrease in oxygen affinity in active states when the demand for oxygen is highest, is paradoxical from a functional point of view [20]. However, if the increase in P_{50} is accompanied by a greater increase in maximum flux (J_{max}), the J_{max}/P_{50} ratio still increases and indicates elevated apparent catalytic efficiency with activation by ADP [20]. When plotted as a function of the specific oxygen flux normalized to protein content, the P_{50} values in both our KD cell lines increased without a corresponding increase in oxygen flux (Figure 4C). Therefore the increase in P_{50} in our KD cells is most likely to be due to decreased affinity of CcO for oxygen, i.e. an increased apparent K_m for oxygen. Marked CcO deficiency with almost unchanged normoxic cellular respiratory rates accompanied by increased P_{50} values were also found in fibroblasts from patients with Leigh syndrome owing to Surf1 deficiency [17]. In addition to reduced holoenzyme levels, Surf1-deficient fibroblasts were characterized by increased accumulation of CcO subcomplexes. It was hypothesized that, under conditions of high oxygen pressure, the

accumulated subcomplexes could restore near normal respiration, and contribute to the increased P_{50} value [17,37]. However, it was repeatedly demonstrated that subcomplexes found in Surf1-deficient fibroblasts are devoid of the catalytic core subunit Cox2 [11,38]. Similar subcomplexes, i.e. devoid of Cox2, also accumulate in *COX5A*-KD mitochondria. Cox2 is known to mediate electrostatic binding of cytochrome *c* and represents the initial entry site for electrons. The subcomplexes in *COX6A1*-KD cells are represented mainly by incomplete CcO assemblies that lack only few peripheral nuclear-encoded subunits. Exposure of isolated monomeric bovine CcO to hydrostatic pressure results in a mixture of 13-, 11- and nine-subunit CcO complexes [31]. Analysis of separated forms showed that both the 13-subunit complex as well as the 11-subunit form devoid of subunits Cox6a and Cox6b retained 85–90% of electron transport activity of the untreated enzyme. The nine-subunit form that lacks two additional subunits (Cox3 and Cox7a) had only 40–45% activity of intact enzyme. The authors were not able to determine the loss of which of the two subunits led to such marked reduction in enzyme activity [31]. Nevertheless, the results of other studies suggest that the loss of Cox3 is likely to be responsible for the majority of CcO inactivation observed [39,40]. Both of the major intermediates found in our Cox6a-deficient cells (a_2 and S3) are thus likely to be capable of electron transfer, unlike the subcomplexes from *COX5A*-KD cells. Indeed, the capacity of CcO in *COX5A*-KD cells as measured by oxygen consumption after ascorbate/TMPD was significantly decreased, and the P_{50} value was significantly increased when compared with both control and *COX6A1*-KD samples. Therefore it appears likely that the presence of the high-molecular-mass CcO subcomplexes in *COX6A*-KD cells might contribute to cellular respiration at low oxygen levels and lead to higher apparent CcO excess capacity. In contrast, uncoupled respiration did not change at normoxic levels of oxygen after natural substrates, and spectrophotometric measurement indicated a decrease of specific CcO activity to the same extent in both cell lines.

Nonetheless, the decreased oxygen affinity of CcO in both KD cell lines appears paradoxical, as there apparently seems to be no rational reason for the decreased catalytic competence of the residual CcO enzyme. Furthermore, the substantial reduction in CcO content was accompanied by less diminished specific activity of CcO in *COX5A*- and *COX6A1*-KD cells, suggesting compensatory catalytic stimulation of the residual CcO. Taken together, we assume that decreased oxygen affinity of CcO in our KD cells results from quantitative changes in the CcO pool which, when reduced, undergoes normal flux at high oxygen pressure, but is significantly more sensitive to decreased oxygen levels. Such an assumption is in line with the oxygen dependence of CcO

flux control demonstrated previously [41]. In this study, a lower experimental concentration of oxygen was related to a steeper initial slope of the cyanide titration curve for maximal succinate oxidation rate. Moreover, a lower concentration of CcO inhibitor was necessary to cause complete inhibition of respiration [41].

Both *COX5A*- and *COX6A*-KD mitochondria showed, in addition to a reduction in the CcO monomer, an even more pronounced reduction of the dimeric form of CcO. Indeed, the pattern of respiratory supercomplexes showed that species containing the dimeric form of the CcO complex (III_2IV_2 and $\text{I}_1\text{III}_2\text{IV}_2$) are significantly reduced in KD cells. In contrast, supercomplexes containing monomeric CcO were unaltered or even slightly increased. A similar effect was shown recently to stem from a CcO defect induced by KD of the human CcO-specific copper metallochaperone Cox17 [42]. The majority of mammalian CcO is thought to exist in a dimeric form within the inner mitochondrial membrane [43]. Indeed, it appears that dimerization of CcO plays a crucial structural and functional role, conferring maximal structural stability on the complex [31].

In yeast, it was shown that complex IV associates with complex III already in the form of incomplete subcomplexes, and that some of the late assembled subunits are probably added directly to the III/IV supercomplex [44]. An example of such a subunit is Cox13, the yeast homologue of human Cox6a [45]. Indeed, BN/PAGE immunoblots for both control and down-regulated cells revealed additional spots that migrate at the level of supercomplexes in the first dimension, but with an apparent molecular mass lower than that of the CcO holoenzyme. Although we cannot, in principle, exclude the removal of some of the peripheral subunits because of detergent treatment, these spots might represent incomplete CcO assemblies that are already present in supercomplexes. Further analyses are required to confirm this hypothesis.

Despite remarkable conservation of secondary structure in Cox6a isoforms, mature Cox6a1 and Cox6a2 subunits (non-muscle and heart/muscle isoform) were found to share lower intra-species (approx. 60%) than inter-species (80–88%) amino acid sequence identity in humans, rats and cows, suggesting that the *COX6A1* and *COX6A2* genes arose before mammalian radiation [46]. The tissue-specific pattern of these isoforms is established during tissue differentiation [47–49]. A switch from *COX6A1* to *COX6A2* isoforms was described to occur during mammalian postnatal development in skeletal muscle and heart as well as during differentiation of myogenic cells *in vitro*, and is assumed to be essential for normal function of tissues with high aerobic metabolic demands [48,49]. In the heart of mice lacking the *COX6A2* gene, the content of the CcO holoenzyme was virtually equal to the level of Cox6a1 isoform in wild-type control, which accounted for 20% of the total Cox6a content. Thus the content of CcO comprising Cox6a1 appeared to be unchanged; in other words, without apparent compensation by induction of the expression of subunit Cox6a1 in the knockout heart [28]. HEK-293 cells used in this study are derived from embryonic kidney tissue, which is specific by almost exclusive (both prenatal and postnatal) expression of the *COX6A1* isoform [47–49]. Indeed, the vast majority of the *COX6A* transcripts in HEK-293 cells is represented by the *COX6A1* isoform. The *COX6A1* RNAi constructs were designed to target the 3'-UTR of the *COX6A1* transcript, which is lacking in the *COX6A2* isoform. Indeed, similar to the results from *COX6A2*-knockout heart, the decrease in the major isoform in our *COX6A1*-KD cells was not accompanied by up-regulation of the minor isoform (*COX6A2*). However, ectopic expression of Cox6a2 in *COX6A1*-KD cells tends to complement the CcO defect. It therefore appears that the mechanisms responsible for maintenance of tissue-specific

patterns of *COX6A* isoforms cannot react in response to actual cellular state. In contrast, it is also possible that the pronounced biochemical defect still did not provoke sufficient physiological impairment, which would otherwise trigger the expression of the minor subunit.

In conclusion, our results indicate that, whereas nuclear-encoded CcO subunits Cox4 and Cox5a are required for the assembly of the functional CcO complex, the Cox6a subunit is required for the overall stability of the holoenzyme. Consequently, the heterogeneous CcO population of Cox6a-deficient cells exhibits higher residual respiration at low oxygen levels than the various CcO forms found in *COX5A*-KD cells. The fact that the ectopic expression of heart/muscle-specific isoform of Cox6a can complement the CcO defect in *COX6A1*-KD cells is in sharp contrast with unaltered levels of this isoform in our CcO-deficient model, and suggests the existence of a fixed differentiation programme regarding human Cox6a isoforms. The description of a novel assembly intermediate at the very last step of CcO assembly suggests additional regulatory level of the process. The normal amount and function of complex I in all of our CcO-deficient cell lines suggest that even relatively small residual amounts of CcO can maintain normal biogenesis of this respiratory complex in human cells.

AUTHOR CONTRIBUTION

Daniela Fornuskova designed the study, prepared the KD cell lines, performed Western blot analyses and wrote the paper. Lukas Stiburek helped to interpret the data and write the paper. Laszlo Wenrich performed high-resolution respirometry. Kamila Vinsova quantified mRNA levels. Hana Hansikova measured specific enzyme activities. Jiri Zeman was involved in experimental planning, data analysis and writing the final paper.

FUNDING

This work was supported by grants from the Grant Agency of Charles University [grant number GAUK 1/2006/R], the Grant Agency of Czech Republic [grant number GACR 303/07/0781], the Internal Grant Agency of the Ministry of Health of the Czech Republic [grant number IGA MZ NS 10581/3] and the Center of Applied Genomics [grant number CAG 1M0520], and by institutional project [grant number MSM 0021620806].

REFERENCES

- Zhen, Y., Hoganson, C. W., Babcock, G. T. and Ferguson-Miller, S. (1999) Definition of the interaction domain for cytochrome *c* on cytochrome *c* oxidase. I. Biochemical, spectral, and kinetic characterization of surface mutants in subunit II of *Rhodobacter sphaeroides* cytochrome *aa*₃. *J. Biol. Chem.* **274**, 38032–38041
- Stiburek, L., Hansikova, H., Tesarova, M., Cerna, L. and Zeman, J. (2006) Biogenesis of eukaryotic cytochrome *c* oxidase. *Physiol. Res.* **55**, (Suppl. 2), S27–S41
- Huttemann, M., Lee, I., Pecinova, A., Pecina, P., Przyklenk, K. and Doan, J. W. (2008) Regulation of oxidative phosphorylation, the mitochondrial membrane potential, and their role in human disease. *J. Bioenerg. Biomembr.* **40**, 445–456
- Fontanesi, F., Soto, I. C. and Barrientos, A. (2008) Cytochrome *c* oxidase biogenesis: new levels of regulation. *IUBMB Life* **60**, 557–568
- Helling, S., Vogt, S., Rhiel, A., Ramzan, R., Wen, L., Marcus, K. and Kadenbach, B. (2008) Phosphorylation and kinetics of mammalian cytochrome *c* oxidase. *Mol. Cell. Proteomics* **7**, 1714–1724
- Huttemann, M., Kadenbach, B. and Grossman, L. I. (2001) Mammalian subunit IV isoforms of cytochrome *c* oxidase. *Gene* **267**, 111–123
- Kadenbach, B., Huttemann, M., Arnold, S., Lee, I. and Bender, E. (2000) Mitochondrial energy metabolism is regulated via nuclear-coded subunits of cytochrome *c* oxidase. *Free Radical Biol. Med.* **29**, 211–221
- Tsukihara, T., Aoyama, H., Yamashita, E., Tomizaki, T., Yamaguchi, H., Shinzawa-Itoh, K., Nakashima, R., Yaono, R. and Yoshikawa, S. (1996) The whole structure of the 13-subunit oxidized cytochrome *c* oxidase at 2.8 Å. *Science* **272**, 1136–1144
- Arnold, S. and Kadenbach, B. (1997) Cell respiration is controlled by ATP, an allosteric inhibitor of cytochrome-*c* oxidase. *Eur. J. Biochem.* **249**, 350–354

- 10 Horvat, S., Beyer, C. and Arnold, S. (2006) Effect of hypoxia on the transcription pattern of subunit isoforms and the kinetics of cytochrome *c* oxidase in cortical astrocytes and cerebellar neurons. *J. Neurochem.* **99**, 937–951
- 11 Stiburek, L., Vesela, K., Hansikova, H., Pecina, P., Tesarova, M., Cerna, L., Houstek, J. and Zeman, J. (2005) Tissue-specific cytochrome *c* oxidase assembly defects due to mutations in SCO2 and SURF1. *Biochem. J.* **392**, 625–632
- 12 Schlerf, A., Droste, M., Winter, M. and Kadenbach, B. (1988) Characterization of two different genes (cDNA) for cytochrome *c* oxidase subunit VIa from heart and liver of the rat. *EMBO J.* **7**, 2387–2391
- 13 Nijtmans, L. G., Taanman, J. W., Muijsers, A. O., Speijer, D. and Van den Bogert, C. (1998) Assembly of cytochrome-*c* oxidase in cultured human cells. *Eur. J. Biochem.* **254**, 389–394
- 14 Stiburek, L., Fornuskova, D., Wenchich, L., Pejznochova, M., Hansikova, H. and Zeman, J. (2007) Knockdown of human Oxa11 impairs the biogenesis of F₁F₀-ATP synthase and NADH:ubiquinone oxidoreductase. *J. Mol. Biol.* **374**, 506–516
- 15 Wittig, I., Braun, H. P. and Schagger, H. (2006) Blue native PAGE. *Nat. Protoc.* **1**, 418–428
- 16 Lowry, O. H., Rosebrough, N. J., Farr, A. L. and Randall, R. J. (1951) Protein measurement with the Folin phenol reagent. *J. Biol. Chem.* **193**, 265–275
- 17 Pecina, P., Gnaiger, E., Zeman, J., Pronicka, E. and Houstek, J. (2004) Decreased affinity for oxygen of cytochrome-*c* oxidase in Leigh syndrome caused by SURF1 mutations. *Am. J. Physiol. Cell. Physiol.* **287**, C1384–C1388
- 18 Massa, V., Fernandez-Vizarra, E., Alshahwan, S., Bakhsh, E., Goffrini, P., Ferrero, I., Mereghetti, P., D'Adamo, P., Gasparini, P. and Zeviani, M. (2008) Severe infantile encephalomyopathy caused by a mutation in COX6B1, a nucleus-encoded subunit of cytochrome *c* oxidase. *Am. J. Hum. Genet.* **82**, 1281–1289
- 19 Schagger, H. and Pfeiffer, K. (2000) Supercomplexes in the respiratory chains of yeast and mammalian mitochondria. *EMBO J.* **19**, 1777–1783
- 20 Gnaiger, E., Lassnig, B., Kuznetsov, A., Rieger, G. and Margreiter, R. (1998) Mitochondrial oxygen affinity, respiratory flux control and excess capacity of cytochrome *c* oxidase. *J. Exp. Biol.* **201**, 1129–1139
- 21 Diaz, F. (2010) Cytochrome *c* oxidase deficiency: patients and animal models. *Biochim. Biophys. Acta* **1802**, 100–110
- 22 Shoubridge, E. A. (2001) Cytochrome *c* oxidase deficiency. *Am. J. Med. Genet.* **106**, 46–52
- 23 Suthamarak, W., Yang, Y. Y., Morgan, P. G. and Sedensky, M. M. (2009) Complex I function is defective in complex IV-deficient *Caenorhabditis elegans*. *J. Biol. Chem.* **284**, 6425–6435
- 24 Li, Y., D'Aurelio, M., Deng, J. H., Park, J. S., Manfredi, G., Hu, P., Lu, J. and Bai, Y. (2007) An assembled complex IV maintains the stability and activity of complex I in mammalian mitochondria. *J. Biol. Chem.* **282**, 17557–17562
- 25 Baden, K. N., Murray, J., Capaldi, R. A. and Guillemain, K. (2007) Early developmental pathology due to cytochrome *c* oxidase deficiency is revealed by a new zebrafish model. *J. Biol. Chem.* **282**, 34839–34849
- 26 Poyton, R. O., Trueblood, C. E., Wright, R. M. and Farrell, L. E. (1988) Expression and function of cytochrome *c* oxidase subunit isoforms: modulators of cellular energy production? *Ann. N.Y. Acad. Sci.* **550**, 289–307
- 27 Liu, W., Gnanasambandam, R., Benjamin, J., Kaur, G., Getman, P. B., Siegel, A. J., Shortridge, R. D. and Singh, S. (2007) Mutations in cytochrome *c* oxidase subunit VIa cause neurodegeneration and motor dysfunction in *Drosophila*. *Genetics* **176**, 937–946
- 28 Radford, N. B., Wan, B., Richman, A., Szczepaniak, L. S., Li, J. L., Li, K., Pfeiffer, K., Schagger, H., Garry, D. J. and Moreadith, R. W. (2002) Cardiac dysfunction in mice lacking cytochrome-*c* oxidase subunit VIaH. *Am. J. Physiol. Heart Circ. Physiol.* **282**, H726–H733
- 29 Taanman, J. W. and Capaldi, R. A. (1993) Subunit VIa of yeast cytochrome *c* oxidase is not necessary for assembly of the enzyme complex but modulates the enzyme activity: isolation and characterization of the nuclear-coded gene. *J. Biol. Chem.* **268**, 18754–18761
- 30 Sedlak, E. and Robinson, N. C. (2009) Sequential dissociation of subunits from bovine heart cytochrome *c* oxidase by urea. *Biochemistry* **48**, 8143–8150
- 31 Stanicova, J., Sedlak, E., Musatov, A. and Robinson, N. C. (2007) Differential stability of dimeric and monomeric cytochrome *c* oxidase exposed to elevated hydrostatic pressure. *Biochemistry* **46**, 7146–7152
- 32 Barrientos, A., Gouget, K., Horn, D., Soto, I. C. and Fontanesi, F. (2009) Suppression mechanisms of COX assembly defects in yeast and human: insights into the COX assembly process. *Biochim. Biophys. Acta* **1793**, 97–107
- 33 Khalimonchuk, O., Bestwick, M., Meunier, B., Watts, T. C. and Winge, D. R. (2010) Formation of the redox cofactor centers during Cox1 maturation in yeast cytochrome oxidase. *Mol. Cell. Biol.* **30**, 1004–1017
- 34 Rossignol, R., Faustin, B., Rocher, C., Malgat, M., Mazat, J. P. and Letellier, T. (2003) Mitochondrial threshold effects. *Biochem. J.* **370**, 751–762
- 35 Diaz, F., Fukui, H., Garcia, S. and Moraes, C. T. (2006) Cytochrome *c* oxidase is required for the assembly/stability of respiratory complex I in mouse fibroblasts. *Mol. Cell. Biol.* **26**, 4872–4881
- 36 Galati, D., Srinivasan, S., Raza, H., Prabu, S. K., Hardy, M., Chandran, K., Lopez, M., Kalyanaraman, B. and Avadhani, N. G. (2009) Role of nuclear-encoded subunit Vb in the assembly and stability of cytochrome *c* oxidase complex: implications in mitochondrial dysfunction and ROS production. *Biochem. J.* **420**, 439–449
- 37 Pecina, P., Capkova, M., Chowdhury, S. K., Drahota, Z., Dubot, A., Vojtkova, A., Hansikova, H., Houstkova, H., Zeman, J., Godinot, C. and Houstek, J. (2003) Functional alteration of cytochrome *c* oxidase by SURF1 mutations in Leigh syndrome. *Biochim. Biophys. Acta* **1639**, 53–63
- 38 Williams, S. L., Valnot, I., Rustin, P. and Taanman, J. W. (2004) Cytochrome *c* oxidase subassemblies in fibroblast cultures from patients carrying mutations in COX10, SCO1, or SURF1. *J. Biol. Chem.* **279**, 7462–7469
- 39 Bratton, M. R., Pressler, M. A. and Hosler, J. P. (1999) Suicide inactivation of cytochrome *c* oxidase: catalytic turnover in the absence of subunit III alters the active site. *Biochemistry* **38**, 16236–16245
- 40 Penttila, T. (1983) Properties and reconstitution of a cytochrome oxidase deficient in subunit III. *Eur. J. Biochem.* **133**, 355–361
- 41 Wiedemann, F. R. and Kunz, W. S. (1998) Oxygen dependence of flux control of cytochrome *c* oxidase: implications for mitochondrial diseases. *FEBS Lett.* **422**, 33–35
- 42 Oswald, C., Krause-Buchholz, U. and Rodel, G. (2009) Knockdown of human COX17 affects assembly and supramolecular organization of cytochrome *c* oxidase. *J. Mol. Biol.* **389**, 470–479
- 43 Musatov, A. and Robinson, N. C. (2002) Cholate-induced dimerization of detergent- or phospholipid-solubilized bovine cytochrome *c* oxidase. *Biochemistry* **41**, 4371–4376
- 44 Mick, D. U., Wagner, K., van der Laan, M., Frazier, A. E., Perschil, I., Pawlas, M., Meyer, H. E., Warscheid, B. and Rehling, P. (2007) Shy1 couples Cox1 translational regulation to cytochrome *c* oxidase assembly. *EMBO J.* **26**, 4347–4358
- 45 Brandner, K., Mick, D. U., Frazier, A. E., Taylor, R. D., Meisinger, C. and Rehling, P. (2005) Taz1, an outer mitochondrial membrane protein, affects stability and assembly of inner membrane protein complexes: implications for Barth Syndrome. *Mol. Biol. Cell* **16**, 5202–5214
- 46 Fabrzi, G. M., Sadlock, J., Hirano, M., Mita, S., Koga, Y., Rizzuto, R., Zeviani, M. and Schon, E. A. (1992) Differential expression of genes specifying two isoforms of subunit VIa of human cytochrome *c* oxidase. *Gene* **119**, 307–312
- 47 Bonne, G., Seibel, P., Possekkel, S., Marsac, C. and Kadenbach, B. (1993) Expression of human cytochrome *c* oxidase subunits during fetal development. *Eur. J. Biochem.* **217**, 1099–1107
- 48 Kim, K., Lecordier, A. and Bowman, L. H. (1995) Both nuclear and mitochondrial cytochrome *c* oxidase mRNA levels increase dramatically during mouse postnatal development. *Biochem. J.* **306**, 353–358
- 49 Taanman, J. W., Herzberg, N. H., De Vries, H., Bolhuis, P. A. and Van den Bogert, C. (1992) Steady-state transcript levels of cytochrome *c* oxidase genes during human myogenesis indicate subunit switching of subunit VIa and co-expression of subunit VIa isoforms. *Biochim. Biophys. Acta* **1139**, 155–162

SUPPLEMENTARY ONLINE DATA

Novel insights into the assembly and function of human nuclear-encoded cytochrome *c* oxidase subunits 4, 5a, 6a, 7a and 7b

Daniela FORNUSKOVA, Lukas STIBUREK, Laszlo WENCHICH, Kamila VINSOVA, Hana HANSIKOVA and Jiri ZEMAN¹

Department of Pediatrics, First Faculty of Medicine, Charles University in Prague, Ke Karlovu 2, Prague 2, 128 08, Czech Republic

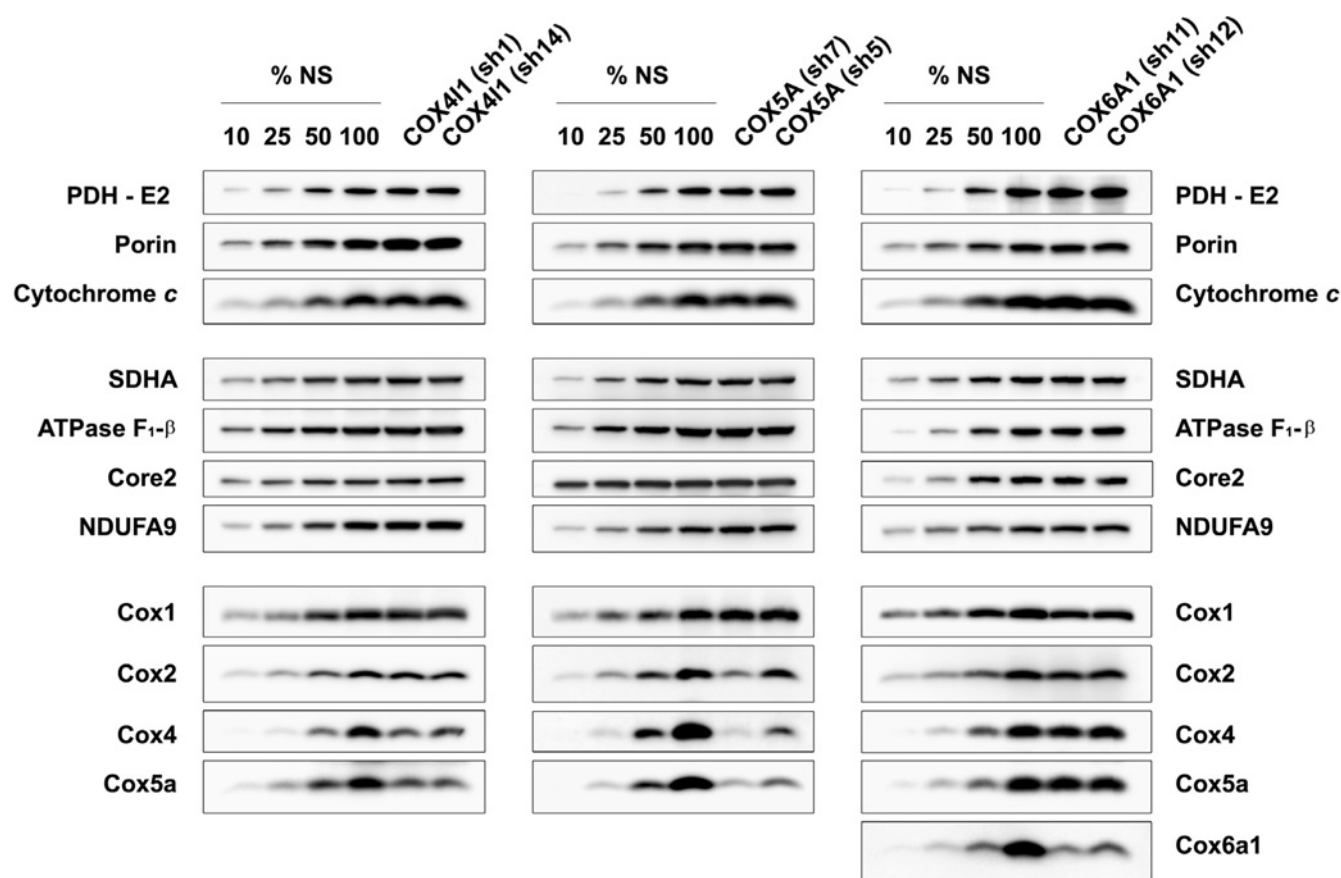


Figure S1 Steady-state levels of selected respiratory chain subunits and several mitochondrial proteins in *COX4*-, *COX5A*- and *COX6A1*-KD cells

Equal amounts (~20 μ g) of mitochondrial protein from *COX4*-, *COX5A*- and *COX6A1*-KD cells, together with serial dilutions of control (NS) samples, were fractionated using SDS/PAGE and subjected to Western blot analysis using antibodies specific for the complex IV subunits Cox1, Cox2, Cox4, Cox5a and Cox6a1, the pyruvate dehydrogenase subunit E2 (PDH-E2), the outer membrane protein porin, the electron carrier cytochrome *c*, the SDHA subunit of complex II, the ATP synthase subunit F₁- β (ATPase F₁- β), the complex III subunit Core 2 and the complex I subunit NDUFA9 [NADH dehydrogenase (ubiquinone) 1 α subcomplex 9].

Received 5 November 2009/12 March 2010; accepted 22 March 2010
Published as BJ Immediate Publication 22 March 2010, doi:10.1042/BJ20091714

¹To whom correspondence should be addressed (email jzem@lf1.cuni.cz).

5.2. Characterization of the biochemical properties of OXA1L, the human homologue of the yeast mitochondrial Oxa1 translocase, and study of its role for CcO biogenesis (*specific aim 1b*)

Stiburek L, **Fornuskova D**, Wenchich L, Pejznochova M, Hansikova H and Zeman J

Knockdown of human Oxa11 impairs the biogenesis of F₁F₀-ATP synthase and NADH:ubiquinone oxidoreductase.

J Mol Biol 2007; 374: 506-516.

We addressed the role of human Oxa11 in the biogenesis of oxidative phosphorylation system.

To study the molecular role and biochemical properties of human OXA1L gene product, we employed expression cloning and propagation of plasmid constructs in bacteria, rabbit OXA1L antibody design and preparation, immunocytochemistry, confocal microscopy, co-immunoprecipitation as well as subcellular and submitochondrial fractionation and localization. To estimate functionality and integrity of OXPHOS in context of Oxa11 deficiency, we prepared stable human HEK-293 knockdown lines using human microRNA-adopted design evoking RNA interference. The obtained material was analyzed with use of isolation of crude mitochondrial fraction by cellular fractionation and differential centrifugation, FACS analysis, spectrophotometric measurements of specific enzyme activities, high-resolution respirometry and blue-native (BN), denaturing (SDS) and two-dimensional (BN/SDS) PAGE with downstream immunoblot detections using monoclonal or polyclonal antibodies against various mitochondrial proteins.

The Oxa1 protein is a member of the evolutionarily conserved Oxa1/Alb3/YidC protein family, which is involved in the biogenesis of membrane proteins in mitochondria, chloroplasts and bacteria. The predicted human homologue, Oxa11, was originally identified by partial functional complementation of the respiratory growth defect of the yeast *oxa1* mutant. Here we demonstrate that both the endogenous human Oxa11, with an apparent molecular mass of 42 kDa, and the Oxa11-FLAG chimeric protein localize exclusively to mitochondria in HEK-293 cells. Furthermore, human Oxa11 was found to be an integral membrane protein, and, using two-dimensional blue native/denaturing PAGE, the majority of the protein was identified as part of a 600-700 kDa complex. The stable short hairpin (sh) RNA-mediated knockdown of

Oxa11 in HEK-293 cells resulted in markedly decreased steady-state levels and ATP hydrolytic activity of the ATP synthase and moderately reduced levels and activity of NADH:ubiquinone oxidoreductase (complex I). However, no significant accumulation of corresponding sub-complexes could be detected on blue native immunoblots. Intriguingly, the achieved depletion of Oxa11 protein did not adversely affect the assembly or activity of cytochrome c oxidase or complex III. Taken together, our results indicate that human Oxa11 represents a mitochondrial integral membrane protein required for the correct biogenesis of ATP synthase and complex I.

I contributed to this study by assisting in research design, by cloning of pCMV-GIN-ZEO plasmid derivatives coding for candidate shRNAs to achieve the most efficient knockdown and by performing the part of electrophoretic and immunoblot analyses.

Knockdown of Human Oxa1 Impairs the Biogenesis of F₁F_o-ATP Synthase and NADH:Ubiquinone Oxidoreductase

Lukas Stiburek, Daniela Fornuskova, Laszlo Wenchich
Martina Pejznochova, Hana Hansikova and Jiri Zeman*

Department of Pediatrics and
Center of Applied Genomics
1st Faculty of Medicine
Charles University, Prague
128 08, Czech Republic

Received 26 June 2007;
received in revised form
17 September 2007;
accepted 17 September 2007
Available online
20 September 2007

The Oxa1 protein is a founding member of the evolutionarily conserved Oxa1/Alb3/YidC protein family, which is involved in the biogenesis of membrane proteins in mitochondria, chloroplasts and bacteria. The predicted human homologue, Oxa1l, was originally identified by partial functional complementation of the respiratory growth defect of the yeast *oxa1* mutant. Here we demonstrate that both the endogenous human Oxa1l, with an apparent molecular mass of 42 kDa, and the Oxa1l-FLAG chimeric protein localize exclusively to mitochondria in HEK293 cells. Furthermore, human Oxa1l was found to be an integral membrane protein, and, using two-dimensional blue native/denaturing PAGE, the majority of the protein was identified as part of a 600–700 kDa complex. The stable short hairpin (sh) RNA-mediated knockdown of Oxa1l in HEK293 cells resulted in markedly decreased steady-state levels and ATP hydrolytic activity of the F₁F_o-ATP synthase and moderately reduced levels and activity of NADH:ubiquinone oxidoreductase (complex I). However, no significant accumulation of corresponding sub-complexes could be detected on blue native immunoblots. Intriguingly, the achieved depletion of Oxa1l protein did not adversely affect the assembly or activity of cytochrome *c* oxidase or the cytochrome *bc*₁ complex. Taken together, our results indicate that human Oxa1l represents a mitochondrial integral membrane protein required for the correct biogenesis of F₁F_o-ATP synthase and NADH:ubiquinone oxidoreductase.

© 2007 Elsevier Ltd. All rights reserved.

Keywords: mitochondria; Oxa1l; ATP synthase; NADH:ubiquinone oxidoreductase; biogenesis

Edited by J. Karn

Introduction

The mitochondrial oxidative phosphorylation system (OXPHOS) is responsible for the vast majority of ATP produced in aerobic cells. It is composed of four respiratory chain complexes and the F₁F_o-ATP syn-

thase (complex V) embedded within the inner membrane of the organelle. The biogenesis of OXPHOS is complicated by its sub-cellular location, dual genetic origin, the large number of constituent subunits and prosthetic groups, and the high hydrophobicity of some of the membrane subunits. Consequently, a number of specific gene products have evolved to accommodate such complex requirements. One of them is the Oxa1 protein, a founding member of the evolutionarily conserved Oxa1/Alb3/YidC protein family, which is involved in the biogenesis of membrane proteins in mitochondria, chloroplasts and bacteria.^{1,2} The best characterized member of this family, *Saccharomyces cerevisiae* Oxa1, is an intrinsic protein of the inner mitochondrial membrane that mediates the insertion of mitochondrial translation products as well as of conservatively sorted nuclear gene products into the inner membrane from the mitochondrial matrix.^{1,3,4} Although the yeast Oxa1 was shown to represent a rather

*Corresponding author. E-mail address: jzem@lf1.cuni.cz.

Abbreviations used: OXPHOS, oxidative phosphorylation system; CcO, cytochrome *c* oxidase; SDH, succinate:ubiquinone oxidoreductase; CS, citrate synthase; SDHA, 70 kDa flavoprotein subunit of SDH; PDH, pyruvate dehydrogenase; HEK293, human embryonic kidney 293; RNAi, RNA interference; shRNA, short hairpin RNA; shRNAmir, miR-30-based shRNA; FCCP, carbonyl cyanide *p*-(trifluoromethoxy) phenylhydrazone; GFP, green fluorescent protein; TMPD, *N,N,N',N'*-tetramethyl-*p*-phenylenediamine dihydrochloride.

general export machinery of the inner membrane, the co-translational membrane insertion of the mitochondrially encoded Cox2 precursor appears to exhibit the strictest dependency on its function.⁵⁻⁷ The other substrates of Oxa1, including Oxa1 itself, can be inserted independently of its function, albeit with significantly reduced efficiencies.^{8,9} Very recently, a novel post-translational role in the biogenesis of OXPHOS was demonstrated for yeast Oxa1. The protein was shown to stably interact in a post-translational manner with the ATP synthase subunit *c*, mediating its assembly into the ATP synthase complex.¹⁰ Yeast *oxa1* cells are respiratory-deficient, with undetectable cytochrome *c* oxidase (CcO or complex IV) activity and markedly reduced levels of the F₁F_o-ATP synthase and cytochrome *bc*₁ complex (complex III).^{3,4} *Schizosaccharomyces pombe* contains two distinct Oxa1 orthologues, both of which are able to complement the respiratory defect of yeast Oxa1-null cells. The double inactivation of these genes is lethal to this petite-negative yeast.¹¹ The depletion of Oxa1 in *Neurospora crassa* results in a slow-growth phenotype accompanied by reduced subunit levels of CcO and NADH:ubiquinone oxidoreductase (complex I). The *N. crassa*, Oxa1 was shown to form a 170–180 kDa homo-oligomeric complex, most likely containing four Oxa1 monomers.¹² Mitochondrial Oxa1 homologues possess a hydrophobic core domain composed of five transmembrane helices, and a C-terminal matrix domain that was shown in yeast to bind mitochondrial ribosome, thereby mediating co-translational membrane recruitment of nascent mitochondrial translation products.^{13,14}

The predicted human Oxa1 orthologue, referred to as Oxa1l, shares 33% sequence identity with the corresponding yeast polypeptide. The human *OXA1L* cDNA was originally cloned by partial functional complementation of the respiratory growth defect of the yeast *oxa1-79* mutant.¹⁵ It contains an open reading frame predicted to encode a protein of 435 amino acids. It was suggested that the ten exons of *OXA1L* might form an open reading frame able to encode a precursor protein of 495 amino acids,¹⁶ and more recently the cDNA containing those additional 180 bp was cloned.¹⁷ However, this extended version was shown to exhibit an even lower capacity to complement the respiratory growth defect of yeast *oxa1* cells than the original sequence.¹⁸ The human *OXA1L* mRNA was found to be enriched in mitochondria-bound polysomes isolated from HeLa cells, and its 3' untranslated region was shown to be functionally important when expressed in yeast cells.¹⁸

Here we address the role of human Oxa1l in the biogenesis of OXPHOS. We demonstrate here that human Oxa1l is a mitochondrial integral membrane protein that exists as part of a 600–700 kDa complex in mitochondria of human embryonic kidney 293 (HEK293) cells. We further show that the stable short hairpin RNA (shRNA)-mediated knockdown of human Oxa1l in HEK293 cells leads to markedly decreased protein levels and ATP hydrolytic activity of the F₁F_o-ATP synthase and moderately reduced

levels and activity of NADH:ubiquinone oxidoreductase. Intriguingly, the activity and content of cytochrome *c* oxidase and the cytochrome *bc*₁ complex were unaffected or even increased in Oxa1l knockdown cells. Hence, these results indicate that human Oxa1l represents a mitochondrial integral membrane protein which is required for the correct biogenesis of the F₁F_o-ATP synthase and NADH:ubiquinone oxidoreductase.

Results

Human Oxa1l localizes to mitochondria in HEK293 cells

The predicted human Oxa1l precursor (Q15070) has a calculated molecular mass of 48.5 kDa and possesses a characteristic N-terminal mitochondrial targeting sequence. Both Mitopred and MitoProt II predict a significant score for location of the protein within mitochondria. To demonstrate the mitochondrial targeting of Oxa1l, a chimeric construct con-

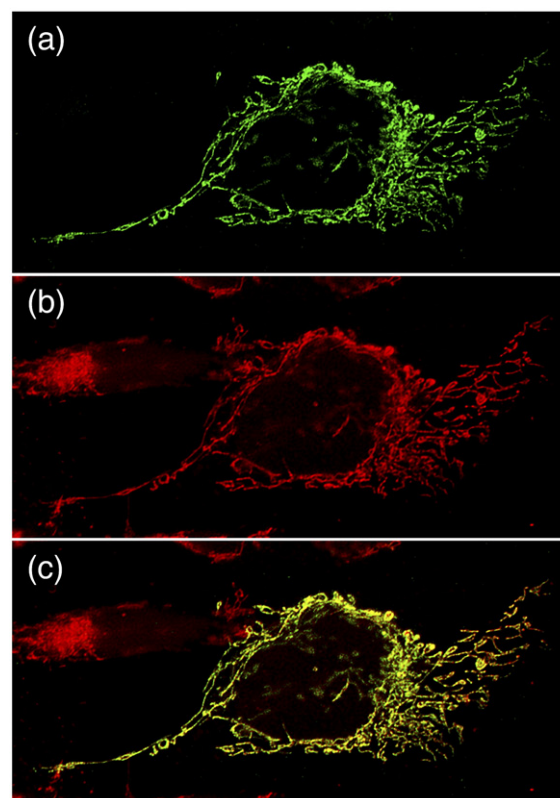


Figure 1. Overexpressed human Oxa1l-FLAG chimeric protein is targeted exclusively to mitochondria in HEK293 cells. (b) HEK293 cells were transiently transfected with the *OXA1L*-FLAG expression construct, stained with MitoTracker Red, and (a) subsequently labeled with a monoclonal M2 anti-FLAG antibody and with an anti-mouse Alexa Fluor 488 antibody. The fluorescence signal was recorded with a Nikon Eclipse TE2000 microscope, and deconvolved using the Huygens Professional Software (SVI). (c) Superimposition of (a) and (b) shows complete overlap of the two staining patterns.

taining the OXA1L coding sequence tagged with a C-terminal FLAG epitope was transiently expressed in HEK293 cells. As shown in Figure 1, labeling of the cells with an anti-FLAG monoclonal antibody and with the mitochondria-selective dye MitoTracker Red followed by confocal microscopy revealed a characteristic mitochondrial staining pattern, as well as a complete overlap of the two signals. To analyze the sub-cellular location of the endogenous human Oxa11, we prepared samples of whole cell lysates, isolated mitochondria and cytoplasmic fractions from HEK293 cells. Immunoblot analysis using an antibody to human Oxa11 showed that the protein, with an apparent molecular mass of approximately 42 kDa, is clearly more enriched in isolated mitochondria than in whole cell lysates, and is absent from the cytoplasmic fraction (Figure 2(a)). Antibodies to Cox1 (mitochondria), eIF2 α (cytoplasm) and mtHSP70 (mitochondria and cytoplasm) were used as compartment markers. These results suggest that human Oxa11 localizes exclusively to mitochondria in HEK293 cells.

Human Oxa11 is an integral membrane protein

Human Oxa11 is predicted to be a transmembrane protein. We have determined its solubility by fractionation of sonically disrupted mitochondria into soluble matrix proteins and membrane vesicles. Immunoblot analysis of the two fractions revealed that Oxa11 is found exclusively in the membrane fraction (Figure 2(b)). To find out whether Oxa11 is a peripheral or integral membrane protein, its sus-

ceptibility to alkaline carbonate extraction was assessed. Mitochondria were extracted with sodium carbonate (pH 11.5), and the supernatant and pellet fractions were subjected to immunoblot analysis. Oxa11 was found exclusively in the pellet fraction, indicating that it is an integral membrane protein (Figure 2(b)).

Human Oxa11 exists as part of a 600–700 kDa complex in the mitochondria of HEK293 cells

The fact that both *S. cerevisiae* and *N. crassa* Oxa1 proteins were reported to be part of an oligomeric assembly prompted us to assess this property in the human protein. Mitochondria isolated from HEK293 cells were solubilized with 1.3% (w/v) dodecyl maltoside and fractionated using two-dimensional blue native/denaturing PAGE, on a 6%–16% (w/v) polyacrylamide gradient in the first dimension. Probing of the resulting immunoblots with the antibody to Oxa11 and with the corresponding pre-immune serum revealed that Oxa11 is specifically present in one major, high molecular mass complex, and in several minor, faster migrating assemblies. As shown in Figure 2(c), simultaneous detection with the antibody to Oxa11 and with an antibody to ATPase F₁- α revealed that the major Oxa11-containing complex has an estimated molecular mass of approximately 600–700 kDa. Since the yeast Oxa1 was recently shown to physically interact with components of ATP synthase holoenzyme, we have asked whether the human Oxa11 complex also contains some of the ATP synthase subunits.

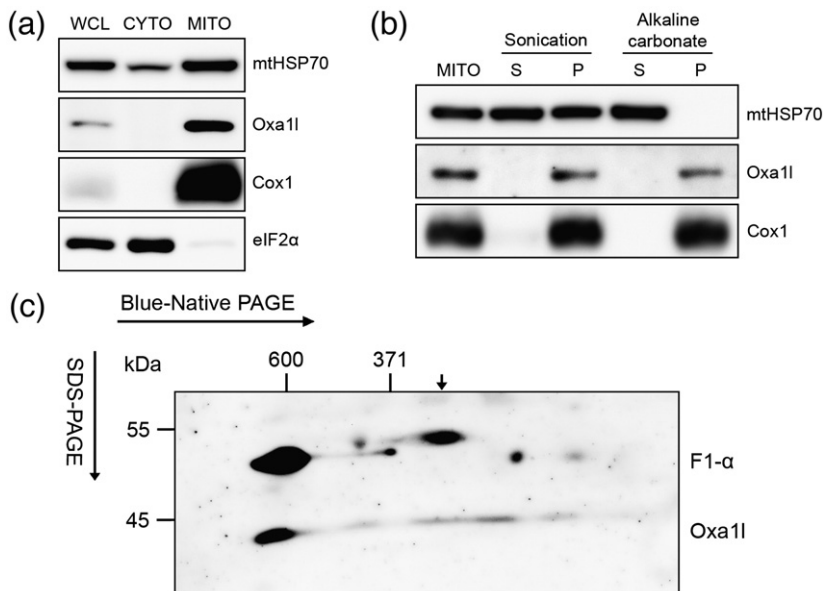


Figure 2. Human Oxa11 is a mitochondrial integral membrane protein that exists as part of a 600–700 kDa complex. (a) Equal amounts of protein (20 μ g) from isolated mitochondria, cytoplasmic fraction and whole cell lysate from the HEK293 cells were fractionated using SDS–10% PAGE, and the resulting immunoblots were decorated with an antibody to Oxa11. Antibodies to Cox1 (mitochondria), eIF2 α (cytoplasm) and mtHSP70 (mitochondria and cytoplasm) were used as compartment markers. (b) Mitochondria isolated from HEK293 cells were either sonically disrupted or extracted with sodium carbonate (pH 11.5) and centrifuged at 100,000g for 30 min, and the resulting fractions were processed for SDS–PAGE. The aliquots of

resulting samples (5 μ g of protein) were, together with the whole mitochondria lysate, used to prepare denaturing immunoblots that were subsequently decorated with antibodies to Oxa11, mtHSP70 (peripheral protein) and Cox1 (integral protein). s, supernatant; p, pellet. (c) Mitochondria isolated from HEK293 cells were solubilized with 1.3% dodecyl maltoside and fractionated (50 μ g of protein) using two-dimensional blue native/denaturing PAGE, on a 6%–16% polyacrylamide gradient in the first dimension. The resulting immunoblot was decorated with antibodies to Oxa11 and ATPase F₁- α . Under the conditions employed, an antibody to F₁- α recognized the ATP synthase holoenzyme of approximately 600 kDa and the F₁-ATPase sub-complex of 371 kDa. The small arrow indicates a non-specific binding of Oxa11 antibody that was also achieved using the Oxa11 preimmune serum alone.

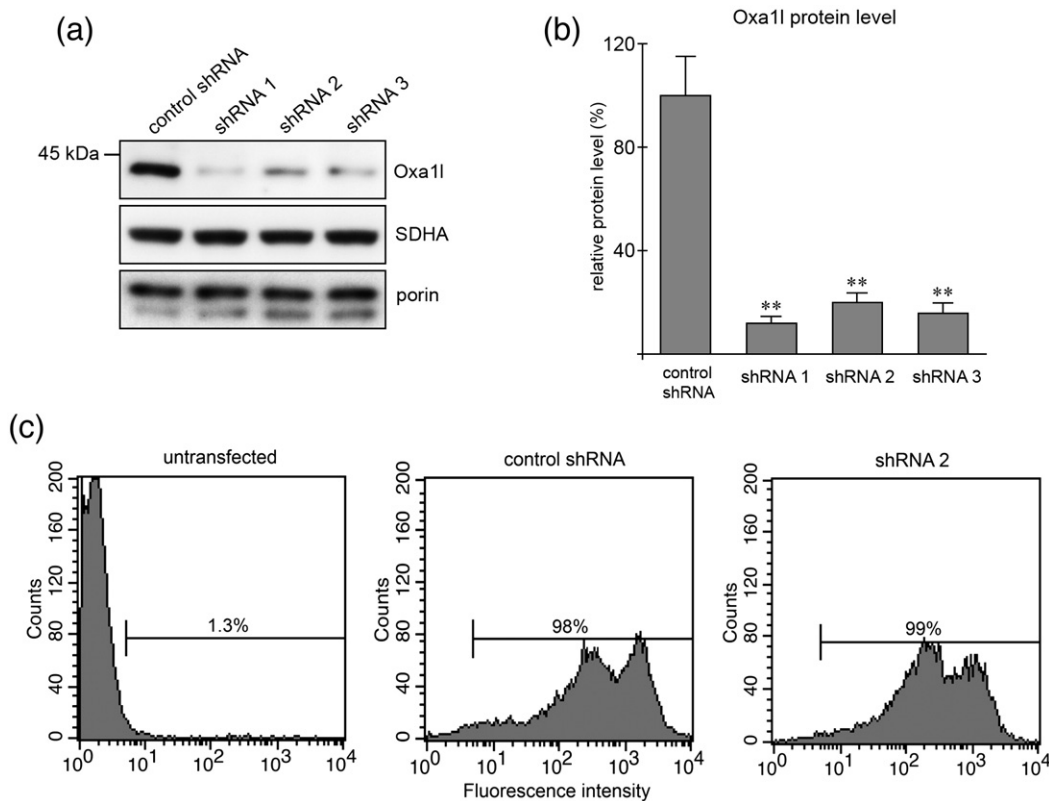


Figure 3. *Oxa1l* is substantially depleted in HEK293 cells by the stable expression of shRNAmir. (a) Equal amounts of protein (10 μ g) from mitochondria isolated from G418-resistant cells stably transfected with one of the OXA1L-targeted shRNA constructs (shRNA 1, 2 and 3) and from cells expressing the negative control shRNA were fractionated using SDS–10% PAGE. The resulting immunoblot was decorated with antibodies to *Oxa1l*, SDHA and porin. (b) The results of densitometric quantification (Quantity One; Bio-Rad) of three independent experiments from (a) are presented in the histogram. **, $p < 0.01$ (c) Flow cytometric analysis of GFP expression in HEK293 cells stably transfected with the OXA1L-targeted shRNA construct (shRNA 2) or with the negative control shRNA construct. The analysis of untransfected parental HEK293 cells is included as a negative control.

HEK293 cells were transiently transfected with the OXA1L–FLAG expression construct and solubilized with 1% (v/v) Triton X-100 and the fusion protein was then immunoprecipitated from the lysate using an ANTI-FLAG® M2 affinity agarose resin. The immunoprecipitate was fractionated using SDS–PAGE and the resulting immunoblots were probed with available antibodies against the ATP synthase subunits and against various respiratory chain subunits. However, despite high efficiency of *Oxa1l*–FLAG protein precipitation we could not detect any OXPHOS subunits in the immunoprecipitate using available antibodies (data not shown). These results suggest that a substantial fraction of human *Oxa1l* exists in the mitochondria of HEK293 cells as part of an approximately 600–700 kDa assembly that do not appear to contain any of the mitochondrial OXPHOS complexes.

Stable knockdown of *Oxa1l* in HEK293 cells

To uncover the functional involvement of human *Oxa1l* in the biogenesis of OXPHOS, we down-regulated its expression in HEK293 cells using RNA interference (RNAi). Given the considerable half-life of the OXPHOS complexes, a stable vector-based

approach was utilized that incorporates the RNA polymerase II-driven expression of short hairpin RNAs embedded within the context of a mammalian miR-30 microRNA primary transcript. This method was shown to provide high-level knockdown even in polyclonal cell populations of single-copy integrants.¹⁹ Sequences of eight different miR-30-based shRNAs (shRNAmirs) targeted to the coding sequence of human OXA1L were downloaded from the publicly accessible RNAi Codex database†, synthesized, cloned into the lentiviral pCMV-GIN-Zeo vector, and functionally validated by their transient co-expression with the OXA1L–FLAG construct (data not shown). The three shRNA constructs that proved to be effective were selected (shRNA 1, mp_id 433861; shRNA 2, mp_id 19616 and shRNA 3, mp_id 19615), and together with the negative control (non-silencing) shRNA construct and the empty vector were used to establish G418-resistant stably expressing cells. The fact that the expression of shRNAmir in the pCMV-GIN-Zeo vector is transcriptionally coupled with that of green fluorescent protein (GFP) permitted an estimation of

† <http://codex.cshl.org>

shRNA expression levels in stable cells. Flow cytometric analysis revealed that practically all the cells were GFP positive, without marked differences in expression levels (Figure 3(c)). The extent of endogenous Oxa11 protein depletion was then determined by immunoblot analysis of mitochondrial fractions isolated from pooled colonies of stable cells (Figure 3(a)). The cells carrying the OXA1L-targeted constructs expressing shRNA 1, shRNA 2 and shRNA 3 showed substantial reductions in Oxa11 protein levels to approximately 12%, 20% and 16% of control values, respectively (Figure 3(b)). No significant differences in the Oxa11 protein levels were observed between cells carrying the negative control shRNA construct and cells carrying the empty vector (data not shown). Given the substantial reduction in Oxa11 protein levels, pooled colonies were used for subsequent analysis, obviating the need for additional sub-cloning.

Knockdown of human Oxa11 leads to markedly diminished protein content and ATP hydrolytic activity of the F₁F_o-ATP synthase and moderately reduced content and activity of NADH:ubiquinone oxidoreductase (complex I)

We initially determined the steady-state levels of several mitochondrial proteins, mainly OXPHOS subunits, in our cellular Oxa11 knockdown model. Since we did not detect significant alterations in the content of mitochondria (porin, 70 kDa flavoprotein

subunit of succinate:ubiquinone oxidoreductase (SDHA)), the whole-cell lysates, normalized to the immunoblot signal of α -tubulin, were used for denaturing immunoblots. The steady-state levels of SDHA, core protein 2, porin, mtHSP70 and pyruvate dehydrogenase (PDH)-E2 were found to be similar to those in negative controls, whereas the levels of Cox1, Cox2 and Cox5a were either unaffected or slightly increased to approximately 120%–130% of control values. In contrast, the steady-state levels of ATP synthase subunits F1- α , F1- β , OSCP and subunit d were reduced to approximately 25%–50%. In addition, the levels of complex I subunits NDUFB6 and NDUFA9 were decreased to approximately 50%–60% of control values in Oxa11-depleted cells (Figure 4(a), or data not shown).

To determine the holoenzyme content and assembly state of each of the OXPHOS complexes, blue native immunoblots of dodecyl maltoside-solubilized mitochondria were prepared. Consistent with denaturing analysis, native immunoblots showed unaffected levels of respiratory complexes II and III, whereas the content of cytochrome *c* oxidase holoenzyme was increased to approximately 130% of control values (Figure 4(b)). On the contrary, the levels of F₁F_o-ATP synthase holoenzyme were reduced to approximately 25%–50%, whereas the holoenzyme content of complex I was decreased to approximately 50%–60% of control values in the mitochondria of Oxa11-depleted cells (Figure 4(b)). However, no significant accumulation of either the

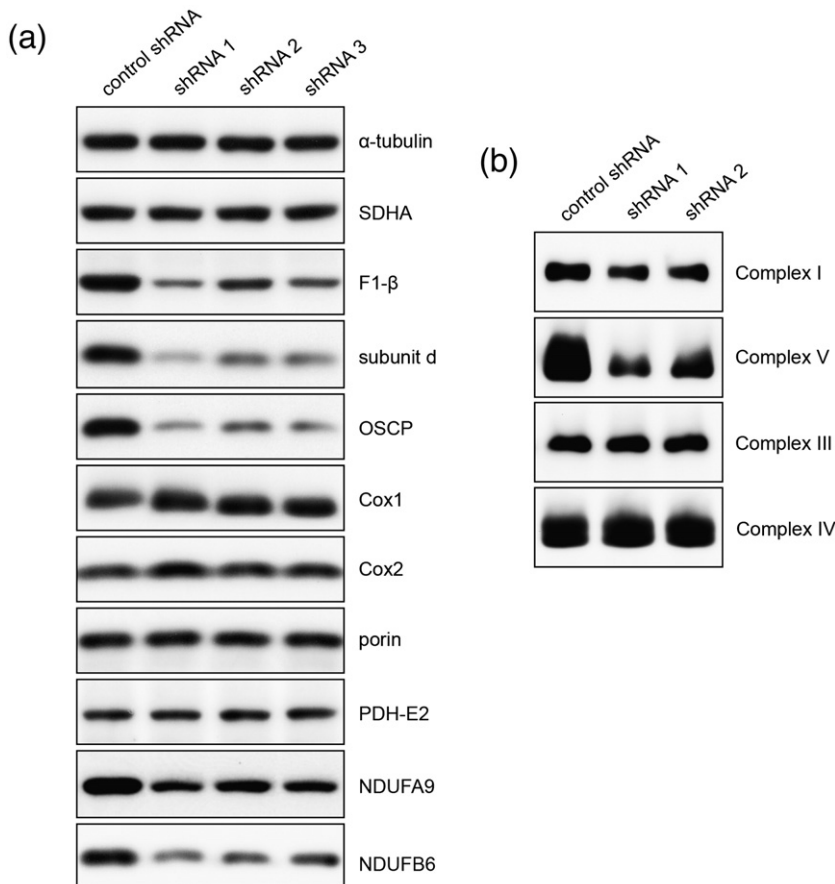


Figure 4. Depletion of Oxa11 in HEK293 cells results in decreased steady-state levels of the F₁F_o-ATP synthase and NADH:ubiquinone oxidoreductase holoenzyme and subunits. (a) Equal amounts of protein (10 μ g) from whole cell lysates prepared from G418-resistant cells stably transfected with one of the OXA1L-targeted shRNA constructs (shRNA 1, 2 and 3) and from cells carrying the negative control shRNA construct were fractionated using SDS-PAGE. The resulting immunoblots were decorated with antibodies to α -tubulin, SDHA, F1- β , subunit d, OSCP, Cox1, Cox2, porin, PDH-E2, NDUFA9 and NDUFB6. (b) Isolated mitochondria were solubilized with 1.3% dodecyl maltoside and fractionated using blue native PAGE on 6%–15% polyacrylamide gradient. The amount of protein loaded per lane (\sim 5 μ g) was normalized to the immunoblot signals of porin and SDHA. The resulting immunoblots were decorated with antibodies to NDUFA9 (complex I), subunit d (complex V), Cox1 (complex IV) and core protein 2 (complex III). The immunoblots shown are representative of at least three independent experiments.

ATP synthase or complex I sub-complexes could be detected on blue native immunoblots using available antibodies (data not shown).

To confirm and extend the above results, enzymatic activities of respiratory chain complexes, as well as the aurovertin-sensitive ATP hydrolytic activity, were determined. The activities of succinate:ubiquinone oxidoreductase (SDH), cytochrome *c* reductase and citrate synthase (CS) were found to be at control levels (data not shown), whereas the activity of CcO, normalized to that of CS, was either unaffected or insignificantly increased to approximately 110%–120% of control values. In contrast, the aurovertin-sensitive ATP hydrolytic activity was substantially decreased to approximately 30%–60% of control values in the mitochondria of *Oxa1l*-depleted cells (Figure 5(a)). In line with the moderately reduced protein content, the activity of complex I, normalized to that of CS, was diminished to approximately 70%–80% of control values. The values of aurovertin-sensitive ATPase activity correlated with the relative residual content of ATP synthase holoenzyme, consistent with the fact that no significant accumulation of F₁ sub-complex(es) could be detected on blue native immunoblots.

To further confirm the results of CcO activity and content determination, high-resolution polarographic measurements of ascorbate/*N,N,N',N'*-tetramethyl-*p*-phenylenediamine dihydrochloride (TMPD)-fuelled, sodium azide-sensitive oxygen consumption were carried out with digitonin-permeabilized cells. The measurements showed significantly increased ascorbate/TMPD-fuelled respiration in *Oxa1l*-depleted cells to approximately 150%–160% of control values, indicating increased activity and/or content of the membrane-embedded CcO complex in these cells (Figure 5(b)).

Discussion

This study represents the first characterization of a mammalian member of the evolutionarily con-

served *Oxa1*/Alb3/YidC family of proteins. The evidence presented herein indicates that human *Oxa1l* is a mitochondrial integral membrane protein that exists as part of a 600–700 kDa complex in the mitochondria of HEK293 cells. We further demonstrate here that the shRNA-mediated depletion of human *Oxa1l* leads to compromised biogenesis of the F₁F₀-ATP synthase and, to a lesser extent, NADH:ubiquinone oxidoreductase.

The mitochondrial membrane localization of human *Oxa1l* is supported by several lines of evidence. First, the protein possesses a characteristic N-terminal mitochondrial targeting sequence and a hydrophobic core region composed of five predicted transmembrane helices. Second, the sub-cellular fractionation of HEK293 cells together with subsequent immunoblotting using an antibody to *Oxa1l* revealed that the protein, with an apparent molecular mass of approximately 42 kDa, is highly enriched in isolated mitochondria and absent from the cytoplasmic fraction. Third, immunofluorescence labeling of HEK293 cells transfected with the OXA1L-FLAG expression construct, followed by confocal microscopy, showed an exclusive mitochondrial targeting of the overexpressed *Oxa1l*-FLAG chimeric protein. Finally, the human *Oxa1l* was found exclusively in the pellet fraction of sonically disrupted mitochondria, and could not be extracted from the mitochondrial membrane by alkaline carbonate treatment. Similarly, the yeast *Oxa1* was shown to be a mitochondrial integral membrane protein, spanning the inner membrane with five transmembrane helices.^{20,21}

Both *S. cerevisiae* and *N. crassa* *Oxa1* were reported to be part of an oligomeric assembly.^{8,12,22} Here we demonstrate that the majority of human *Oxa1l* exists in the mitochondria of HEK293 cells as part of a 600–700 kDa complex of unknown composition. In contrast to yeast *Oxa1*,¹⁰ no ATP synthase subunits to which we have antibodies were found to co-purify with the human *Oxa1l*-FLAG protein expressed in HEK293 cells. Similarly, we could not detect any respiratory chain subunits in the *Oxa1l*-

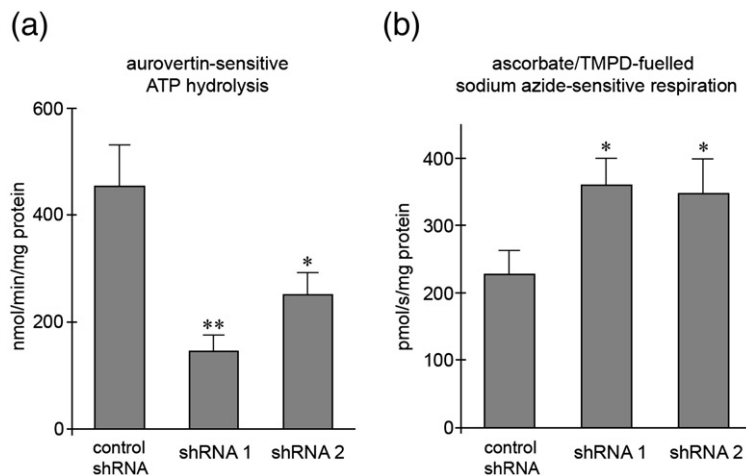


Figure 5. Depletion of *Oxa1l* in HEK293 cells leads to diminished aurovertin-sensitive ATP hydrolytic activity and increased ascorbate/TMPD-fuelled, sodium azide-sensitive oxygen consumption. (a) Aurovertin-sensitive ATP hydrolytic activity was measured using an ATP-regenerating system in mitochondria isolated from G418-resistant cells stably transfected with one of the OXA1L-targeted shRNA constructs (shRNA 1 and 2) and from cells carrying the negative control shRNA construct. (b) Ascorbate/TMPD-fuelled, sodium azide-sensitive oxygen consumption was

measured in digitonin-permeabilized cells in the presence of FCCP using an OROBOROS oxygraph. Values are expressed as mean \pm S.D. *, $p < 0.05$; **, $p < 0.01$.

FLAG immunoprecipitate. Since the Oxa1 complex from *N. crassa* was shown to be composed exclusively of Oxa1 monomers,¹² it is possible that also the human complex might be similarly organized. However, given the higher estimated molecular mass of the human complex, it seems likely that some other protein(s) might be involved.

To investigate the functional involvement of human Oxa11 in the biogenesis of OXPHOS, we down-regulated its expression in HEK293 cells by the stable expression of shRNAmir. The depletion of Oxa11 achieved was specific, since a qualitatively identical loss-of-function phenotype was induced using three different shRNA species. The Oxa11-depleted cells showed largely normal mitochondrial content, and both functionally and quantitatively intact respiratory chain complexes II and III. Intriguingly, the cytochrome oxidase activity and content of CcO, as well as the ascorbate/TMPD-fuelled, sodium azide-sensitive oxygen uptake, were either unaffected or even increased when compared to negative controls. On the contrary, markedly reduced protein content and ATPase activity of the F₁F_o-ATP synthase and moderately reduced content and activity of NADH:ubiquinone oxidoreductase were found in Oxa11-depleted cells, indicating selectively compromised assembly or stability of these two OXPHOS complexes. However, no significant accumulation of sub-complexes containing either the ATP synthase or complex I subunits could be detected in the mitochondria of Oxa11-depleted cells.

The observed defect of ATP synthase and complex I is consistent with the mitochondrial localization and integral membrane nature of Oxa11 and, to a certain extent, with the functional involvement of fungal Oxa1 homologues. However, the inactivation of OXA1 in yeast was shown to cause more pleiotropic OXPHOS defects, characterized mainly by the complete absence of CcO activity,⁴ pointing to the essential requirement of Oxa1 in the biogenesis of CcO.²³ In our opinion, there are at least four reasons that might account for the observed difference between the human cell line and fungi. First, the human protein might have functionally diverged from its fungal counterparts, most likely in terms of an adapted substrate preference. Since the yeast Oxa1 is strictly required for the N-terminal export of Cox2 precursor, it is possible that the complete absence of the N-terminal leader peptide in nascent human Cox2 might be responsible for the observed Oxa1-independent assembly of human CcO. Second, another protein that provides a partially overlapping function (e.g. Cox18) might be able to compensate, to a certain extent, for the lack of Oxa11 in human mitochondria. Third, Oxa11 may exhibit a tissue-specific loss-of-function phenotype, similar to several other factors involved in human OXPHOS biogenesis.²⁴ Finally, the depletion of Oxa11 achieved might not reach the threshold necessary to induce a detectable defect of cytochrome *c* oxidase and cytochrome *bc*₁ complex, though the increased respi-

ratory activity and content of CcO argues against this alternative.

The fact that human Oxa11 is able to partially restore the respiratory growth of yeast *oxa1* cells suggests that both proteins share at least basic functional features. However, given the wide exchangeability among the members of the Oxa1/Alb3/YidC family,²⁵ this cannot be extrapolated to a precise endogenous role. In this context, it was suggested that the potential homo-oligomerization of Oxa1 proteins might be responsible for their functional conservation, as interaction with other components may be dispensable for basic (translocase) function.¹²

The slightly increased activity and content of CcO in Oxa11-depleted cells may likely represent a part of an adaptive response to OXPHOS impairment. This explanation appears conceivable, since CcO was repeatedly shown to exhibit a low reserve capacity and a large control coefficient over the respiratory chain.^{26–28} Furthermore, CcO was shown to be required for the assembly/stability of complex I in mouse fibroblasts.²⁹ Indeed, a similar increase in the protein content of CcO was observed in human fibroblasts with a selectively reduced content of complex I holoenzyme.³⁰ The observed discrepancy between the cytochrome oxidase activity and ascorbate/TMPD-driven respiration was reported³¹ and probably stems from different preparations of the enzyme complex. Unlike the low-concentration digitonin treatment (respirometry), which preserves the inner membrane intact, the lauryl maltoside solubilization (spectrophotometric CcO assay) removes the enzyme complex from the inner membrane, eventually leading to altered enzyme function (e.g. due to abrogated allosteric interactions).

Since we did not detect any significant accumulation of ATP synthase or complex I sub-complexes in Oxa11-depleted mitochondria, it seems unlikely that the holoenzyme reduction observed could stem from a compromised stability of the complex. The lack of significant accumulation of F₁-ATPase also suggests that the assembly defect of ATP synthase cannot be attributed solely to selectively affected accumulation of mitochondrially encoded subunits *a* and *A6L*, since human ρ^0 cells were shown to contain high levels of F₁-ATPase.³² The F₁-ATPase was, however, repeatedly found to be more or less stably associated with subunit *c* (oligomer) in ρ^0 cells.^{33,34} In contrast to yeast and *S. pombe*, the biogenesis of mammalian (and *N. crassa*) ATP synthase is likely to be further complicated by the fact that the highly hydrophobic subunit *c* is encoded in the nucleus and has to be imported from the cytoplasm prior to its membrane insertion and assembly. Nargang *et al.*¹² have studied the *N. crassa oxa1* mutant but the authors did not address the effects of Oxa1 depletion on the ATP synthase in their paper. Recently, it was reported that the ATP synthase defect of yeast *oxa1* cells probably stems directly from the compromised assembly of subunit *c* into the holoenzyme.¹⁰ Indeed, the expression level of

subunit c was suggested to determine the content of ATP synthase in mammalian tissues.³⁵ It was shown that in mouse and rat thermogenic brown fat, the low expression level of subunit c mRNA correlates with the low relative content of ATP synthase in this tissue, irrespective of high mRNA levels of the remaining ATP synthase subunits.^{36–38} Furthermore, no accumulated ATP synthase sub-complexes could be detected in brown adipose tissue.³⁹ Therefore, we speculate that the ATP synthase defect of human *Oxa1l*-depleted cells could stem from the impaired assembly and/or membrane integration of the nuclear-encoded ATP synthase subunit c.

In conclusion, this study has revealed a possible role for the human member of the *Oxa1/Alb3/YidC* protein family in the biogenesis of OXPHOS that differs to a certain extent from that demonstrated for fungal *Oxa1* homologues. The specific RNAi phenotype suggests that *Oxa1l* is involved in the biogenesis of ATP synthase and complex I in human mitochondria, consistent with its mitochondrial localization and integral membrane properties. Future work will involve investigation of the exact composition of the *Oxa1l*-containing high molecular mass complex, as well as knockdown of *Oxa1l* expression in another (primary) human cell type.

Materials and Methods

Cell culture, transfections and flow cytometry

Human embryonic kidney cells (HEK293, CRL-1573) were obtained from ATCC (Rockville, MD) and grown at 37 °C in a 5% (v/v) CO₂ atmosphere in high-glucose Dulbecco's modified Eagle's medium (PAA, Austria) supplemented with 10% (v/v) fetal calf serum (PAA). Cell transfections were carried out either with a Nucleofector™ device (Amaxa, Cologne, Germany) using the HEK293 cell-specific transfection kit (Amaxa) or with the Lipofectamine 2000 reagent (Invitrogen, Paisley, UK). The GFP fluorescence of stable G418-resistant HEK293 cells was measured with a FACSCalibur flow cytometer and analyzed using the Cell Quest 3.3 application (Becton Dickinson, San Jose, CA).

Immunofluorescence

HEK293 cells (1.5×10^5) grown on 70 mm² glass chamber slides (BD Falcon, Palo Alto, CA) were transfected with an *OXA1L*-FLAG expression construct using the Lipofectamine 2000 reagent. At 24 h after the transfection, the cells were incubated with 200 nM MitoTracker Red CMX Ros (Molecular Probes, Eugene, OR) for 15 min, and then fixed and permeabilized with phosphate-buffered saline, 4% (v/v) paraformaldehyde and 0.1% (v/v) Triton X-100 solutions, respectively. Subsequently, the cells were incubated in phosphate-buffered saline, 10% (w/v) bovine serum albumin solution for 1 h at 37 °C to block non-specific binding. Immunocytochemical detection was then performed with a monoclonal M2 anti-FLAG antibody (1:1000) and with an anti-mouse IgG₁ Alexa Fluor® 488 antibody (1:500).

Laser scanning confocal microscopy

xyz images sampled according to the Nyquist criterion were acquired using a Nikon Eclipse TE2000 microscope equipped with a C1si confocal scanning head and an Apo TIRF 60× (N.A. 1.49) objective. The 488 nm and 543 nm laser lines and appropriate 515(±15) and 590(±15) nm band pass filter sets were used for excitation and fluorescence detection, respectively. Individual channel images were acquired separately. Images were restored using the measured point spread function (PSF) and the classic maximum likelihood deconvolution algorithm in Huygens Professional Software (SVI, Hilversum, Netherlands).

Plasmid construction

The nucleotide sequences of eight different miR-30-based shRNAs (shRNAmirs) targeted to the coding sequence of human *OXA1L* were downloaded from the publicly accessible RNAi Codex database.⁴⁰ The corresponding 97-mer oligonucleotides were synthesized (Invitrogen) and used as template sequences for PCR amplification to produce clonable double-stranded products. The corresponding XhoI/EcoRI restriction fragments were inserted downstream of the CMV-GFP-IRES-Neo expression cassette of the lentiviral pCMV-GIN-Zeo vector (Open Biosystems, Huntsville, AL). The negative control (non-silencing) shRNAmir pCMV-GIN-Zeo derivative was obtained from Open Biosystems. The full-length human *OXA1L* coding sequence was amplified from the IMAGE (integrated molecular analysis of genomes and their expression) clone 40017377 and inserted into the C-FLAG fusion mammalian expression vector pCMV-Tag4 (Stratagene, La Jolla, CA). The fidelity of all constructs was confirmed by automated DNA sequencing.

Validation of shRNAs and generation of stable transfectants

To assess the efficiency of the shRNAmir constructs, HEK293 cells were co-transfected using a Nucleofector™ device with either one of the eight *OXA1L*-targeted shRNA constructs or the negative control (non-silencing) shRNA construct and with the *OXA1L*-FLAG expression construct. At 48 h after the transfection, the cells were lysed and the expression level of the *Oxa1l*-FLAG fusion protein was examined by immunoblot analysis. The three *OXA1L*-targeted constructs that contained shRNA 1 (mp_d 433861, 5'-CAAGTTAGCAGGAGAC-CAT-3'), shRNA 2 (mp_id 19616, 5'-CCTACAACCTG-GAAAG GAT-3') and shRNA 3 (mp_id 19615, 5'-GAGACCATATGAGTATA-3') (RNAi Codex) showed the highest potential to interfere with the expression of *Oxa1l*-FLAG protein in the transient assay. For the generation of stable transfectants, HEK293 cells (10^6) were transfected using a Nucleofector™ device with the three functionally validated *OXA1L*-targeted shRNA constructs, the negative control (non-silencing) shRNA construct and with the empty vector. At 48 h after the transfection the cells were split into culture medium containing 720 µg/ml of G418 sulfate (Clontech, Mountain View, CA) and antibiotic-resistant colonies were selected over a period of three weeks. The cells were further maintained in the presence of 720 µg/ml G418.

Preparation of a polyclonal antibody to human Oxa11

An Oxa11-specific antiserum was generated by immunizing chicken with a synthetic peptide (KLH-coupled) corresponding to the C-terminal part of human Oxa11 (CKPKSKYPWHDT). The polyclonal antibody to human Oxa11 was affinity-purified from the total IgY with the respective peptide-packed column. The specificity of the produced antibody was tested by immunodetection of the Oxa11-FLAG fusion protein.

Immunoblot analysis

Protein sample preparations, electrophoresis and immunoblot analysis were performed essentially as described.²⁴ Monoclonal antibodies against the mitochondrial outer membrane protein porin, CcO subunits Cox1, Cox2 and Cox5a, the 70 kDa flavoprotein subunit of SDH (SDHA), complex III subunit core protein 2, complex I subunits NDUF9 and NDUF6, complex V subunits F1- α , F1- β , subunit d and OSCP, and pyruvate dehydrogenase (PDH) subunit E2 were obtained from Mitosciences (Eugene, OR). The mouse monoclonal antibody to mtHSP70 was from Alexis Biochemicals (San Diego, CA). Polyclonal antibodies to α -tubulin and eIF2 α were from Cell Signaling Technology (Beverly, MA), and the monoclonal anti-FLAG antibody was from Sigma (Prague, Czech Republic). Signal acquisition was performed using either a VersaDoc 4000 imaging system (Bio-Rad Laboratories, Hercules, CA) or Kodak BioMax Light films (Eastman Kodak Co., Rochester, NY). Digital images were analyzed using the Quantity One application (Bio-Rad Laboratories).

Immunoprecipitation of Oxa11-FLAG protein

HEK293 cells ($\sim 10^6$) were transiently (48 h) transfected with the Oxa11-FLAG expression construct, lysed with a buffer containing 1% Triton X-100, 150 mM NaCl, 1 mM EDTA and 50 mM Tris-HCl (pH 7.4), and the lysate was incubated for 6 h at 4 °C with previously washed 50 μ l of an ANTI-FLAG[®] M2 affinity agarose resin (flagipt-1; Sigma, Prague, Czech Republic). Subsequently, the resin was washed five times with a buffer containing 150 mM NaCl, 50 mM Tris-HCl (pH 7.4), and the bound protein was eluted by competition with 3 \times FLAG peptide. Finally, the eluted immunoprecipitate was combined with SDS sample buffer and resolved using SDS-PAGE.

Enzyme activity assays

The activities of enzyme complexes NADH:ubiquinone oxidoreductase (complex I), succinate:ubiquinone oxidoreductase (SDH or complex II), cytochrome *bc*₁ complex (complex III), cytochrome *c* oxidase (complex IV) and citrate synthase (CS) were measured spectrophotometrically in whole cell extracts and isolated mitochondria using standard methods.⁴¹ Aurovertin-sensitive ATP hydrolytic activity was measured in isolated mitochondria using an ATP-regenerating system as described.^{41,42}

Polarographic measurements

The ascorbate/TMPD-fuelled sodium azide-sensitive oxygen consumption of digitonin-permeabilized HEK293 cells was measured at 30 °C using an OROBOROS

Oxygraph (Anton Paar, Innsbruck, Austria) in a medium containing 0.5 mM EGTA, 3 mM MgCl₂, 60 mM potassium lactobionate, 20 mM taurine, 10 mM KH₂PO₄, 110 mM sucrose, 1 g/l BSA, 20 mM Hepes (pH 7.1). The measurements were carried out in the presence of 30 μ g/ml of digitonin, 2.5 μ M antimycin A, 2 mM ascorbate, 500 μ M TMPD and 1.5 μ M carbonyl cyanide *p*-(trifluoromethoxy) phenylhydrazone (FCCP). Respiration was inhibited by the addition of sodium azide to a final concentration of 10 mM.

Sub-cellular and submitochondrial fractionation

HEK293 cells (10^7) were harvested, washed twice with phosphate-buffered saline, resuspended in an isotonic buffer containing 250 mM sucrose, 10 mM Tris-HCl (pH 7.4), 1 mM EDTA, 1% (w/v) Protease inhibitor cocktail (Sigma), and disrupted on ice using a Dounce homogenizer. Unbroken cells and nuclei were removed from the homogenate by centrifugation at 600g for 15 min. The post-nuclear supernatant was centrifuged at 10,000g for 25 min to pellet the mitochondria. The resulting supernatant corresponding to the cytoplasmic fraction was collected, and the mitochondrial pellet was washed once with the isotonic buffer. For sonical disruption, isolated mitochondria were adjusted to a protein concentration of 2.5 mg/ml, sonicated and centrifuged at 100,000g for 30 min. Alkaline sodium carbonate extraction of mitochondrial membranes was performed essentially as described.⁴³

Statistical analysis

A Student's *t* test was performed using Microsoft Excel. Results are expressed as mean \pm S.D. A *p* value of less than 0.05 was considered as statistically significant, and asterisks are used to denote significance as follows: *, *p* < 0.05; **, *p* < 0.01.

Acknowledgements

The work was supported by grants from the Grant Agency of Charles University (GAUK 87607 and GAUK 1/2006/R), by institutional project MSM 0021620806 and by the European Union's Sixth Framework Programme for Research, Priority 1 "Life sciences, genomics and biotechnology for health" LSHMCT-2004-503116. We thank Dr J. Sikora for carrying out confocal microscopy imaging.

References

1. Yi, L. & Dalbey, R. E. (2005). Oxa1/Alb3/YidC system for insertion of membrane proteins in mitochondria, chloroplasts and bacteria (review). *Mol. Membr. Biol.* **22**, 101–111.
2. Herrmann, J. M. & Neupert, W. (2003). Protein insertion into the inner membrane of mitochondria. *IUBMB Life*, **55**, 219–225.
3. Bonnefoy, N., Chalvet, F., Hamel, P., Slonimski, P. P. & Dujardin, G. (1994). OXA1, a *Saccharomyces cerevisiae* nuclear gene whose sequence is conserved from

- prokaryotes to eukaryotes controls cytochrome oxidase biogenesis. *J. Mol. Biol.* **239**, 201–212.
4. Altamura, N., Capitanio, N., Bonnefoy, N., Papa, S. & Dujardin, G. (1996). The *Saccharomyces cerevisiae* OXA1 gene is required for the correct assembly of cytochrome c oxidase and oligomycin-sensitive ATP synthase. *FEBS Letters*, **382**, 111–115.
 5. Hell, K., Herrmann, J., Pratje, E., Neupert, W. & Stuart, R. A. (1997). Oxa1p mediates the export of the N- and C-termini of pCoxII from the mitochondrial matrix to the intermembrane space. *FEBS Letters*, **418**, 367–370.
 6. He, S. & Fox, T. D. (1997). Membrane translocation of mitochondrially coded Cox2p: distinct requirements for export of N and C termini and dependence on the conserved protein Oxa1p. *Mol. Biol. Cell*, **8**, 1449–1460.
 7. Lemaire, C., Guibet-Grandmougin, F., Angles, D., Dujardin, G. & Bonnefoy, N. (2004). A yeast mitochondrial membrane methyltransferase-like protein can compensate for oxa1 mutations. *J. Biol. Chem.* **279**, 47464–47472.
 8. Hell, K., Herrmann, J. M., Pratje, E., Neupert, W. & Stuart, R. A. (1998). Oxa1p, an essential component of the N-tail protein export machinery in mitochondria. *Proc. Natl Acad. Sci. USA*, **95**, 2250–2255.
 9. Hell, K., Neupert, W. & Stuart, R. A. (2001). Oxa1p acts as a general membrane insertion machinery for proteins encoded by mitochondrial DNA. *EMBO J.* **20**, 1281–1288.
 10. Jia, L., Dienhart, M. K. & Stuart, R. A. (2007). Oxa1 Directly Interacts with Atp9 and Mediates Its Assembly into the Mitochondrial F1Fo-ATP Synthase Complex. *Mol. Biol. Cell*, **18**, 1897–1908.
 11. Bonnefoy, N., Kermorgant, M., Groudinsky, O. & Dujardin, G. (2000). The respiratory gene OXA1 has two fission yeast orthologues which together encode a function essential for cellular viability. *Mol. Microbiol.* **35**, 1135–1145.
 12. Nargang, F. E., Preuss, M., Neupert, W. & Herrmann, J. M. (2002). The Oxa1 protein forms a homooligomeric complex and is an essential part of the mitochondrial export translocase in *Neurospora crassa*. *J. Biol. Chem.* **277**, 12846–12853.
 13. Jia, L., Dienhart, M., Schram, M., McCauley, M., Hell, K. & Stuart, R. A. (2003). Yeast Oxa1 interacts with mitochondrial ribosomes: the importance of the C-terminal region of Oxa1. *EMBO J.* **22**, 6438–6447.
 14. Szyrach, G., Ott, M., Bonnefoy, N., Neupert, W. & Herrmann, J. M. (2003). Ribosome binding to the Oxa1 complex facilitates co-translational protein insertion in mitochondria. *EMBO J.* **22**, 6448–6457.
 15. Bonnefoy, N., Kermorgant, M., Groudinsky, O., Minet, M., Slonimski, P. P. & Dujardin, G. (1994). Cloning of a human gene involved in cytochrome oxidase assembly by functional complementation of an oxa1-mutation in *Saccharomyces cerevisiae*. *Proc. Natl Acad. Sci. USA*, **91**, 11978–11982.
 16. Rotig, A., Parfait, B., Heidet, L., Dujardin, G., Rustin, P. & Munnich, A. (1997). Sequence and structure of the human OXA1L gene and its upstream elements. *Biochim. Biophys. Acta*, **1361**, 6–10.
 17. Strausberg, R. L., Feingold, E. A., Grouse, L. H., Derge, J. G., Klausner, R. D., Collins, F. S. *et al.* (2002). Generation and initial analysis of more than 15,000 full-length human and mouse cDNA sequences. *Proc. Natl Acad. Sci. USA*, **99**, 16899–16903.
 18. Sylvestre, J., Margeot, A., Jacq, C., Dujardin, G. & Corral-Debrinski, M. (2003). The role of the 3' untranslated region in mRNA sorting to the vicinity of mitochondria is conserved from yeast to human cells. *Mol. Biol. Cell*, **14**, 3848–3856.
 19. Stegmeier, F., Hu, G., Rickles, R. J., Hannon, G. J. & Elledge, S. J. (2005). A lentiviral microRNA-based system for single-copy polymerase II-regulated RNA interference in mammalian cells. *Proc. Natl Acad. Sci. USA*, **102**, 13212–13217.
 20. Kermorgant, M., Bonnefoy, N. & Dujardin, G. (1997). Oxa1p, which is required for cytochrome c oxidase and ATP synthase complex formation, is embedded in the mitochondrial inner membrane. *Curr. Genet.* **31**, 302–307.
 21. Herrmann, J. M., Neupert, W. & Stuart, R. A. (1997). Insertion into the mitochondrial inner membrane of a polytopic protein, the nuclear-encoded Oxa1p. *Embo J.* **16**, 2217–2226.
 22. Reif, S., Randelj, O., Domanska, G., Dian, E. A., Krimmer, T., Motz, C. & Rassow, J. (2005). Conserved mechanism of Oxa1 insertion into the mitochondrial inner membrane. *J. Mol. Biol.* **354**, 520–528.
 23. Stiburek, L., Hansikova, H., Tesarova, M., Cerna, L. & Zeman, J. (2006). Biogenesis of eukaryotic cytochrome c oxidase. *Physiol. Res.* **55**, S27–S41.
 24. Stiburek, L., Vesela, K., Hansikova, H., Pecina, P., Tesarova, M., Cerna, L. *et al.* (2005). Tissue-specific cytochrome c oxidase assembly defects due to mutations in SCO2 and SURF1. *Biochem. J.* **392**, 625–632.
 25. Preuss, M., Ott, M., Funes, S., Luirink, J. & Herrmann, J. M. (2005). Evolution of mitochondrial oxa proteins from bacterial YidC. Inherited and acquired functions of a conserved protein insertion machinery. *J. Biol. Chem.* **280**, 13004–13011.
 26. Villani, G., Greco, M., Papa, S. & Attardi, G. (1998). Low reserve of cytochrome c oxidase capacity in vivo in the respiratory chain of a variety of human cell types. *J. Biol. Chem.* **273**, 31829–31836.
 27. Piccoli, C., Scrima, R., Boffoli, D. & Capitanio, N. (2006). Control by cytochrome c oxidase of the cellular oxidative phosphorylation system depends on the mitochondrial energy state. *Biochem. J.* **396**, 573–583.
 28. Villani, G. & Attardi, G. (2000). *In vivo* control of respiration by cytochrome c oxidase in human cells. *Free Radic. Biol. Med.* **29**, 202–210.
 29. Diaz, F., Fukui, H., Garcia, S. & Moraes, C. T. (2006). Cytochrome c oxidase is required for the assembly/stability of respiratory complex I in mouse fibroblasts. *Mol. Cell. Biol.* **26**, 4872–4881.
 30. Ugalde, C., Janssen, R. J., van den Heuvel, L. P., Smeitink, J. A. & Nijtmans, L. G. (2004). Differences in assembly or stability of complex I and other mitochondrial OXPHOS complexes in inherited complex I deficiency. *Hum. Mol. Genet.* **13**, 659–667.
 31. Pecina, P., Capkova, M., Chowdhury, S. K., Drahot, Z., Dubot, A., Vojtiskova, A. *et al.* (2003). Functional alteration of cytochrome c oxidase by SURF1 mutations in Leigh syndrome. *Biochim. Biophys. Acta*, **1639**, 53–63.
 32. Buchet, K. & Godinot, C. (1998). Functional F1-ATPase essential in maintaining growth and membrane potential of human mitochondrial DNA-depleted rho degrees cells. *J. Biol. Chem.* **273**, 22983–22989.
 33. Garcia, J. J., Ogilvie, I., Robinson, B. H. & Capaldi, R. A. (2000). Structure, functioning, and assembly of the ATP synthase in cells from patients with the T8993G mitochondrial DNA mutation. Comparison with the enzyme in Rho(0) cells completely lacking mtDNA. *J. Biol. Chem.* **275**, 11075–11081.
 34. Carrozzo, R., Wittig, I., Santorelli, F. M., Bertini, E., Hofmann, S., Brandt, U. & Schagger, H. (2006). Sub-complexes of human ATP synthase mark mitochondrial biosynthesis disorders. *Ann. Neurol.* **59**, 265–275.

35. Houstek, J., Pickova, A., Vojtiskova, A., Mracek, T., Pecina, P. & Jesina, P. (2006). Mitochondrial diseases and genetic defects of ATP synthase. *Biochim. Biophys. Acta*, **1757**, 1400–1405.
36. Houstek, J., Andersson, U., Tvrdik, P., Nedergaard, J. & Cannon, B. (1995). The expression of subunit c correlates with and thus may limit the biosynthesis of the mitochondrial F₀F₁-ATPase in brown adipose tissue. *J. Biol. Chem.* **270**, 7689–7694.
37. Andersson, U., Houstek, J. & Cannon, B. (1997). ATP synthase subunit c expression: physiological regulation of the P1 and P2 genes. *Biochem. J.* **323**, 379–385.
38. Sangawa, H., Himeda, T., Shibata, H. & Higuti, T. (1997). Gene expression of subunit c(P1), subunit c (P2), and oligomycin sensitivity-conferring protein may play a key role in biogenesis of H⁺-ATP synthase in various rat tissues. *J. Biol. Chem.* **272**, 6034–6037.
39. Kramarova, T. (2006). *Limiting factors in ATP synthesis*, PhD thesis. Stockholm University.
40. Olson, A., Sheth, N., Lee, J. S., Hannon, G. & Sachidanandam, R. (2006). RNAi Codex: a portal/database for short-hairpin RNA (shRNA) gene-silencing constructs. *Nucl. Acids Res.* **34**, D153–D157.
41. Rustin, P., Chretien, D., Bourgeron, T., Gerard, B., Rotig, A., Saudubray, J. M. & Munnich, A. (1994). Biochemical and molecular investigations in respiratory chain deficiencies. *Clin. Chim. Acta*, **228**, 35–51.
42. Jesina, P., Tesarova, M., Fornuskova, D., Vojtiskova, A., Pecina, P., Kaplanova, V. *et al.* (2004). Diminished synthesis of subunit a (ATP6) and altered function of ATP synthase and cytochrome c oxidase due to the mtDNA 2 bp microdeletion of TA at positions 9205 and 9206. *Biochem. J.* **383**, 561–571.
43. Fujiki, Y., Hubbard, A. L., Fowler, S. & Lazarow, P. B. (1982). Isolation of intracellular membranes by means of sodium carbonate treatment: application to endoplasmic reticulum. *J. Cell Biol.* **93**, 97–102.

5.3. Analysis of the tissue-specific effects of mt-tRNA point mutations in patients affected by Leigh syndrome (8363G>A), MERRF syndrome (8344A>G), and MELAS syndrome (3243A>G) on the steady-state levels and activity of OXPHOS complexes (specific aim 2a)

Fornuskova D, Brantova O, Tesarova M, Stiburek L, Honzik T, Wenchich L, Tietzeova E, Hansikova H and Zeman J

The impact of mitochondrial tRNA mutations on the amount of ATP synthase differs in the brain compared to other tissues.

Biochim Biophys Acta 2008; 1782: 317-325.

Numerous studies have characterized the molecular mechanisms of point mutations in mitochondrial tRNA genes *in vitro*, but less was known how these mutations affect the amount and stability of OXPHOS complexes in human tissues. We have characterized the tissue- and gene-specific impact of 8363G>A, 8344A>G and 3243A>G mutations affecting mt-tRNA^{Lys} and mt-tRNA^{Leu(UUR)} on OXPHOS complexes in various tissues of patients carrying these mutations with clinical phenotypes of Leigh, MERRF and MELAS syndromes.

We used spectrophotometric measurements of specific enzyme activities, high-resolution respirometry and isolation of crude mitochondrial fraction by cellular fractionation and differential centrifugation to perform blue-native (BN) and two-dimensional (BN/SDS) PAGE with downstream immunoblot detections using monoclonal antibodies against various mitochondrial proteins.

In skeletal muscle mitochondria, both mutations that affect mt-tRNA^{Lys} (8363G>A, 8344A>G) resulted in severe combined deficiency of complexes I and IV, compared to an isolated severe defect of complex I in the 3243A>G sample (mt-tRNA^{Leu(UUR)}). Furthermore, we compared obtained patterns with those found in the heart, frontal cortex, and liver of 8363G>A and 3243A>G patients. In the frontal cortex mitochondria of both patients, the patterns of OXPHOS deficiencies differed substantially from those observed in other tissues, and this difference was particularly striking for ATP synthase. Surprisingly, in the frontal cortex of the 3243A>G patient, whose ATP synthase level was below the detection limit, the assembly of complex IV,

as inferred from 2D-PAGE immunoblotting, appeared to be hindered by some factor other than the availability of mtDNA-encoded subunits.

I contributed to this study by designing the research, carrying out the part of one-dimensional and two-dimensional electrophoretic and immunoblot analyses, and by writing the paper.



ELSEVIER

Available online at www.sciencedirect.com

Biochimica et Biophysica Acta 1782 (2008) 317–325

www.elsevier.com/locate/bbadis

The impact of mitochondrial tRNA mutations on the amount of ATP synthase differs in the brain compared to other tissues

Daniela Fornuskova, Olga Brantova, Marketa Tesarova, Lukas Stiburek, Tomas Honzik, Laszlo Wenchich, Evzenie Tietzeova, Hana Hansikova, Jiri Zeman*

Department of Pediatrics and Center of Applied Genomics, First Faculty of Medicine, Charles University in Prague, Ke Karlovu 2, Prague 2, 128 08, Czech Republic

Received 20 September 2007; received in revised form 1 February 2008; accepted 1 February 2008

Available online 15 February 2008

Abstract

The impact of point mutations in mitochondrial tRNA genes on the amount and stability of respiratory chain complexes and ATP synthase (OXPHOS) has been broadly characterized in cultured skin fibroblasts, skeletal muscle samples, and mitochondrial cybrids. However, less is known about how these mutations affect other tissues, especially the brain. We have compared OXPHOS protein deficiency patterns in skeletal muscle mitochondria of patients with Leigh (8363G>A), MERRF (8344A>G), and MELAS (3243A>G) syndromes. Both mutations that affect mt-tRNA^{Lys} (8363G>A, 8344A>G) resulted in severe combined deficiency of complexes I and IV, compared to an isolated severe defect of complex I in the 3243A>G sample (mt-tRNA^{Leu(UUR)}). Furthermore, we compared obtained patterns with those found in the heart, frontal cortex, and liver of 8363G>A and 3243A>G patients. In the frontal cortex mitochondria of both patients, the patterns of OXPHOS deficiencies differed substantially from those observed in other tissues, and this difference was particularly striking for ATP synthase. Surprisingly, in the frontal cortex of the 3243A>G patient, whose ATP synthase level was below the detection limit, the assembly of complex IV, as inferred from 2D-PAGE immunoblotting, appeared to be hindered by some factor other than the availability of mtDNA-encoded subunits.

© 2008 Elsevier B.V. All rights reserved.

Keywords: Brain; COX — cytochrome *c* oxidase; Leigh syndrome; MELAS syndrome; MERRF syndrome; Tissue specificity

1. Introduction

The mammalian organism fully depends on the oxidative phosphorylation system (OXPHOS) as the major energy (ATP) producer of the cell. Disturbances of OXPHOS may be caused by mutations in either mitochondrial DNA (mtDNA) or nuclear DNA, and environmental factors have also been shown to have important effects on OXPHOS. In human mitochondria, a small circular DNA molecule (16 659 bp) codes for 13 polypeptides that form, together with nuclear-encoded subunits, five inner-membrane OXPHOS complexes.

For the translation of these 11 mRNAs (nine monocistronic and two bicistronic), mitochondria contain a separate translational system made of protein components, encoded exclusively by nuclear genes and RNA components encoded by the mitochondrial genome (two ribosomal RNA (rRNA) genes and 22 transfer RNA (tRNA) genes). Mitochondrial translation is precisely controlled to meet tissue-specific demands for mtDNA-encoded structural subunits of the OXPHOS complexes [1]. Although the basal components of the mitochondrial expression system are known, the mechanism of regulation of the system in response to the metabolic needs of the cell is poorly understood [2,3].

Since the late 1980s, large-scale deletions and point mutations in mtDNA (approximately 120 in tRNAs and 11 in rRNAs) have been identified to cause disorders of mitochondrial protein synthesis, which is associated with defects of mitochondrial bioenergetics in tissues that most depend on OXPHOS. Despite numerous clinical studies on patients with mt-tRNA mutations,

Abbreviations: BN-PAGE, Blue-Native PAGE; COX, cytochrome *c* oxidase, complex IV; CS, citrate synthase; mt-tRNA, mitochondrial tRNA; mtDNA, mitochondrial DNA; OXPHOS, oxidative phosphorylation system; SQR, succinate:coenzyme Q₁₀ reductase, complex II

* Corresponding author. Tel.: +420 2 24967733; fax: +420 2 24967099.

E-mail address: jzem@lfl.cuni.cz (J. Zeman).

0925-4439/\$ - see front matter © 2008 Elsevier B.V. All rights reserved.

doi:10.1016/j.bbadis.2008.02.001

which usually involve morphological and functional characterization of OXPHOS insufficiency in skin fibroblast cultures or skeletal muscle, little is known regarding tissue specificity of OXPHOS deficiencies.

The aim of this study was to determine the steady-state levels of OXPHOS protein complexes in the mitochondria of various tissues (skeletal muscle, heart, frontal cortex and liver) of patients with mt-tRNA mutations. We chose (i) a patient with an 8363G>A mutation in mt-tRNA^{Lys}, who died of Leigh syndrome; (ii) a patient with an 8344A>G mutation in the same tRNA, who suffers from MERRF syndrome (myoclonic epilepsy with ragged-red fibers); and (iii) a patient with a 3243A>G mutation in mt-tRNA^{Leu(UUR)}, who died of MELAS syndrome (mitochondrial encephalomyopathy, lactic acidosis and stroke-like episodes). In the skeletal muscle of these patients, the mutations manifested themselves as described in previous studies [4–11]; however, these results disclose new aspects of OXPHOS deficiencies in the brain, particularly in the case of ATP synthase. Furthermore, the 3243A>G frontal cortex mitochondria showed a marked loss of the complex IV holoenzyme, accompanied by accumulation of assembly intermediates, which might be caused by the virtual absence of complex V in this sample. A similar phenomenon was described in yeast ATP synthase mutants [12–15].

2. Patients, materials and methods

2.1. Ethics

This study was carried out in accordance with the Declaration of Helsinki of the World Medical Association, and was approved by the Committee of Medical Ethics of the Faculty of Medicine and General Faculty Hospital. Informed parental consent, in accordance with the guidelines of the Faculty of Medicine, Charles University, was obtained for all biopsies and autopsies.

2.2. Case reports

2.2.1. Patient 1, with an 8363G>A mtDNA mutation

The boy was born at term with a birth weight of 2590 g (5th percentile) and a length of 48 cm. The early postnatal adaptation was uneventful, but a failure to thrive and progressive hypotony developed beginning in infancy, and he was wheelchair-dependent from the age of 8 years. Psychological investigations revealed moderate mental retardation, which later became severe. At the age of 8 he had his first epileptic paroxysm, and at the age of 11, an acute stroke-like encephalopathy developed, resulting in generalized weakness and respiratory failure requiring ventilatory support. The liver function was unaffected and aminotransferases were always within the reference range. The EEG pattern was abnormal; an EMG demonstrated peripheral neuropathy, echocardiography showed hypertrophic cardiomyopathy, and MRI revealed bilateral necrotic basal ganglia lesions typical of Leigh syndrome. The boy died at the age of twelve. Metabolic analyses revealed hyperlactacidemia (2.5–5.5 mmol/l, controls <2.1 mmol/l) with an increased lactate/pyruvate ratio (L/P 28).

2.2.2. Patient 2, with a 3243A>G mtDNA mutation

The girl was born at term with a birth weight of 3140 g and a length of 50 cm. Her early postnatal adaptation was uneventful, but a failure to thrive and growth retardation were observed beginning in infancy. At the age of 16 years, her weight and height were 30 kg and 140 cm (<3rd percentile). Cardiac evaluation revealed dilated cardiomyopathy and Wolf–Parkinson–White syndrome. At the age of 18 years, blurred vision, emesis and tiredness developed, and subsequently, seizures and coma. An MRI study showed symmetrical lesions within the basal ganglia, compatible with Leigh syndrome, in addition to several hypodensities in the subcortical regions of the frontal and occipital parts of the brain, which are

consistent with a diagnosis of acute ischemia. Metabolic analyses revealed metabolic acidosis (BE-10 to -25 mmol/l, controls \pm 2 mmol/l), as well as increased levels of lactate in the blood (4–10 mmol/l, controls <2.1 mmol/l), cerebrospinal fluid (12 mmol/l, controls <2.1 mmol/l), and urine (4976 mM/mol creatinine, controls <60 mM/mol creatinine). Despite intensive treatment, the girl died of progressive encephalomyopathy and respiratory failure due to acquired infection during the terminal phase of the disease, at the age of 18 years.

2.2.3. Patient 3, with an 8344A>G mtDNA mutation

The boy was born at term with a birth weight of 3500 g and length of 51 cm, with normal postnatal adaptation. Beginning at the age of 11 years, he developed progressive muscle weakness and paresthesia. Now, at the age of 15, he has generalized muscle hypotrophy and hyporeflexia. No mental deterioration has been observed. An EMG disclosed diffuse myopathic abnormalities and normal nerve conduction velocities. The EEG and cardiac evaluation were normal. Metabolic analyses revealed an increased level of lactate in the blood (5.6–7.88 mmol/l, controls <2.1 mmol/l) and lactate in the urine (5148 mM/mol creatinine, controls <60 mM/mol creatinine).

2.3. Tissues

All studied tissues were obtained from three patients harbouring one of two mutations in mt-tRNA^{Lys} (8363G>A and 8344A>G) or one mutation in mt-tRNA^{Leu(UUR)} (3243A>G), as well as from age-related controls. Open muscle biopsies from the tibialis anterior muscle were frozen at -80 °C. Post-mortem tissue specimens obtained at autopsy of 8363G>A and 3243A>G patients, and controls were frozen less than 2 h after death. The studies were performed in available stored material from the muscle (tibialis anterior), heart, liver, and brain (frontal cortex).

2.4. mtDNA analysis

Total genomic DNA was isolated by phenol extraction from available tissues. The DNA sample from the muscle biopsy of patient 1 was used for the sequencing of the whole mtDNA molecule on an AbiPrism 3100 Avant Genetic Analyser (Applied Biosystems).

To determine the amount of mtDNA containing the mutation, PCR/RFLP analysis was performed. PCR products (8279–8485) were radioactively labelled with [α -³²P]dCTP in the final cycle of PCR, and run on a non-denaturing 10% (w/v) polyacrylamide gel after complete digestion with TspRI (New England BioLabs). The mutation abolishes one of two TspRI restriction sites on the fragment. The proportions of wild-type to mutant mtDNA were measured using a PhosphorImager and ImageQuant software (Molecular Dynamics). The levels of heteroplasmy of the 3243A>G and 8344A>G mutations were determined as described elsewhere [16].

2.5. Electrophoresis

BN-PAGE (Blue-Native PAGE) [17] was used for the separation of mitochondrial membrane protein complexes on polyacrylamide 6–15% (w/v) gradient gels using a MiniProtean® 3 System (Bio-Rad Laboratories). 5–50 μ g of protein, which was prepared as described previously [18], was loaded in each lane. Two-dimensional BN/SDS/PAGE [17] was performed as described previously [18]. The protein content was measured by the Bio-Rad Protein Assay (Bio-Rad Laboratories), using BSA as a standard.

2.6. Immunoblot analysis

Proteins were electroblotted from the gels onto Immobilon™-P PVDF membranes (Millipore) using semi-dry transfer for 90 min at a constant current of 0.8 mA/cm². Membranes were air-dried overnight, rinsed twice with 100% (v/v) methanol, and blocked in TBS and 10% (w/v) non-fat dried milk for 1–2 h. Primary detection of BN/PAGE-blot was performed with mouse monoclonal antibodies raised against the complex I subunit NDUFA9 (2 μ g/ml), ATP synthase subunit alpha (2–3 μ g/ml), complex III subunit Core 2 (0.5 μ g/ml), complex IV subunit COX2 (0.5–1 μ g/ml), and complex II subunit 70 kDa protein (1 μ g/

ml) (Mitosciences), at indicated dilutions. Primary detection of two-dimensional BN/SDS/PAGE-blot for the COX assembly was performed according to Stiburek et al. [18]. Blots were incubated with primary antibodies in TBS, 0.3% (v/v) Tween 20, and 2% non-fat dried milk for 2 h. Secondary detection was carried out with a goat anti-mouse IgG-horseradish peroxidase conjugate (1:1000–1:4000) (Sigma–Aldrich) in TBS, 0.1% Tween 20, and 2% non-fat dried milk, for 1 h. The immunoblots were developed with SuperSignal West Femto Maximum Sensitivity Substrate (Pierce). The immunoblot-images of chemiluminescence signals were captured using the VersaDoc Imaging System, Model 4000 (Bio-Rad Laboratories), and analysed by the Quantity One application (Bio-Rad Laboratories). All blotting experiments were repeated with independently isolated mitochondrial samples. Duplicate experiments yielded consistent results.

2.7. Spectrophotometric assays

The activities of respiratory chain complexes in isolated muscle mitochondria were measured spectrophotometrically by standard methods at 37 °C. NADH:coenzyme Q10 reductase (NQR, complex I), succinate:coenzyme Q10 reductase (SQR, complex II), succinate:cytochrome *c* reductase (SCCR, complex II+III), NADH:cytochrome *c* reductase (NCCR, complex I+III), coenzyme Q10:cytochrome *c* reductase (QCCR, complex III), and cytochrome *c* oxidase (COX, complex IV) were measured according to Rustin et al. [19], and citrate synthase (CS) according to [20]. Total protein amount was determined by the method of Lowry [21].

2.8. High resolution oxygraphy in muscle fibers

Muscle fibers were separated mechanically according to [22], and oxygen consumption by saponin-skinned muscle fibers was determined using multiple substrate inhibitor titrations as described previously [23].

3. Results

3.1. Heteroplasmy of mt-tRNA mutations in investigated tissues

Analyses of heteroplasmy by radioactive PCR-RFLP showed 80 – 97% heteroplasmy of mt-tRNA mutations in the tissues of all patients (Table 1). Despite the narrow range of the mutation load found in patient tissues, the severity of the clinical/functional phenotype did not correlate with the level of heteroplasmy.

3.2. Steady-state levels of OXPHOS complexes in 8363G>A, 8344A>G and 3243A>G skeletal muscle

To investigate the impact of mtDNA mutations on the system of oxidative phosphorylation, immunoblots of mitochondrial fractions resolved by BN-PAGE were prepared. Dilutions of samples from control mitochondria were loaded on the same gels in order to express the residual steady-state levels of OXPHOS complexes in the patient tissues as a percentage of control values.

In the 8363G>A skeletal muscle sample obtained at autopsy, profoundly decreased levels of complex I (5% of control) and IV (<10% of control) were detected. The sample also revealed a diminished amount of complex V holoenzyme (35% of control), along with accumulated sub-complexes, most likely V* (F1-ATPase with several c-subunits) and F1-ATPase (Fig. 1A). The same sub-complexes were also detected in a bioptic muscle sample from the 8363G>A patient using BN-PAGE with Coomassie staining, followed by the second denaturing electrophoretic dimension with silver staining (Fig. 2).

A very similar pattern, although less severe, was found in the 8344A>G skeletal muscle sample. The amount of complex I was reduced to approximately 25% of control, the level of complex IV holoenzyme was <15% of control, and the holoenzyme level of complex V was decreased to 60% of the control value. Immunodetection of complex V further showed sub-complexes similar to those observed in the 8363G>A sample (Figs. 1A, 2A).

In 3243A>G skeletal muscle, relative levels of OXPHOS holoenzymes were normal, except for a decrease in the content of complex I to 30% of control and complex IV to 60% of control (Fig. 1A).

3.3. Steady-state levels of OXPHOS complexes in other 8363G>A and 3243A>G tissues

Only the 8363G>A and 3243A>G samples of heart, frontal cortex, and liver tissue were available for comparison of the

Table 1
Summary of clinical consequences, mtDNA mutation loads and character of OXPHOS deficiencies in investigated tissues of the patients

	8363G>A	3243A>G	8344A>G
Skeletal muscle	8363G>A	3243A>G	8344A>G
Clinical phenotype	Myopathy (+++)	Myopathy (++)	Myopathy (++)
Heteroplasmy	80%	90%	89%
OXPHOS protein deficiencies*	I and IV (↓↓↓), V (↓↓), V ^{sub}	I (↓↓)	I and IV (↓↓↓), V (↓), V ^{sub}
ADP-stimulated respiration after pyruvate/glutamate/succinate	↓↓/↓/↑↑	nd	↓/N/↑↑↑
Heart	8363G>A	3243A>G	8344A>G
Clinical phenotype	Cardiomyopathy ^H (++)	Cardiomyopathy ^D (++)	–
Heteroplasmy	89%	89%	nd
OXPHOS protein deficiencies	I and IV and V (↓↓↓), V ^{sub}	I (↓↓↓)	nd
Frontal cortex	8363G>A	3243A>G	8344A>G
Clinical phenotype	Encephalopathy (++)	Encephalopathy (++)	–
Heteroplasmy	87%	89%	nd
OXPHOS protein deficiencies	V (↓↓↓), I and IV (↓↓)	V (↓↓↓), I and IV (↓↓↓), IV ^{sub}	nd
Liver	8363G>A	3243A>G	8344A>G
Clinical phenotype	–	–	–
Heteroplasmy	97%	87%	nd
OXPHOS protein deficiencies	I (↓↓)	N	nd

–, absent; ++, moderate; +++, severe; ↓↓↓, <30% of control; ↓↓, 30 – 50% of control/mean control value; ↓, >50% of control/mean control value; ↑↑, 160% of mean control value; ↑↑↑, >200% of mean control value; N, normal; nd, not done; ^{sub}-assembly intermediates of indexed complex were present; ^D- dilated; ^H- hypertrophic.

* relative steady-state protein levels (Western blot) correlated with activities of respiratory chain complexes (spectrophotometry), (Fig. 3).

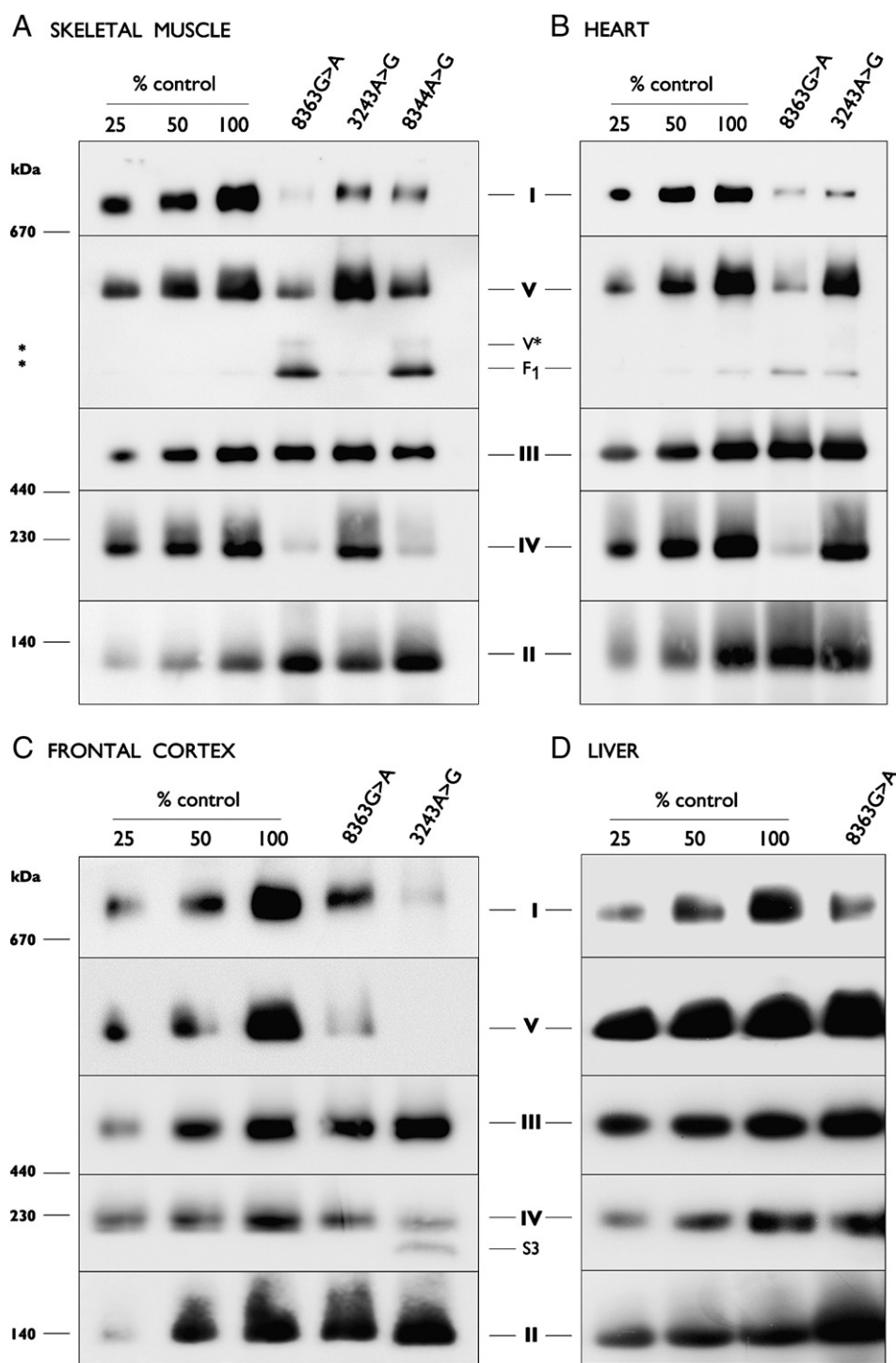


Fig. 1. Analysis of the assembly of OXPHOS complexes by immunoblotting of BN-PAGE. BN-PAGE of lauryl maltoside-solubilised mitochondria isolated from autoptic (8363G>A, 3243A>G) and bioptic (8344A>G) muscle (A) and from autoptic (8363G>A, 3243A>G) heart (B), frontal cortex (C) and liver (D) was electroblotted onto PVDF membranes and probed with monoclonal antibodies that detect the native forms of the OXPHOS complexes. Three aliquots of control mitochondria corresponding to the indicated dilutions of control samples were loaded on the same gels. The migration of holoenzymes (I–V) and molecular mass standards (kDa) are indicated; the actual position of sub-complex V* and/or F1 of complex V (*) in skeletal muscle (A) and heart (B) is directly below complex III (around 370–470 kDa).

impact of mtDNA mutations on the system of oxidative phosphorylation in skeletal muscle and other tissues (Table 1).

The 8363G>A heart sample showed the same considerable reduction in complexes I (5% of control) and IV (<10% of control) content as skeletal muscle, but despite the greater reduction of complex V holoenzyme (15% of control), there was a

significantly lower accumulation of F1-ATPase. The 3243A>G heart sample had a pronounced reduction of complex I (20% of control), similar to skeletal muscle (Fig. 1B).

In the 8363G>A frontal cortex, the assembly of complexes I and IV were less affected than in the above-mentioned tissues. The amount of complex I was decreased to 40% of control, and

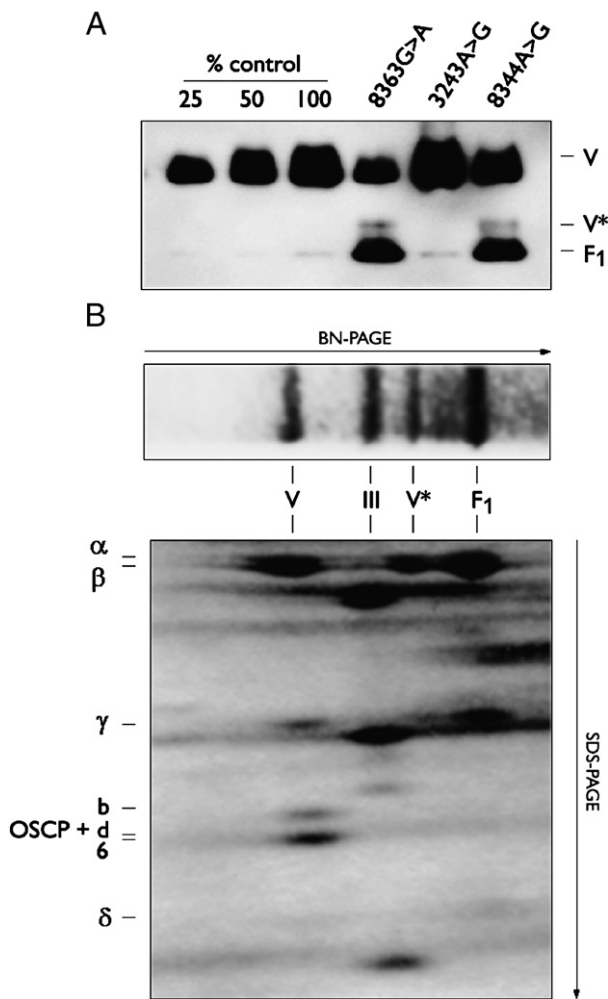


Fig. 2. Complex V (V) subassemblies V* and F₁-ATPase (F₁), compatible with those described previously for T8993G mitochondria, ρ⁰ cells, or where mitochondrial translation has been inhibited. Long exposure of complex V immunodetection with the monoclonal antibody against the ATP-alpha subunit from Fig. 1A (A). Coomassie staining of BN-PAGE (above) and silver staining of two-dimensional BN/SDS/PAGE (below) of the 8363G>A sample obtained from skeletal muscle (bioptic sample) (B).

the holoenzyme level of complex IV was reduced to 50% of control. Conversely, complex V (<20% of control) appeared to be the most severely affected member of the OXPHOS system. The decrease was more substantial than in skeletal muscle; nevertheless, no detectable sub-complexes could be found. The 3243A>G frontal cortex sample showed a dramatic reduction of complex V to below the detection limits of the method, and of complex I to 10% of the control value. Probing of the immunoblots with an anti-COX2 antibody showed a reduction of complex IV to 20% of control, as well as the presence of a high

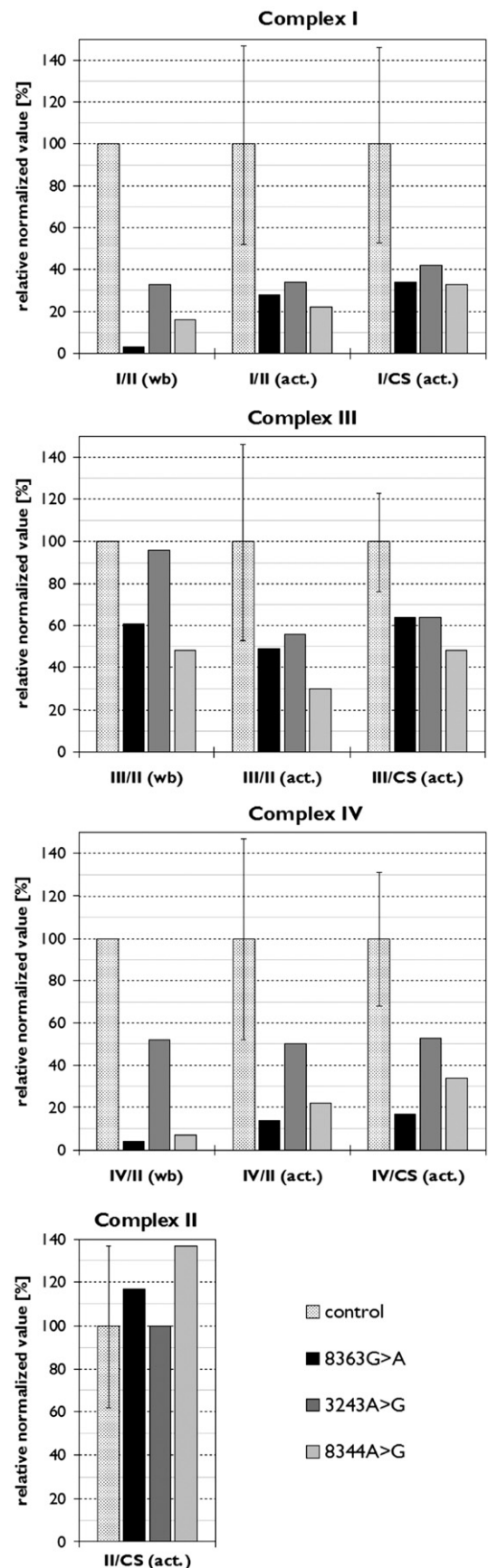


Fig. 3. Relative steady-state protein levels and activities of respiratory chain complexes normalized to complex II (II) or citrate synthase (CS) in isolated muscle mitochondria. The ratios of specific activities are expressed as the percentage of the mean of the control values (reference ranges are shown). Fractions by the x-axis indicate which ratios are concerned; I — complex I, III — complex III, IV — complex IV, (wb) — the ratio of holoenzyme levels obtained from a Western blot, (act.) — the ratio of specific activities obtained using spectrophotometry.

molecular weight sub-complex (Fig. 1C). Due to the unexpected OXPHOS deficiency pattern observed in brain tissue, particularly in the 3243A>G patient, the immunoblotting was also performed on the frontal cortex sample from another 3243A>G patient. In the only available sample with a 65% level of heteroplasmy, the immunoblotting analysis revealed normal levels of OXPHOS complexes in comparison to control (data not shown).

Despite the highest level of heteroplasmy (Table 1), the 8363G>A liver sample only showed an isolated deficiency of complex I (40% of control) (Fig. 1D). Steady-state levels of OXPHOS complexes in the 3243A>G liver mitochondria were comparable to control (data not shown).

3.4. Activities of respiratory chain complexes in 8363G>A, 8344A>G and 3243A>G skeletal muscle

To characterize the impact of the 8363G>A, 8344A>G and 3243A>G mutations on the function of respiratory chain complexes, the specific activities of the respective enzymes and citrate synthase (CS, control enzyme) were measured spectrophotometrically. The values expressed as relative ratios of the activities of complexes I, III and IV normalized to complex II (II, SQR) or CS were compared to the relative ratios of steady-state protein levels normalized to complex II (Fig. 3). Consistent with immunoblotting results, the spectrophotometry revealed lower activity ratios for complex I (I/II and I/CS) in the isolated muscle mitochondria of all three patients, and a severe deficiency of complex IV in 8363G>A and 8344A>G isolated muscle mitochondria. The COX/SQR (IV/II) and COX/CS (IV/CS) activity ratios in the 3243A>G patient were just below the control range.

3.5. Oxygraphic analysis in 8363G>A and 8344A>G skeletal muscle fibers

The functional consequences of the 8363G>A mutation in comparison to the 8344A>G mutation were analysed by high-resolution oxygraphy of the patients' skeletal muscle fibers permeabilized by a low concentration saponin treatment (Table 2).

Table 2
Oxygen consumption by saponin-permeabilized skeletal muscle fibers with 8363G>A and 8344A>G mutations

	8363G>A	8344A>G	Controls (n=9)
<i>Mitochondrial respiration (nmol O₂ min⁻¹ per mg of wet weight)</i>			
Pyruvate/malate	6.9	14.7	16–26
Glutamate/malate	5.1	16.5	10–22
Succinate	21.4	30.0	9–18
Ascorbate/TMPD	66.0	57.0	43–83
<i>Value normalized to respiration after succinate addition</i>			
Pyruvate/malate	0.32	0.49	0.96–1.85
Glutamate/malate	0.24	0.55	0.83–1.72
Ascorbate/TMPD	3.08	1.90	3.50–5.98

Polarographic measurements were performed as multiple substrate-inhibitor titration in the presence of 1 mM ADP with subsequent additions of pyruvate (10 mM)/malate (5 mM) or glutamate (10 mM)/malate (5 mM); succinate (10 mM); ascorbate (2 mM)/TMPD (500 μM).

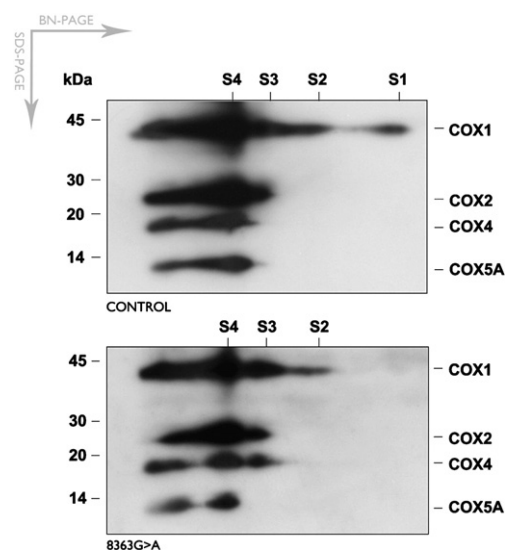


Fig. 4. Subunit composition of complex IV subassemblies in skeletal muscle obtained from the 8363G>A patient (bioptic sample). Two-dimensional BN/SDS-PAGE of lauryl maltoside-solubilised mitochondria isolated from the skeletal muscle of a control or the 8363G>A patient, obtained at biopsy, were electroblotted onto PVDF membranes and probed with monoclonal antibodies specific for the subunits COX1, COX2, COX4 and COX5A. The positions of the holoenzyme (S4) and subassemblies (S1–S3) are indicated, along with the migration of the molecular mass standard (kDa).

In both samples, a decrease of ADP-stimulated oxygen consumption compared to control fibers was observed using pyruvate as a substrate, and an increase was found after succinate addition. A pronounced reduction in ADP-stimulated respiration was found after pyruvate (33% of the mean control value) as well as after glutamate (32% of the mean control value) additions in 8363G>A muscle fibers. Indeed, ADP-stimulated respiration after succinate treatment increased to 158% of the mean control value. In 8344A>G muscle fibers, ADP-stimulated respiration after pyruvate addition was 70% of the mean control value, but after glutamate, it was within the reference range. Similarly to 8363G>A muscle fibers, the ADP-stimulated respiration after succinate addition increased to 222% of the mean control value in the 8344A>G sample. The absolute oxygen consumption after ascorbate+TMPD treatment was, in both samples, within control levels; however, normalization of the data to the level of respiration after succinate addition revealed decreased ratios after treatment with all of the substrates (Table 2).

3.6. Mitochondrial content in skeletal muscles with mt-tRNA^{Lys} mutations

In isolated muscle mitochondria, Western blotting showed an increased level of complex II holoenzyme, which is entirely encoded by nuclear DNA, up to 150% and 160% of control in 8363G>A and 8344A>G patient samples, respectively (Fig. 1A). After normalization, this leads to artificially decreased amounts of complex III in the skeletal muscle mitochondria of both patients (Fig. 3, Complex III). Accordingly, the II/CS activity ratio remained on the upper border of

the reference range (Fig. 3, Complex II), indicating a higher mitochondrial membrane content (altered mitochondrial morphology).

In tissue homogenates, the specific activity of CS was increased to 380% and 285% of the mean control value in the 8363G>A and 8344A>G patient samples, respectively. Histochemistry revealed increased amounts of SDH product in 8363G>A skeletal muscle and ragged-red fibers in 8344A>G skeletal muscle.

Based on the above-mentioned observations and on the increased ADP-stimulated oxygen consumption after succinate treatment (antimycin A-sensitive) of patients' skeletal muscle fibers (Section 3.5), a proliferation of mitochondria with altered morphology could be expected as a result of cellular energetic imbalance.

3.7. Immunoblots of two-dimensional native/denaturing gels

Immunoblotting of BN/SDS/PAGE (native in the first dimension and denaturing in the second dimension) with COX1, COX2, COX4 and COX5A antibodies was used to analyze the assembly of complex IV in 8363G>A skeletal muscle, and to confirm the alignment of the high molecular weight band identified in the 3243A>G frontal cortex after immunoblotting of BN/PAGE with COX2 antibody.

In 8363G>A skeletal muscle, the level of free S1 sub-complex was found to be below the detection limit of the method (Fig. 4). This probably reflects the limiting character of the COX1 subunit in the holoenzyme assembly.

In 3243A>G frontal cortex, significantly increased levels of all known complex IV assembly intermediates were observed, including free apoCOX1 (S1 sub-complex), apoCOX2, and apoCOX5A (Fig. 5). The high molecular weight band just below

the COX holoenzyme, which was detected with anti-COX2 antibody (Fig. 1C), very likely represents the S3 assembly intermediate (Fig. 5). Long exposure of the same immunoblot also revealed the band representing free apoCOX2 subunit (data not shown). This finding further supports the assumption that the final reduction in the content of COX holoenzyme in the 3243A>G frontal cortex mitochondria is not caused solely by the limiting character of mtDNA-encoded subunits of COX (translational defect, Fig. 4).

4. Discussion

This paper has presented a detailed analysis disclosing the tissue-specific impact of the 8363G>A mtDNA mutation on the amount, stability, and function of the OXPHOS complexes in a patient who died of Leigh syndrome. Furthermore, these data were compared with that from two other mtDNA mutations; the first one in the same tRNA (8344A>G) and the other one in mt-tRNA^{Leu(UUR)} (3243A>G), both of which are at least twice as common as the total number of other mtDNA point mutations known to cause disorders affecting the central nervous system [24,25]. Although just one patient with a comparable level of heteroplasmy was available per studied mutation, the observed data demonstrate intriguing tissue-specific patterns of OXPHOS protein deficiencies, with the most unexpected findings in the 3243A>G frontal cortex.

In the skeletal muscle of patient 1, the lowest level of heteroplasmy but the most severe OXPHOS defect suggests a more profound impact of the 8363G>A mutation on the translational system than that of the 8344A>G mutation. Concerning the 3243A>G mutation, the relatively proportional levels of heteroplasmy in 8344A>G and 3243A>G skeletal muscles, the more significant decrease in the content of complex I, the severe decrease in the amount of complex IV, and the slightly lower level of complex V in patient 2 all indicate a less pronounced impact of the 3243A>G mutation on mitochondrial translation in this tissue. However, the different nuclear backgrounds [26–30], distributions of heteroplasmy levels in cells and mitochondria [25,31,32], and environmental factors [33,34] which have been shown to influence expression of mitochondrial respiratory insufficiency, prevent the reduction of these results to any simple quantitative trait.

The frequency of UUR (Leu) codons in mitochondrially-translated subunits of OXPHOS implies decreased steady-state levels of complex I subunits, namely ND6, ND3, ND2 and ND5 (14–9 UURs) in 3243A>G mitochondria. In 8363G>A and 8344A>G mitochondria, the distribution of AAR (Lys) codons anticipates diminished levels of ND5, ND2, ND4 and COX1 (21–10 AARs). Moreover, all these subunits contain two X/Lys/Lys/X motifs, or one X/Lys/Lys/X and one Lys/X/Lys motif (<http://www.mitomap.org>), which are apparently strong stalling points for the ribosome. The particular abundance and distribution of codons in mitochondrially-translated subunits of respiratory chain complexes appears to be a plausible explanation for the isolated defect of complex I in the patient with a mutation in mt-tRNA^{Leu(UUR)}, along with the combined deficiency of complexes I and IV in patients with mutations in mt-tRNA^{Lys}.

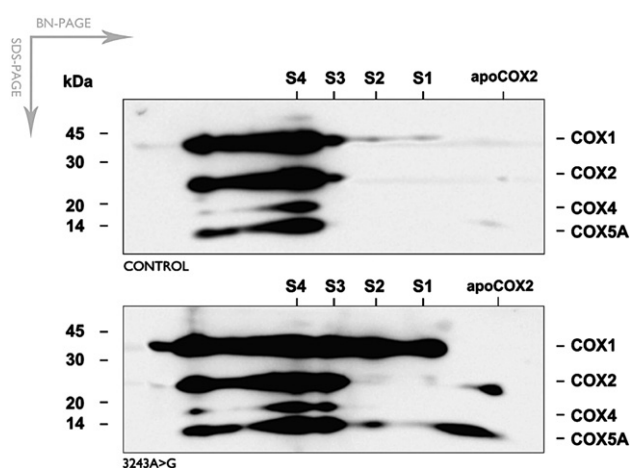


Fig. 5. Subunit composition of complex IV subassemblies in the frontal cortex obtained at autopsy of the 3243A>G patient. Two-dimensional BN/SDS/PAGE of lauryl maltoside-solubilised mitochondria isolated from the frontal cortex of a control or the 3243A>G patient, obtained at autopsy, were electroblotted onto PVDF membranes and probed with monoclonal antibodies specific for the subunits COX1, COX2, COX4 and COX5A. The positions of holoenzyme (S4) and subassemblies (S1–S3, apoCOX2) are indicated, along with the migration of the molecular mass standard (kDa).

Furthermore, the complete absence of unassembled apoCOX1 (S1) in the skeletal muscle of the 8363G>A patient, as revealed by BN/SDS/PAGE immunoblotting, conforms to the limiting character of the COX1 subunit in holoenzyme assembly. On the contrary, the OXPHOS deficiency patterns found in the frontal cortex mitochondria of the 8363G>A and 3243A>G patients could suggest, similarly to [18], a specific character for brain OXPHOS. First, in both frontal cortex samples, the decrease in the content of complex V was more profound than in that of complexes I and IV. Second, despite such a pronounced defect of complex V, no sub-complexes similar to those observed in skeletal muscle and heart could be detected, even when the immunoblot exposure was prolonged (data not shown). Unfortunately, no 8344A>G frontal cortex specimen was available for the analysis. However, a selectively decreased expression of COX2 subunit was previously reported in frontal cortex and cerebellum of a MERRF patient [35]. F1-ATPase, which was observed in heart, was found along with a sub-complex denoted V* in skeletal muscle. The sub-complex V* is likely composed of F1-ATPase and several c-F₀ subunits. These sub-complexes were described previously in 8993T>G mitochondria [36,37], ρ⁰ cells [37], and in cells with inhibited mitochondrial translation [38]. The observed steady-state levels of OXPHOS complexes suggest that the brain ATP synthase is most sensitive to disturbances of the mitochondrial translational system caused by the studied mt-tRNA mutations. Such a tissue-specific impact of mt-tRNA mutations with comparable tissue heteroplasmy is likely to result from tissue-specific variations in the nature of mitochondria. Indeed, it was shown that the brain, liver and kidney OXPHOS system is mainly controlled at the phosphorylation level by ATP synthase and a phosphate carrier, in contrast to the muscle and heart, where it is essentially controlled at the level of the respiratory chain [39]. On the other hand, instead of diminished energy provisions, an insufficient discharge of mitochondrial membrane potential leading to reactive oxygen species (ROS) production was proposed as the underlying pathogenic mechanism of ATP synthase deficiency [40]. Accordingly, the complete lack of complex V from 3243A>G frontal cortex may be, apart from the translational defect, responsible for the unusual assembly pattern of COX in this sample. Indeed, it was shown in yeast that (i) cells deficient in ATP synthase have a severe reduction of COX holoenzyme [12–15] and (ii) no decrease in COX synthesis is observed in uncoupled ATP synthase mutants, where the maintenance of mitochondrial potential is severely compromised by a massive proton leak through the F₀ sector [41,42]. Although the COX1 subunit was shown to be a key regulatory target for COX reduction in yeast cells [12], some other mechanism is likely to be involved in the hindered assembly of COX in the 3243A>G frontal cortex mitochondria, since this sample had high accumulated levels of all three mitochondrially encoded subunits, either free or partially assembled.

Although it is necessary to analyze considerably more samples with high levels of heteroplasmy (such samples are difficult to obtain), these data show new effects of mt-tRNA mutations on the brain which differ substantially from those described for skeletal muscle, heart, and liver tissues.

Acknowledgements

This work was supported by the European Union's Sixth Framework Programme for Research, Priority 1 'Life sciences, genomics and biotechnology for health' (LSHMCT-2004-503116), Research Projects MSM 0021620806 and 1M6837805002 and a grant from the Grant Agency of the Czech Republic (GACR 303/03/H065).

References

- [1] H. Antonicka, F. Sasarman, N.G. Kennaway, E.A. Shoubridge, The molecular basis for tissue specificity of the oxidative phosphorylation deficiencies in patients with mutations in the mitochondrial translation factor EFG1, *Hum. Mol. Genet.* 15 (2006) 1835–1846.
- [2] J. Asin-Cayuela, C.M. Gustafsson, Mitochondrial transcription and its regulation in mammalian cells, *Trends Biochem. Sci.* 32 (2007) 111–117.
- [3] J.W. Taanman, The mitochondrial genome: structure, transcription, translation and replication, *Biochim. Biophys. Acta* 1410 (1999) 103–123.
- [4] A. Shtilbans, S. Shanske, S. Goodman, C.M. Sue, C. Bruno, T.L. Johnson, N.S. Lova, N. Waheed, S. DiMauro, G8363A mutation in the mitochondrial DNA transfer ribonucleic acidLys gene: another cause of Leigh syndrome, *J. Child Neurol.* 15 (2000) 759–761.
- [5] M. Ozawa, I. Nishino, S. Horai, I. Nonaka, Y.I. Goto, Myoclonus epilepsy associated with ragged-red fibers: a G-to-A mutation at nucleotide pair 8363 in mitochondrial tRNA(Lys) in two families, *Muscle Nerve* 20 (1997) 271–278.
- [6] F.M. Santorelli, S.C. Mak, M. El-Schahawi, C. Casali, S. Shanske, T.Z. Baram, R.E. Madrid, S. DiMauro, Maternally inherited cardiomyopathy and hearing loss associated with a novel mutation in the mitochondrial tRNA(Lys) gene (G8363A), *Am. J. Hum. Genet.* 58 (1996) 933–939.
- [7] L. Boulet, G. Karpati, E.A. Shoubridge, Distribution and threshold expression of the tRNA(Lys) mutation in skeletal muscle of patients with myoclonic epilepsy and ragged-red fibers (MERRF), *Am. J. Hum. Genet.* 51 (1992) 1187–1200.
- [8] E.J. Okhuijsen-Kroes, J.M. Trijbels, R.C. Sengers, E. Mariman, L.P. van den Heuvel, U. Wendel, G. Koch, J.A. Smeitink, Infantile presentation of the mtDNA A3243G tRNA(Leu (UUR)) mutation, *Neuropediatrics* 32 (2001) 183–190.
- [9] Y. Koga, Y. Akita, N. Takane, Y. Sato, H. Kato, Heterogeneous presentation in A3243G mutation in the mitochondrial tRNA(Leu(UUR)) gene, *Arch. Dis. Child.* 82 (2000) 407–411.
- [10] G. Silvestri, M. Rana, F. Odoardi, A. Modoni, E. Paris, M. Papacci, P. Tonali, S. Servidei, Single-fiber PCR in MELAS(3243) patients: correlations between intratissue distribution and phenotypic expression of the mtDNA(A3243G) genotype, *Am. J. Med. Genet.* 94 (2000) 201–206.
- [11] J.A. Morgan-Hughes, M.G. Sweeney, J.M. Cooper, S.R. Hammans, M. Brockington, A.H. Schapira, A.E. Harding, J.B. Clark, Mitochondrial DNA (mtDNA) diseases: correlation of genotype to phenotype, *Biochim. Biophys. Acta* 1271 (1995) 135–140.
- [12] M. Rak, E. Tetaud, F. Godard, I. Sagot, B. Salin, S. Duvezin-Caubet, P. Slonimski, J. Rytka, J.P. di Rago, Yeast cells lacking the mitochondrial gene encoding the ATP synthase subunit 6 exhibit a selective loss of complex IV and unusual mitochondrial morphology, *J. Biol. Chem.* 282 (2007) 10853–10864.
- [13] W.M. Choo, R.G. Hadikusumo, S. Marzuki, Mitochondrial adenosine triphosphatase in mit-mutants of *Saccharomyces cerevisiae* with defective subunit 6 of the enzyme complex, *Biochim. Biophys. Acta* 806 (1985) 290–304.
- [14] S. Marzuki, L.C. Watkins, W.M. Choo, Mitochondrial H⁺-ATPase in mutants of *Saccharomyces cerevisiae* with defective subunit 8 of the enzyme complex, *Biochim. Biophys. Acta* 975 (1989) 222–230.
- [15] M.F. Paul, J. Velours, G. Arselin de Chateaubodeau, M. Aigle, B. Guerin, The role of subunit 4, a nuclear-encoded protein of the F₀ sector of yeast mitochondrial ATP synthase, in the assembly of the whole complex, *Eur. J. Biochem.* 185 (1989) 163–171.
- [16] O. Brantova, M. Tesarova, H. Hansikova, M. Elleder, J. Zeman, J. Sladkova, Ultrastructural changes of mitochondria in the cultivated skin fibroblasts of

- patients with point mutations in mitochondrial DNA, *Ultrastruct. Pathol.* 30 (2006) 239–245.
- [17] H. Schagger, G. von Jagow, Blue native electrophoresis for isolation of membrane protein complexes in enzymatically active form, *Anal. Biochem.* 199 (1991) 223–231.
- [18] L. Stiburek, K. Vesela, H. Hansikova, P. Pecina, M. Tesarova, L. Cerna, J. Houstek, J. Zeman, Tissue-specific cytochrome c oxidase assembly defects due to mutations in SCO2 and SURF1, *Biochem. J.* 392 (2005) 625–632.
- [19] P. Rustin, D. Chretien, T. Bourgeron, B. Gerard, A. Rotig, J.M. Saudubray, A. Munnich, Biochemical and molecular investigations in respiratory chain deficiencies, *Clin. Chim. Acta* 228 (1994) 35–51.
- [20] P.A. Srere, Citrate synthase, in: S.P. Colowick, N.O. Kaplan (Eds.), *Methods in Enzymology*, 1969, pp. 3–26.
- [21] O.H. Lowry, N.J. Rosebrough, A.L. Farr, R.J. Randall, Protein measurement with the Folin phenol reagent, *J. Biol. Chem.* 193 (1951) 265–275.
- [22] W.S. Kunz, A.V. Kuznetsov, W. Schulze, K. Eichhorn, L. Schild, F. Strigow, R. Bohnensack, S. Neuhofer, H. Grasshoff, H.W. Neumann, et al., Functional characterization of mitochondrial oxidative phosphorylation in saponin-skinned human muscle fibers, *Biochim. Biophys. Acta* 1144 (1993) 46–53.
- [23] L. Wenich, Z. Drahota, T. Honzik, H. Hansikova, M. Tesarova, J. Zeman, J. Houstek, Polarographic evaluation of mitochondrial enzymes activity in isolated mitochondria and in permeabilized human muscle cells with inherited mitochondrial defects, *Physiol. Res.* 52 (2003) 781–788.
- [24] P.F. Chinnery, D.T. Brown, K. Archibald, A. Curtis, D.M. Turnbull, Spinocerebellar ataxia and the A3243G and A8344G mtDNA mutations, *J. Med. Genet.* 39 (2002) E22.
- [25] J. Betts, E. Jaros, R.H. Perry, A.M. Schaefer, R.W. Taylor, Z. Abdel-All, R.N. Lightowlers, D.M. Turnbull, Molecular neuropathology of MELAS: level of heteroplasmy in individual neurones and evidence of extensive vascular involvement, *Neuropathol. Appl. Neurobiol.* 32 (2006) 359–373.
- [26] M. Feuermann, S. Francisci, T. Rinaldi, C. De Luca, H. Rohou, L. Frontali, M. Bolotin-Fukuhara, The yeast counterparts of human ‘MELAS’ mutations cause mitochondrial dysfunction that can be rescued by overexpression of the mitochondrial translation factor EF-Tu, *EMBO Rep.* 4 (2003) 53–58.
- [27] T. Rinaldi, A. Gambadoro, S. Francisci, L. Frontali, Nucleo-mitochondrial interactions in *Saccharomyces cerevisiae*: characterization of a nuclear gene suppressing a defect in mitochondrial tRNA(Asp) processing, *Gene* 303 (2003) 63–68.
- [28] H. Hao, L.E. Morrison, C.T. Moraes, Suppression of a mitochondrial tRNA gene mutation phenotype associated with changes in the nuclear background, *Hum. Mol. Genet.* 8 (1999) 1117–1124.
- [29] M.X. Guan, N. Fischel-Ghodsian, G. Attardi, A biochemical basis for the inherited susceptibility to aminoglycoside ototoxicity, *Hum. Mol. Genet.* 9 (2000) 1787–1793.
- [30] K.R. Johnson, Q.Y. Zheng, Y. Bykhovskaya, O. Spirina, N. Fischel-Ghodsian, A nuclear-mitochondrial DNA interaction affecting hearing impairment in mice, *Nat. Genet.* 27 (2001) 191–194.
- [31] S.E. Durham, D.C. Samuels, L.M. Cree, P.F. Chinnery, Normal levels of wild-type mitochondrial DNA maintain cytochrome c oxidase activity for two pathogenic mitochondrial DNA mutations but not for m.3243A->G, *Am. J. Hum. Genet.* 81 (2007) 189–195.
- [32] E. Bua, J. Johnson, A. Herbst, B. Delong, D. McKenzie, S. Salamat, J.M. Aiken, Mitochondrial DNA-deletion mutations accumulate intracellularly to detrimental levels in aged human skeletal muscle fibers, *Am. J. Hum. Genet.* 79 (2006) 469–480.
- [33] R.J. Levy, Mitochondrial dysfunction, bioenergetic impairment, and metabolic down-regulation in sepsis, *Shock* 28 (2007) 24–28.
- [34] T. Hassanein, T. Frederick, Mitochondrial dysfunction in liver disease and organ transplantation, *Mitochondrion* 4 (2004) 609–620.
- [35] M. Sparaco, E.A. Schon, S. DiMauro, E. Bonilla, Myoclonic epilepsy with ragged-red fibers (MERRF): an immunohistochemical study of the brain, *Brain Pathol.* 5 (1995) 125–133.
- [36] L.G. Nijtmans, N.S. Henderson, G. Attardi, I.J. Holt, Impaired ATP synthase assembly associated with a mutation in the human ATP synthase subunit 6 gene, *J. Biol. Chem.* 276 (2001) 6755–6762.
- [37] R. Carozzo, I. Wittig, F.M. Santorelli, E. Bertini, S. Hofmann, U. Brandt, H. Schagger, Subcomplexes of human ATP synthase mark mitochondrial biosynthesis disorders, *Ann. Neurol.* 59 (2006) 265–275.
- [38] L.G. Nijtmans, P. Klement, J. Houstek, C. van den Bogert, Assembly of mitochondrial ATP synthase in cultured human cells: implications for mitochondrial diseases, *Biochim. Biophys. Acta* 1272 (1995) 190–198.
- [39] R. Rossignol, T. Letellier, M. Maltat, C. Rocher, J.P. Mazat, Tissue variation in the control of oxidative phosphorylation: implication for mitochondrial diseases, *Biochem. J.* 347 (Pt 1) (2000) 45–53.
- [40] J. Houstek, T. Mracek, A. Vojtiskova, J. Zeman, Mitochondrial diseases and ATPase defects of nuclear origin, *Biochim. Biophys. Acta* 1658 (2004) 115–121.
- [41] S. Duvezin-Caubet, M. Caron, M.F. Giraud, J. Velours, J.P. di Rago, The two rotor components of yeast mitochondrial ATP synthase are mechanically coupled by subunit delta, *Proc. Natl. Acad. Sci. U. S. A.* 100 (2003) 13235–13240.
- [42] E. Guelin, J. Chevallier, M. Rigoulet, B. Guerin, J. Velours, ATP synthase of yeast mitochondria. Isolation and disruption of the ATP epsilon gene, *J. Biol. Chem.* 268 (1993) 161–167.

5.4. Study of molecular and biochemical impact of mtDNA mutation in the ATP6 gene (9205 Δ TA) on the biosynthesis of ATPase subunit a and its structural and functional consequences (specific aim 2b)

Jesina P, Tesarova M, **Fornuskova D**, Vojtiskova A, Pecina P, Kaplanova V,
Hansikova H, Zeman J and Houstek J

Diminished synthesis of subunit a (ATP6) and altered function of ATP synthase and cytochrome c oxidase due to the mtDNA 2 bp microdeletion of TA at positions 9205 and 9206.

Biochem J 2004; 383: 561-571.

In patient with combined deficiency of complexes IV and V, we identified and studied rare mtDNA mutation in the ATP6 gene – a 2bp microdeletion at positions 9205 and 9206 (9205 Δ TA). This mutation cancels the STOP codon of ATP6 gene and changes the cleavage site between the *ATP6* and *COX3* transcripts.

To unravel the molecular basis of combined cytochrome c oxidase and ATP synthase deficiency in patient with fatal infantile encephalopathy, severe psychomotor delay, frontal lobe atrophy and lactic acidosis, we used mtDNA sequencing. The amount of mtDNA containing the microdeletion was determined by the PCR/RFLP analysis in available tissues of the patient and his relatives. The functionality and integrity of OXPHOS, especially of complexes IV and V, was studied using isolation of crude mitochondrial fraction by cellular fractionation and differential centrifugation, spectrophotometric measurements of specific enzyme activities, rate of ATP synthesis, quantitative real-time RT-PCR and Northern blot analyses, assay for biosynthesis of mitochondrial proteins, high-resolution respirometry, cytofluorimetric analysis of mitochondrial membrane potential, and blue-native (BN), denaturing (SDS) and two-dimensional (BN/SDS) PAGE with downstream immunoblot detections using monoclonal or polyclonal antibodies against various mitochondrial proteins.

The mutation was present at increasing load in a three-generation family (in blood: grandmother - 16%, mother - 82%, proband - >98%). In the affected boy with severe encephalopathy, a homoplasmic mutation was present in blood, fibroblasts and muscle. The fibroblasts from the patient showed normal aurovertin-sensitive ATPase hydrolytic activity, a 70 % decrease in ATP synthesis and an 85 % decrease in CcO activity.

ADP-stimulated respiration and the ADP-induced decrease in the mitochondrial membrane potential at state 4 were decreased by 50 %. The content of subunit a was decreased 10-fold compared with other ATP synthase subunits, and [³⁵S] methionine labelling showed a 9-fold decrease in subunit a biosynthesis. The content of CcO subunits 1, 4 and 6c was decreased by 30–60 %. Northern Blot and quantitative real-time reverse transcription–PCR analysis further demonstrated that the primary *ATP6-COX3* transcript is cleaved to the *ATP6* and *COX3* mRNAs 2-3-fold less efficiently. Structural studies by blue-native and two-dimensional electrophoresis revealed an altered pattern of CcO assembly and instability of the ATP synthase complex, which dissociated into subcomplexes. The results indicate that the 9205ΔTA mutation prevents the synthesis of ATP synthase subunit a, and causes the formation of incomplete ATP synthase complexes that are capable of ATP hydrolysis but not ATP synthesis. The mutation also affects the biogenesis of CcO, which is present in a decreased amount in cells from affected individuals.

I contributed to this study by identification of the 9205ΔTA mutation in mitochondrial genome of the patient and his relatives.

Vojtiskova A, Jesina P, Kalous M, Kaplanova V, Houstek J, Tesarova M, **Fornuskova D**, Zeman J, Dubot A and Godinot C

Mitochondrial membrane potential and ATP production in primary disorders of ATP synthase.

Toxicol Mech Methods 2004; 14: 7-11.

We summarize the functional consequences of primary ATP synthase defects resulting from 8993T>G, 9205ΔTA and 8527A>G mutations in the *ATP6* gene at the level of mitochondrial ATP synthesis and maintenance as well as discharge of the mitochondrial membrane potential.

Studies of fibroblasts with primary defects in mitochondrial ATP synthase due to heteroplasmic mtDNA mutations in the *ATP6* gene, affecting protonophoric function or synthesis of subunit a, show that at high mutation loads, mitochondrial membrane potential $\Delta\Psi_m$ at state 4 is normal, but ADP-induced discharge of $\Delta\Psi_m$ is impaired and ATP synthesis at state 3-ADP is decreased. Increased $\Delta\Psi_m$ and low ATP synthesis is also found when the ATP synthase content is diminished by altered biogenesis of the enzyme complex. Irrespective of the different pathogenic mechanisms, elevated $\Delta\Psi_m$ in

primary ATP synthase disorders could increase mitochondrial production of reactive oxygen species and decrease energy provision.

I contributed to this study by molecular analysis and preparation of cultured skin fibroblasts derived from patients.

Diminished synthesis of subunit a (ATP6) and altered function of ATP synthase and cytochrome *c* oxidase due to the mtDNA 2 bp microdeletion of TA at positions 9205 and 9206

Pavel JEŠINA*¹, Markéta TESAŘOVÁ†¹, Daniela FORNŮSKOVÁ†, Alena VOJTÍŠKOVÁ*, Petr PECINA*, Vilma KAPLANOVÁ*, Hana HANSÍKOVÁ†, Jiří ZEMAN† and Josef HOUŠTĚK*²

*Department of Bioenergetics, Institute of Physiology and Centre for Integrated Genomics, Academy of Sciences of the Czech Republic, Vídeňská 1083, 142 20 Prague, Czech Republic, and †Department of Pediatrics and Institute for Inherited Metabolic Disorders, 1st Faculty of Medicine, Charles University, 120 00 Prague, Czech Republic

Dysfunction of mitochondrial ATPase (F_1F_0 -ATP synthase) due to missense mutations in ATP6 [mtDNA (mitochondrial DNA)-encoded subunit a] is a frequent cause of severe mitochondrial encephalomyopathies. We have investigated a rare mtDNA mutation, i.e. a 2 bp deletion of TA at positions 9205 and 9206 (9205 Δ TA), which affects the STOP codon of the *ATP6* gene and the cleavage site between the RNAs for *ATP6* and *COX3* (cytochrome *c* oxidase 3). The mutation was present at increasing load in a three-generation family (in blood: 16%/82%/>98%). In the affected boy with severe encephalopathy, a homoplasmic mutation was present in blood, fibroblasts and muscle. The fibroblasts from the patient showed normal aurovertin-sensitive ATPase hydrolytic activity, a 70% decrease in ATP synthesis and an 85% decrease in COX activity. ADP-stimulated respiration and the ADP-induced decrease in the mitochondrial membrane potential at state 4 were decreased by 50%. The content of subunit a was decreased 10-fold compared with other ATPase subunits, and [³⁵S]-

methionine labelling showed a 9-fold decrease in subunit a biosynthesis. The content of COX subunits 1, 4 and 6c was decreased by 30–60%. Northern Blot and quantitative real-time reverse transcription-PCR analysis further demonstrated that the primary ATP6-COX3 transcript is cleaved to the ATP6 and COX3 mRNAs 2–3-fold less efficiently. Structural studies by Blue-Native and two-dimensional electrophoresis revealed an altered pattern of COX assembly and instability of the ATPase complex, which dissociated into subcomplexes. The results indicate that the 9205 Δ TA mutation prevents the synthesis of ATPase subunit a, and causes the formation of incomplete ATPase complexes that are capable of ATP hydrolysis but not ATP synthesis. The mutation also affects the biogenesis of COX, which is present in a decreased amount in cells from affected individuals.

Key words: *ATP6*, ATP synthase, *COX3*, cytochrome *c* oxidase, mitochondrial disease, mitochondrial DNA (mtDNA).

INTRODUCTION

The mammalian ATPase (F_1F_0 -ATP synthase) complex catalyses the synthesis of ATP from ADP and P_i , the final step of the OXPHOS (oxidative phosphorylation) pathway. The ATPase complex consists of 16 different subunits [1], and is composed of the globular F_1 catalytic part connected by two stalks to the membrane-embedded F_0 moiety that translocates protons across the mitochondrial inner membrane. Only two F_0 subunits, subunit a (ATP6) and A6L (ATP8), are encoded by mtDNA (mitochondrial DNA) [2]. Both are essential for the biogenesis and assembly of the ATPase complex [3].

Mutations in mtDNA represent a frequent cause of mitochondrial diseases. They can involve tRNAs, rRNAs or protein-encoding genes (for review see [4]) and are associated with a wide variety of clinical pictures, ranging from isolated myopathy to multisystem disorders, affecting primarily tissues with high energy demands, such as skeletal muscle, heart and nervous system. Most pathogenic mtDNA mutations are in tRNAs. Mutations in protein-encoding genes are much less frequent, with the exception of those associated with complex I or ATPase dysfunction.

All maternally inherited ATPase diseases are caused by mutations in the *ATP6* gene; no mutation has been reported in the *ATP8* (A6L) gene. Mutations in the *ATP6* gene disturb the function of the ATPase proton channel, which consists of subunit a and multiple copies of subunit c. The most frequent are heteroplasmic T8993G [5] or less severe T8993C mutations [6], which result in replacement of Leu¹⁵⁶ by Arg or Pro in subunit a, and often present as a NARP (neurogenic muscle weakness, ataxia, retinitis pigmentosa) [5] or MILS (maternally inherited Leigh syndrome) [7] phenotype. Several other, less frequent, mutations of *ATP6* at positions 9176 or 8851 have also been described (for review see [8]), resulting in similar lesions in brain, particularly in the striatum (familial bilateral striatal necrosis). The T8993G mutation results in a decrease in mitochondrial ATP production [9] without a significant effect on ATP hydrolysis [7], and in structural changes in the ATPase complex [10], which, however, could not be found in some cases [11]. It has been observed that the ATPase deficiency is associated with a decreased ability of cells from affected individuals to assemble correctly the ATPase complex, which shows instability in BN-PAGE (Blue-Native PAGE) experiments [10,12].

Abbreviations used: ATPase, F_1F_0 -ATP synthase; BN-PAGE, Blue-Native PAGE; COX, cytochrome *c* oxidase; CS, citrate synthase; 2D, two-dimensional; DDM, dodecyl maltoside; FCCP, carbonyl cyanide 4-trifluoromethoxyphenylhydrazone; LRPPRC, leucine-rich pentatricopeptide repeat cassette; mtDNA, mitochondrial DNA; OXPHOS, oxidative phosphorylation; $\Delta\Psi_m$, mitochondrial membrane potential; RFLP, restriction fragment length polymorphism; RT-PCR, reverse transcription-PCR; SDH, succinate dehydrogenase; TMPD, *N,N,N',N'*-tetramethyl-*p*-phenylenediamine; TMRM, tetramethylrhodamine methyl ester; WB, Western blot.

¹ These authors contributed equally to this work.

² To whom correspondence should be addressed (email houstek@biomed.cas.cz).

In the present paper we have studied a very rare mtDNA mutation in the *ATP6* gene – a 2 bp microdeletion at positions 9205 and 9206 (9205 Δ TA). This mutation cancels the STOP codon of *ATP6* gene and changes the cleavage site between the *ATP6* and *COX3* (cytochrome *c* oxidase subunit 3) transcripts. It was originally discovered in a newborn with transient lactic acidosis [13]. Recently we found a second case of a 9205 Δ TA mutation that was present in a child with severe encephalopathy and hyperlactacidaemia [14]. Here we present the results of molecular and biochemical studies of *ATPase* and *COX* that focus on the biosynthesis of *ATPase* subunit *a* and the structural and functional consequences of the 9205 Δ TA mutation.

EXPERIMENTAL

Ethics

This study was carried out in accordance with the Declaration of Helsinki of the World Medical Association, and was approved by the Committees of Medical Ethics at all collaborating institutions. Informed consent was obtained from the parents of the child.

Case report

The boy was born at term from a second, uncomplicated pregnancy, with birth weight 3450 g and length 52 cm. Failure to thrive, spastic quadraparesis and microcephalia were observed from the 3rd month of life, followed by practical arrest of any psychomotor development. Metabolic investigations revealed intermittent hyperlactacidaemia (B-lactate, 0.95–3.4 mmol/l; controls < 2.1 mmol/l), with increased levels of lactate and alanine in the cerebrospinal fluid [lactate, 4.8 mmol/l (controls < 1.8 mmol/l); alanine, 36 μ mol/l (controls < 34 μ mol/l)]. He is 5 years old at present. Both parents are healthy, but an older brother (from the first marriage of the mother) died due to a respiratory failure at the age of 3 years. He presented with fatal infantile encephalopathy, severe psychomotor delay, frontal lobe atrophy and lactic acidosis.

Cell cultures and isolation of mitochondria

Fibroblast cultures were established from skin biopsies, and cells were grown in Dulbecco's modified Eagle's medium supplemented with 10% (v/v) fetal calf serum (Sigma) at 37 °C in 5% CO₂ in air. Cells were grown to approx. 90% confluence and harvested using 0.05% (w/v) trypsin and 0.02% (w/v) EDTA. Detached cells were diluted with an ice-cold culture medium, sedimented by centrifugation and washed twice in PBS.

Mitochondria were isolated from fibroblasts by a hypo-osmotic shock method [15]. The freshly harvested cells were disrupted in 10 mM Tris buffer (pH 7.4) and quickly homogenized in a Teflon/glass homogenizer at 4 °C. Sucrose was added to a final concentration of 0.25 M immediately after homogenization. The nuclei were removed by centrifugation for 10 min at 4 °C and 600 g and the mitochondrial fraction was isolated from the postnuclear supernatant by centrifugation for 10 min at 4 °C and 10 000 g. The mitochondrial pellet was washed and finally resuspended in 0.25 M sucrose, 2 mM EGTA, 40 mM KCl and 20 mM Tris, pH 7.4, and stored at –70 °C.

Mitoplasts were prepared from fibroblasts as described previously [16]. In brief, trypsinized cells suspended in an STE medium (0.25 M sucrose, 10 mM Tris, 1 mM EDTA, pH 7.4) were treated with digitonin (0.4 mg/mg of protein; Fluka) on ice for 15 min. The suspension was diluted 10-fold with STE and centrifuged for 10 min at 4 °C and 12 000 g. The pellet was

washed by centrifugation and resuspended in STE to a final concentration of 1–2 mg of protein/ml. Based on immunodetection and enzyme activity measurements, > 95% of the mitochondrial inner membrane proteins were recovered in this fraction.

Muscle mitochondria were isolated according to [17], but without use of protease. Tissue samples were homogenized at 4 °C in a KCl medium (100 mM KCl, 50 mM Tris, 2 mM EDTA, 10 mg/ml aprotinin, pH 7.5). The homogenate was centrifuged for 10 min at 4 °C and 600 g, the supernatant was filtered through a 100 μ m nylon screen, and mitochondria were sedimented by centrifugation for 10 min at 4 °C and 10 000 g. The mitochondrial pellet was washed by centrifugation and resuspended to a final protein concentration of 20–25 mg/ml.

DNA analysis and sequencing

Total genomic DNA from muscle and cultured fibroblasts was isolated by phenol extraction. The entire mtDNA was amplified in six overlapping fragments by PCR (7–3148, 2073–5719, 5645–8815, 8403–11 132, 11 005–14 684 and 13 863–136). Purified fragments were sequenced on the automatic sequencer ALFExpress II (Amersham Biosciences) using cycle sequencing with 41 Cy5-labelled internal sequencing primers.

Restriction analysis

To determine the amount of mtDNA containing the microdeletion, the PCR/RFLP (restriction fragment length polymorphism) analysis method was performed according to [18] using the mismatched (bold) primers 5'-CCT CTA CCT GCA CGA CAA TGC A-3' (forward) and 5'-CGT TAT GCA TTG GAA GTG AAA TCA C-3' (reverse), which introduce two novel *NsiI* restriction sites in the case of the wild-type mtDNA and one *NsiI* restriction site in the case of mutant mtDNA. PCR products were radioactively labelled with [α -³²P]dCTP in the final cycle of PCR and run on a non-denaturing 13% (w/v) polyacrylamide gel after complete digestion. The proportions of wild-type and mutant mtDNA were measured using a PhosphorImager and ImageQuant software (Molecular Dynamics).

Northern blot analysis

Total RNA was isolated from cultured fibroblasts by phenol/guanidium thiocyanate/chloroform extraction [19]. Approx. 20 μ g of total RNA per lane was separated through a 1.2% (w/v) agarose/formaldehyde gel and transferred to a Hybond-N nylon membrane (Amersham) in 20 \times SSC (1 \times SSC is 0.15 M NaCl/0.015 M sodium citrate). The membrane was prehybridized for 2 h at 45 °C in 5 \times SSC, Denhardt's solution, 0.5% SDS and 100 μ g/ml sonicated herring sperm. The membranes were hybridized overnight at 45 °C with [α -³²P]dCTP-labelled probes corresponding to regions of the genes *ATP6* (8361–9060), *COX3* (9269–9912), *ND1* (3313–4252) and *COX1* (6120–6960). The radioactivity was detected by phosphor imaging (as above).

Quantitative RT-PCR (reverse transcription-PCR) analysis

Total RNA was isolated from cultured fibroblasts using RNA Blue reagent (Top-Bio, Prague, Czech Republic). Following DNase I treatment (Invitrogen), first-strand cDNA was synthesized from 1 μ g RNA aliquots with 200 units SuperScript II reverse transcriptase using either 200 ng of random hexamer primers or 500 ng of oligo(dT)_{12–18} (all Invitrogen) according to the manufacturer's instructions. Real-time quantitative RT-PCR was performed on a LightCycler instrument (Roche Diagnostics) using a QuantiTect SYBR Green PCR kit (Qiagen). PCR reactions were performed

on cDNAs using primer pairs specific for the *ATP6* gene transcript (forward, 5'-CCT TAT GAG CGG GCA CAG T-3'; reverse, 5'-CAG GGC TAT TGG AA-3'; nt 8846–8994), for the *COX3* gene transcript (forward, 5'-GCC CTC TCA GCC CTC CTA ATG-3'; reverse, 5'-GTG GCC TTG GTA TGT GCT TTC TCG-3'; nt 9267–9416), for the *ATP6-COX3* gene transcript (forward, 5'-AAT CCA AGC CTA CGT TTT CAC ACT-3'; reverse, 5'-TAG GCC GGA GGT CAT TAG G-3'; nt 9150–9299), for the *CYTb* gene transcript (forward, 5'-GAC CTC CCC ACC CCA TCC A-3'; reverse, 5'-AAA GGC GGT TGA GGC GTC TG-3'; nt 14804–14935) and for the *ND1* gene transcript (forward, 5'-CAA CCT CAA CCT AGG CCT CCT-3'; reverse, 5'-ACG GCT AGG CTA GAG GTG GC-3'; nt 3595–3644). The primer pair for *ATP6-COX3* was designed to flank the splice site of the *ATP6-COX3* transcript. Amplified regions of the *ATP6* or *COX3* transcript were present in both processed and unprocessed RNAs. All reactions were run at an annealing temperature of 60 °C. The PCR mixture contained 5 μ l of 2 \times SYBR Green PCR Master Mix, 2 μ l of 100 \times diluted reverse transcription product and 200 nM of each primer in a total volume of 10 μ l. All reactions were performed in triplicate. For each primer pair, non-template controls were included to check for the absence of contaminants and primer-dimers that would interfere with quantification when SYBR Green is used. The external standard curve was generated in parallel for all reactions using serial dilutions of cDNA synthesized from control RNA. For each sample, the relative amounts of *ATP6*, *COX3*, *CYTb*, *ND1* and unprocessed *ATP6-COX3* transcripts were determined from the standard curves. Each sample was analysed in two separate experiments.

Electrophoresis and WB (Western blot) analysis

BN-PAGE [20] was used for the separation of native mitochondrial OXPHOS complexes on 6–15 % (w/v) polyacrylamide gradient minigels (Mini Protean system; Bio-Rad) as described previously [16]. Mitoplasts were pelleted by centrifugation for 10 min at 4 °C and 10 000 *g*, and solubilized using 1 g of DDM (dodecyl maltoside)/g of protein for 20 min on ice in a buffer containing 1.75 M aminocaproic acid, 2 mM EDTA and 75 mM Bis-Tris (pH 7.0). Samples were centrifuged for 20 min at 20 000 *g* and Serva Blue G dye was added to collected supernatants at a concentration of 0.1 g/g of detergent. Electrophoresis was performed at 50 V for 30 min and then at 90 V.

SDS/PAGE [21] was performed on 10 % (w/v) polyacrylamide slab minigels, and analysis of [³⁵S]methionine-labelled proteins was performed on a 16 cm long 15–20 % (w/v) gradient polyacrylamide slab gels (Protean system; Bio-Rad). The samples were boiled for 3 min in sample lysis buffer [2 % (v/v) mercaptoethanol, 4 % (w/v) SDS, 10 mM Tris/HCl, 10 % (v/v) glycerol]. For 2D (two-dimensional) analysis, strips of the first-dimension BN-PAGE gel were incubated for 1 h in 1 % (w/v) SDS and 1 % (v/v) mercaptoethanol and then subjected to SDS/PAGE (10 % polyacrylamide) for separation in the second dimension [21].

Gels were blotted on to Hybond C-extra nitrocellulose membranes (Amersham) by semi-dry electrotransfer for 1 h at 0.8 mA/cm² and the membrane was blocked in PBS containing 0.2 % (v/v) Tween 20 (PBST). The membranes were used whole or were cut according to molecular mass markers into portions containing individual OXPHOS complexes or their subunits. Membranes were incubated for 3 h with primary antibodies diluted in PBS containing 2 % (w/v) BSA (PBSTA). Previously characterized polyclonal antibodies were used at the indicated titres: those against the *F₀c* subunit of ATPase (1:900) [22] and those against the *F₀a* (*ATP6*) subunit of ATPase (1:500) [23]. In addition, we used monoclonal antibodies against subunits COX1

(1:330; Molecular Probes A-6403), COX4 (1:670; Molecular Probes A-6409), COX6c (1:200; Molecular Probes A-6401), NADH39 (1:250; Molecular Probes A-11 140), SDH70 (succinate dehydrogenase 70 kDa subunit; 1:2000; Molecular Probes A-11 142) and subunit α of *F₁-ATPase* (1:200 000; lot 20D6 [24]). Incubation with peroxidase-labelled secondary antibodies in PBSTA was performed for 1 h using either goat anti-mouse IgG (1:1000; Sigma A8924) or goat anti-rabbit IgG (1:1000; Sigma F0382). The chemiluminescence reaction with an ECL[®] kit (Amersham) was detected on an LAS 1000 instrument (Fuji) and the signal was quantified using Aida 2.11 Image Analyser software.

Spectrophotometric assays

The activities of the mitochondrial enzymes NADH:CoQ reductase (complex I), succinate:CoQ reductase (complex II), CoQ:cytochrome *c* reductase (complex III), COX (complex IV), NADH:cytochrome *c* reductase (complex I + III), succinate:cytochrome *c* reductase (complex II + III) and CS (citrate synthase) were measured spectrophotometrically by standard methods at 37 °C in muscle homogenate and isolated muscle mitochondria [17,25–28] or in cultured fibroblasts [29].

ATPase hydrolytic activity was measured in a ATP-regenerating system as described in [30]. Mitochondria (8–22 μ g of protein/ml) were incubated in a medium containing 40 mM Tris (pH 7.4), 5 mM MgCl₂, 10 mM KCl, 2 mM phosphoenolpyruvate, 0.2 mM NADH, 1 μ g/ml rotenone, 0.1 % (w/v) BSA, 5 units of pyruvate kinase and 5 units of lactate dehydrogenase for 2 min. The reaction was started by the addition of 1 mM ATP and the rate of NADH oxidation, equimolar to ATP hydrolysis, was monitored as the decrease in absorbance at 340 nm. Sensitivity to aurovertin was determined by parallel measurements in the presence of 2 μ M inhibitor.

High-resolution oxygraphy

Oxygen consumption by cultured fibroblasts was determined at 30 °C as described previously [29,31] using an Oxygraph-2k (Oroboros, Innsbruck, Austria). Freshly harvested fibroblasts were suspended in a KCl medium (80 mM KCl, 10 mM Tris/HCl, 3 mM MgCl₂, 1 mM EDTA, 5 mM potassium phosphate, pH 7.4) and cells were permeabilized by digitonin (0.1 mg of detergent/mg of protein). Respiratory substrates and inhibitors were used at the concentrations indicated. Oxygen consumption was expressed in pmol of oxygen/s per mg of protein. COX activity was measured with 5 mM ascorbate and 1 mM TMPD (*N,N,N',N'*-tetramethyl-*p*-phenylenediamine), and was corrected for substrate auto-oxidation (determined as oxygen uptake insensitive to 0.33 mM KCN).

Cytofluorimetric analysis of $\Delta\Psi_m$ (mitochondrial membrane potential)

Cytofluorimetric measurements were performed on a FACSort flow cytometer (Becton Dickinson) according to [32]. Fibroblasts were suspended in a KCl medium containing 10 mM succinate to a protein concentration of 1 mg/ml and permeabilized by 0.1 mg of digitonin/mg of protein. Permeabilized fibroblasts were diluted to 0.2 mg of protein/ml and incubated with 20 nM TMRM (tetramethylrhodamine methyl ester; Molecular Probes) for 15 min. OXPHOS inhibitors and ADP at the concentrations indicated were added 1 min before cytofluorimetric analysis. Approx. 10 000 cells were used for each measurement. Data were acquired on a logarithmic scale using CellQuest (Becton Dickinson) and analysed with WinMDI 2.8 software (J. Trotter, TSRI, La Jolla, CA, U.S.A.). Arithmetic mean values of fluorescence signal in

Table 1 Respiratory chain enzyme and mitochondrial ATPase activities in isolated muscle mitochondria and cultured skin fibroblasts

SCCR, succinate:cytochrome *c* reductase; NCCR, NADH:cytochrome *c* reductase; SQR, succinate:CoQ reductase; QCCR, CoQ:cytochrome *c* reductase; NQR, NADH:CoQ reductase; ND, not determined. Values for age-related controls are presented as means \pm S.D. and as a control range (parentheses).

(A)

Enzyme	Activity (nmol/min per mg of protein)					
	Muscle homogenate		Muscle mitochondria		Fibroblasts (mitochondria*)	
	Patient	Controls (<i>n</i> = 20)	Patient	Controls (<i>n</i> = 20)	Patient	Controls (<i>n</i> = 30)
COX	122	125 \pm 72 (53–197)	331	682 \pm 395 (287–1077)	5.1	29 \pm 11 (18–40)
CS	241	114 \pm 29 (85–143)	284	419 \pm 221 (200–640)	40.6	58 \pm 12 (46–70)
COX/CS	0.50	1.04 \pm 0.44 (0.60–1.48)	1.16	1.66 \pm 0.57 (1.09–2.23)	0.12	0.51 \pm 0.18 (0.33–0.69)
SCCR	ND		98	127 \pm 77 (50–206)	ND	
NCCR	ND		76	99 \pm 57 (42–156)	16.3	28 \pm 14 (14–42)
SQR	ND		43	64 \pm 44 (20–108)	10.6	13 \pm 8 (5–21)
QCCR	ND		54	178 \pm 79 (100–257)	14.1	17 \pm 10 (7–27)
NQR	ND		192	274 \pm 80 (194–354)	33.8	23 \pm 10 (15–50)
ATPase	ND		ND		320 \pm 33.1*	254 \pm 16.0*

(B)

Enzyme	Activity (nmol/min per mg of protein)				
	Patient		Mother	Grandmother	Controls (<i>n</i> = 30)
	Expt 1	Expt 2			
COX	7.9	2.4	16.9	34.4	29 \pm 11
CS	45.5	33.8	50.6	52.2	58 \pm 12
COX/CS	0.17	0.07	0.33	0.66	0.51 \pm 0.18

arbitrary units were determined for each sample for subsequent graphic presentation.

ATP synthesis

The rate of ATP synthesis was measured at 37 °C in 150 mM KCl, 25 mM Tris/HCl, 10 mM potassium phosphate, 2 mM EDTA and 1% (w/v) BSA, pH 7.2, using 0.5 mM ADP and 10 mM succinate or 10 mM pyruvate + 10 mM malate as substrate, as described previously [33]. Protein concentration was 1 mg/ml. For permeabilization of fibroblasts, 0.1 mg of digitonin/mg of protein was used. The reaction was started by addition of fibroblasts and performed for the indicated time intervals. Reaction mixture aliquots of 200 μ l were added to 200 μ l of DMSO, and ATP content was determined in DMSO-quenched samples by a luciferase assay according to [34]. ATP production was expressed in nmol of ATP/min per mg of protein.

Biosynthesis of mitochondrial proteins

Growth medium was removed from cultured fibroblasts, and the cells were rinsed with methionine-free medium without serum (Gibco medium 21013; 1 mM pyruvate, 2 mM glutamine and 30 mg/l cysteine) and incubated in the same medium containing 10% (v/v) dialysed fetal calf serum and 100 μ g/ml emetine for 10 min. The cells were labelled for 3 h with 300 μ Ci/ml L-[³⁵S]methionine, as described in [35]. The products were separated by 15–20% (w/v) polyacrylamide gradient SDS/PAGE. A small aliquot of the samples prepared for electrophoresis was used to measure the total incorporation of radioactivity in the mitochondrial fraction as trichloroacetic acid-precipitable counts. The radioactivity of proteins was quantified in dried gels using a BAS-5000 system (Fuji). Labelled proteins were identified according to their molecular mass as reported previously in *ex vivo* translation assays [35].

Protein determination

The protein content was measured by the Bradford or Micro BCA protein kit assays (Bio-Rad), using BSA as a standard. Samples were sonicated for 20 s prior to protein determination.

RESULTS

Activities of respiratory chain enzymes and mitochondrial ATPase

The activities of respiratory chain enzymes (Table 1A) in a muscle homogenate from a patient with encephalopathy and lactic acidosis showed a decrease in the COX/CS ratio. In isolated muscle mitochondria, both COX activity and the COX/CS ratio were at the lower end of the control range, complex I activity was below the control range and complex III activity was moderately decreased. In fibroblasts from the patient, we found a pronounced decrease in COX activity to 15% of the control, CS was just below the control range, and the activities of other respiratory chain enzymes were normal. ATPase hydrolytic activity was determined in isolated mitochondria from the patient's fibroblasts. It was measured as aurovertin-sensitive activity at a constant ATP concentration and was found to be normal.

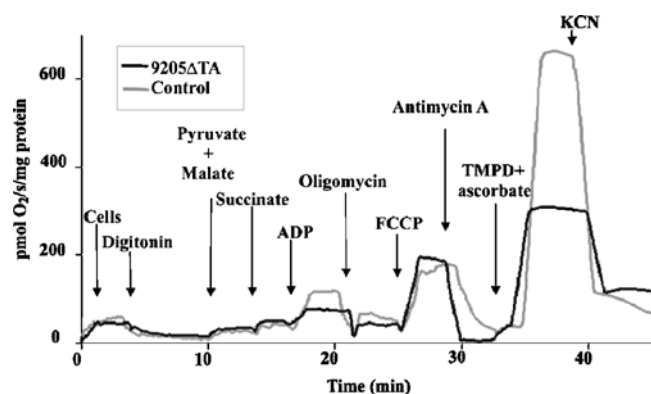
When COX activity was measured in fibroblasts from the patient's asymptomatic mother and grandmother, decreased COX activity and a COX/CS ratio near the lower limit of the reference range were found in the mother, but not in the grandmother (Table 1B).

mtDNA 9205 Δ TA mutation in the affected family

Sequencing of the patient's mtDNA revealed a very rare mtDNA mutation – a heteroplasmic 2 bp deletion TA at positions 9205 and 9206 (9205 Δ TA) in the *ATP6-COX3* genes. Analysis of mutation heteroplasmy in tissues of the affected boy by radioactive RFLP (using *Nsi*I restrictase; Table 2) showed practically homoplasmic

Table 2 9205 Δ TA mutation load in family members

Sample	Heteroplasmy (%)
mtDNA	
Grandmother – blood DNA	16
Grandmother – fibroblast DNA	9
Mother – blood DNA	82
Mother – fibroblast DNA	92
Patient – blood DNA	> 98
Patient – muscle DNA	> 98
Patient – fibroblasts DNA	> 98
cDNA	
Patient – fibroblasts cDNA oligo(dT)	> 98
Patient – fibroblasts cDNA oligo(dT) + random primers	> 98

**Figure 1** Oxygen consumption by digitonin-permeabilized skin fibroblasts

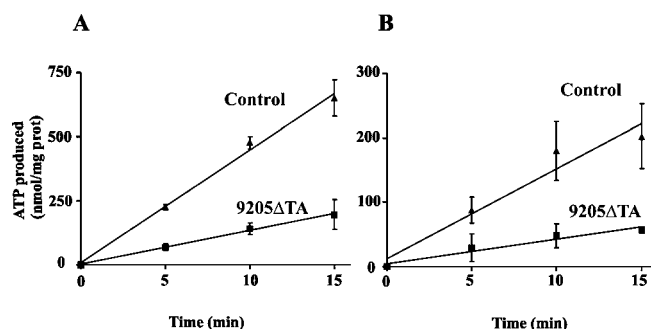
Measurements were performed using 0.45–0.62 mg of cell protein/ml and 0.1 mg of digitonin/mg of protein. Subsequent additions of pyruvate (5 mM), malate (1.5 mM), succinate (10 mM), ADP (0.5 mM), oligomycin (1 μ M), FCCP (1 μ M), antimycin A (0.2 μ g/ml), ascorbate (5 mM), TMPD (1 mM) and KCN (0.33 mM) are indicated. Oxygen consumption is expressed as negative values of the first time derivative of changes in oxygen tension (pmol of O_2 /s per mg of protein).

9205 Δ TA mtDNA mutation in fibroblasts, muscle and blood (> 98%). Analysis of blood DNA confirmed the presence of the 9205 Δ TA mutation at lower loads both in the mother (82%) and in the grandmother (16%). Interestingly, a similar mutation load was found in their fibroblasts (mother 92%; grandmother 9%), in correspondence with the observed decrease in COX activity in the mother's fibroblasts (see above).

An equal mutation load in the patient's fibroblasts was found using RFLP of isolated DNA as well as of cDNA reverse-transcribed from isolated RNA using either oligo(dT) or oligo(dT) + random primers, indicating that the mutation is fully retained in ATP6–COX3 RNA and poly(A) RNA (Table 2).

Oxygraphic analysis of cultured fibroblasts

The functional consequences of the 9205 Δ TA mutation were analysed by high-resolution oxygraphy of the patient's fibroblasts that had been permeabilized by a low concentration of digitonin. The 9205 Δ TA cells showed a pronounced decrease in ADP-stimulated oxygen consumption using pyruvate, malate and succinate as substrate, which contrasted with a normal rate of state 3 respiration in the presence of the uncoupler FCCP (carbonyl cyanide 4-trifluoromethoxyphenylhydrazone). We also observed a decrease in COX activity determined with TMPD and ascorbate (Figure 1). In 9205 Δ TA cells from the patient, ADP-stimulated respiration

**Figure 2** Production of ATP by control and 9205 Δ TA fibroblasts

The rate of ATP synthesis was measured in the presence of 0.5 mM ADP in 9205 Δ TA (■) and control (▲) cultured skin fibroblasts treated with 0.1 mg of digitonin/mg of protein. Substrates were 10 mM pyruvate + 10 mM malate (A) or 10 mM succinate (B). ATP was determined in DMSO-quenched aliquots by a luciferase assay. Data represent means \pm S.D. for three experiments.

was 50–60%, FCCP-stimulated respiration was 100–110% and COX activity was 40–50% of values in control cells. Although well coupled, the mitochondria of 9205 Δ TA cells thus showed a strongly impaired effect of ADP, indicating a decreased ability to synthesize ATP.

Low ATP production in 9205 Δ TA cells

The ability of fibroblasts to synthesize ATP by the mitochondrial OXPHOS pathway was measured directly in cells suspended in mitochondrial medium, permeabilized by digitonin and supplied with respiratory substrates and ADP, as in the oxygraphic experiments. With either succinate or pyruvate + malate as substrate, linear production of ATP was observed in control cells for 15 min, corresponding to ATP production of 16.4 ± 1.8 and 45.4 ± 1.5 nmol/min per mg of protein respectively, in accordance with the oxygraphic measurements. In 9205 Δ TA fibroblasts, a steadily diminished ATP production was observed during the 15 min interval with both types of substrate, giving values of 4.8 ± 0.7 and 13.7 ± 0.4 nmol/min per mg of protein respectively, which are approx. 30% of control values (Figure 2).

Changes in $\Delta\Psi_m$

$\Delta\Psi_m$ was analysed cytofluorimetrically in digitonin-permeabilized fibroblasts using the membrane potential-sensitive cationic probe TMRM. We found that the $\Delta\Psi_m$ of the patient's fibroblasts was practically normal at state 4 using succinate as a substrate, but the effect of the addition of ADP on $\Delta\Psi_m$ was significantly decreased in 9205 Δ TA cells (Figure 3). Whereas in control cells the TMRM fluorescence was decreased by the addition of ADP (state 3 ADP) to approx. 28% of the state 4 value, in the 9205 Δ TA cells the TMRM fluorescence decreased to only 50%. The observed 2-fold difference in TMRM fluorescence would correspond to an even more pronounced difference in $\Delta\Psi_m$ values in mV, because the accumulation of the fluorophore obeys the Nernst equation and depends exponentially on $\Delta\Psi_m$ [36]. In both types of cells, the effect of ADP was fully reversible by oligomycin (Figure 3), atractyloside or aurovertin (results not shown), indicating that the effect of ADP requires the transport of ADP to the mitochondrial matrix as well as the catalytic activity of ATPase. In accordance with the measurements of ATP production and respirometry, these results suggest that ATP synthesis by mitochondrial ATPase is strongly impaired in 9205 Δ TA cells from the affected individual.

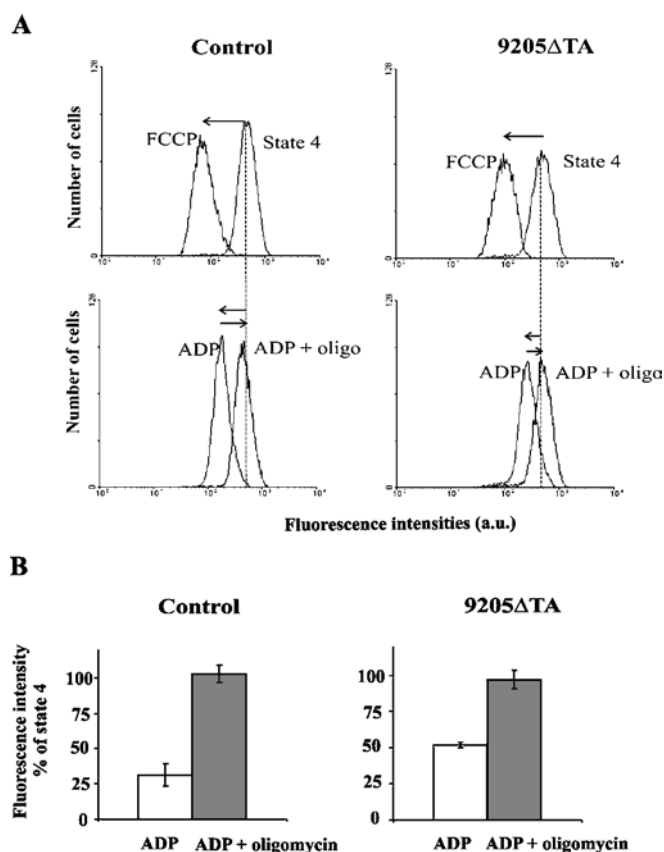


Figure 3 Cytofluorimetric analysis of control and 9205ΔTA fibroblasts

Cytofluorimetric analysis was performed in digitonin-treated fibroblasts (0.1 mg of digitonin/mg of protein) and stained with 20 nM TMRM in a KCl medium containing 10 mM succinate. (A) Typical reading of TMRM fluorescence at state 4 and effect of 1 μM FCCCP is shown in the upper panels. Lower panels show the effect of 0.1 mM ADP and its sensitivity to 1 μM oligomycin (oligo). (B) TMRM fluorescence of state 3-ADP and effect of oligomycin is expressed as percentage of the state 4 signal. The $\Delta\Psi_m$ -independent signal (after addition of FCCCP) was subtracted from all data. The data represent means \pm S.D. for four independent experiments.

Altered composition and increased lability of ATPase and COX

In order to assess the cellular content of ATPase and COX subunits, we analysed the mitochondrial proteins of isolated fibroblasts by SDS/PAGE and WB. It is clearly apparent from Figure 4(A) that 9205ΔTA fibroblasts had a selectively diminished content of ATPase subunit a and a significantly decreased content of COX subunits. In comparison with control cells, 9205ΔTA mitochondria contained 11 \pm 5.9% of F_0 subunit a, 127 \pm 13.0% of F_1 α subunit, 85% of OSCP (oligomycin-sensitivity-conferring protein), 108 \pm 18.0% of F_0 subunit c, 47 \pm 2.8% of COX1 subunit, 69 \pm 8.5% of COX4 subunit and 36 \pm 21.2% of COX6c subunit (average values of four experiments; data normalized to the content of the SDH 70 kDa subunit). The same pattern was obtained when analysing complete cell protein extracts (results not shown).

To resolve the native ATPase complex, we solubilized mitochondrial OXPHOS complexes from mitoplasts by DDM and analysed them by BN-PAGE and WB using an antibody against ATPase F_1 α subunit. As shown in Figure 4(B), in 9205ΔTA cells we found a decreased content of the full-size ATPase and the accumulation of an incomplete form of the ATPase with a molecular mass of approx. 390 kDa. A parallel WB analysis of complex I using an antibody to the NADH39 subunit showed an

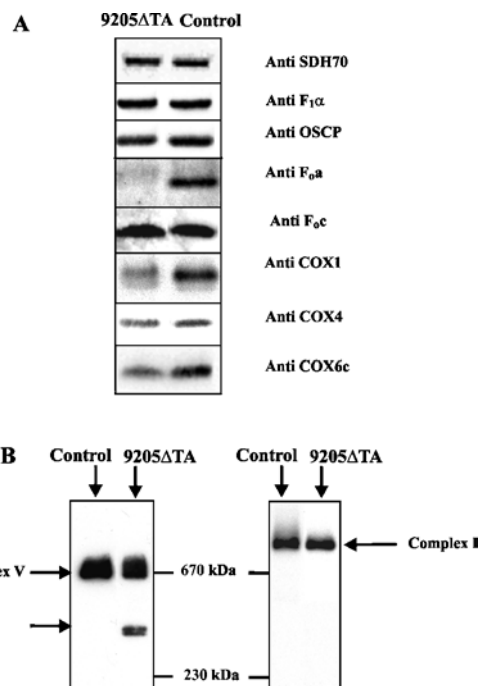


Figure 4 Electrophoretic analysis of OXPHOS complexes

(A) SDS/PAGE WB of ATPase, COX and SDH subunits was performed using aliquots of 7.5 μg of protein of mitochondria from control and 9205ΔTA cells. Detection was done with monoclonal antibodies against subunits SDH70, F_1 α , OSCP (oligomycin-sensitivity-conferring protein), COX1, COX4 and COX6c, and with polyclonal antibodies against ATPase subunits F_0 a and F_0 c. (B) BN-PAGE WB with monoclonal antibody against F_1 α and NADH39 subunit was performed using 15 μg aliquots of protein solubilized using 1 g of DDM/g of protein from mitoplasts of control and 9205ΔTA cells. The migration of molecular mass standards is indicated.

identical pattern in control and 9205ΔTA cells – we observed only intact complex with a molecular mass above 800 kDa (Figure 4B) that was present in the same amounts in 9205ΔTA and control cells.

2D electrophoretic analysis of ATPase and COX

Detailed analysis of the different forms of ATPase present in DDM-solubilized enzyme complexes was performed by 2D electrophoresis, whereby proteins resolved by BN-PAGE in the first dimension were separated by SDS/PAGE in the second dimension and detected by WB. The ATPase complex with an apparent molecular mass of approx. 620 kDa was significantly decreased in 9205ΔTA cells, but several other, smaller ATPase subcomplexes were detected by F_1 subunit α - and F_0 subunit c-immunoreactive signals (Figure 5A). In addition to the 390 kDa F_1 subcomplex containing the α subunit, which was present in the 9205ΔTA cells in increased amounts, a larger 460 kDa complex containing both subunits α and c was also found in the 9205ΔTA cells. Moreover, an additional, subunit c-containing complex with a molecular mass of approx. 120 kDa and a markedly increased amount of free subunit α (approx. 60 kDa) were seen. However, none of the above complexes showed a detectable reaction with an antibody against subunit a in the 9205ΔTA cells.

2D analysis of COX was performed using antibodies to COX1 and COX4 subunits (Figure 5B). A pronounced decrease in the amount of COX was observed in the DDM solubilize of 9205ΔTA cells. In control cells, most of the COX was present as a monomer, but a significant amount of COX dimers (approx. 420–440 kDa) and small amounts of COX supercomplex (approx.

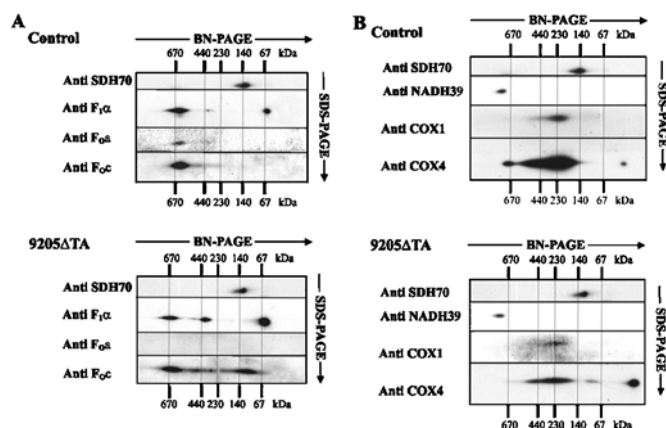


Figure 5 2D electrophoretic analysis and immunodetection of OXPHOS complexes

Aliquots (15 μ g of protein) of DDM-solubilized mitoplasts from 9205 Δ TA and control fibroblasts were separated in the first dimension by BN-PAGE and in the second dimension by SDS/PAGE. WB analysis was performed with an antibody against the SDH70 subunit and with antibodies (A) against ATPase subunits $F_{1\alpha}$, F_{0a} and F_{0c} , or (B) against complex I subunit NADH39 and against COX subunits COX1 and COX4. The migration of molecular mass standards is indicated.

670 kDa; probably COX- bc_1 supercomplex) as well as some monomeric COX4 subunits were clearly seen. In the 9205 Δ TA cells the pattern was different. An additional band of molecular mass approx. 100 kDa was present, and the relative content of the free COX4 subunit was much higher (approx. 15-fold) than in control cells.

WB analysis of complex I on 2D gels using a monoclonal antibody to the NADH39 subunit showed no difference between control and 9205 Δ TA cells. Only the full-size, assembled complex I was found, and was present in similar amounts in both types of cells. No assembly intermediates were detected. Similarly, no difference was found in the case of complex II using the anti-SDH70 antibody. Thus, unlike ATPase and COX, the biosynthesis and/or stability of complex I were not affected by the 9205 Δ TA mutation.

Steady-state levels and processing of ATP6 and COX3 mRNAs

The 9205 Δ TA microdeletion is situated between the genes *ATP6* and *COX3*, which are transcribed in one polycistronic transcript that is subsequently cleaved stepwise and polyadenylated into mature mRNA. Therefore we studied the steady-state levels and processing of ATP6 and COX3 mRNAs. Northern blot analysis using cDNA complementary to mtDNA sequences 8361–9060 and 9269–9912 as a probe was performed to determine whether the mutation disturbs the RNA processing of ATP6 and COX3 transcripts (Figure 6A). The primary, unprocessed, and the secondary ATP8–ATP6–COX3 transcripts occurred in both 9205 Δ TA cells and control cells in similar amounts. The steady-state levels of processed COX3 and ATP8–ATP6 transcripts were decreased in 9205 Δ TA cells. The relative values of the ATP8–ATP6/ATP8–ATP6–COX3 and COX3/ATP8–ATP6–COX3 RNA ratios revealed approx. 40% and 50% decreases respectively in ATP8–ATP6 and COX3 RNA levels. In parallel, we also determined the steady-state levels of the transcripts of two other genes encoded by mtDNA, i.e. *ND1* and *COX1*. We observed the same content of the mature ND1 transcript (Figure 6B) in control and 9205 Δ TA cells. Similarly, there was no difference in the content of COX1 transcripts (results not shown).

These Northern blot data were fully confirmed by quantitative RT-PCR experiments (Figure 7). Using PCR products

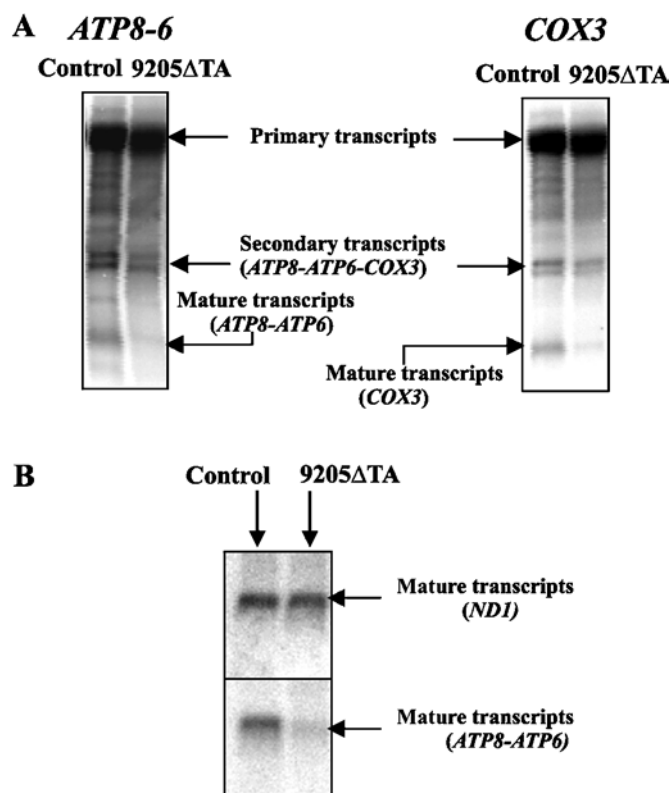


Figure 6 Northern blot analysis of ATP6 and COX3 transcripts

Northern blot analysis of COX3, ATP8–ATP6 and ND1 transcripts was performed in control and 9205 Δ TA cells. The mRNA species representing (A) the primary mtDNA polycistronic transcript, partially processed ATP8–ATP6–COX3 transcripts and mature COX3 and ATP8–ATP6 transcripts and (B) mature ND1 and ATP8–ATP6 transcripts are indicated.

corresponding to *ATP6* (nt 8846–8994), *COX3* (nt 9267–9416) and the *ATP6*–*COX3* cleavage site (nt 9150–9299), we found that ATP6 as well as COX3 RNA levels were decreased 2–3-fold relative to those of the uncleaved polycistronic ATP8–ATP6–COX3 transcript. The decrease was also confirmed when relating ATP6 and COX3 RNA levels to *CYTB* and *ND1* expression (PCR product of 14804–14935 for *CYTB* and 3595–3644 for *ND1*). As also shown in Figure 7, similar results were obtained using cDNA prepared by oligo(dT) or random primers, indicating that polyadenylation is neither impaired nor affects transcript processing.

Specific decrease in the biosynthesis of ATPase subunit a

To assess how the 9205 Δ TA mutation affects the biosynthesis of subunit a and other mtDNA-encoded proteins, [35 S]methionine labelling of proteins in 9205 Δ TA cells was performed in the presence of emetine (an inhibitor of cytosolic proteosynthesis). The extent of labelling (Figure 8) was comparable in 9205 Δ TA and control cells, and the pattern of labelled proteins was also similar, with two exceptions – markedly decreased labelling of a band of approx. 22 kDa and increased labelling of a band of approx. 12 kDa. The first band was identified as ATPase subunit a, based on WB analysis performed on the same gel with an antibody against subunit a (Figure 8), in accordance with the size and mobility of subunit a in this type of SDS/PAGE [37]. On the basis of its size, the second band was identified as ATPase subunit 8 (A6L). The COX3 subunit was weakly labelled in both types of

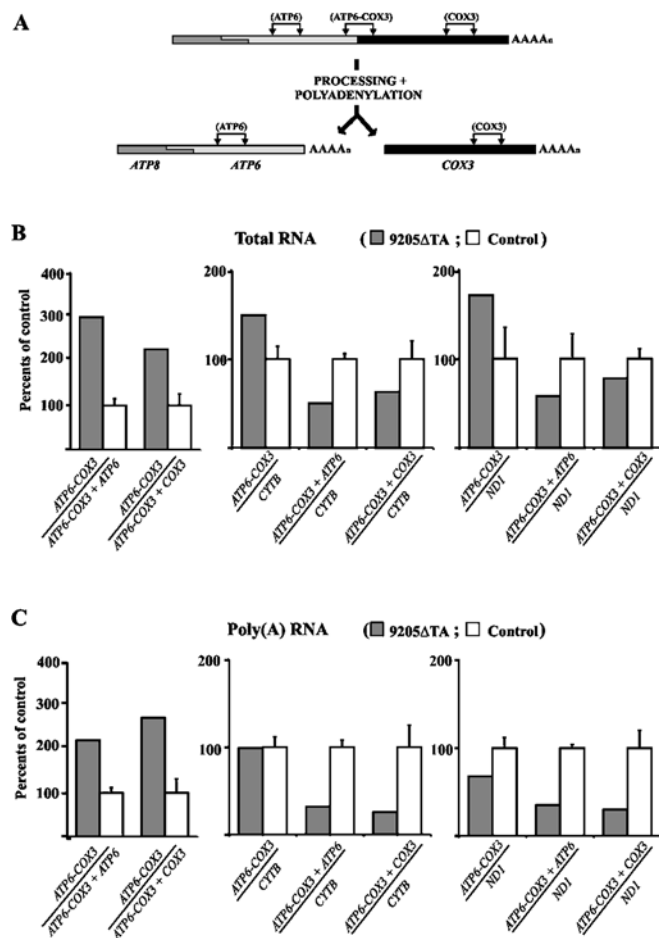


Figure 7 Quantitative real-time RT-PCR analysis of *ATP6*, *COX3*, cytochrome *b* and *ND1* transcripts

(A) Scheme of *ATP6*–*COX3* RNA processing and PCR products analysed. For experiments, cDNAs obtained from (B) total RNA (reverse transcription with random primers) or (C) mRNA [reverse transcription with oligo(dT) primers] were used. The relative amount of uncleaved *ATP6*–*COX3* transcript and the amounts of all *ATP6* or *COX3* transcripts present either in unprocessed form or in mature form were measured and correlated. The values were also correlated to the expression of mitochondrial *CYTB* and *ND1* as reference genes. Graphs depict results obtained in 9205ΔTA fibroblasts expressed as a percentage of the mean \pm S.D. for three controls.

cells, and no significant difference could be seen between the 9205ΔTA and control cells. Three independent experiments gave essentially the same result, and clearly showed, in accordance with all WB data, that mutation of the *ATP6* STOP codon greatly decreases the synthesis of ATPase subunit a (to 12.7 ± 0.73 % of the control). In turn, up-regulation of *ATP8* synthesis is apparent.

DISCUSSION

We present a detailed analysis of the impact of a maternally inherited 2 bp microdeletion TA at position 9205 and 9206 in the mtDNA (9205ΔTA) on the respiratory chain complexes, with the aim of disclosing the pathogenic mechanism in a patient with severe encephalomyopathy, spastic quadraparesis, microcephalia and hyperlactacidaemia.

Biochemically, the patient presented with a pronounced selective decrease in COX activity in his fibroblasts (15 % of control), while a lowered COX/CS ratio and a mild decrease in com-

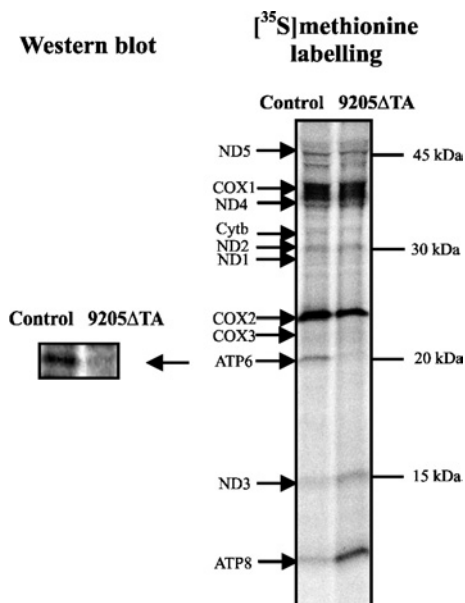


Figure 8 Incorporation of [35 S]methionine into proteins encoded by mtDNA

mtDNA-specific translation was performed in control and 9205ΔTA fibroblasts in the presence of emetine. Radioactive proteins were separated by SDS/PAGE on a 15–20 % (w/v) gradient polyacrylamide gel and detected by phosphorimaging. On the left side, the WB from the same SDS/PAGE run using an antibody against subunit F_0a is shown. The migration of mtDNA-encoded polypeptides and of molecular mass standards is indicated.

plex III activity were found in muscle. Sequencing of mtDNA revealed a 2 bp microdeletion, which disrupts the STOP codon of the *ATP6* gene. This mutation has been described only once previously, in a patient with seizures and repetitive bouts of lactic acidemia [13]. It was reported as being homoplasmic (lymphocytes and fibroblasts), but was not detected in that patient's mother or grandmother. In our patient, the mutation was also found to be homoplasmic (> 98 %) in all tissues tested. In addition, the heteroplasmic mutation 9205ΔTA was present in the asymptomatic mother (82 %) and grandmother (16 %). Importantly, a high mutation load in the mother's fibroblasts was also associated with a decrease in COX activity.

The mtDNA mutation 9205ΔTA lies on the boundary of two genes, *ATP6* and *COX3*, and it is highly probable that it influences the transcription and post-transcriptional modification of these genes. Assuming that this is the main cause of the patient's phenotype, insufficient energy provision is to be expected in the tissues, particularly in brain (explaining the dominating encephalopathy). Our measurements in the patient's fibroblasts showed a 3-fold decrease in mitochondrial ATP production. In fact, the observed decrease was even higher than that observed in cases of missense mutations in the *ATP6* gene (T9176G, T8993G and T8993C), where higher values of residual mitochondrial ATP production have been reported [10–12,38]. By analogy with these mutations, we found completely normal ATPase hydrolytic activity. Thus it appears that only a fraction of ATPase complexes can utilize $\Delta\Psi_m$ to drive ATP synthesis in 9205ΔTA cells. This view is further supported by the normal $\Delta\Psi_m$ observed at state 4 and its decrease by FCCP, while ADP (state 3-ADP) caused a much smaller decrease in $\Delta\Psi_m$ in the patient. These data indicate that mitochondria in 9205ΔTA cells can be fully energized and that the mutation does not enhance the passive H^+ transport at state 4 via the F_0 proton channel of the ATPase complexes, which are known to contribute to the proton conductivity of the mitochondrial inner

membrane [39]. When, however, ADP becomes available, the discharge by ATP synthesis of $\Delta\Psi_m$ in 9205 Δ TA cells is significantly decreased.

Our functional data support the view that the F_0 part has an altered function in the majority of ATPase complexes of the patient's fibroblasts, due to the absence of subunit a (an essential component of the ATPase proton channel) or an alteration of its structure (for review, see [40]). The absence of the *ATP6* STOP codon could interfere with synthesis of the subunit by decreasing the translational efficacy of the *ATP6* mRNA, resulting in a low amount of subunit a being produced and in the formation of ATPase complexes lacking subunit a and incapable of synthesizing ATP. Another possibility might be production of subunit a modified in the C-terminal part, as a poly(A) tail in the absence of a regular STOP codon could cause extension of several lysine residues at the C-terminus. Indeed, several amino acid residues involved in H^+ translocation are located in this part of the protein [8].

To delineate the subunit composition and native structure of ATPase, we employed electrophoretic/WB analysis using subunit-specific antibodies, including a polyclonal antibody against subunit a [23]. We have found that the content of subunit a is greatly decreased (to 11 % of control) in the patient's fibroblasts, whereas other ATPase subunits are unchanged. The antibody was raised against 10 amino acids at the N-terminal part of human subunit a, and most probably would react with a putative form of subunit a elongated at the C-terminus. However, no larger forms of subunit a could be detected by WB. A low content of subunit a was confirmed by 9-fold decreased labelling of this subunit by [35 S]methionine, and the labelling pattern also did not indicate the accumulation of a larger form of this subunit in 9205 Δ TA cells.

Under native electrophoretic conditions, we found in the 9205 Δ TA cells a decreased content of DDM-solubilized, normal-sized F_1F_0 -ATPase, together with an increased content of an F_1 subcomplex of 390 kDa. There was no apparent difference between the mobility of the 620 kDa ATPase complex in the 9205 Δ TA and control samples; however, subunit a, present in the ATPase in one copy, represents only 4 % of the total ATPase mass, and the expected difference in mobility of the whole, subunit a-lacking complex is below the resolution of BN-PAGE. Furthermore, we found yet another larger, F_1 -containing subcomplex of 460 kDa that consists of F_1 -ATPase and some F_0 subunits, including subunit c. This pattern closely resembles that in cells with a T8993G mutation in the *ATP6* gene [10,12], or in cells with doxycycline-inhibited mitochondrial protein synthesis [3]. Interestingly, these three different mechanisms that affect the biosynthesis of subunit a gave a very similar picture at the level of ATPase structure. In the case of the 9205 Δ TA mutation, the ATPase complexes exert lability upon DDM extraction that is not observed in those from control cells; however, even the subunit a-lacking ATPase complexes maintain structural interactions between the F_1 and F_0 parts of the enzyme, although these are weaker. It appears that incomplete F_0 is also able to 'gate' the F_1 in these complexes, as no H^+ leak has been detected by measurement of membrane potential.

In addition to changes in ATPase, we also found changes in the structure and function of COX. The pronounced decrease in COX activity observed in spectrophotometric assays was confirmed by the oxidation of TMPD + ascorbate in 9205 Δ TA cells. The remaining COX activity, however, did not limit the generation of $\Delta\Psi_m$, and it was also sufficient for substrate oxidation in the uncoupled state. The functional consequences at the level of COX resembled to some extent COX assembly defects due to *SURF1* mutations [41]. The total amount of COX subunits detected by WB was also decreased, indicating a 30–50 % decrease in enzyme

content. Some of the COX complexes showed a normal size, but some COX subunits detected by 2D/WB analysis were found to be present in COX subcomplexes or as free subunits. The 2D pattern resembled the pattern observed in cells with a 15 bp deletion (9480 Δ 15) in *COX3* [37] that show a failure to assemble the holoenzyme complex and instability of the COX1–COX2 interaction [42].

When comparing the changes in ATPase and COX, it appears that 9205 Δ TA cells contain approx. 10 % of the control content of normal ATPase complexes and 30–50 % of that of normal COX complexes. Both enzymes are present in mitochondria at normal, physiological conditions in excess in most tissues, and their threshold values are known to vary in individual cell types [43]. With regard to the dominating encephalopathy in our patient, it is interesting that the reserve capacity of COX appears to be rather high in brain, while the reserve capacity of ATPase appears to be much lower.

All of the data presented herein are in accordance with the hypothesis that the mechanism by which the 9205 Δ TA mutation affects mitochondrial function is associated with changes in the transcription of the *ATP6* and *COX3* genes and their translational competence and efficacy. Using two independent approaches, i.e. Northern blot and quantitative real-time PCR analysis of cDNA, we found that processing of the primary *ATP8*–*ATP6*–*COX3* transcript is impaired in our patient. Both methods revealed a 2–3-fold decrease in the content of mature *ATP6* and *COX3* transcripts, while the content of *ND1* and *COX1* transcripts was unaffected. The same picture emerged when analysing polyadenylated forms of *ATP6* and *COX3* RNAs. These differences found in the patient's cells were also confirmed when relating the steady-state levels of *ATP6* and *COX3* RNAs and mRNAs to the levels of *CYTB* or *ND1* transcripts.

The decrease in the amount of the mature *ATP6* transcript agreed well with the decreased synthesis and content of subunit a. Interestingly, the labelling of subunit 8 was increased, indicating up-regulated translation of the *ATP8* gene, which precedes and partially overlaps the *ATP6* gene. The translation of the *ATP8* and *ATP6* mRNAs is well described in yeast, but the structure of these genes and its regulation differs completely from that in mammalian mitochondria, where the mechanism of *ATP8* and *ATP6* biosynthesis is largely unknown. The question arises whether increased labelling of subunit 8 could be caused by translation of *ATP8* from an unspliced form of the *ATP8*–*ATP6*–*COX3* transcript, part of which is, according to our results, polyadenylated [cDNA synthesis with random primers and oligo(dT) primer] and could be therefore subjected to translation.

Recently, Seneca and co-workers continued an analysis of the fibroblasts from the first patient identified with the 9205 Δ TA deletion [18,44]. They investigated the levels and fate of *ATP6* and *COX3* mRNAs and did not find any difference in primary transcript processing in their patient, but some differences in the deadenylation of mRNAs were present. In the second paper they investigated the biochemical consequences of the mutation, and the only difference they found was an accumulation of the F_1 -ATPase intermediate and increased *ATP8* labelling. Therefore two patients with the same 9205 Δ TA homoplasmic mutation differ dramatically, and this difference is difficult to understand. There appears to be a good correlation between changes in mature transcripts, pronounced biochemical consequences and severe encephalopathy in our patient, compared with unchanged RNA processing, insignificant biochemical changes and much weaker clinical presentation in the Seneca study. On the other hand, both patients harbour the same homoplasmic 9205 Δ TA mutation. Thus in one case the mutation is pathogenic, and in the other it has little effect. We have no explanation for this difference at the

moment, but several aspects might be important. In both cases numerous other changes in mtDNA sequence were found. In our case all were identified as more or less frequent polymorphisms, one of which was present in the *ATP6* gene (A8860G) and one in the *COX3* gene (G9477A). In the Seneca case mtDNA sequencing revealed 42 changes from the revised Cambridge Reference Sequence, including three rare polymorphisms (C9335T, A11362G and A12822G) and two novel transitions (T15287C and T15705C) in the *CYTB* gene. The two types of mtDNA also belong to different haplogroups.

The question arises as to whether in the Seneca case the absence of pathogenicity might be due to some compensatory mechanism affecting the post-transcriptional processing and translation of the *ATP6* and *COX3* mRNAs. Two revertants have been described in human mtDNA, in cells carrying tRNA mutations. A suppressor mutation at position 12300 was found, generating tRNA^{Leu} (CUN), which compensated for the 3243 (MELAS; mitochondrial encephalomyopathy, lactic acidosis and stroke-like episodes) mutation of tRNA^{Leu} (UUR) [45]. In the second case, a G5703A mutation in tRNA^{Asn} was functionally rescued without changes in mtDNA upon cultivation in a galactose medium [46]. A compensatory import of surrogate tRNA due to nuclear mutation was proposed, but not shown. Moreover, a similar compensatory import of RNAs or proteins is highly unlikely in 9205ΔTA cells.

A possible compensatory mechanism could be connected with factors that affect (and/or correct) the processing of mitochondrial transcripts and their translation in 9205ΔTA cells. Interestingly, several nuclear-encoded factors have been described in yeast (NCA2, NCA3, NAM1/MTF2, Aep3p) that are essential for proper processing of mitochondrial RNAs, namely the *ATP8*–*ATP6* co-transcript (for references see [47]), but their mammalian orthologues have not been found, possibly reflecting differences in the structure of mitochondrial RNAs between yeast and mammals. Another group of factors is represented by proteins mediating the mRNA–ribosome interaction. The search for mammalian orthologues in this group was more successful. A LRPPRC (leucine-rich pentatricopeptide repeat cassette) protein was identified using a functional genomics approach [48], and it was shown that mutation in the *LRPPRC* gene causes the Leigh syndrome of French–Canadian type, which is a human mitochondrial *COX* deficiency [49]. However, the divergence of the LRPPRC protein sequence from that of the analogous yeast protein is very large and, therefore, it has not yet been possible to identify other mammalian proteins by a sequence similarity approach.

This work was supported by grants from the Grant Agency of the Ministry of Health of the Czech Republic (NR/7790-3, 8065-3), the Grant Agency of Charles University (GAUK 14/2004), the Grant Agency of the Czech Republic (303/03/0749) and by institutional projects (AVOZ5011922, VZ 111100003). The expert technical assistance of V. Fialová and V. Brožková is gratefully acknowledged.

REFERENCES

- Walker, J. E. and Collinson, I. R. (1994) The role of the stalk in the coupling mechanism of *F₁F₀*-ATPases. *FEBS Lett.* **346**, 39–43
- Anderson, S., Bankier, A. T., Barrell, B. G., de Bruijn, M. H. L., Coulson, A. R., Drouin, J., Eperon, I. C., Nierlich, D. P., Roe, B. A., Sanger, F. et al. (1981) Sequence and organization of the human mitochondrial genome. *Nature (London)* **290**, 457–465
- Nijtmans, L. G., Klement, P., Houstek, J. and van den Bogert, C. (1995) Assembly of mitochondrial ATP synthase in cultured human cells: implications for mitochondrial diseases. *Biochim. Biophys. Acta* **1272**, 190–198
- DiMauro, S. and Schon, E. A. (2001) Mitochondrial DNA mutations in human disease. *Am. J. Med. Genet.* **106**, 18–26
- Holt, I. J., Harding, A. E., Petty, R. K. H. and Morgan-Hughes, J. A. (1990) A new mitochondrial disease associated with mitochondrial DNA heteroplasmy. *Am. J. Hum. Genet.* **46**, 428–433
- de Vries, D. D., van Engelen, B. G., Gabreels, F. J., Ruitenbeek, W. and van Oost, B. A. (1993) A second missense mutation in the mitochondrial *ATPase 6* gene in Leigh's syndrome. *Ann. Neurol.* **34**, 410–412
- Tatuch, Y., Christodoulou, J., Feigenbaum, A., Clarke, J. T., Wherret, J., Smith, C., Rudd, N., Petrova Benedict, R. and Robinson, B. H. (1992) Heteroplasmic mtDNA mutation (T → G) at 8993 can cause Leigh disease when the percentage of abnormal mtDNA is high. *Am. J. Hum. Genet.* **50**, 852–858
- Schon, E. A., Santra, S., Pallotti, F. and Girvin, M. E. (2001) Pathogenesis of primary defects in mitochondrial ATP synthesis. *Semin. Cell Dev. Biol.* **12**, 441–448
- Tatuch, Y. and Robinson, B. H. (1993) The mitochondrial DNA mutation at 8993 associated with NARP slows the rate of ATP synthesis in isolated lymphoblast mitochondria. *Biochem. Biophys. Res. Commun.* **192**, 124–128
- Houstek, J., Klement, P., Hermanska, J., Houstkova, H., Hansikova, H., van den Bogert, C. and Zeman, J. (1995) Altered properties of mitochondrial ATP-synthase in patients with a T → G mutation in the *ATPase 6* (subunit a) gene at position 8993 of mtDNA. *Biochim. Biophys. Acta* **1271**, 349–357
- Garcia, J. J., Oglivie, I., Robinson, B. H. and Capaldi, R. A. (2000) Structure, functioning, and assembly of the ATP synthase in cells from patients with the T893G mitochondrial DNA mutation. Comparison with the enzyme in Rho⁰ cells completely lacking mtDNA. *J. Biol. Chem.* **275**, 11075–11081
- Nijtmans, L. G., Henderson, N. S., Attardi, G. and Holt, I. J. (2001) Impaired ATP synthase assembly associated with a mutation in the human ATP synthase subunit 6 gene. *J. Biol. Chem.* **276**, 6755–6762
- Seneca, S., Abramowicz, M., Lissens, W., Muller, M. F., Vamos, E. and de Meirleir, L. (1996) A mitochondrial DNA microdeletion in a newborn girl with transient lactic acidosis. *J. Inher. Metab. Dis.* **19**, 115–118
- Fornuskova, D., Tesarova, M., Hansikova, H. and Zeman, J. (2003) New mtDNA mutation 9204delTA in a family with mitochondrial encephalopathy and ATP synthase defect. *Cas. Lek. Cesk.* **142**, 313
- Bentlage, H. A., Wendel, U., Schagger, H., ter Laak, H. J., Janssen, A. J. and Trijbels, J. M. (1996) Lethal infantile mitochondrial disease with isolated complex I deficiency in fibroblasts but with combined complex I and IV deficiencies in muscle. *Neurology* **47**, 243–248
- Klement, P., Nijtmans, L. G., Van den Bogert, C. and Houstek, J. (1995) Analysis of oxidative phosphorylation complexes in cultured human fibroblasts and amniocytes by blue-native-electrophoresis using mitoplasts isolated with the help of digitonin. *Anal. Biochem.* **231**, 218–224
- Makinen, M. and Lee, C. P. (1968) Biochemical studies of skeletal muscle mitochondria: I. Microanalysis of cytochrome content, oxidative and phosphorylative activities of mammalian skeletal muscle mitochondria. *Arch. Biochem. Biophys.* **126**, 75–82
- Chrzanowska-Lightowlers, Z. M., Temperley, R. J., Smith, P. M., Seneca, S. H. and Lightowlers, R. N. (2004) Functional polypeptides can be synthesized from human mitochondrial transcripts lacking termination codons. *Biochem. J.* **377**, 725–731
- Sambrook, J. and Russell, D. W. (2001) *Molecular Cloning: A Laboratory Manual*, 3rd edn., Cold Spring Harbor Laboratory Press, Cold Spring Harbor, NY
- Schagger, H. and von Jagow, G. (1991) Blue native electrophoresis for isolation of membrane protein complexes in enzymatically active form. *Anal. Biochem.* **199**, 223–231
- Schagger, H. and von Jagow, G. (1987) Tricine-sodium dodecyl sulfate-polyacrylamide gel electrophoresis for the separation of proteins in the range from 1 to 100 kDa. *Anal. Biochem.* **166**, 368–379
- Houstek, J., Andersson, U., Tvrdik, P., Nedergaard, J. and Cannon, B. (1995) The expression of subunit c correlates with and thus may limit the biosynthesis of the mitochondrial *F₀F₁*-ATPase in brown adipose tissue. *J. Biol. Chem.* **270**, 7689–7694
- Dubot, A., Godinot, C., Dumur, V., Sablonniere, B., Stojkovic, T., Cuisset, J. M., Vojtiskova, A., Pecina, P., Jesina, P. and Houstek, J. (2004) GUG is an efficient initiation codon to translate the human mitochondrial *ATP6* gene. *Biochem. Biophys. Res. Commun.* **313**, 687–693
- Moradi-Ameli, M. and Godinot, C. (1983) Characterization of monoclonal antibodies against mitochondrial *F₁*-ATPase. *Proc. Natl. Acad. Sci. U.S.A.* **80**, 6167–6171
- Wharton, D. C. and Tzagoloff, A. (1967) Cytochrome oxidase from beef heart mitochondria. *Methods Enzymol.* **10**, 245–253
- Rustin, P., Chretien, D., Bourgeron, T., Gerard, B., Rotig, A., Saudubray, J. M. and Munnich, A. (1994) Biochemical and molecular investigations in respiratory chain deficiencies. *Clin. Chim. Acta* **228**, 35–51
- Fischer, J. C., Ruitenbeek, W., Trijbels, J. M. F., Veerkamp, J. H., Stadhouders, A. M., Sengers, R. C. A. and Janssen, A. J. M. (1985) Differential investigation of the capacity of succinate oxidation in human skeletal muscle. *Clin. Chim. Acta* **153**, 37–42
- Fischer, J. C., Ruitenbeek, W., Trijbels, J. M. F., Veerkamp, J. H., Stadhouders, A. M., Sengers, R. C. A. and Janssen, A. J. M. (1986) Estimation of NADH oxidation in human skeletal muscle mitochondria. *Clin. Chim. Acta* **155**, 263–274

- 29 Chowdhury, S. K., Drahota, Z., Floryk, D., Calda, P. and Houstek, J. (2000) Activities of mitochondrial oxidative phosphorylation enzymes in cultured amniocytes. *Clin. Chim. Acta* **298**, 157–173
- 30 Baracca, A., Amler, E., Solaini, G., Parenti-Castelli, G., Lenaz, G. and Houstek, J. (1989) Temperature-induced states of isolated F_1 -ATPase affect catalysis, enzyme conformation and high-affinity nucleotide binding sites. *Biochim. Biophys. Acta* **976**, 77–84
- 31 Pecina, P., Capkova, M., Chowdhury, S. K., Drahota, Z., Dubot, A., Vojtiskova, A., Hansikova, H., Houstkova, H., Zeman, J., Godinot, C. and Houstek, J. (2003) Functional alteration of cytochrome *c* oxidase by SURF1 mutations in Leigh syndrome. *Biochim. Biophys. Acta* **1639**, 53–63
- 32 Floryk, D. and Houstek, J. (1999) Tetramethyl rhodamine methyl ester (TMRM) is suitable for cytofluorometric measurements of mitochondrial membrane potential in cells treated with digitonin. *Biosci. Rep.* **19**, 27–34
- 33 Wanders, R. J. A., Ruiter, J. P. N., Wijburg, F. A., Zeman, J., Klement, P. and Houstek, J. (1996) Prenatal diagnosis of systemic disorders of the respiratory chain in cultured chorionic villus fibroblasts by study of ATP synthesis in digitonin-permeabilized cells. *J. Inher. Metab. Dis.* **19**, 133–136
- 34 Ouhabi, R., Boue-Grabot, M. and Mazat, J. P. (1998) Mitochondrial ATP synthesis in permeabilized cells: assessment of the ATP/O values *in situ*. *Anal. Biochem.* **263**, 169–175
- 35 Chomyn, A. (1996) *In vivo* labeling and analysis of human mitochondrial translation products. *Methods Enzymol.* **264**, 197–211
- 36 Plasek, J. and Sigler, K. (1996) Slow fluorescent indicators of membrane potential: a survey of different approaches to probe response analysis. *J. Photochem. Photobiol. B* **33**, 101–124
- 37 Hoffbuhr, K. C., Davidson, E., Filiano, B. A., Davidson, M., Kennaway, N. G. and King, M. P. (2000) A pathogenic 15-base pair deletion in mitochondrial DNA-encoded cytochrome *c* oxidase subunit III results in the absence of functional cytochrome *c* oxidase. *J. Biol. Chem.* **275**, 13994–14003
- 38 Carrozzo, R., Murray, J., Santorelli, F. M. and Capaldi, R. A. (2000) The T9176G mutation of human mtDNA gives a fully assembled but inactive ATP synthase when modeled in *Escherichia coli*. *FEBS Lett.* **486**, 297–299
- 39 Pansini, A., Guerrieri, F. and Papa, S. (1978) Control of proton conduction by the H^+ -ATPase in the inner mitochondrial membrane. *Eur. J. Biochem.* **92**, 545–551
- 40 Hutcheon, M. L., Duncan, T. M., Ngai, H. and Cross, R. L. (2001) Energy-driven subunit rotation at the interface between subunit a and the c oligomer in the F_0 sector of *Escherichia coli* ATP synthase. *Proc. Natl. Acad. Sci. U.S.A.* **98**, 8519–8524
- 41 Buchet, K. and Godinot, C. (1998) Functional F_1 -ATPase is essential in maintaining growth and membrane potential of human mitochondrial DNA-depleted rho degrees cells. *J. Biol. Chem.* **273**, 22983–22989
- 42 Shoubridge, E. A. (2001) Cytochrome *c* oxidase deficiency. *Am. J. Med. Genet.* **106**, 46–52
- 43 Rossignol, R., Faustin, B., Rocher, C., Malgat, M., Mazat, J. P. and Letellier, T. (2003) Mitochondrial threshold effects. *Biochem. J.* **370**, 751–762
- 44 Temperley, R. J., Seneca, S. H., Tonska, K., Bartnik, E., Bindoff, L. A., Lightowlers, R. N. and Chrzanowska-Lightowlers, Z. M. (2003) Investigation of a pathogenic mtDNA microdeletion reveals a translation-dependent deadenylation decay pathway in human mitochondria. *Hum. Mol. Genet.* **12**, 2341–2348
- 45 El Meziane, A., Lehtinen, S. K., Hance, N., Nijtmans, L. G., Dunbar, D., Holt, I. J. and Jacobs, H. T. (1998) A tRNA suppressor mutation in human mitochondria. *Nat. Genet.* **18**, 350–353
- 46 Hao, H., Morrison, L. E. and Moraes, C. T. (1999) Suppression of a mitochondrial tRNA gene mutation phenotype associated with changes in the nuclear background. *Hum. Mol. Genet.* **8**, 1117–1124
- 47 Ellis, T. P., Helfenbein, K. G., Tzagoloff, A. and Dieckmann, C. L. (2004) Aep3p stabilizes the mitochondrial bicistronic mRNA encoding subunits 6 and 8 of the H^+ -translocating ATP synthase of *Saccharomyces cerevisiae*. *J. Biol. Chem.* **279**, 15728–15733
- 48 Mili, S. and Pinol-Roma, S. (2003) LRP130, a pentatricopeptide motif protein with a noncanonical RNA-binding domain, is bound *in vivo* to mitochondrial and nuclear RNAs. *Mol. Cell. Biol.* **23**, 4972–4982
- 49 Mootha, V. K., Lepage, P., Miller, K., Bunkenborg, J., Reich, M., Hjerrild, M., Delmonte, T., Villeneuve, A., Sladek, R., Xu, F. et al. (2003) Identification of a gene causing human cytochrome *c* oxidase deficiency by integrative genomics. *Proc. Natl. Acad. Sci. U.S.A.* **100**, 605–610

Received 12 March 2004/12 July 2004; accepted 21 July 2004

Published as BJ Immediate Publication 21 July 2004, DOI 10.1042/BJ20040407

Mitochondrial Membrane Potential and ATP Production in Primary Disorders of ATP Synthase

Alena Vojtíšková, Pavel Ješina, Martin Kalous, Vilma Kaplanová,
and Josef Houštěk

*Institute of Physiology and Centre for Integrated Genomics, Academy of Sciences of the Czech Republic,
Prague, Czech Republic*

Markéta Tesařová, Daniela Fornusková, and Jiří Zeman

Department of Pediatrics, First Faculty of Medicine, Charles University, Prague, Czech Republic

Audrey Dubot and Catherine Godinot

Centre of Molecular and Cellular Genetics, Claude Bernard University of Lyon, Villeurbanne, France

Studies of fibroblasts with primary defects in mitochondrial ATP synthase (ATPase) due to heteroplasmic mtDNA mutations in the *ATP6* gene, affecting protonophoric function or synthesis of subunit a, show that at high mutation loads, mitochondrial membrane potential $\Delta\Psi_m$ at state 4 is normal, but ADP-induced discharge of $\Delta\Psi_m$ is impaired and ATP synthesis at state 3-ADP is decreased. Increased $\Delta\Psi_m$ and low ATP synthesis is also found when the ATPase content is diminished by altered biogenesis of the enzyme complex. Irrespective of the different pathogenic mechanisms, elevated $\Delta\Psi_m$ in primary ATPase disorders could increase mitochondrial production of reactive oxygen species and decrease energy provision.

Keywords ATP Synthase, *ATP6*, Flow Cytometry, Membrane Potential, Mitochondrial diseases, mtDNA

Mitochondrial encephalomyopathies due to defects in mitochondrial F_0F_1 -adenosine 5'-triphosphate (ATP) synthase (ATPase) are less common than disorders of the respiratory-chain complexes, but they are usually very severe and can be caused by mitochondrial DNA (mtDNA) mutations or by mutations in nuclear genes. Mitochondrial ATPase is the key enzyme of cellular energy conversion. By means of a fascinating rotary motor mechanism (Kinosita et al. 1998; Stock et al. 2000), it couples the H^+ gradient generated by the respiratory

chain to the synthesis of ATP from adenosine 5'-diphosphate (ADP) and phosphate. The ATPase complex comprises 16 different subunits (Walker and Collinson 1994). It is composed of the globular F_1 catalytic part, which is connected by two stalks to the membrane-embedded F_0 moiety; the latter translocates protons across the inner mitochondrial membrane. Two F_0 subunits, subunit a (*ATP6*) and subunit A6L, are coded by mtDNA (Anderson et al. 1981); all other subunits are nuclear encoded.

The most common cause of ATPase defects are missense heteroplasmic mtDNA mutations in the *ATP6* gene, which affect the protonophoric function of subunit a, an essential component, together with multiple copies of subunit c of the ATPase proton channel (Hutcheon et al. 2001; Stock et al. 1999). Higher prevalence show T8993G(C) mutations (Ciafaloni et al. 1993; Holt et al. 1990; Puddu et al. 1993; Shoffner et al. 1992; Tatuch et al. 1994) which change Leu¹⁵⁶ to Arg or Pro. At a lower mutation load, they manifest as neurogenic muscle weakness, ataxia, and retinitis pigmentosa (NARP syndrome); at heteroplasmy exceeding 90% they present as maternally inherited Leigh syndrome (severe and fatal encephalopathy). Less common are T9176G(C) mutations, which change Leu²¹⁷ (Carrozzo et al. 2001; Dionisi-Vici et al. 1998; Thyagarajan et al. 1995), or a T8851G mutation (De Meirleir et al. 1995) that changes Trp¹⁰⁹, all manifesting also as striatal necrosis syndromes (Schon et al. 2001). Impairment of the ATPase H^+ channel results often, but not always, in decreased ATP production, whereas the ATPase hydrolytic activity remains largely unchanged (Houstek et al. 1995; Tatuch and Robinson 1993). A different type of pathogenic mechanism represents mtDNA 2bp microdeletion 9205delTA, which was found in a newborn with transient lactic acidosis (Seneca et al. 1996) and also in a child with encephalopathy and severe psychomotor retardation (Fornuskova et al. 2003).

Received 1 July 2003; accepted 10 July 2003.

This work was supported by Grant Agency of Ministry of Health of the Czech Republic (NE6533-3) and institutional projects AVOZ5011922 and VZ111100003.

Address correspondence to Josef Houštěk, Institute of Physiology, Academy of Sciences of the Czech Republic, Vídeňská 1083, 14220 Prague, Czech Republic. E-mail: houstek@biomed.cas.cz

A 9205delTA mutation removes the stop codon of the *ATP6* gene and affects the cleavage site between the *ATP6* and *COXIII* transcripts. Most recently, a new mutation, in which A8527G changes the ATPase 6 initiation codon AUG into GUG (Met > Val), has been found in an adult patient with neuropathy, mental retardation, myopathy, suprarenal peripheral insufficiency, and retinopathy (Dubot et al. 2003).

ATPase defects due to nuclear genome mutations are very rare and appear to be caused by diminished biosynthesis of the ATPase complex. ATPase deficiency of possible nonmitochondrial origin was first described in a child with 3-methylglutaconic aciduria and severe lactic acidosis (Holme et al. 1992). Extremely low ATPase activity and low, tightly coupled respiration rates were observed in muscle mitochondria, but no mutation was found in mtDNA genes encoding ATPase subunits. A nuclear origin of ATP synthase deficiency was demonstrated for the first time in 1999 (Houstek et al. 1999) in a new type of fatal mitochondrial disorder: a child with severe lactic acidosis, cardiomegaly, and hepatomegaly died 2 days after birth. 70 to 80% decrease in ATPase activity and ATP production was associated with a corresponding selective decrease in the ATPase complex, which had normal size and subunit composition. Increased biosynthesis of the β subunit with a very short half-life contrasted with decreased biosynthesis of the assembled ATPase and indicated assembly defect at the level of F_1 -ATPase. Cybrid cells made of patient fibroblasts fully complemented the ATPase defect and confirmed the nuclear origin of impaired biogenesis of the enzyme complex (Houstek et al. 1999). Later on several other selective ATPase defects of varying severity have been found, including a fatal ATPase defect described in Belgium (Van Coster et al. 2001); a milder case of ATPase deficiency found in an Austrian patient (Mayr et al. 2002); and two new families with ATPase deficiency of nuclear origin found in the Czech Republic. In this article, we summarize our studies of the functional consequences of various types of primary ATPase defects at the level of mitochondrial ATP synthesis and maintenance and discharge of the mitochondrial membrane potential.

MATERIALS AND METHODS

Cell Cultures

Human skin fibroblasts were cultured in Dulbecco's Modified Eagle's Medium (DMEM) medium with 10% fetal calf serum at 37°C in 5% carbon dioxide in air to approximately 90% confluence. Cells were harvested using 0.05% trypsin and 0.02% ethylenediaminetetraacetic acid (EDTA). Previously established fibroblast cultures with different heteroplasmic mtDNA mutations in the *ATP6* gene (Table 1), and fibroblast cultures with selective ATPase deficiency of nuclear origin from three unrelated Czech families (Table 2) were used for the experiments. Derived transmitochondrial cybrids were prepared as before by the method of Tiranti and colleagues (1995).

TABLE 1

ATP production in fibroblasts with different mtDNA mutations in the *ATP6* gene

Mutation	Mutation type	Heteroplasmy	ATP production ^a
T8993G	Missense Leu → Arg	97%	35–54%
9205delTA	Stop codon → Lys	86%	20–40%
A8527G	Met → Val, change of initiation codon AUG → GUG	97%	90–100%

^aAntimycin A-sensitive production using succinate or pyruvate + malate as a substrate.

Cytofluorometric Analysis

Freshly harvested fibroblasts were resuspended in 80 mM KCl; 10 mM Tris Cl pH 7.4; 3 mM MgCl₂; 1 mM EDTA; 5 mM KH₂PO₄; and 10 mM succinate at a protein concentration of 1 mg/mL. Cells were permeabilized by 0.1 mg digitonin per mg protein (Sigma Chemical, St. Louis, MO) and stained with 20 nM tetramethylrhodamine methyl ester (TMRM; Molecular Probes, Eugene, OR) for 15 min at room temperature. ADP, inhibitors, or both were added at indicated concentrations 1 min before cytofluorometric measurements, which were performed as described elsewhere (Floryk and Houstek 1999) on a FACSort flow cytometer (Becton Dickinson, San Jose, CA) equipped with an argon laser, 488 nm. The TMRM signal was analyzed in the FL2 channel, equipped with a band pass filter 585 ± 21 nm; the photomultiplier value of the detector was at 631 V in FL2. Data were acquired in log scale using CellQuest (Becton Dickinson, San Jose, CA) and analyzed with WinMDI 2.8 software (TSRI, La Jolla, CA). Arithmetic mean values of the fluorescence signal in arbitrary units were determined for each sample for the purpose of subsequent graphic representation.

ATP Production Measurements

The rate of ATP synthesis (Wanders et al. 1993) was measured in 150 mM KCl; 25 mM Tris/HCl; 10 mM KPi; 2 mM EDTA; 1% BSA, pH 7.2; using 0.5 mM ADP and succinate, ketglutarate + malate, or pyruvate + malate as a substrate, all in 10 mM concentration. For permeabilization of fibroblasts and cybrids, 0.1 and 0.03 mg digitonin per mg protein, respectively, was used. ATP was determined in DMSO-quenched aliquots according to Ouhabi and colleagues (1998) by a luciferase assay.

Ethics

The described studies were carried out in accordance with the Declaration of Helsinki of the World Medical Association and were approved by the Committees of Medical Ethics at all collaborating institutions. Informed consent was obtained from investigated individuals or their parents.

TABLE 2
ATP production in fibroblasts from three patients with selective deficiency of ATP synthase

Case	I	II	III
Phenotype	LA, CM, H	LA, CM	LA, CM, EM, dev. delay
Onset/survival	Newborn/2 days	Newborn/32 days	Neonate/7 years
ATPase activity in fibroblasts (% of control) ^a	30%	20%	30%
ATP production in fibroblasts (% of control) ^b	28–32%	32–47%	18–23%
ATP production in cybrids (% of control) ^b	102–116%	220–380%	230%

^aOligomycin-sensitive ATPase activity.

^bAntimycin A-sensitive production using succinate, ketoglutarate + malate, or glutamate + malate as a substrate. CM, cardiomyopathy; EM, encephalomyopathy; H, hepatomegaly; LA, lactic acidosis.

Note: The data for Case I are from the work of Houstek and colleagues (1999); the data for Cases II and III are from two new patients from unrelated families.

RESULTS AND DISCUSSION

The pathogenic mechanisms underlying different types of ATPase defects and disorders seem to range from a dysfunction of mutated subunit a, through insufficient or altered biosynthesis of subunit a, to a diminished production of otherwise normal ATPase complex. With the aim of assessing how these different ATPase defects influence the mitochondrial energy provision, mitochondrial membrane potential $\Delta\Psi_m$ and ATP production were studied. As summarized in Table 1, three types of heteroplasmic mutations in the *ATP6* gene, all present in high mutation loads (86 to 97%), affected substrate-supported ATP production to different extents. The most pronounced decrease in ATP synthesis was in 9205delTA cells; higher rates were found in T8993G fibroblasts; the A8527G mutation was without any effect. Flow cytometry using TMRM as a fluorescent probe further showed that these mutations have varying influences on the $\Delta\Psi_m$. Steady-state levels of $\Delta\Psi_m$ were determined under state 4 conditions, when no ADP is available and $\Delta\mu H^+$ cannot be utilized for ATP synthesis. In all types of fibroblasts, the state 4 $\Delta\Psi_m$ values were within the control range, and the addition of an uncoupler, FCCP, similarly decreased the TMRM signal, indicating that none of the *ATP6* mutations studied increases the passive H^+ flow at state 4. The addition of ADP (state 3-ADP) caused a significant decrease of $\Delta\Psi_m$ in both the control and the A8527G cells, and this ADP-dependent decrease was fully prevented by the ATPase inhibitor oligomycin (Fig. 1). A much smaller, although fully reversible, effect of ADP was seen in 9205delTA cells, and only a minute effect was found in T8993G fibroblasts. Both types of studies, thus, convincingly showed that near-homoplasmic T8993G mutation largely, but not completely, prevented the discharge of $\Delta\Psi_m$ and the synthesis of ATP by mitochondrial ATPase.

It is interesting to note that the behavior of cells with 9205delTA is very similar, and alteration of the *ATP6* stop codon probably interferes with the synthesis of subunit a; or an elon-

gated form of subunit a could be produced, resulting in nonfunctional ATP synthase. In the first case, some incomplete, subunit a-lacking ATPase complexes would be formed. In the second case, the subunit a would be modified in the C-terminal part, where several AA residues that are involved in H^+ -translocation are located (Schon et al. 2001). Both types of measurements also clearly showed that A8527G mutation is without detectable effect on mitochondrial ATP synthesis and, very likely, the GUG initiation codon, replacing the canonical AUG, is somehow operative in human mitochondrial *ATP6* mRNA translation, as is the case of *COXI* and *COXII* in some vertebrates (Johansen et al. 1990; Pan et al. 1993).

A completely different pathogenic mechanism is associated with primary ATPase defects of nuclear origin (Houstek et al. 1999), where the mitochondrial content of ATPase complex is selectively reduced relative to the content of respiratory-chain enzymes, while the subunit composition and the hydrolytic as well as the synthetic function of the remaining ATPase complexes are normal. This relative lack of ATPase was found to cause an increase in membrane potential at state 4 (Houstek et al. 1999), which is indicative of decreased passive H^+ leak and which resulted in a pronounced decrease in ATP production (see Table 2 and Houstek et al. 1999). As is shown in Table 2, a similarly pronounced decrease of ATP production was found in two new patients from different families, in whom a 70–80% decrease of mitochondrial ATPase was found. Their clinical presentations also included lactic acidosis and cardiomyopathy. In one case the patient survived for several weeks; the other case was milder and presented with lactic acidosis, cardiomyopathy, encephalopathy, and developmental delay. In order to find out the genetic origin of these new ATPase defects, transmitochondrial cybrids were prepared by fusing enucleated patient fibroblasts with mtDNA-less (ρ^0) 143B. TK⁻ osteosarcoma cells. As shown in Table 2, the ATP synthesis was fully restored in both types of cybrids, indicating again that the underlying genetic defect is not a mtDNA mutation.

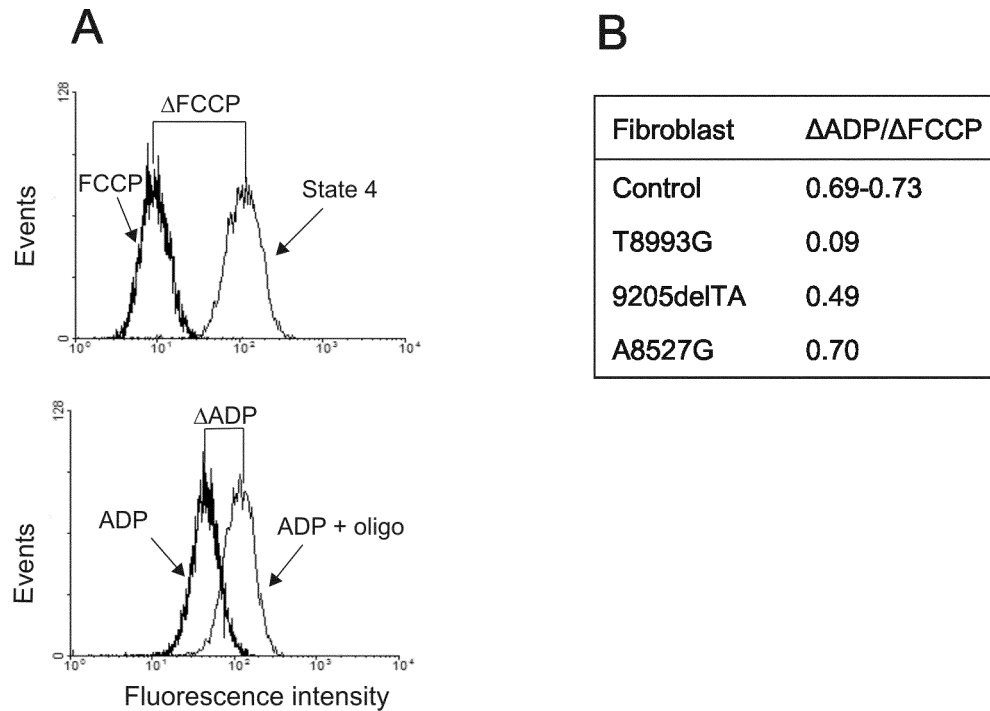


FIG. 1. Changes in the mitochondrial membrane potential $\Delta\Psi_m$ in fibroblasts with different *ATP6* mutations. Cytofluorometric analysis of the mitochondrial membrane potential by TMRM fluorescence was performed in a digitonin-permeabilized fibroblast supplied with 10 mM succinate. (A) The effect of 1 μM FCCCP, 0.1 mM ADP, and ADP followed by 1 μM oligomycin (oligo) in control cells. (B) The ADP-induced decrease of TMRM fluorescence relative to the FCCCP-induced decrease was analyzed in cells with indicated mtDNA mutations.

All the known primary deficiencies of mitochondrial ATPase can significantly affect the mitochondrial ATP production, irrespective of whether the cause is an insufficient amount of normal enzyme or altered properties of ATPase complex that is present in normal quantities. It is also quite clear that in all types of ATPase defects, the production of ATP is only partly inhibited, even in very severe cases. It is difficult to understand how only a partial decline of energy provision (sometimes only 50% or less) can have such serious and often fatal effects. All ATP synthesis data are based on cell cultures, and the situations in the most commonly affected tissues, which have high energy demands, such as brain, heart, and skeletal muscle, can be completely different. On the other hand, inhibitor titration studies in muscle tissue (Rossignol et al. 1999, 2003) show an especially high threshold for ATPase, indicating that some 10% of the normal activity of the enzyme is sufficient for more than 50% functionality of the whole respiratory chain.

It is well established that along with energy shortage, other metabolic consequences, in particular the production of reactive oxygen species (ROS) and the induction of apoptosis and tissue necrosis, are major components of the pathogenic mechanism in mitochondrial OXPHOS diseases (Lenaz et al. 2002; Wallace 1999). An exponential increase in mitochondrial ROS production has been demonstrated at levels of $\Delta\Psi_m$ above 140 mV (Korshunov et al. 1997; Liu 1999), whereas a decrease in $\Delta\Psi_m$ via stimulation of ATP synthase activity, a low ATP/ADP ratio, substrate limitation, or increased proton permeability due

to external or internal uncoupling lower the amount of ROS produced (Kadenbach 2003). The main conclusion we draw from our cytofluorometric studies is that in ATPase disorders, higher levels of $\Delta\Psi_m$ can be expected because a low amount of enzyme or altered function of the F_0 proton channel apparently limit the physiological discharge of respiration-generated $\Delta\mu\text{H}^+$. If this is the case, increased and unbalanced ROS production, rather than diminished energy provision, would be the key pathogenic process in primary ATPase diseases.

REFERENCES

- Anderson, S., Bankier, A. T., Barrell, B. G., de Bruijn, M. H. L., Coulson, A. R., Drouin, J., Eperon, I. C., Nierlich, D. P., Roe, B. A., Sanger, F., Schreier, P. H., Smith, A. J. H., Staden, R., and Young, I. G. 1981. Sequence and organization of the human mitochondrial genome. *Nature* 290:457–465.
- Carozzo, R., Tessa, A., Vazquez-Memije, M. E., Piemonte, F., Patrono, C., Malandrini, A., Dionisi-Vici, C., Vilarinho, L., Villanova, M., Schagger, H., Federico, A., Bertini, E., and Santorelli, F. M. 2001. The T9176G mtDNA mutation severely affects ATP production and results in Leigh syndrome. *Neurology* 56:687–690.
- Ciafaloni, E., Santorelli, F. M., Shanske, S., Deonna, T., Roulet, E., Janzer, C., Pescia, G., and DiMauro, S. 1993. Maternally inherited Leigh syndrome. *J. Pediatr.* 122:419–422.
- De Meirleir, L., Seneca, S., Lissens, W., Schoentjes, E., and Desprechins, B. 1995. Bilateral striatal necrosis with a novel point mutation in the mitochondrial ATPase 6 gene. *Pediatr. Neurol.* 13:242–246.
- Dionisi-Vici, C., Seneca, S., Zeviani, M., Fariello, G., Rimoldi, M., Bertini, E., and De Meirleir, L. 1998. Fulminant Leigh syndrome and sudden unexpected

- death in a family with the T9176C mutation of the mitochondrial ATPase 6 gene. *J. Inherit. Metab. Dis.* 21:2–8.
- Dubot, A., Godinot, C., Vojtiskova, A., Pecina, P., Jesina, P., and Houstek, J. 2003. Use of GUG as initiation codon for the human mitochondria-encoded ATP6 subunit. In *Functional Genomics and Disease*, European Science Foundation, PD4/171, <http://www.esffg2003.org>.
- Floryk, D., and Houstek, J. 1999. Tetramethyl rhodamine methyl ester (TMRM) is suitable for cytofluorometric measurements of mitochondrial membrane potential in cells treated with digitonin. *Biosci. Rep.* 19:27–34.
- Fornuskova, D., Tesarova, M., Hansikova, H., and Zeman, J. 2003. New mtDNA mutation 9204delTA in a family with mitochondrial encephalopathy and ATP-synthase defect. *Cas. Lek. Cesk.* 142:313.
- Holme, E., Greter, J., Jacobson, C. E., Larsson, N. G., Lindstedt, S., Nilsson, K. O., Oldfors, A., and Tulinius, M. 1992. Mitochondrial ATP-synthase deficiency in a child with 3-methylglutaconic aciduria. *Pediatr. Res.* 32:731–735.
- Holt, I. J., Harding, A. E., Petty, R. K. H., and Morgan-Hughes, J. A. 1990. A new mitochondrial disease associated with mitochondrial DNA heteroplasmy. *Am. J. Hum. Genet.* 46:428–433.
- Houstek, J., Klement, P., Floryk, D., Antonicka, H., Hermanska, J., Kalous, M., Hansikova, H., Hout'kova, H., Chowdhury, S. K., Rosipal, T., Kmoch, S., Stratilova, L., and Zeman, J. 1999. A novel deficiency of mitochondrial ATPase of nuclear origin. *Hum. Mol. Genet.* 8:1967–1974.
- Houstek, J., Klement, P., Hermanska, J., Houstkova, H., Hansikova, H., van den Bogert, C., and Zeman, J. 1995. Altered properties of mitochondrial ATP-synthase in patients with a T → G mutation in the ATPase 6 (subunit a) gene at position 8993 of mtDNA. *Biochim. Biophys. Acta* 1271:349–357.
- Hutcheon, M. L., Duncan, T. M., Ngai, H., and Cross, R. L. 2001. Energy-driven subunit rotation at the interface between subunit a and the c oligomer in the F(O) sector of *Escherichia coli* ATP synthase. *Proc. Natl. Acad. Sci. USA* 98:8519–8524.
- Johansen, S., Guddal, P. H., and Johansen, T. 1990. Organization of the mitochondrial genome of Atlantic cod, *Gadus morhua*. *Nucleic Acids Res.* 18: 411–419.
- Kadenbach, B. 2003. Intrinsic and extrinsic uncoupling of oxidative phosphorylation. *Biochim. Biophys. Acta* 1604:77–94.
- Kinosita, K., Jr., Yasuda, R., Noji, H., Ishiwata, S., and Yoshida, M. 1998. F1-ATPase: a rotary motor made of a single molecule. *Cell* 93:21–24.
- Korshunov, S. S., Skulachev, V. P., and Starkov, A. A. 1997. High protonic potential actuates a mechanism of production of reactive oxygen species in mitochondria. *FEBS Lett.* 416:15–18.
- Lenaz, G., Bovina, C., D'Aurelio, M., Fato, R., Formiggini, G., Genova, M. L., Giuliano, G., Pich, M. M., Paolucci, U., Castelli, G. P., and Ventura, B. 2002. Role of mitochondria in oxidative stress and aging. *Ann. N.Y. Acad. Sci.* 959:199–213.
- Liu, S. S. 1999. Cooperation of a “reactive oxygen cycle” with the Q cycle and the proton cycle in the respiratory chain: superoxide generating and cycling mechanisms in mitochondria. *J. Bioenerg. Biomembr.* 31:367–376.
- Mayr, J. A., Paul, J., Kurnik, P., Fotschl, U., Houstek, J., and Sperl, W. 2002. Increased uncoupling in a patient with a quantitative defect of the F0F1-ATP-synthase. *J. Inherit. Metab. Dis.* 25(suppl. 1):178.
- Ouhabi, R., Boue-Grabot, M., and Mazat, J. P. 1998. Mitochondrial ATP synthesis in permeabilized cells: assessment of the ATP/O values in situ. *Anal. Biochem.* 263:169–175.
- Pan, Y. F., Lee, Y. W., Wei, Y. H., and Chiang, A. N. 1993. A gene for cytochrome c oxidase subunit II in duck mitochondrial DNA: structural features and sequence evolution. *Biochem. Mol. Biol. Int.* 30:479–489.
- Puddu, P., Barboni, P., Mantovani, V., Montagna, P., Cerullo, A., Braglini, M., Molinotti, C., and Caramazza, R. 1993. Retinitis pigmentosa, ataxia, and mental retardation associated with mitochondrial DNA mutation in an Italian family. *Br. J. Ophthalmol.* 77:84–88.
- Rossignol, R., Faustin, B., Rocher, C., Malgat, M., Mazat, J. P., and Letellier, T. 2003. Mitochondrial threshold effects. *Biochem. J.* 370:751–762.
- Rossignol, R., Malgat, M., Mazat, J. P., and Letellier, T. 1999. Threshold effect and tissue specificity: implication for mitochondrial cytopathies. *J. Biol. Chem.* 274:33426–33432.
- Schon, E. A., Santra, S., Pallotti, F., and Girvin, M. E. 2001. Pathogenesis of primary defects in mitochondrial ATP synthesis. *Semin. Cell Dev. Biol.* 12:441–448.
- Seneca, S., Abramowicz, M., Lissens, W., Muller, M. F., Vamos, E., and de Meirleir, L. 1996. A mitochondrial DNA microdeletion in a newborn girl with transient lactic acidosis. *J. Inherit. Metab. Dis.* 19:115–118.
- Shoffner, J. M., Fernhoff, P. M., Krawiecki, N. S., Caplan, D. B., Holt, P. J., Koontz, D. A., Takei, Y., Newman, N. J., Ortiz, R. G., Polak, M., Ballinger, S. W., Lott, M. T., and Wallace, D. C. 1992. Subacute necrotizing encephalopathy: oxidative phosphorylation defects and the ATPase 6 point mutation. *Neurology* 42:2168–2174.
- Stock, D., Gibbons, C., Arechaga, I., Leslie, A. G., and Walker, J. E. 2000. The rotary mechanism of ATP synthase. *Curr. Opin. Struct. Biol.* 10:672–679.
- Stock, D., Leslie, A. G., and Walker, J. E. 1999. Molecular architecture of the rotary motor in ATP synthase. *Science* 286:1700–1705.
- Tatuch, Y., Pagon, R. A., Vlcek, B., Roberts, R., Korson, M., and Robinson, B. H. 1994. The 8993mtDNA mutation: heteroplasmy and clinical presentation in three families. *Eur. J. Hum. Genet.* 2:35–43.
- Tatuch, Y., and Robinson, B. H. 1993. The mitochondrial DNA mutation at 8993 associated with NARP slows the rate of ATP synthesis in isolated lymphoblast mitochondria. *Biochem. Biophys. Res. Commun.* 192:124–128.
- Thyagarajan, D., Shanske, S., Vazquez Memije, M., De Vivo, D., and DiMauro, S. 1995. A novel mitochondrial ATPase 6 point mutation in familial bilateral striatal necrosis. *Ann. Neurol.* 38:468–472.
- Tiranti, V., Munaro, M., Sandona, D., Lamantea, E., Rimoldi, M., DiDonato, S., Bisson, R., and Zeviani, M. 1995. Nuclear DNA origin of cytochrome c oxidase deficiency in Leigh's syndrome: Genetic evidence based on patient-derived rho degrees transformants. *Hum. Mol. Genet.* 4:2017–2023.
- Van Coster, R., Smet, J., and Eyskens, F. 2001. Severe complex V deficiency with fatal outcome in neonatal period. In *Society for the Study of Inborn Errors of Metabolism*, ed. G. T. N. Besley, 24, p. 83. Prague, Czech Republic: Kluwer Academic.
- Walker, J. E., and Collinson, I. R. 1994. The role of the stalk in the coupling mechanism of F1F0-ATPases. *FEBS Lett.* 346:39–43.
- Wallace, D. C. 1999. Mitochondrial diseases in man and mouse. *Science* 283:1482–1488.
- Wanders, R. J., Ruijter, J. P., and Wijburg, F. A. 1993. Studies on mitochondrial oxidative phosphorylation in permeabilized human skin fibroblasts: application to mitochondrial encephalomyopathies. *Biochim. Biophys. Acta* 1181:219–222.

6 CONCLUSIONS

- Whereas nDNA-encoded CcO subunits Cox4 and Cox5a are required for the assembly of the functional CcO complex, the Cox6a subunit is required for the overall stability of the holoenzyme. Consequently, the heterogeneous CcO population of Cox6a-deficient cells exhibits higher residual respiration at low oxygen levels than the various CcO forms found in COX5A-KD cells. The description of a novel assembly intermediate at the very last step of CcO assembly suggests additional regulatory level of the process.
- The fact that the ectopic expression of heart/muscle-specific isoform of Cox6a can complement the CcO defect in COX6A1-KD cells is in sharp contrast with unaltered levels of this isoform in our CcO-deficient model, and suggests the existence of a fixed differentiation programme regarding human Cox6a isoforms. The normal amount and function of complex I in all of our CcO-deficient cell lines suggest that even relatively small residual amounts of CcO can maintain normal biogenesis of this respiratory complex in human cells.
- The RNAi knockdown of OXA1L in HEK-293 cells showed that the protein plays an important role in the biogenesis of ATP synthase and respiratory complex I. In sharp contrast to the yeast orthologue, the loss of human Oxa1l does not lead to any impairments of assembly of CcO or the complex III, suggesting functional divergence during evolution.
- In skeletal muscle tissue, comparably high mutant loads (~ 90%) of 3243A>G affecting mt-tRNA^{Leu(UUR)} and 8344A>G affecting mt-tRNA^{Lys} have been associated with severe defect of complex I, but only 8344A>G mutation also resulted in severe deficiency of complex IV. Similarly, 80% heteroplasmy of 8363G>A mutation affecting mt-tRNA^{Lys} resulted in combined severe deficiency of complexes I and IV. Virtually the same patterns of OXPHOS holoenzyme deficiencies were observed in heart mitochondrial samples. However, the patterns of OXPHOS deficiencies in frontal cortex mitochondria of 8363G>A and 3243A>G patients differed substantially from those of other tissues. This difference was particularly striking for ATP synthase. Although it is necessary to analyze considerably more samples with high levels of heteroplasmy (such samples are difficult to obtain), effects of mt-tRNA mutations on the brain OXPHOS are likely to be particularly different from those described for skeletal muscle, heart, and liver tissues.

- The mechanism by which the 9205 Δ TA mutation affects mitochondrial function is associated with changes in the transcription of the *ATP6* and *COX3* genes and their translational competence and efficacy. The decrease in the amount of the mature *ATP6* transcript agreed well with the decreased synthesis and content of subunit a. Interestingly, the labelling of subunit 8 was increased, indicating up-regulated translation of the *ATP8* gene, which precedes and partially overlaps the *ATP6* gene. The translation of the *ATP8* and *ATP6* mRNAs is well described in yeast, but the structure of these genes and its regulation differs completely from that in mammalian mitochondria, where the mechanism of *ATP8* and *ATP6* biosynthesis is largely unknown. The question arises whether increased labelling of subunit 8 could be caused by translation of *ATP8* from an unspliced form of the *ATP8-ATP6-COX3* transcript, part of which is, according to our results, polyadenylated [cDNA synthesis with random primers and oligo(dT) primer] and could be therefore subjected to translation.
- Based on the cytofluorometric studies in cultured skin fibroblasts from patients with complex V defects, higher physiological levels of $\Delta\Psi_m$ can be expected because of low amount of enzyme or altered function of the F_o proton channel. Consequently, increased and unbalanced ROS production, rather than diminished energy provision, would be the key pathogenic process in primary ATP synthase diseases.

7 SUMMARY

In this PhD thesis, we utilized molecular approaches to manipulating the gene expression in human HEK-293 cell line and rare autoptic/biopic tissue materials or cultured skin fibroblasts from patients with mitochondrial disorders to deal with molecular, biochemical and functional aspects of OXPHOS deficiencies.

We prepared stable HEK-293 cell lines with downregulated expression of selected structural CcO subunits (Cox4i1, Cox5a and Cox6a1) and OXA1L gene to study new aspects of the CcO assembly pathway. The obtained knockdown samples in combination with ectopic expression of C-end epitope-tagged Cox6a, Cox7a and Cox7b in wild-type HEK-293 cells and knockdown cell lines allowed us to elucidate early and very late events of CcO assembly and let us to propose new scheme of human CcO holoenzyme assembly pathway. Based on the study of OXA1L knockdown material, we showed that OXA1L is to a great extent expendable, unlike the loss of OXA1 in yeast, for CcO biogenesis.

Due to unique collection of tissues from patients with comparably high heteroplasmy of mt-tRNA mutations resulting in MELAS, MERRF and Leigh syndromes, we found that in skeletal muscle of the patients, the impact of mt-tRNA mutations seems to be gene-specific, whereas tissue-specificity of OXPHOS deficiency patterns was found among different tissues of the patients. Furthermore, we clarified at molecular and biochemical level a mechanism by which very rare mutation 9205 Δ TA affects mitochondrial function. The data on complex V deficient cultured skin fibroblasts contributes to the growing idea that insufficient supply of ATP to meet cellular needs is not necessarily the only factor decisive for pathogenic processes in primary ATPase diseases but also increased and/or unbalanced ROS production might be underlying.

The data presented in this PhD thesis were published in 5 scientific journals and were reported at specialized national or international meetings.

8 REFERENCES

- Acin-Perez R, Bayona-Bafaluy MP, Fernandez-Silva P, Moreno-Loshuertos R, Perez-Martos A, Bruno C, Moraes CT, Enriquez JA. **2004**. Respiratory complex III is required to maintain complex I in mammalian mitochondria. **Mol Cell** 13(6):805-15.
- Acin-Perez R, Fernandez-Silva P, Peleato ML, Perez-Martos A, Enriquez JA. **2008**. Respiratory active mitochondrial supercomplexes. **Mol Cell** 32(4):529-39.
- Adrian GS, McCammon MT, Montgomery DL, Douglas MG. **1986**. Sequences required for delivery and localization of the ADP/ATP translocator to the mitochondrial inner membrane. **Mol Cell Biol** 6(2):626-34.
- Allen RD, Schroeder CC, Fok AK. **1989**. An investigation of mitochondrial inner membranes by rapid-freeze deep-etch techniques. **J Cell Biol** 108(6):2233-40.
- Altamura N, Capitanio N, Bonnefoy N, Papa S, Dujardin G. **1996**. The *Saccharomyces cerevisiae* OXA1 gene is required for the correct assembly of cytochrome c oxidase and oligomycin-sensitive ATP synthase. **FEBS Lett** 382(1-2):111-5.
- Andersson SG, Karlberg O, Canback B, Kurland CG. **2003**. On the origin of mitochondria: a genomics perspective. **Philos Trans R Soc Lond B Biol Sci** 358(1429):165-77; discussion 77-9.
- Andersson SG, Zomorodipour A, Andersson JO, Sicheritz-Ponten T, Alsmark UC, Podowski RM, Naslund AK, Eriksson AS, Winkler HH, Kurland CG. **1998**. The genome sequence of *Rickettsia prowazekii* and the origin of mitochondria. **Nature** 396(6707):133-40.
- Aquila H, Link TA, Klingenberg M. **1985**. The uncoupling protein from brown fat mitochondria is related to the mitochondrial ADP/ATP carrier. Analysis of sequence homologies and of folding of the protein in the membrane. **EMBO J** 4(9):2369-76.
- Aquila H, Misra D, Eulitz M, Klingenberg M. **1982**. Complete amino acid sequence of the ADP/ATP carrier from beef heart mitochondria. **Hoppe Seylers Z Physiol Chem** 363(3):345-9.
- Arends H, Sebald W. **1984**. Nucleotide sequence of the cloned mRNA and gene of the ADP/ATP carrier from *Neurospora crassa*. **EMBO J** 3(2):377-82.
- Arnold I, Pfeiffer K, Neupert W, Stuart RA, Schagger H. **1998**. Yeast mitochondrial F1F0-ATP synthase exists as a dimer: identification of three dimer-specific subunits. **EMBO J** 17(24):7170-8.
- Arnold S, Kadenbach B. **1997**. Cell respiration is controlled by ATP, an allosteric inhibitor of cytochrome-c oxidase. **Eur J Biochem** 249(1):350-4.
- Baracca A, Amler E, Solaini G, Parenti Castelli G, Lenaz G, Houstek J. **1989**. Temperature-induced states of isolated F1-ATPase affect catalysis, enzyme conformation and high-affinity nucleotide binding sites. **Biochim Biophys Acta** 976(1):77-84.
- Barrientos A, Barros MH, Valnot I, Rotig A, Rustin P, Tzagoloff A. **2002**. Cytochrome oxidase in health and disease. **Gene** 286(1):53-63.
- Barrientos A, Gouget K, Horn D, Soto IC, Fontanesi F. **2009**. Suppression mechanisms of COX assembly defects in yeast and human: insights into the COX assembly process. **Biochim Biophys Acta** 1793(1):97-107.
- Baysal BE, Ferrell RE, Willett-Brozick JE, Lawrence EC, Myssiorek D, Bosch A, van der Mey A, Taschner PE, Rubinstein WS, Myers EN and others. **2000**. Mutations in SDHD, a mitochondrial complex II gene, in hereditary paraganglioma. **Science** 287(5454):848-51.

- Beke-Somfai T, Lincoln P, Norden B. **2010**. Mechanical control of ATP synthase function: activation energy difference between tight and loose binding sites. **Biochemistry** 49(3):401-3.
- Belogradov GI, Tomich JM, Hatefi Y. **1996**. Membrane topography and near-neighbor relationships of the mitochondrial ATP synthase subunits e, f, and g. **J Biol Chem** 271(34):20340-5.
- Benard G, Faustin B, Passerieux E, Galinier A, Rocher C, Bellance N, Delage JP, Casteilla L, Letellier T, Rossignol R. **2006**. Physiological diversity of mitochondrial oxidative phosphorylation. **Am J Physiol Cell Physiol** 291(6):C1172-82.
- Bentlage HA, Wendel U, Schagger H, ter Laak HJ, Janssen AJ, Trijbels JM. **1996**. Lethal infantile mitochondrial disease with isolated complex I deficiency in fibroblasts but with combined complex I and IV deficiencies in muscle. **Neurology** 47(1):243-8.
- Berman SB, Pineda FJ, Hardwick JM. **2008**. Mitochondrial fission and fusion dynamics: the long and short of it. **Cell Death Differ** 15(7):1147-52.
- Berry EA, Trumpower BL. **1985**. Isolation of ubiquinol oxidase from *Paracoccus denitrificans* and resolution into cytochrome bc₁ and cytochrome c-aa₃ complexes. **J Biol Chem** 260(4):2458-67.
- Betina S, Gavurnikova G, Haviernik P, Sabova L, Kolarov J. **1995**. Expression of the AAC2 gene encoding the major mitochondrial ADP/ATP carrier in *Saccharomyces cerevisiae* is controlled at the transcriptional level by oxygen, heme and HAP2 factor. **Eur J Biochem** 229(3):651-7.
- Bianchi C, Genova ML, Parenti Castelli G, Lenaz G. **2004**. The mitochondrial respiratory chain is partially organized in a supercomplex assembly: kinetic evidence using flux control analysis. **J Biol Chem** 279(35):36562-9.
- Birch-Machin MA, Taylor RW, Cochran B, Ackrell BA, Turnbull DM. **2000**. Late-onset optic atrophy, ataxia, and myopathy associated with a mutation of a complex II gene. **Ann Neurol** 48(3):330-5.
- Blakely EL, Mitchell AL, Fisher N, Meunier B, Nijtmans LG, Schaefer AM, Jackson MJ, Turnbull DM, Taylor RW. **2005**. A mitochondrial cytochrome b mutation causing severe respiratory chain enzyme deficiency in humans and yeast. **FEBS J** 272(14):3583-92.
- Bohm M, Pronicka E, Karczmarewicz E, Pronicki M, Piekutowska-Abramczuk D, Sykut-Cegielska J, Mierzewska H, Hansikova H, Vesela K, Tesarova M and others. **2006**. Retrospective, multicentric study of 180 children with cytochrome C oxidase deficiency. **Pediatr Res** 59(1):21-6.
- Bonne G, Seibel P, Possekkel S, Marsac C, Kadenbach B. **1993**. Expression of human cytochrome c oxidase subunits during fetal development. **Eur J Biochem** 217(3):1099-107.
- Bourgeron T, Rustin P, Chretien D, Birch-Machin M, Bourgeois M, Viegas-Pequignot E, Munnich A, Rotig A. **1995**. Mutation of a nuclear succinate dehydrogenase gene results in mitochondrial respiratory chain deficiency. **Nat Genet** 11(2):144-9.
- Boyer PD. **1993**. The binding change mechanism for ATP synthase--some probabilities and possibilities. **Biochim Biophys Acta** 1140(3):215-50.
- Boyer PD. **1998**. ATP synthase--past and future. **Biochim Biophys Acta** 1365(1-2):3-9.
- Boyer PD. **2000**. Catalytic site forms and controls in ATP synthase catalysis. **Biochim Biophys Acta** 1458(2-3):252-62.

- Brandner K, Mick DU, Frazier AE, Taylor RD, Meisinger C, Rehling P. **2005**. Taz1, an outer mitochondrial membrane protein, affects stability and assembly of inner membrane protein complexes: implications for Barth Syndrome. **Mol Biol Cell** 16(11):5202-14.
- Brandt U, Trumppower B. **1994**. The protonmotive Q cycle in mitochondria and bacteria. **Crit Rev Biochem Mol Biol** 29(3):165-97.
- Brantova O, Tesarova M, Hansikova H, Elleder M, Zeman J, Sladkova J. **2006**. Ultrastructural changes of mitochondria in the cultivated skin fibroblasts of patients with point mutations in mitochondrial DNA. **Ultrastruct Pathol** 30(4):239-45.
- Braun HP, Emmermann M, Krufft V, Schmitz UK. **1992**. The general mitochondrial processing peptidase from potato is an integral part of cytochrome c reductase of the respiratory chain. **EMBO J** 11(9):3219-27.
- Braun HP, Schmitz UK. **1995**. Are the 'core' proteins of the mitochondrial bc1 complex evolutionary relics of a processing protease? **Trends Biochem Sci** 20(5):171-5.
- Brustovetsky N, Becker A, Klingenberg M, Bamberg E. **1996**. Electrical currents associated with nucleotide transport by the reconstituted mitochondrial ADP/ATP carrier. **Proc Natl Acad Sci U S A** 93(2):664-8.
- Buschges R, Bahrenberg G, Zimmermann M, Wolf K. **1994**. NADH: ubiquinone oxidoreductase in obligate aerobic yeasts. **Yeast** 10(4):475-9.
- Buzhynskyy N, Sens P, Prima V, Sturgis JN, Scheuring S. **2007**. Rows of ATP synthase dimers in native mitochondrial inner membranes. **Biophys J** 93(8):2870-6.
- Capaldi RA. **1982**. Arrangement of proteins in the mitochondrial inner membrane. **Biochim Biophys Acta** 694(3):291-306.
- Capaldi RA, Aggeler R. **2002**. Mechanism of the F(1)F(0)-type ATP synthase, a biological rotary motor. **Trends Biochem Sci** 27(3):154-60.
- Carroll J, Fearnley IM, Shannon RJ, Hirst J, Walker JE. **2003**. Analysis of the subunit composition of complex I from bovine heart mitochondria. **Mol Cell Proteomics** 2(2):117-26.
- Carroll J, Fearnley IM, Skehel JM, Shannon RJ, Hirst J, Walker JE. **2006**. Bovine complex I is a complex of 45 different subunits. **J Biol Chem** 281(43):32724-7.
- Carrozzo R, Tessa A, Vazquez-Memije ME, Piemonte F, Patrono C, Malandrini A, Dionisi-Vici C, Vilarinho L, Villanova M, Schagger H and others. **2001**. The T9176G mtDNA mutation severely affects ATP production and results in Leigh syndrome. **Neurology** 56(5):687-90.
- Cervený KL, Tamura Y, Zhang Z, Jensen RE, Sesaki H. **2007**. Regulation of mitochondrial fusion and division. **Trends Cell Biol** 17(11):563-9.
- Ciafaloni E, Santorelli FM, Shanske S, Deonna T, Roulet E, Janzer C, Pescia G, DiMauro S. **1993**. Maternally inherited Leigh syndrome. **J Pediatr** 122(3):419-22.
- Civitarese AE, Ravussin E. **2008**. Mitochondrial energetics and insulin resistance. **Endocrinology** 149(3):950-4.
- Cizkova A, Stranecky V, Mayr JA, Tesarova M, Havlickova V, Paul J, Ivanek R, Kuss AW, Hansikova H, Kaplanova V and others. **2008**. TMEM70 mutations cause isolated ATP synthase deficiency and neonatal mitochondrial encephalomyopathy. **Nat Genet** 40(11):1288-90.
- Claypool SM, Oktay Y, Boonthung P, Loo JA, Koehler CM. **2008**. Cardiolipin defines the interactome of the major ADP/ATP carrier protein of the mitochondrial inner membrane. **J Cell Biol** 182(5):937-50.

- Crofts AR, Barquera B, Gennis RB, Kuras R, Guergova-Kuras M, Berry EA. **1999a**. Mechanism of ubiquinol oxidation by the bc(1) complex: different domains of the quinol binding pocket and their role in the mechanism and binding of inhibitors. **Biochemistry** 38(48):15807-26.
- Crofts AR, Guergova-Kuras M, Huang L, Kuras R, Zhang Z, Berry EA. **1999b**. Mechanism of ubiquinol oxidation by the bc(1) complex: role of the iron sulfur protein and its mobility. **Biochemistry** 38(48):15791-806.
- Csordas G, Renken C, Varnai P, Walter L, Weaver D, Buttle KF, Balla T, Mannella CA, Hajnoczky G. **2006**. Structural and functional features and significance of the physical linkage between ER and mitochondria. **J Cell Biol** 174(7):915-21.
- de Brito OM, Scorrano L. **2008**. Mitofusin 2 tethers endoplasmic reticulum to mitochondria. **Nature** 456(7222):605-10.
- De Meirleir L, Seneca S, Lissens W, De Clercq I, Eyskens F, Gerlo E, Smet J, Van Coster R. **2004**. Respiratory chain complex V deficiency due to a mutation in the assembly gene ATP12. **J Med Genet** 41(2):120-4.
- De Meirleir L, Seneca S, Lissens W, Schoentjes E, Desprechins B. **1995**. Bilateral striatal necrosis with a novel point mutation in the mitochondrial ATPase 6 gene. **Pediatr Neurol** 13(3):242-6.
- Di Donato S. **2009**. Multisystem manifestations of mitochondrial disorders. **J Neurol** 256(5):693-710.
- Diaz F. **2010**. Cytochrome c oxidase deficiency: patients and animal models. **Biochim Biophys Acta** 1802(1):100-10.
- Diaz F, Fukui H, Garcia S, Moraes CT. **2006**. Cytochrome c oxidase is required for the assembly/stability of respiratory complex I in mouse fibroblasts. **Mol Cell Biol** 26(13):4872-81.
- Dickson VK, Silvester JA, Fearnley IM, Leslie AG, Walker JE. **2006**. On the structure of the stator of the mitochondrial ATP synthase. **EMBO J** 25(12):2911-8.
- DiMauro S, Schon EA. **2008**. Mitochondrial disorders in the nervous system. **Annu Rev Neurosci** 31:91-123.
- Dionisi-Vici C, Seneca S, Zeviani M, Fariello G, Rimoldi M, Bertini E, De Meirleir L. **1998**. Fulminant Leigh syndrome and sudden unexpected death in a family with the T9176C mutation of the mitochondrial ATPase 6 gene. **J Inherit Metab Dis** 21(1):2-8.
- Distelmaier F, Koopman WJ, van den Heuvel LP, Rodenburg RJ, Mayatepek E, Willems PH, Smeitink JA. **2009**. Mitochondrial complex I deficiency: from organelle dysfunction to clinical disease. **Brain** 132(Pt 4):833-42.
- Dolce V, Fiermonte G, Messina A, Palmieri F. **1991**. Nucleotide sequence of a human heart cDNA encoding the mitochondrial phosphate carrier. **DNA Seq** 2(2):133-5.
- Dolce V, Iacobazzi V, Palmieri F, Walker JE. **1994**. The sequences of human and bovine genes of the phosphate carrier from mitochondria contain evidence of alternatively spliced forms. **J Biol Chem** 269(14):10451-60.
- Dolce V, Scarcia P, Iacopetta D, Palmieri F. **2005**. A fourth ADP/ATP carrier isoform in man: identification, bacterial expression, functional characterization and tissue distribution. **FEBS Lett** 579(3):633-7.
- Drgon T, Sabova L, Nelson N, Kolarov J. **1991**. ADP/ATP translocator is essential only for anaerobic growth of yeast *Saccharomyces cerevisiae*. **FEBS Lett** 289(2):159-62.
- Dubot A, Godinot C, Dumur V, Sablonniere B, Stojkovic T, Cuisset JM, Vojtiskova A, Pecina P, Jesina P, Houstek J. **2004**. GUG is an efficient initiation codon to

- translate the human mitochondrial ATP6 gene. **Biochem Biophys Res Commun** 313(3):687-93.
- Dudkina NV, Eubel H, Keegstra W, Boekema EJ, Braun HP. **2005**. Structure of a mitochondrial supercomplex formed by respiratory-chain complexes I and III. **Proc Natl Acad Sci U S A** 102(9):3225-9.
- Dudkina NV, Sunderhaus S, Braun HP, Boekema EJ. **2006**. Characterization of dimeric ATP synthase and cristae membrane ultrastructure from *Saccharomyces* and *Polytomella* mitochondria. **FEBS Lett** 580(14):3427-32.
- Duee ED, Vignais PV. **1969**. Kinetics and specificity of the adenine nucleotide translocation in rat liver mitochondria. **J Biol Chem** 244(14):3920-31.
- Duvezin-Caubet S, Caron M, Giraud MF, Velours J, di Rago JP. **2003**. The two rotor components of yeast mitochondrial ATP synthase are mechanically coupled by subunit delta. **Proc Natl Acad Sci U S A** 100(23):13235-40.
- Eng C, Kiuru M, Fernandez MJ, Aaltonen LA. **2003**. A role for mitochondrial enzymes in inherited neoplasia and beyond. **Nat Rev Cancer** 3(3):193-202.
- Eubel H, Jansch L, Braun HP. **2003**. New insights into the respiratory chain of plant mitochondria. Supercomplexes and a unique composition of complex II. **Plant Physiol** 133(1):274-86.
- Fabrizi GM, Sadlock J, Hirano M, Mita S, Koga Y, Rizzuto R, Zeviani M, Schon EA. **1992**. Differential expression of genes specifying two isoforms of subunit VIa of human cytochrome c oxidase. **Gene** 119(2):307-12.
- Fernandez-Moreira D, Ugalde C, Smeets R, Rodenburg RJ, Lopez-Laso E, Ruiz-Falco ML, Briones P, Martin MA, Smeitink JA, Arenas J. **2007**. X-linked NDUFA1 gene mutations associated with mitochondrial encephalomyopathy. **Ann Neurol** 61(1):73-83.
- Fernandez-Vizarra E, Tiranti V, Zeviani M. **2009**. Assembly of the oxidative phosphorylation system in humans: what we have learned by studying its defects. **Biochim Biophys Acta** 1793(1):200-11.
- Fiermonte G, Dolce V, Palmieri F. **1998**. Expression in *Escherichia coli*, functional characterization, and tissue distribution of isoforms A and B of the phosphate carrier from bovine mitochondria. **J Biol Chem** 273(35):22782-7.
- Fischer JC, Ruitenbeek W, Trijbels JM, Veerkamp JH, Stadhouders AM, Sengers RC, Janssen AJ. **1986**. Estimation of NADH oxidation in human skeletal muscle mitochondria. **Clin Chim Acta** 155(3):263-73.
- Floryk D, Houstek J. **1999**. Tetramethyl rhodamine methyl ester (TMRM) is suitable for cytofluorometric measurements of mitochondrial membrane potential in cells treated with digitonin. **Biosci Rep** 19(1):27-34.
- Fontanesi F, Palmieri L, Scarcia P, Lodi T, Donnini C, Limongelli A, Tiranti V, Zeviani M, Ferrero I, Viola AM. **2004**. Mutations in AAC2, equivalent to human adPEO-associated ANT1 mutations, lead to defective oxidative phosphorylation in *Saccharomyces cerevisiae* and affect mitochondrial DNA stability. **Hum Mol Genet** 13(9):923-34.
- Fontanesi F, Soto IC, Barrientos A. **2008**. Cytochrome c oxidase biogenesis: new levels of regulation. **IUBMB Life** 60(9):557-68.
- Fornuskova D, Brantova O, Tesarova M, Stiburek L, Honzik T, Wenchich L, Tietzeova E, Hansikova H, Zeman J. **2008**. The impact of mitochondrial tRNA mutations on the amount of ATP synthase differs in the brain compared to other tissues. **Biochim Biophys Acta** 1782(5):317-25.

- Fornuskova D, Stiburek L, Wenchich L, Vinsova K, Hansikova H, Zeman J. **2010**. Novel insights into the assembly and function of human nuclear-encoded cytochrome c oxidase subunits 4, 5a, 6a, 7a and 7b. **Biochem J** 428(3):363-74.
- Frey TG, Mannella CA. **2000**. The internal structure of mitochondria. **Trends Biochem Sci** 25(7):319-24.
- Fronzes R, Weimann T, Vaillier J, Velours J, Brethes D. **2006**. The peripheral stalk participates in the yeast ATP synthase dimerization independently of e and g subunits. **Biochemistry** 45(21):6715-23.
- Fujiki Y, Hubbard AL, Fowler S, Lazarow PB. **1982**. Isolation of intracellular membranes by means of sodium carbonate treatment: application to endoplasmic reticulum. **J Cell Biol** 93(1):97-102.
- Galati D, Srinivasan S, Raza H, Prabu SK, Hardy M, Chandran K, Lopez M, Kalyanaraman B, Avadhani NG. **2009**. Role of nuclear-encoded subunit Vb in the assembly and stability of cytochrome c oxidase complex: implications in mitochondrial dysfunction and ROS production. **Biochem J** 420(3):439-49.
- Gavin PD, Prescott M, Devenish RJ. **2005**. F1F0-ATP synthase complex interactions in vivo can occur in the absence of the dimer specific subunit e. **J Bioenerg Biomembr** 37(2):55-66.
- Genova ML, Baracca A, Biondi A, Casalena G, Faccioli M, Falasca AI, Formiggini G, Sgarbi G, Solaini G, Lenaz G. **2008**. Is supercomplex organization of the respiratory chain required for optimal electron transfer activity? **Biochim Biophys Acta** 1777(7-8):740-6.
- Ghezzi D, Goffrini P, Uziel G, Horvath R, Klopstock T, Lochmuller H, D'Adamo P, Gasparini P, Strom TM, Prokisch H and others. **2009**. SDHAF1, encoding a LYR complex-II specific assembly factor, is mutated in SDH-defective infantile leukoencephalopathy. **Nat Genet**.
- Giorgi C, De Stefani D, Bononi A, Rizzuto R, Pinton P. **2009**. Structural and functional link between the mitochondrial network and the endoplasmic reticulum. **Int J Biochem Cell Biol** 41(10):1817-27.
- Giraud MF, Paumard P, Soubannier V, Vaillier J, Arselin G, Salin B, Schaeffer J, Brethes D, di Rago JP, Velours J. **2002**. Is there a relationship between the supramolecular organization of the mitochondrial ATP synthase and the formation of cristae? **Biochim Biophys Acta** 1555(1-3):174-80.
- Gostimskaya IS, Grivennikova VG, Cecchini G, Vinogradov AD. **2007**. Reversible dissociation of flavin mononucleotide from the mammalian membrane-bound NADH: ubiquinone oxidoreductase (complex I). **FEBS Lett** 581(30):5803-6.
- Graham BH, Waymire KG, Cottrell B, Trounce IA, MacGregor GR, Wallace DC. **1997**. A mouse model for mitochondrial myopathy and cardiomyopathy resulting from a deficiency in the heart/muscle isoform of the adenine nucleotide translocator. **Nat Genet** 16(3):226-34.
- Gray MW, Burger G, Lang BF. **1999**. Mitochondrial evolution. **Science** 283(5407):1476-81.
- Grivennikova VG, Vinogradov AD. **2006**. Generation of superoxide by the mitochondrial Complex I. **Biochim Biophys Acta** 1757(5-6):553-61.
- Groen AK, Wanders RJ, Westerhoff HV, van der Meer R, Tager JM. **1982**. Quantification of the contribution of various steps to the control of mitochondrial respiration. **J Biol Chem** 257(6):2754-7.
- Guelin E, Chevallier J, Rigoulet M, Guerin B, Velours J. **1993**. ATP synthase of yeast mitochondria. Isolation and disruption of the ATP epsilon gene. **J Biol Chem** 268(1):161-7.

- Guenebaut V, Schlitt A, Weiss H, Leonard K, Friedrich T. **1998**. Consistent structure between bacterial and mitochondrial NADH:ubiquinone oxidoreductase (complex I). **J Mol Biol** 276(1):105-12.
- Gupte SS, Hackenbrock CR. **1988**. The role of cytochrome c diffusion in mitochondrial electron transport. **J Biol Chem** 263(11):5248-53.
- Hackenbreg H, Klingenberg M. **1980**. Molecular weight and hydrodynamic parameters of the adenosine 5'-diphosphate--adenosine 5'-triphosphate carrier in Triton X-100. **Biochemistry** 19(3):548-55.
- Hackenbrock CR. **1968**. Chemical and physical fixation of isolated mitochondria in low-energy and high-energy states. **Proc Natl Acad Sci U S A** 61(2):598-605.
- Hadikusumo RG, Meltzer S, Choo WM, Jean-Francois MJ, Linnane AW, Marzuki S. **1988**. The definition of mitochondrial H⁺ ATPase assembly defects in mutants of *Saccharomyces cerevisiae* with a monoclonal antibody to the enzyme complex as an assembly probe. **Biochim Biophys Acta** 933(1):212-22.
- Hagerhall C. **1997**. Succinate: quinone oxidoreductases. Variations on a conserved theme. **Biochim Biophys Acta** 1320(2):107-41.
- Hatefi Y. **1985**. The mitochondrial electron transport and oxidative phosphorylation system. **Annu Rev Biochem** 54:1015-69.
- Haut S, Brivet M, Touati G, Rustin P, Lebon S, Garcia-Cazorla A, Saudubray JM, Boutron A, Legrand A, Slama A. **2003**. A deletion in the human QP-C gene causes a complex III deficiency resulting in hypoglycaemia and lactic acidosis. **Hum Genet** 113(2):118-22.
- Heldt HW, Klingenberg M, Milovancev M. **1972**. Differences between the ATP-ADP ratios in the mitochondrial matrix and in the extramitochondrial space. **Eur J Biochem** 30(3):434-40.
- Helling S, Vogt S, Rhiel A, Ramzan R, Wen L, Marcus K, Kadenbach B. **2008**. Phosphorylation and kinetics of mammalian cytochrome c oxidase. **Mol Cell Proteomics** 7(9):1714-24.
- Herrmann JM, Neupert W. **2003**. Protein insertion into the inner membrane of mitochondria. **IUBMB Life** 55(4-5):219-25.
- Hirst J. **2010**. Towards the molecular mechanism of respiratory complex I. **Biochem J** 425(2):327-39.
- Holland HD. **1990**. ATMOSPHERIC EVOLUTION - ORIGINS OF BREATHABLE AIR. **Nature** 347(6288):17-.
- Holme E, Greter J, Jacobson CE, Larsson NG, Lindstedt S, Nilsson KO, Oldfors A, Tulinius M. **1992**. Mitochondrial ATP-synthase deficiency in a child with 3-methylglutaconic aciduria. **Pediatr Res** 32(6):731-5.
- Holt IJ, Harding AE, Petty RK, Morgan-Hughes JA. **1990**. A new mitochondrial disease associated with mitochondrial DNA heteroplasmy. **Am J Hum Genet** 46(3):428-33.
- Hong S, Pedersen PL. **2002**. ATP synthase of yeast: structural insight into the different inhibitory potencies of two regulatory peptides and identification of a new potential regulator. **Arch Biochem Biophys** 405(1):38-43.
- Horvat S, Beyer C, Arnold S. **2006**. Effect of hypoxia on the transcription pattern of subunit isoforms and the kinetics of cytochrome c oxidase in cortical astrocytes and cerebellar neurons. **J Neurochem** 99(3):937-51.
- Houstek J, Andersson U, Tvrđik P, Nedergaard J, Cannon B. **1995a**. The expression of subunit c correlates with and thus may limit the biosynthesis of the mitochondrial F₀F₁-ATPase in brown adipose tissue. **J Biol Chem** 270(13):7689-94.

- Houstek J, Klement P, Floryk D, Antonicka H, Hermanska J, Kalous M, Hansikova H, Hout'kova H, Chowdhury SK, Rosipal T and others. **1999**. A novel deficiency of mitochondrial ATPase of nuclear origin. **Hum Mol Genet** 8(11):1967-74.
- Houstek J, Klement P, Hermanska J, Houstkova H, Hansikova H, Van den Bogert C, Zeman J. **1995b**. Altered properties of mitochondrial ATP-synthase in patients with a T->G mutation in the ATPase 6 (subunit a) gene at position 8993 of mtDNA. **Biochim Biophys Acta** 1271(2-3):349-57.
- Houstek J, Mracek T, Vojtiskova A, Zeman J. **2004**. Mitochondrial diseases and ATPase defects of nuclear origin. **Biochim Biophys Acta** 1658(1-2):115-21.
- Hunte C, Koepke J, Lange C, Rossmanith T, Michel H. **2000**. Structure at 2.3 Å resolution of the cytochrome bc(1) complex from the yeast *Saccharomyces cerevisiae* co-crystallized with an antibody Fv fragment. **Structure** 8(6):669-84.
- Hutcheon ML, Duncan TM, Ngai H, Cross RL. **2001**. Energy-driven subunit rotation at the interface between subunit a and the c oligomer in the F(O) sector of *Escherichia coli* ATP synthase. **Proc Natl Acad Sci U S A** 98(15):8519-24.
- Huttemann M, Kadenbach B, Grossman LI. **2001**. Mammalian subunit IV isoforms of cytochrome c oxidase. **Gene** 267(1):111-23.
- Huttemann M, Lee I, Pecinova A, Pecina P, Przyklenk K, Doan JW. **2008**. Regulation of oxidative phosphorylation, the mitochondrial membrane potential, and their role in human disease. **J Bioenerg Biomembr** 40(5):445-56.
- Chen C, Ko Y, Delannoy M, Ludtke SJ, Chiu W, Pedersen PL. **2004**. Mitochondrial ATP synthasome: three-dimensional structure by electron microscopy of the ATP synthase in complex formation with carriers for Pi and ADP/ATP. **J Biol Chem** 279(30):31761-8.
- Chen H, Chan DC. **2005**. Emerging functions of mammalian mitochondrial fusion and fission. **Hum Mol Genet** 14 Spec No. 2:R283-9.
- Chen XJ. **2002**. Induction of an unregulated channel by mutations in adenine nucleotide translocase suggests an explanation for human ophthalmoplegia. **Hum Mol Genet** 11(16):1835-43.
- Chomyn A. **1996**. In vivo labeling and analysis of human mitochondrial translation products. **Methods Enzymol** 264:197-211.
- Choo WM, Hadikusumo RG, Marzuki S. **1985**. Mitochondrial adenosine triphosphatase in mit- mutants of *Saccharomyces cerevisiae* with defective subunit 6 of the enzyme complex. **Biochim Biophys Acta** 806(2):290-304.
- Chowdhury SK, Drahota Z, Floryk D, Calda P, Houstek J. **2000**. Activities of mitochondrial oxidative phosphorylation enzymes in cultured amniocytes. **Clin Chim Acta** 298(1-2):157-73.
- Chrzanowska-Lightowlers ZM, Temperley RJ, Smith PM, Seneca SH, Lightowlers RN. **2004**. Functional polypeptides can be synthesized from human mitochondrial transcripts lacking termination codons. **Biochem J** 377(Pt 3):725-31.
- Iwasaki T, Matsuura K, Oshima T. **1995a**. Resolution of the aerobic respiratory system of the thermoacidophilic archaeon, *Sulfolobus* sp. strain 7. I. The archaeal terminal oxidase supercomplex is a functional fusion of respiratory complexes III and IV with no c-type cytochromes. **J Biol Chem** 270(52):30881-92.
- Iwasaki T, Wakagi T, Isogai Y, Iizuka T, Oshima T. **1995b**. Resolution of the aerobic respiratory system of the thermoacidophilic archaeon, *Sulfolobus* sp. strain 7. II. Characterization of the archaeal terminal oxidase subcomplexes and implication for the intramolecular electron transfer. **J Biol Chem** 270(52):30893-901.

- Iwata S, Lee JW, Okada K, Lee JK, Iwata M, Rasmussen B, Link TA, Ramaswamy S, Jap BK. **1998**. Complete structure of the 11-subunit bovine mitochondrial cytochrome bc₁ complex. **Science** 281(5373):64-71.
- Janssen RJ, Nijtmans LG, van den Heuvel LP, Smeitink JA. **2006**. Mitochondrial complex I: structure, function and pathology. **J Inherit Metab Dis** 29(4):499-515.
- Jesina P, Tesarova M, Fornuskova D, Vojtiskova A, Pecina P, Kaplanova V, Hansikova H, Zeman J, Houstek J. **2004**. Diminished synthesis of subunit a (ATP6) and altered function of ATP synthase and cytochrome c oxidase due to the mtDNA 2 bp microdeletion of TA at positions 9205 and 9206. **Biochem J** 383(Pt. 3):561-71.
- Jonckheere AI, Hogeveen M, Nijtmans LG, van den Brand MA, Janssen AJ, Diepstra JH, van den Brandt FC, van den Heuvel LP, Hol FA, Hofste TG and others. **2008**. A novel mitochondrial ATP8 gene mutation in a patient with apical hypertrophic cardiomyopathy and neuropathy. **J Med Genet** 45(3):129-33.
- Kadenbach B. **2003**. Intrinsic and extrinsic uncoupling of oxidative phosphorylation. **Biochim Biophys Acta** 1604(2):77-94.
- Kadenbach B, Arnold S. **1999**. A second mechanism of respiratory control. **FEBS Lett** 447(2-3):131-4.
- Kadenbach B, Huttemann M, Arnold S, Lee I, Bender E. **2000**. Mitochondrial energy metabolism is regulated via nuclear-coded subunits of cytochrome c oxidase. **Free Radic Biol Med** 29(3-4):211-21.
- Kaim G, Dimroth P. **1999**. ATP synthesis by F-type ATP synthase is obligatorily dependent on the transmembrane voltage. **EMBO J** 18(15):4118-27.
- Kakkar P, Singh BK. **2007**. Mitochondria: a hub of redox activities and cellular distress control. **Mol Cell Biochem** 305(1-2):235-53.
- Kaplan RS. **2001**. Structure and function of mitochondrial anion transport proteins. **J Membr Biol** 179(3):165-83.
- Karlberg O, Canback B, Kurland CG, Andersson SG. **2000**. The dual origin of the yeast mitochondrial proteome. **Yeast** 17(3):170-87.
- Kaukonen J, Juselius JK, Tiranti V, Kyttala A, Zeviani M, Comi GP, Keranen S, Peltonen L, Suomalainen A. **2000**. Role of adenine nucleotide translocator 1 in mtDNA maintenance. **Science** 289(5480):782-5.
- Kerscher S, Drose S, Zwicker K, Zickermann V, Brandt U. **2002**. *Yarrowia lipolytica*, a yeast genetic system to study mitochondrial complex I. **Biochim Biophys Acta** 1555(1-3):83-91.
- Kim K, Lecordier A, Bowman LH. **1995**. Both nuclear and mitochondrial cytochrome c oxidase mRNA levels increase dramatically during mouse postnatal development. **Biochem J** 306 (Pt 2):353-8.
- Kirby DM, Thorburn DR. **2008**. Approaches to finding the molecular basis of mitochondrial oxidative phosphorylation disorders. **Twin Res Hum Genet** 11(4):395-411.
- Klement P, Nijtmans LG, Van den Bogert C, Houstek J. **1995**. Analysis of oxidative phosphorylation complexes in cultured human fibroblasts and amniocytes by blue-native-electrophoresis using mitoplasts isolated with the help of digitonin. **Anal Biochem** 231(1):218-24.
- Klingenberg M. **1980**. The ADP-ATP translocation in mitochondria, a membrane potential controlled transport. **J Membr Biol** 56(2):97-105.
- Klingenberg M. **2008**. The ADP and ATP transport in mitochondria and its carrier. **Biochim Biophys Acta** 1778(10):1978-2021.

- Ko YH, Delannoy M, Hullihen J, Chiu W, Pedersen PL. **2003**. Mitochondrial ATP synthasome. Cristae-enriched membranes and a multiwell detergent screening assay yield dispersed single complexes containing the ATP synthase and carriers for Pi and ADP/ATP. **J Biol Chem** 278(14):12305-9.
- Koene S, Smeitink J. **2009**. Mitochondrial medicine: entering the era of treatment. **J Intern Med** 265(2):193-209.
- Kolarov J, Kolarova N, Nelson N. **1990**. A third ADP/ATP translocator gene in yeast. **J Biol Chem** 265(21):12711-6.
- Koonin EV. **2010**. The origin and early evolution of eukaryotes in the light of phylogenomics. **Genome Biol** 11(5):209.
- Koopman WJ, Distelmaier F, Esseling JJ, Smeitink JA, Willems PH. **2008**. Computer-assisted live cell analysis of mitochondrial membrane potential, morphology and calcium handling. **Methods** 46(4):304-11.
- Koopman WJ, Nijtmans LG, Dieteren CE, Roestenberg P, Valsecchi F, Smeitink JA, Willems PH. **2010**. Mammalian mitochondrial complex I: biogenesis, regulation, and reactive oxygen species generation. **Antioxid Redox Signal** 12(12):1431-70.
- Korshunov SS, Skulachev VP, Starkov AA. **1997**. High protonic potential actuates a mechanism of production of reactive oxygen species in mitochondria. **FEBS Lett** 416(1):15-8.
- Kramer R. **1998**. Mitochondrial carrier proteins can reversibly change their transport mode: the cases of the aspartate/glutamate and the phosphate carrier. **Exp Physiol** 83(2):259-65.
- Kramer R, Klingenberg M. **1985**. Structural and functional asymmetry of the ADP/ATP carrier from mitochondria. **Ann N Y Acad Sci** 456:289-90.
- Kroger A, Geisler V, Lemma E, Theis F, Lenger R. **1992**. BACTERIAL FUMARATE RESPIRATION. **Arch. Microbiol.** 158(5):311-4.
- Kroger A, Klingenberg M. **1973**. Further evidence for the pool function of ubiquinone as derived from the inhibition of the electron transport by antimycin. **Eur J Biochem** 39(2):313-23.
- Ku DH, Kagan J, Chen ST, Chang CD, Baserga R, Wurzel J. **1990**. The human fibroblast adenine nucleotide translocator gene. Molecular cloning and sequence. **J Biol Chem** 265(27):16060-3.
- Kuan G, Dassa E, Saurin W, Hofnung M, Saier MH, Jr. **1995**. Phylogenetic analyses of the ATP-binding constituents of bacterial extracytoplasmic receptor-dependent ABC-type nutrient uptake permeases. **Res Microbiol** 146(4):271-8.
- Kucharczyk R, Zick M, Bietenhader M, Rak M, Couplan E, Blondel M, Caubet SD, di Rago JP. **2009**. Mitochondrial ATP synthase disorders: molecular mechanisms and the quest for curative therapeutic approaches. **Biochim Biophys Acta** 1793(1):186-99.
- Kunz WS, Kuznetsov AV, Schulze W, Eichhorn K, Schild L, Striggow F, Bohnensack R, Neuhof S, Grasshoff H, Neumann HW and others. **1993**. Functional characterization of mitochondrial oxidative phosphorylation in saponin-skinned human muscle fibers. **Biochim Biophys Acta** 1144(1):46-53.
- Kurland CG, Andersson SG. **2000**. Origin and evolution of the mitochondrial proteome. **Microbiol Mol Biol Rev** 64(4):786-820.
- Lang BF, Gray MW, Burger G. **1999**. Mitochondrial genome evolution and the origin of eukaryotes. **Annu Rev Genet** 33:351-97.
- Lange C, Hunte C. **2002**. Crystal structure of the yeast cytochrome bc1 complex with its bound substrate cytochrome c. **Proc Natl Acad Sci U S A** 99(5):2800-5.

- Lange C, Nett JH, Trumppower BL, Hunte C. **2001**. Specific roles of protein-phospholipid interactions in the yeast cytochrome bc₁ complex structure. **EMBO J** 20(23):6591-600.
- LaNoue K, Mizani SM, Klingenberg M. **1978**. Electrical imbalance of adenine nucleotide transport across the mitochondrial membrane. **J Biol Chem** 253(1):191-8.
- Lawson JE, Gawaz M, Klingenberg M, Douglas MG. **1990**. Structure-function studies of adenine nucleotide transport in mitochondria. I. Construction and genetic analysis of yeast mutants encoding the ADP/ATP carrier protein of mitochondria. **J Biol Chem** 265(24):14195-201.
- Lebon S, Chol M, Benit P, Mugnier C, Chretien D, Giurgea I, Kern I, Girardin E, Hertz-Pannier L, de Lonlay P and others. **2003**. Recurrent de novo mitochondrial DNA mutations in respiratory chain deficiency. **J Med Genet** 40(12):896-9.
- Lecocq J, Ballou CE. **1964**. On the Structure of Cardiolipin. **Biochemistry** 3:976-80.
- Lee I, Bender E, Arnold S, Kadenbach B. **2001**. New control of mitochondrial membrane potential and ROS formation--a hypothesis. **Biol Chem** 382(12):1629-36.
- Leigh D. **1951**. Subacute necrotizing encephalomyelopathy in an infant. **J Neurol Neurosurg Psychiatry** 14(3):216-21.
- Lemos RS, Fernandes AS, Pereira MM, Gomes CM, Teixeira M. **2002**. Quinol:fumarate oxidoreductases and succinate:quinone oxidoreductases: phylogenetic relationships, metal centres and membrane attachment. **Biochim Biophys Acta** 1553(1-2):158-70.
- Lenaz G, Genova ML. **2007**. Kinetics of integrated electron transfer in the mitochondrial respiratory chain: random collisions vs. solid state electron channeling. **Am J Physiol Cell Physiol** 292(4):C1221-39.
- Lenaz G, Genova ML. **2009**. Structural and functional organization of the mitochondrial respiratory chain: a dynamic super-assembly. **Int J Biochem Cell Biol** 41(10):1750-72.
- Leonard K, Wingfield P, Arad T, Weiss H. **1981**. Three-dimensional structure of ubiquinol:cytochrome c reductase from *Neurospora* mitochondria determined by electron microscopy of membrane crystals. **J Mol Biol** 149(2):259-74.
- Levy SE, Chen YS, Graham BH, Wallace DC. **2000**. Expression and sequence analysis of the mouse adenine nucleotide translocase 1 and 2 genes. **Gene** 254(1-2):57-66.
- Li Y, D'Aurelio M, Deng JH, Park JS, Manfredi G, Hu P, Lu J, Bai Y. **2007**. An assembled complex IV maintains the stability and activity of complex I in mammalian mitochondria. **J Biol Chem** 282(24):17557-62.
- Lin CS, Hackenberg H, Klingenberg EM. **1980**. The uncoupling protein from brown adipose tissue mitochondria is a dimer. A hydrodynamic study. **FEBS Lett** 113(2):304-6.
- Lin MT, Beal MF. **2006**. Mitochondrial dysfunction and oxidative stress in neurodegenerative diseases. **Nature** 443(7113):787-95.
- Liu SS. **1999**. Cooperation of a "reactive oxygen cycle" with the Q cycle and the proton cycle in the respiratory chain--superoxide generating and cycling mechanisms in mitochondria. **J Bioenerg Biomembr** 31(4):367-76.
- Logan DC. **2006**. The mitochondrial compartment. **J Exp Bot** 57(6):1225-43.
- Lowry OH, Rosebrough NJ, Farr AL, Randall RJ. **1951**. Protein measurement with the Folin phenol reagent. **J Biol Chem** 193(1):265-75.

- Luft R, Ikkos D, Palmieri G, Ernster L, Afzelius B. **1962**. A case of severe hypermetabolism of nonthyroid origin with a defect in the maintenance of mitochondrial respiratory control: a correlated clinical, biochemical, and morphological study. **J Clin Invest** 41:1776-804.
- Macfarlane MG. **1964**. The structure of cardiolipin. **Biochem J** 92(2):12C-4C.
- Makinen MW, Lee CP. **1968**. Biochemical studies of skeletal muscle mitochondria. I. Microanalysis of cytochrome content, oxidative and phosphorylative activities of mammalian skeletal muscle mitochondria. **Arch Biochem Biophys** 126(1):75-82.
- Mannella CA. **2000**. Introduction: our changing views of mitochondria. **J Bioenerg Biomembr** 32(1):1-4.
- Mannella CA. **2006a**. The relevance of mitochondrial membrane topology to mitochondrial function. **Biochim Biophys Acta** 1762(2):140-7.
- Mannella CA. **2006b**. Structure and dynamics of the mitochondrial inner membrane cristae. **Biochim Biophys Acta** 1763(5-6):542-8.
- Mannella CA. **2008**. Structural diversity of mitochondria: functional implications. **Ann N Y Acad Sci** 1147:171-9.
- Mannella CA, Marko M, Buttle K. **1997**. Reconsidering mitochondrial structure: new views of an old organelle. **Trends Biochem Sci** 22(2):37-8.
- Mannella CA, Marko M, Penczek P, Barnard D, Frank J. **1994**. The internal compartmentation of rat-liver mitochondria: tomographic study using the high-voltage transmission electron microscope. **Microsc Res Tech** 27(4):278-83.
- Mannella CA, Pfeiffer DR, Bradshaw PC, Moraru, II, Slepchenko B, Loew LM, Hsieh CE, Buttle K, Marko M. **2001**. Topology of the mitochondrial inner membrane: dynamics and bioenergetic implications. **IUBMB Life** 52(3-5):93-100.
- Marques I, Dencher NA, Videira A, Krause F. **2007**. Supramolecular organization of the respiratory chain in *Neurospora crassa* mitochondria. **Eukaryot Cell** 6(12):2391-405.
- Marques I, Duarte M, Assuncao J, Ushakova AV, Videira A. **2005**. Composition of complex I from *Neurospora crassa* and disruption of two "accessory" subunits. **Biochim Biophys Acta** 1707(2-3):211-20.
- Marsy S, Frachon P, Dujardin G, Lombes A, Lemaire C. **2008**. Respiratory mutations lead to different pleiotropic effects on OXPHOS complexes in yeast and in human cells. **FEBS Lett** 582(23-24):3489-93.
- Marzuki S, Watkins LC, Choo WM. **1989**. Mitochondrial H⁺-ATPase in mutants of *Saccharomyces cerevisiae* with defective subunit 8 of the enzyme complex. **Biochim Biophys Acta** 975(2):222-30.
- Massa V, Fernandez-Vizarra E, Alshahwan S, Bakhsh E, Goffrini P, Ferrero I, Mereghetti P, D'Adamo P, Gasparini P, Zeviani M. **2008**. Severe infantile encephalomyopathy caused by a mutation in COX6B1, a nucleus-encoded subunit of cytochrome c oxidase. **Am J Hum Genet** 82(6):1281-9.
- Mayr JA, Havlickova V, Zimmermann F, Magler I, Kaplanova V, Jesina P, Pecinova A, Nuskova H, Koch J, Sperl W and others. **2010**. Mitochondrial ATP synthase deficiency due to a mutation in the ATP5E gene for the F1 epsilon subunit. **Hum Mol Genet** 19(17):3430-9.
- Mayr JA, Merkel O, Kohlwein SD, Gebhardt BR, Bohles H, Fotschl U, Koch J, Jaksch M, Lochmuller H, Horvath R and others. **2007**. Mitochondrial phosphate-carrier deficiency: a novel disorder of oxidative phosphorylation. **Am J Hum Genet** 80(3):478-84.

- Mazat JP, Rossignol R, Malgat M, Letellier T. **2000**. Simple models of threshold curves in the expression of inborn errors of metabolism: application to some experimental observations. **Dev Neurosci** 22(5-6):399-403.
- McKenzie M, Lazarou M, Thorburn DR, Ryan MT. **2006**. Mitochondrial respiratory chain supercomplexes are destabilized in Barth Syndrome patients. **J Mol Biol** 361(3):462-9.
- Meier T, Krah A, Bond PJ, Pogoryelov D, Diederichs K, Faraldo-Gomez JD. **2009**. Complete ion-coordination structure in the rotor ring of Na⁺-dependent F-ATP synthases. **J Mol Biol** 391(2):498-507.
- Meier T, Polzer P, Diederichs K, Welte W, Dimroth P. **2005**. Structure of the rotor ring of F-Type Na⁺-ATPase from *Ilyobacter tartaricus*. **Science** 308(5722):659-62.
- Meyer B, Wittig I, Trifilieff E, Karas M, Schagger H. **2007**. Identification of two proteins associated with mammalian ATP synthase. **Mol Cell Proteomics** 6(10):1690-9.
- Mick DU, Wagner K, van der Laan M, Frazier AE, Perschil I, Pawlas M, Meyer HE, Warscheid B, Rehling P. **2007**. Shy1 couples Cox1 translational regulation to cytochrome c oxidase assembly. **EMBO J** 26(20):4347-58.
- Mitchell P. **1961**. Coupling of phosphorylation to electron and hydrogen transfer by a chemi-osmotic type of mechanism. **Nature** 191:144-8.
- Mitchell P. **1976**. Possible molecular mechanisms of the protonmotive function of cytochrome systems. **J Theor Biol** 62(2):327-67.
- Mootha VK, Lepage P, Miller K, Bunkenborg J, Reich M, Hjerrild M, Delmonte T, Villeneuve A, Sladek R, Xu F and others. **2003**. Identification of a gene causing human cytochrome c oxidase deficiency by integrative genomics. **Proc Natl Acad Sci U S A** 100(2):605-10.
- Moradi-Ameli M, Godinot C. **1983**. Characterization of monoclonal antibodies against mitochondrial F₁-ATPase. **Proc Natl Acad Sci U S A** 80(20):6167-71.
- Munnich A, Rotig A, Chretien D, Cormier V, Bourgeron T, Bonnefont JP, Saudubray JM, Rustin P. **1996**. Clinical presentation of mitochondrial disorders in childhood. **J Inherit Metab Dis** 19(4):521-7.
- Nakamoto RK, Baylis Scanlon JA, Al-Shawi MK. **2008**. The rotary mechanism of the ATP synthase. **Arch Biochem Biophys** 476(1):43-50.
- Neupert W, Herrmann JM. **2007**. Translocation of proteins into mitochondria. **Annu Rev Biochem** 76:723-49.
- Nicastro D, Frangakis AS, Typke D, Baumeister W. **2000**. Cryo-electron tomography of neurospora mitochondria. **J Struct Biol** 129(1):48-56.
- Niebisch A, Bott M. **2003**. Purification of a cytochrome bc-aa₃ supercomplex with quinol oxidase activity from *Corynebacterium glutamicum*. Identification of a fourth subunit of cytochrome aa₃ oxidase and mutational analysis of diheme cytochrome c₁. **J Biol Chem** 278(6):4339-46.
- Niemann S, Muller U. **2000**. Mutations in SDHC cause autosomal dominant paraganglioma, type 3. **Nat Genet** 26(3):268-70.
- Nicholls D, Ferguson S. **2002**. Bioenergetics₃, 3rd edn., Academic Press, London.
- Nijtmans LG, Taanman JW, Muijsers AO, Speijer D, Van den Bogert C. **1998**. Assembly of cytochrome-c oxidase in cultured human cells. **Eur J Biochem** 254(2):389-94.
- Nosek J, Tomaska L, Fukuhara H, Suyama Y, Kovac L. **1998**. Linear mitochondrial genomes: 30 years down the line. **Trends Genet.** 14(5):184-8.

- Olson A, Sheth N, Lee JS, Hannon G, Sachidanandam R. **2006**. RNAi Codex: a portal/database for short-hairpin RNA (shRNA) gene-silencing constructs. **Nucleic Acids Res** 34(Database issue):D153-7.
- Ouhabi R, Boue-Grabot M, Mazat JP. **1998**. Mitochondrial ATP synthesis in permeabilized cells: assessment of the ATP/O values in situ. **Anal Biochem** 263(2):169-75.
- Palmieri L, Alberio S, Pisano I, Lodi T, Meznaric-Petrusa M, Zidar J, Santoro A, Scarcia P, Fontanesi F, Lamantea E and others. **2005**. Complete loss-of-function of the heart/muscle-specific adenine nucleotide translocator is associated with mitochondrial myopathy and cardiomyopathy. **Hum Mol Genet** 14(20):3079-88.
- Parfait B, Chretien D, Rotig A, Marsac C, Munnich A, Rustin P. **2000**. Compound heterozygous mutations in the flavoprotein gene of the respiratory chain complex II in a patient with Leigh syndrome. **Hum Genet** 106(2):236-43.
- Pasini B, Stratakis CA. **2009**. SDH mutations in tumorigenesis and inherited endocrine tumours: lesson from the pheochromocytoma-paranglioma syndromes. **J Intern Med** 266(1):19-42.
- Paul MF, Velours J, Arselin de Chateaubodeau G, Aigle M, Guerin B. **1989**. The role of subunit 4, a nuclear-encoded protein of the F₀ sector of yeast mitochondrial ATP synthase, in the assembly of the whole complex. **Eur J Biochem** 185(1):163-71.
- Paumard P, Vaillier J, Couлары B, Schaeffer J, Soubannier V, Mueller DM, Brethes D, di Rago JP, Velours J. **2002**. The ATP synthase is involved in generating mitochondrial cristae morphology. **EMBO J** 21(3):221-30.
- Pecina P, Capkova M, Chowdhury SK, Drahota Z, Dubot A, Vojtiskova A, Hansikova H, Houst'kova H, Zeman J, Godinot C and others. **2003**. Functional alteration of cytochrome c oxidase by SURF1 mutations in Leigh syndrome. **Biochim Biophys Acta** 1639(1):53-63.
- Pecina P, Gnaiger E, Zeman J, Pronicka E, Houstek J. **2004**. Decreased affinity for oxygen of cytochrome-c oxidase in Leigh syndrome caused by SURF1 mutations. **Am J Physiol Cell Physiol** 287(5):C1384-8.
- Perales M, Eubel H, Heinemeyer J, Colaneri A, Zabaleta E, Braun HP. **2005**. Disruption of a nuclear gene encoding a mitochondrial gamma carbonic anhydrase reduces complex I and supercomplex I + III₂ levels and alters mitochondrial physiology in Arabidopsis. **J Mol Biol** 350(2):263-77.
- Pfaff E, Klingenberg M. **1968**. Adenine nucleotide translocation of mitochondria. 1. Specificity and control. **Eur J Biochem** 6(1):66-79.
- Pfeiffer K, Gohil V, Stuart RA, Hunte C, Brandt U, Greenberg ML, Schagger H. **2003**. Cardiolipin stabilizes respiratory chain supercomplexes. **J Biol Chem** 278(52):52873-80.
- Pfeiffer T, Schuster S, Bonhoeffer S. **2001**. Cooperation and competition in the evolution of ATP-producing pathways. **Science** 292(5516):504-7.
- Phelps A, Schobert CT, Wohlrab H. **1991**. Cloning and characterization of the mitochondrial phosphate transport protein gene from the yeast *Saccharomyces cerevisiae*. **Biochemistry** 30(1):248-52.
- Phelps A, Wohlrab H. **2004**. Homodimeric mitochondrial phosphate transport protein. Transient subunit/subunit contact site between the transport relevant transmembrane helices A. **Biochemistry** 43(20):6200-7.

- Pogoryelov D, Yildiz O, Faraldo-Gomez JD, Meier T. **2009**. High-resolution structure of the rotor ring of a proton-dependent ATP synthase. **Nat Struct Mol Biol** 16(10):1068-73.
- Preiss L, Yildiz O, Hicks DB, Krulwich TA, Meier T. **2010**. A new type of proton coordination in an F(1)F(o)-ATP synthase rotor ring. **PLoS Biol** 8(8):e1000443.
- Puddu P, Barboni P, Mantovani V, Montagna P, Cerullo A, Bragliani M, Molinotti C, Caramazza R. **1993**. Retinitis pigmentosa, ataxia, and mental retardation associated with mitochondrial DNA mutation in an Italian family. **Br J Ophthalmol** 77(2):84-8.
- Radermacher M, Ruiz T, Clason T, Benjamin S, Brandt U, Zickermann V. **2006**. The three-dimensional structure of complex I from *Yarrowia lipolytica*: a highly dynamic enzyme. **J Struct Biol** 154(3):269-79.
- Radford NB, Wan B, Richman A, Szczepaniak LS, Li JL, Li K, Pfeiffer K, Schagger H, Garry DJ, Moreadith RW. **2002**. Cardiac dysfunction in mice lacking cytochrome-c oxidase subunit VIaH. **Am J Physiol Heart Circ Physiol** 282(2):H726-33.
- Rahman S, Blok RB, Dahl HH, Danks DM, Kirby DM, Chow CW, Christodoulou J, Thorburn DR. **1996**. Leigh syndrome: clinical features and biochemical and DNA abnormalities. **Ann Neurol** 39(3):343-51.
- Rak M, Tetaud E, Godard F, Sagot I, Salin B, Duvezin-Caubet S, Slonimski PP, Rytka J, di Rago JP. **2007**. Yeast cells lacking the mitochondrial gene encoding the ATP synthase subunit 6 exhibit a selective loss of complex IV and unusual mitochondrial morphology. **J Biol Chem** 282(15):10853-64.
- Rossignol R, Letellier T, Malgat M, Rocher C, Mazat JP. **2000**. Tissue variation in the control of oxidative phosphorylation: implication for mitochondrial diseases. **Biochem J** 347 Pt 1:45-53.
- Rossignol R, Malgat M, Mazat JP, Letellier T. **1999**. Threshold effect and tissue specificity. Implication for mitochondrial cytopathies. **J Biol Chem** 274(47):33426-32.
- Rubinstein JL, Dickson VK, Runswick MJ, Walker JE. **2005**. ATP synthase from *Saccharomyces cerevisiae*: location of subunit h in the peripheral stalk region. **J Mol Biol** 345(3):513-20.
- Runswick MJ, Powell SJ, Nyren P, Walker JE. **1987**. Sequence of the bovine mitochondrial phosphate carrier protein: structural relationship to ADP/ATP translocase and the brown fat mitochondria uncoupling protein. **EMBO J** 6(5):1367-73.
- Rustin P, Rotig A. **2002**. Inborn errors of complex II--unusual human mitochondrial diseases. **Biochim Biophys Acta** 1553(1-2):117-22.
- Rutter GA, Rizzuto R. **2000**. Regulation of mitochondrial metabolism by ER Ca²⁺ release: an intimate connection. **Trends Biochem Sci** 25(5):215-21.
- Ryan MT, Muller H, Pfanner N. **1999**. Functional staging of ADP/ATP carrier translocation across the outer mitochondrial membrane. **J Biol Chem** 274(29):20619-27.
- Sambrook J, Russell DW. **2001**. Molecular cloning: A Laboratory Manual, 3rd edn., Cold Spring Harbor Laboratory Press, NY.
- Saraste M. **1999**. Oxidative phosphorylation at the fin de siecle. **Science** 283(5407):1488-93.
- Saraste M, Walker JE. **1982**. Internal sequence repeats and the path of polypeptide in mitochondrial ADP/ATP translocase. **FEBS Lett** 144(2):250-4.

- Scott SV, Cassidy-Stone A, Meeusen SL, Nunnari J. **2003**. Staying in aerobic shape: how the structural integrity of mitochondria and mitochondrial DNA is maintained. **Curr Opin Cell Biol** 15(4):482-8.
- Sedlak E, Robinson NC. **1999**. Phospholipase A(2) digestion of cardiolipin bound to bovine cytochrome c oxidase alters both activity and quaternary structure. **Biochemistry** 38(45):14966-72.
- Seneca S, Abramowicz M, Lissens W, Muller MF, Vamos E, de Meirleir L. **1996**. A mitochondrial DNA microdeletion in a newborn girl with transient lactic acidosis. **J Inherit Metab Dis** 19(2):115-8.
- Shoffner JM, Fernhoff PM, Krawiecki NS, Caplan DB, Holt PJ, Koontz DA, Takei Y, Newman NJ, Ortiz RG, Polak M and others. **1992**. Subacute necrotizing encephalopathy: oxidative phosphorylation defects and the ATPase 6 point mutation. **Neurology** 42(11):2168-74.
- Shoubridge EA. **2001**. Cytochrome c oxidase deficiency. **Am J Med Genet** 106(1):46-52.
- Shteyer E, Saada A, Shaag A, Al-Hijawi FA, Kidess R, Revel-Vilk S, Elpeleg O. **2009**. Exocrine pancreatic insufficiency, dyserythropoietic anemia, and calvarial hyperostosis are caused by a mutation in the COX4I2 gene. **Am J Hum Genet** 84(3):412-7.
- Schaefer AM, Taylor RW, Turnbull DM, Chinnery PF. **2004**. The epidemiology of mitochondrial disorders--past, present and future. **Biochim Biophys Acta** 1659(2-3):115-20.
- Schagger H, de Coo R, Bauer MF, Hofmann S, Godinot C, Brandt U. **2004**. Significance of respirasomes for the assembly/stability of human respiratory chain complex I. **J Biol Chem** 279(35):36349-53.
- Schagger H, Link TA, Engel WD, von Jagow G. **1986**. Isolation of the eleven protein subunits of the bc1 complex from beef heart. **Methods Enzymol** 126:224-37.
- Schagger H, Pfeiffer K. **2000**. Supercomplexes in the respiratory chains of yeast and mammalian mitochondria. **EMBO J** 19(8):1777-83.
- Schagger H, Pfeiffer K. **2001**. The ratio of oxidative phosphorylation complexes I-V in bovine heart mitochondria and the composition of respiratory chain supercomplexes. **J Biol Chem** 276(41):37861-7.
- Schagger H, von Jagow G. **1987**. Tricine-sodium dodecyl sulfate-polyacrylamide gel electrophoresis for the separation of proteins in the range from 1 to 100 kDa. **Anal Biochem** 166(2):368-79.
- Schagger H, von Jagow G. **1991**. Blue native electrophoresis for isolation of membrane protein complexes in enzymatically active form. **Anal Biochem** 199(2):223-31.
- Schlame M, Rua D, Greenberg ML. **2000**. The biosynthesis and functional role of cardiolipin. **Prog Lipid Res** 39(3):257-88.
- Schlerf A, Droste M, Winter M, Kadenbach B. **1988**. Characterization of two different genes (cDNA) for cytochrome c oxidase subunit VIa from heart and liver of the rat. **Embo J** 7(8):2387-91.
- Schon EA, Santra S, Pallotti F, Girvin ME. **2001**. Pathogenesis of primary defects in mitochondrial ATP synthesis. **Semin Cell Dev Biol** 12(6):441-8.
- Schroers A, Burkovski A, Wohlrab H, Kramer R. **1998**. The phosphate carrier from yeast mitochondria. Dimerization is a prerequisite for function. **J Biol Chem** 273(23):14269-76.
- Sicheritz-Ponten T, Kurland CG, Andersson SG. **1998**. A phylogenetic analysis of the cytochrome b and cytochrome c oxidase I genes supports an origin of

- mitochondria from within the Rickettsiaceae. **Biochim Biophys Acta** 1365(3):545-51.
- Smeitink J, Sengers R, Trijbels F, van den Heuvel L. **2001a**. Human NADH:ubiquinone oxidoreductase. **J Bioenerg Biomembr** 33(3):259-66.
- Smeitink J, van den Heuvel L, DiMauro S. **2001b**. The genetics and pathology of oxidative phosphorylation. **Nat Rev Genet** 2(5):342-52.
- Smeitink JA, Zeviani M, Turnbull DM, Jacobs HT. **2006**. Mitochondrial medicine: a metabolic perspective on the pathology of oxidative phosphorylation disorders. **Cell Metab** 3(1):9-13.
- Sone N, Sekimachi M, Kutoh E. **1987**. Identification and properties of a quinol oxidase super-complex composed of a bcl complex and cytochrome oxidase in the thermophilic bacterium PS3. **J Biol Chem** 262(32):15386-91.
- Spannagel C, Vaillier J, Arselin G, Graves PV, Velours J. **1997**. The subunit f of mitochondrial yeast ATP synthase--characterization of the protein and disruption of the structural gene ATP17. **Eur J Biochem** 247(3):1111-7.
- Spiro AJ, Moore CL, Prineas JW, Strasberg PM, Rapin I. **1970**. A cytochrome-related inherited disorder of the nervous system and muscle. **Arch Neurol** 23(2):103-12.
- Stappen R, Kramer R. **1993**. Functional properties of the reconstituted phosphate carrier from bovine heart mitochondria: evidence for asymmetric orientation and characterization of three different transport modes. **Biochim Biophys Acta** 1149(1):40-8.
- Stappen R, Kramer R. **1994**. Kinetic mechanism of phosphate/phosphate and phosphate/OH⁻ antiports catalyzed by reconstituted phosphate carrier from beef heart mitochondria. **J Biol Chem** 269(15):11240-6.
- Stepien G, Torroni A, Chung AB, Hodge JA, Wallace DC. **1992**. Differential expression of adenine nucleotide translocator isoforms in mammalian tissues and during muscle cell differentiation. **J Biol Chem** 267(21):14592-7.
- Stiburek L, Fornuskova D, Wenchich L, Pejznochova M, Hansikova H, Zeman J. **2007**. Knockdown of human Oxa11 impairs the biogenesis of F1Fo-ATP synthase and NADH:ubiquinone oxidoreductase. **J Mol Biol** 374(2):506-16.
- Stiburek L, Hansikova H, Tesarova M, Cerna L, Zeman J. **2006**. Biogenesis of eukaryotic cytochrome c oxidase. **Physiol Res** 55 Suppl 2:S27-41.
- Stiburek L, Vesela K, Hansikova H, Pecina P, Tesarova M, Cerna L, Houstek J, Zeman J. **2005**. Tissue-specific cytochrome c oxidase assembly defects due to mutations in SCO2 and SURF1. **Biochem J** 392(Pt 3):625-32.
- Stiburek L, Zeman J. **2010**. Assembly factors and ATP-dependent proteases in cytochrome c oxidase biogenesis. **Biochim Biophys Acta** 1797(6-7):1149-58.
- Stock D, Leslie AG, Walker JE. **1999**. Molecular architecture of the rotary motor in ATP synthase. **Science** 286(5445):1700-5.
- Strauss M, Hofhaus G, Schroder RR, Kuhlbrandt W. **2008**. Dimer ribbons of ATP synthase shape the inner mitochondrial membrane. **EMBO J** 27(7):1154-60.
- Stroh A, Anderka O, Pfeiffer K, Yagi T, Finel M, Ludwig B, Schagger H. **2004**. Assembly of respiratory complexes I, III, and IV into NADH oxidase supercomplex stabilizes complex I in *Paracoccus denitrificans*. **J Biol Chem** 279(6):5000-7.
- Sun F, Huo X, Zhai Y, Wang A, Xu J, Su D, Bartlam M, Rao Z. **2005**. Crystal structure of mitochondrial respiratory membrane protein complex II. **Cell** 121(7):1043-57.

- Suthammarak W, Yang YY, Morgan PG, Sedensky MM. **2009**. Complex I function is defective in complex IV-deficient *Caenorhabditis elegans*. **J Biol Chem** 284(10):6425-35.
- Szabadkai G, Rizzuto R. **2007**. Chaperones as parts of organelle networks. **Adv Exp Med Biol** 594:64-77.
- Taanman JW, Herzberg NH, De Vries H, Bolhuis PA, Van den Bogert C. **1992**. Steady-state transcript levels of cytochrome c oxidase genes during human myogenesis indicate subunit switching of subunit VIa and co-expression of subunit VIIa isoforms. **Biochim Biophys Acta** 1139(1-2):155-62.
- Tatuch Y, Pagon RA, Vlcek B, Roberts R, Korson M, Robinson BH. **1994**. The 8993 mtDNA mutation: heteroplasmy and clinical presentation in three families. **Eur J Hum Genet** 2(1):35-43.
- Tatuch Y, Robinson BH. **1993**. The mitochondrial DNA mutation at 8993 associated with NARP slows the rate of ATP synthesis in isolated lymphoblast mitochondria. **Biochem Biophys Res Commun** 192(1):124-8.
- Thorburn DR. **2004**. Mitochondrial disorders: prevalence, myths and advances. **J Inherit Metab Dis** 27(3):349-62.
- Thyagarajan D, Shanske S, Vazquez-Memije M, De Vivo D, DiMauro S. **1995**. A novel mitochondrial ATPase 6 point mutation in familial bilateral striatal necrosis. **Ann Neurol** 38(3):468-72.
- Torrioni A, Stepien G, Hodge JA, Wallace DC. **1990**. Neoplastic transformation is associated with coordinate induction of nuclear and cytoplasmic oxidative phosphorylation genes. **J Biol Chem** 265(33):20589-93.
- Tsukihara T, Aoyama H, Yamashita E, Tomizaki T, Yamaguchi H, Shinzawa-Itoh K, Nakashima R, Yaono R, Yoshikawa S. **1996**. The whole structure of the 13-subunit oxidized cytochrome c oxidase at 2.8 Å. **Science** 272(5265):1136-44.
- Tsunoda SP, Aggeler R, Yoshida M, Capaldi RA. **2001**. Rotation of the c subunit oligomer in fully functional F₁F₀ ATP synthase. **Proc Natl Acad Sci U S A** 98(3):898-902.
- Tucker EJ, Compton AG, Thorburn DR. **2010**. Recent advances in the genetics of mitochondrial encephalopathies. **Curr Neurol Neurosci Rep** 10(4):277-85.
- Usui S, Yu L, Yu CA. **1990**. The small molecular mass ubiquinone-binding protein (QPc-9.5 kDa) in mitochondrial ubiquinol-cytochrome c reductase: isolation, ubiquinone-binding domain, and immunoinhibition. **Biochemistry** 29(19):4618-26.
- Viale AM, Arakaki AK. **1994**. The chaperone connection to the origins of the eukaryotic organelles. **FEBS Lett** 341(2-3):146-51.
- Villiers C, Michejda JW, Block M, Lauquin GJ, Vignais PV. **1979**. The electrogenic nature of ADP/ATP transport in inside-out submitochondrial particles. **Biochim Biophys Acta** 546(1):157-70.
- Vinogradov AD. **1998**. Catalytic properties of the mitochondrial NADH-ubiquinone oxidoreductase (complex I) and the pseudo-reversible active/inactive enzyme transition. **Biochim Biophys Acta** 1364(2):169-85.
- Voet D, Voet JG, Pratt CW. **2006**. Fundamentals of Biochemistry: Life at the Molecular Level, 2nd edn., John Wiley & Sons, Inc., MA.
- Vogel RO, Smeitink JA, Nijtmans LG. **2007**. Human mitochondrial complex I assembly: a dynamic and versatile process. **Biochim Biophys Acta** 1767(10):1215-27.
- Vojtiskova A, Jesina P, Kalous M, Kaplanova V, Houstek J, Tesarova M, Fornuskova D, Zeman J, Dubot A, Godinot C. **2004**. Mitochondrial membrane potential and

- ATP production in primary disorders of ATP synthase. **Toxicol Mech Methods** 14(1-2):7-11.
- Vonck J, Schafer E. **2009**. Supramolecular organization of protein complexes in the mitochondrial inner membrane. **Biochim Biophys Acta** 1793(1):117-24.
- Walker JE. **1994**. The regulation of catalysis in ATP synthase. **Curr Opin Struct Biol** 4(6):912-8.
- Walker JE, Dickson VK. **2006**. The peripheral stalk of the mitochondrial ATP synthase. **Biochim Biophys Acta** 1757(5-6):286-96.
- Wanders RJ, Ruiter JP, Wijburg FA, Zeman J, Klement P, Houstek J. **1996**. Prenatal diagnosis of systemic disorders of the respiratory chain in cultured chorionic villus fibroblasts by study of ATP-synthesis in digitonin-permeabilized cells. **J Inherit Metab Dis** 19(2):133-6.
- Weber J, Senior AE. **2000**. ATP synthase: what we know about ATP hydrolysis and what we do not know about ATP synthesis. **Biochim Biophys Acta** 1458(2-3):300-9.
- Weidner U, Geier S, Ptock A, Friedrich T, Leif H, Weiss H. **1993**. The gene locus of the proton-translocating NADH: ubiquinone oxidoreductase in Escherichia coli. Organization of the 14 genes and relationship between the derived proteins and subunits of mitochondrial complex I. **J Mol Biol** 233(1):109-22.
- Wenchich L, Drahota Z, Honzik T, Hansikova H, Tesarova M, Zeman J, Houstek J. **2003**. Polarographic evaluation of mitochondrial enzymes activity in isolated mitochondria and in permeabilized human muscle cells with inherited mitochondrial defects. **Physiol Res** 52(6):781-8.
- Weraarpachai W, Antonicka H, Sasarman F, Seeger J, Schrank B, Kolesar JE, Lochmuller H, Chevrette M, Kaufman BA, Horvath R and others. **2009**. Mutation in TACO1, encoding a translational activator of COX I, results in cytochrome c oxidase deficiency and late-onset Leigh syndrome. **Nat Genet** 41(7):833-7.
- Winge DR, Tzagoloff A. **2009**. Assembly of the mitochondrial respiratory chain. Preface. **Biochim Biophys Acta** 1793(1):1.
- Wittig I, Braun HP, Schagger H. **2006**. Blue native PAGE. **Nat Protoc** 1(1):418-28.
- Wittig I, Schagger H. **2005**. Advantages and limitations of clear-native PAGE. **Proteomics** 5(17):4338-46.
- Wittig I, Schagger H. **2008**. Structural organization of mitochondrial ATP synthase. **Biochim Biophys Acta** 1777(7-8):592-8.
- Wittig I, Schagger H. **2009**. Supramolecular organization of ATP synthase and respiratory chain in mitochondrial membranes. **Biochim Biophys Acta** 1787(6):672-80.
- Wohlrab H. **1986**. Molecular aspects of inorganic phosphate transport in mitochondria. **Biochim Biophys Acta** 853(2):115-34.
- Wohlrab H. **2004**. Novel inter- and intrasubunit contacts between transport-relevant residues of the homodimeric mitochondrial phosphate transport protein. **Biochem Biophys Res Commun** 320(3):685-8.
- Wohlrab H. **2009**. Transport proteins (carriers) of mitochondria. **IUBMB Life** 61(1):40-6.
- Wohlrab H. **2010**. Homodimeric intrinsic membrane proteins. Identification and modulation of interactions between mitochondrial transporter (carrier) subunits. **Biochem Biophys Res Commun** 393(4):746-50.

- Wohlrab H, Flowers N. **1982**. pH gradient-dependent phosphate transport catalyzed by the purified mitochondrial phosphate transport protein. **J Biol Chem** 257(1):28-31.
- Wulf R, Kaltstein A, Klingenberg M. **1978**. H⁺ and cation movements associated with ADP, ATP transport in mitochondria. **Eur J Biochem** 82(2):585-92.
- Xia D, Yu CA, Kim H, Xia JZ, Kachurin AM, Zhang L, Yu L, Deisenhofer J. **1997**. Crystal structure of the cytochrome bc₁ complex from bovine heart mitochondria. **Science** 277(5322):60-6.
- Xiao Y, Metzl M, Mueller DM. **2000**. Partial uncoupling of the mitochondrial membrane by a heterozygous null mutation in the gene encoding the gamma- or delta-subunit of the yeast mitochondrial ATPase. **J Biol Chem** 275(10):6963-8.
- Yankovskaya V, Horsefield R, Tornroth S, Luna-Chavez C, Miyoshi H, Leger C, Byrne B, Cecchini G, Iwata S. **2003**. Architecture of succinate dehydrogenase and reactive oxygen species generation. **Science** 299(5607):700-4.
- Yi L, Dalbey RE. **2005**. Oxa1/Alb3/YidC system for insertion of membrane proteins in mitochondria, chloroplasts and bacteria (review). **Mol Membr Biol** 22(1-2):101-11.
- Zara V, Conte L, Trumppower BL. **2009**. Biogenesis of the yeast cytochrome bc₁ complex. **Biochim Biophys Acta** 1793(1):89-96.
- Zara V, Palmieri F, Mahlke K, Pfanner N. **1992**. The cleavable presequence is not essential for import and assembly of the phosphate carrier of mammalian mitochondria but enhances the specificity and efficiency of import. **J Biol Chem** 267(17):12077-81.
- Zeviani M, Bertagnolio B, Uziel G. **1996**. Neurological presentations of mitochondrial diseases. **J Inherit Metab Dis** 19(4):504-20.
- Zeviani M, Carelli V. **2007**. Mitochondrial disorders. **Curr Opin Neurol** 20(5):564-71.
- Zhang Z, Huang L, Shulmeister VM, Chi YI, Kim KK, Hung LW, Crofts AR, Berry EA, Kim SH. **1998**. Electron transfer by domain movement in cytochrome bc₁. **Nature** 392(6677):677-84.
- Zhen Y, Hoganson CW, Babcock GT, Ferguson-Miller S. **1999**. Definition of the interaction domain for cytochrome c on cytochrome c oxidase. I. Biochemical, spectral, and kinetic characterization of surface mutants in subunit ii of *Rhodobacter sphaeroides* cytochrome aa(3). **J Biol Chem** 274(53):38032-41.
- Zickermann V, Kerscher S, Zwicker K, Tocilescu MA, Radermacher M, Brandt U. **2009**. Architecture of complex I and its implications for electron transfer and proton pumping. **Biochim Biophys Acta** 1787(6):574-83.

9 LIST OF ORIGINAL ARTICLES

9.1. Journal articles

Fornuskova D, Stiburek L, Wenchich L, Vinsova K, Hansikova H, Zeman J. **2010**. Novel insights into the assembly and function of human nuclear-encoded cytochrome c oxidase subunits 4, 5a, 6a, 7a and 7b. **Biochem J** 428(3):363-74. *IF 5.155*

Stiburek L, **Fornuskova D**, Wenchich L, Pejznochova M, Hansikova H, Zeman J. **2007**. Knockdown of human Oxa11 impairs the biogenesis of F1Fo-ATP synthase and NADH:ubiquinone oxidoreductase. **J Mol Biol** 374(2):506-16. *IF 4.472*

Fornuskova D, Brantova O, Tesarova M, Stiburek L, Honzik T, Wenchich L, Tietzeova E, Hansikova H, Zeman J. **2008**. The impact of mitochondrial tRNA mutations on the amount of ATP synthase differs in the brain compared to other tissues. **Biochim Biophys Acta** 1782(5):317-25. *IF 4.579*

Jesina P, Tesarova M, **Fornuskova D**, Vojtiskova A, Pecina P, Kaplanova V, Hansikova H, Zeman J, Houstek J. **2004**. Diminished synthesis of subunit a (ATP6) and altered function of ATP synthase and cytochrome c oxidase due to the mtDNA 2 bp microdeletion of TA at positions 9205 and 9206. **Biochem J** 383(Pt. 3):561-71. *IF 4.278*

Vojtiskova A, Jesina P, Kalous M, Kaplanova V, Houstek J, Tesarova M, **Fornuskova D**, Zeman J, Dubot A, Godinot C. **2004**. Mitochondrial membrane potential and ATP production in primary disorders of ATP synthase. **Toxicol Mech Methods** 14(1-2):7-11. *IF 0.464*

Stiburek L, Kostkova O, **Fornuskova D**, Tesarova J, Wenchich L, Houstek J, Zeman J. **2010**. The mitochondrial ATP-dependent protease YME1L controls the deleterious accumulation of non-assembled OXPHOS subunits. *Submitted for publication to Mol Cell Biol*. *IF 6.057*

9.2. Abstracts in journals

Tesarova M, **Fornuskova D**, Cerna L, Hansikova H, Stiburek L, Zeman J. MtDNA deletions in patients with hypertrophic cardiomyopathy-is there causal relation?

European Human Genetics Conference 2005, 7 - 10 May 2005, Prague, Czech Republic. European Journal of Human genetics 13 (Suppl 1): P0824.

Tesařová M, **Fornůsková D**, Honzík T, Hansíková H, Zeman J. Mutace v mitochondriální DNA u pacientů s encefalopatií a hypertrofickou kardiomyopatií. *Česko-Slovenská pediatrie*, 2006, 61 (5): 323.

Ješina P, Tesařová M, **Fornůsková D**, Vojtíšková A, Pecina P, Kaplanová V, Hansíková H, Zeman J, Houštek J. Structural and functional changes of mitochondrial ATP synthase caused by mtDNA 9205delITA mutation in ATP gene. *10th International congress of Inborn Errors of Metabolism*, 12-16 September 2006, Chiba, Japan. *Journal of Inherited Metabolic Disease* 29 (Suppl):117.

Fornuskova D, Stiburek L, Pejznochova M, Zeman J. Down-regulation of COX5A subunit in HEK293 cells. *32nd FEBS Congress – Molecular Machines*, 7-12 July 2007, Vienna, Austria. *the FEBS Journal* 274 (Suppl 1): 364.

Fornuskova D, Stiburek L, Zeman J. Knock-down of Cox5a in HEK293 cells. *European Human Genetics Conference 2008*, 31 May - 3 June 2008, Barcelona, Spain. *European Journal of Human Genetics* 16 (Suppl 2): 277.

Fornuskova D, Stiburek L, Vinsova, K, Zeman J. Knock-down of cytochrome c oxidase structural subunits in HEK293 cells. *34th FEBS Congress – Life's Molecular Interactions*, 4-9 July 2009, Prague, Czech Republic. *the FEBS Journal* 276 (Suppl 1): 139.

Fornuskova D, Stiburek L, Wenchich L, Vinsova K, Hansikova H, Zeman J. Knockdown of cytochrome c oxidase structural subunits in HEK293 cells. *EBEC 2010*, 17-22 July 2010, Warsaw, Poland. *BBA Bioenergetics*, Suppl to vol 1797: 15.

